An Investigation into the Mechanism of Action of the *SMN2* Bifunctional Oligonucleotide and its Application to Reverse the *RON* Δ165 Pro-Metastatic Splicing Event

Thesis submitted for the degree of

Doctor of Philosophy

at the University of Leicester

Lindsay Denise Smith BSc (Hons)

Department of Biochemistry

University of Leicester

2012

ABSTRACT

An investigation into the mechanism of action of the *SMN2* bifunctional oligonucleotide and its application to reverse the *RON* Δ165 pro-metastatic splicing event

By Lindsay Denise Smith

It is widely accepted that alternative splicing is often a catalyst for the development and progression of disease. Recent advances in oligonucleotide therapeutics have seen these alternative splicing patterns forcibly changed, providing a specific and versatile attack against such diseases.

This study has focused on the use of bifunctional oligonucleotides for the treatment of spinal muscular atrophy (SMA) and cancer. In SMA the bifunctional oligonucleotide is targeted to inhibit exon 7 skipping during splicing of *SMN2*. The current study has confirmed that this oligonucleotide is able to stimulate *SMN2* exon 7 splicing, as has been seen previously (Skordis et al., 2003; Owen et al., 2011). Analysis of the action of this oligonucleotide indicated that it specifically recruits spliceosomal factors to the 3' splice site of *SMN2* intron 6. The tail domain was seen to enhance binding of U2 snRNP to this region and stabilize protein complex formation, while the annealing domain was seen to enhance U2AF65-RNA binding.

A greater understanding of the mechanism of action of the *SMN2* bifunctional oligonucleotide also highlighted flaws in the design of the previously tested *RON* exon 11 bifunctional oligonucleotide (Ghigna et al., 2010). This oligonucleotide was designed to combat the production of *RON* Δ165 mRNA, in which *RON* exon 11 is skipped. Expression of this RON isoform has been linked with the onset of metastasis in some epithelial cell cancers. A systematic analysis of the splicing characteristics of this region in *RON* pre-mRNA, suggested that weak 3' splice site sequences limit *RON* exon 11 splicing. hnRNP H was also shown to bind *RON* introns 10 and 11 and may play a role in the regulation of *RON* exon 11 splicing. A new bifunctional oligonucleotide targeted combat *RON* Δ165 mRNA production, through the stimulation of *RON* exon 11 splicing, was designed with the weakness in *RON* exon 11 splicing and the mechanism of action of the *SMN2* bifunctional oligonucleotide in mind.

Ghigna, C., Toledo, M.D., Bonomi, S., Valacca, C., Gallo, S., Apicella, M., Eperon, I., et al., 2010. Pro-metastatic splicing of Ron proto-oncogene mRNA can be reversed therapeutic potential of bifunctional oligonucleotides and indole derivatives. RNA Biology 7, 495-503.

Owen, N., Zhou, H., Malygin, A. a, Sangha, J., Smith, L.D., Muntoni, F., Eperon, I.C., 2011. Design principles for bifunctional targeted oligonucleotide enhancers of splicing. Nucleic acids research 39, 7194-7208.

Skordis, L. a, Dunckley, M.G., Yue, B., Eperon, I.C., Muntoni, F., 2003. Bifunctional antisense oligonucleotides provide a trans-acting splicing enhancer that stimulates SMN2 gene expression in patient fibroblasts. Proceedings of the National Academy of Sciences of the United States of America 100, 4114-4119.

ACKNOWLEDGEMENTS

I owe my deepest gratitude to my supervisor, Professor Ian Eperon, whose patience, guidance and experience made the completion of this thesis possible. I am extremely grateful for the help of Professor Martin Dyer, Dr Salvador Macip and Dr Simon Wagner, who provided both academic expertise and encouragement throughout my PhD. I am indebted to Giuseppe Biamonti and Claudia Ghigna, who collaborated with us on the RON project and whose work provided inspiration for my research. The help and support of lab members and friends was indispensable throughout my PhD, and I would like to specifically thank Dr Lucy Eperon, Rachel Dumas, Sheree Purmessur, Jennifer Patel, Amy Tomsett, Emily Jones, Julia Howard, Michelle Spiller, Dr Mark Hodson, Paul Smith and Christian Lucus.

I thank my companion and best friend, Angus Webb, for his encouragement, optimism and ambition that have undoubtedly made me who I am today.

Finally, I would like to say thank you to my family and in particular my parents, Robert and Julie Smith. They have supported me throughout my PhD and without whom it would have not been possible. Therefore I dedicate this work to them.

ABBREVIATIONS

A - Adenosine

ATP - Adenosine-5'-triphosphate

ASO – Antisense Oligonucleotide

BPS – Branch-point Sequence

BSA - Bovine Serum Albumin

BF – Bright Field

C - Cytidine

°C - Degree Celsius

CPP – Cell-Penetrating Peptide

CNS – Central Nervous System

DTT - 1,4-dithiothreitol

DNA – Deoxyribonucleic Acid

DMEM – Dulbecco's modified Eagle's medium

dNTP's – Deoxynucleotide triphosphate's (DNA)

EColi - Escherichia coli

ABBREVIATIONS

EDTA - Ethylendiamine-N,N,N',N'-tetraacetic acid

EtOH – Ethanol

EMT – Epithelial-Mesenchymal Transition

Fmol – Femtomole

G - Guanosine

GTP - Guanosine-5'-triphosphate

GFP – Green Fluorescent Protein

H – Hour

Hepes - N-2-hydroxyethylpiperazine-N-2-ethane sulfonic acid

ICV – Intracerebroventricular

KDa- KiloDalton

µ - Micro

M – Molar

Min – Minute

Ml – Millilitre

mRNA – Messenger RNA

ABBREVIATIONS

MSP – Macrophage Stimulating Protein

nM - Nanomolar

NMD – Nonsense-mediated Decay

NP-40 - Nonidet P-40

Nt – Nucleotide

NTP's - Nucleoside triphosphate's (RNA)

PAGE - Polyacrylamide Gel Electrophoresis

PBS – Phosphate Buffered Saline

PCR – Polymerase Chain Reaction

Pre-mRNA – Premature Messenger RNA

Pmole - Picomole

PPT - Polypyrimidine Tract

RNase - Ribonuclease

RNA – Ribonucleic Acid

RNP - Ribonucleoprotein

RT – Reverse Transcription

RON - Receptor d'origine nantais

SDS - Sodium Dodecyl Sulphate

ABBREVIATIONS

snRNA - Small Nuclear Ribonucleic Acid

snRNP - Small Nuclear Ribonucleoprotein

SR - Serine-Arginine

ss - Splice Site

T - Thymidine

TBE - Tris-Borate-EDTA Buffer

TEMED - N,N,N',N'-tetramethylethylenediamine

U snRNP - Uridine-rich Small Nuclear Ribonucleoprotein Particle

UTP - Uridine-5'-triphosphate

UV - Ultraviolet

v/v - Volume per Volume

Oligonucleotides:

2'-*O*-Me – 2'-*O*- Methyl

2'-*O*-MePs – 2'-*O*- Methyl Phosphorothioate

LNA – Locked Nucleic Acid

PNA – Peptide Nucleic Acid

MOE – 2'-*O*-Methoxyethyl

PMO – Morpholino

CONTENTS

CONTENTS

CONTENTS

List of Figures

Chapter 1

Chapter 3

LIST OF FIGURES

LIST OF FIGURES

LIST OF FIGURES

List of Tables

1. INTRODUCTION

1.1. Alternative Splicing

1.1.1. The Big Picture

Splicing is an essential pre-mRNA editing step, whereby intronic regions are removed and exons spliced to form mature mRNA. This process is carried out by the spliceosome - a highly complex molecular machine containing U1, U2, U5 and U4/U6 small nuclear ribonucleoprotein particles (snRNPs), together with other protein factors (Wahl et al., 2009). Splicing occurs in the nucleus and has been shown to be closely integrated with other RNA processes including transcription, polyadenylation and nuclear export (Reed, 2003; Kornblihtt et al., 2004; Rigo and Martinson, 2009).

Some splicing events in mammals are invariant and constitutive. However, there are on average several splicing events per gene in which alternative sites are used (Pan et al., 2008), enabling expansion of the proteome and increasing complexity. Analysis of human mRNA using high-throughput sequencing has indicated that between 95-100 % of mRNAs are spliced alternatively, thus generating more than one mRNA isoform from one original gene sequence (Pan et al., 2008; Wang et al., 2008). In addition, splicing forms another level of quantitative control over gene expression. For instance, alternative splicing of pre-mRNA coding for the splicing regulatory protein SRSF1, leads to the production of a non-viable transcript that is degraded by nonsense-mediated decay (NMD). This regulatory splice is triggered via a

negative feedback loop based on the concentration of SRSF1, that alters splicing and so expression of this protein (Sun et al., 2010). Due to the fundamental role splicing has in tissue-specific expression of mRNA isoforms, this process has been linked to the development and progression of many diseases (Cooper et al., 2009).

1.1.2. Alternative Splicing: A Disease Overview

Approximately 60 % of disease-causing mutations affect splicing (López-Bigas et al., 2005) and incorrect splicing has been shown to contribute to the development and progression of many disease states including: cystic fibrosis (Faà et al., 2009), frontotemporal dementia with parkinsonism (Wang et al., 2011), retinitis pigmentosa (Tanackovic et al., 2011), spinal muscular atrophy (SMA) (Lefebvre et al., 1995) and hutchinson–gilford progeria syndrome (Pollex and Hegele, 2004). These disease causing alterations in splicing are commonly induced through the mutation of splice sites and surrounding regions; the creation of cryptic splice sites; and the loss or gain of splicing enhancers (ESE/ISE) or splicing silencers (ESS/ISS). The most damaging mutations are those affecting the 5' splice site GT and 3' splice site AG (Talerico and Berget, 1990; Fu et al., 2011). For instance, an investigation characterising point mutations at the splice sites of p53 in several cancers and individuals prone to cancer development, identified 29 different splice site mutations that led to the onset of cancer (Holmila et al., 2003). Splice site mutations are common in disease development, with additional examples including a 5' splice site mutation leading to exon skipping in the hSNF5 gene and brain tumour development (Taylor et al., 2000) and 3' splice site mutations triggering exon skipping in the MLH1 and APC gene, that have been linked with the

development of colorectal cancer and hapatoblastoma respectively (Kurahashi et al., 1995; Tanko et al., 2002).

Less severe mutations that alter the sequence surrounding the critical dinucleotides of the 5' and 3' splice site, have also been shown to induce exon skipping events leading to disease development. Such mutations are located both in the surrounding intronic and exonic regions. An example of an exonic mutation is the C6U transition in exon 7 of *SMN2*, which has been shown to be a major determining factor in the skipping of this exon. Skipping of *SMN2* exon 7 is the reason why *SMN2* cannot fully compensate for the loss of *SMN1* and so SMN expression in Spinal Muscular Atrophy (SMA) (Lorson et al., 1999). This exon 7 skipping event in *SMN2* is also an example of where disruption of a splicing enhancer and creation of a silencer alter splicing, allowing for disease development. The C6U transition in exon 7 of *SMN2* (Lorson et al., 1999) causes disruption of an ESE for SRSF1 (Cartegni et al., 2002) and in doing so forms an ESS for hnRNP A1 (Kashima and Manley, 2003; Cartegni et al., 2006). The alteration in protein binding to this region of exon 7 results in a double negative effect on the splicing of this exon, both reducing stimulation of splicing and enhancing repression (Kashima and Manley, 2003; Cartegni et al., 2006).

An example of an intronic splice altering mutation is the mutation upstream of the 3' splice site of exon 2 in the MLH1 gene. This mutation induces skipping of this exon and leads to the development of colorectal cancer (Clarke et al., 2000). Mutations that create cyptic splice sites also cause aberrant splicing and consequently the development of disease. An example of this is the formation of a cryptic splice site in the BRCA1 gene. This mutation, located at the intron 5/exon 6 boundary, adds 11 nucleotides onto the mRNA transcript, which

leads to the synthesis of a non-functional protein product and the development of breast cancer (Hoffman et al., 1998).

In addition, the alteration of expression or mutation of splicing components has also been identified as a catalyst of alternative splicing change, and commonly leads to the development and progression of disease. For example, mutations in U2AF have been identified in myelodysplasia samples, a disease affecting blood function which is often seen prior to the onset of acute myeloid leukaemia (Yoshida et al., 2011). Changes in the expression level of splicing regulatory factors, such as SRSF1, have also been linked with cancer development and progression (Ghigna et al., 2005); so much so, that SRSF1 has been branded as an oncogene (Karni et al., 2007). Splicing plays a dramatic role in events leading to cancer development, with alterations in the pattern of splicing from normal tissue catalysing this change (Warzecha et al., 2009; Valacca et al., 2010; Shapiro et al., 2011)

Both bioinformatic and experimental approaches have been used to identify alterations in the pattern of pre-mRNA splicing in disease. For example, one study identified the expression of cancer specific splice variants of 316 genes, 73 % of which were identified as having a role in tumorigenesis (Xu and Lee, 2003). The expression of splicing variants characteristic to specific diseases has also been identified in lung cancer (Langer et al., 2010; Misquitta-Ali et al., 2011), ovarian and breast cancer (Venables et al., 2009), neuroblastoma (Guo et al., 2011) and neurodegenerative disease for example (Tollervey et al., 2011). Such studies develop an understanding of the expression patterns of disease specific mRNA isoforms and allow for the development of successful diagnostic techniques and therapies.

1.1.3. Splicing Mechanism

The major spliceosome principally utilizes five uridine-rich small ribonucleoprotein particles (U snRNPs) (U1, U2, U4, U5 and U6 snRNP) in order to perform its task of excising introns from pre-mRNA (Smith et al., 2008; Wahl et al., 2009). Centrally to all five U snRNP's is a single snRNA strand and seven Sm or Sm-like (LSm) core proteins, that bind specifically to the snRNA (Hermann et al., 1995; Raker et al., 1996; Mayes et al., 1999). SnRNP's also associate with at least 150 additional auxiliary proteins and assemble on pre-mRNA to form the spliceosome (Hartmuth et al., 2002; Jurica et al., 2002; Zhou et al., 2002; Jurica and Moore, 2003; Behzadnia et al., 2007; Bessonov et al., 2008). The spliceosome arranges on pre-mRNA in response to the presence of specific RNA sequences, known as the 5' splice site (CAG/GTAAGTA), branch point (UACUAAC), polypyrimidine tract and the 3' splice site (NYAG/R) (Figure 1.1.) (N indicates any nucleotide; Y pyrimidine; R, purine; / intron-exon boundary) (Reed, 1989; Zhuang et al., 1989; Zhang, 1998; Wu et al., 1999; Du and Rosbash, 2002). As splicing progresses the structure and composition of the spliceosome is modified through the activity of non-snRNP auxiliary proteins, such as DExD/H-box type RNA-dependent ATPases, helicases and kinases (Wahl et al., 2009).

In vitro investigation in to the splicing mechanism has shown that splicing proceeds through six complexes H, E, A, B, B^{act} and C (Figure 1.1 B) (Brow, 2002; Jurica and Moore, 2003; Bessonov et al., 2010). The initial complex formed on pre-mRNA (complex H) contains U1 snRNP bound to the 5' splice site, together with many sequence specifically bound proteins, including heterogeneous nuclear ribonucleoproteins (hnRNP) (Sharma et al., 2005). The E' complex is the first spliceosomal complex to form on pre-mRNA. This complex

consists of U1 snRNP bound at the 5' splice site, via its 5' end and SF1 bound to the branch-point. This interaction induces a close physical association between the 5' splice site and the branch-point (Kent et al., 2005). Following this, recruitment of U2AF65 to the polypyrimidine tract and U2AF35 to the 3' splice site modifies this initial E' complex to E complex (Kramer and Utans, 1991; Gaur et al., 1995). Also, in addition to U1 snRNP, U2 snRNP has been found to be loosely associated with the RNA in E complex, with its 5' end being situated in proximity of both the 3' and 5' splice site (Dönmez et al., 2007). The loose U2 snRNP association in E complex becomes more stable following progression onto A complex (Das et al., 2000).

Progression to A complex (pre-spliceosome) sees the recruitment and association of U2 snRNP with the branch-point, inducing the branch-point adenosine to bulge outwards in preparation for the first transesterification reaction (Figure 1.1. A) (Query et al., 1994). B complex (pre-catalytic spliceosome) formation sees the recruitment of the U4/U6-U5 Tri-snRNP to the un-spliced pre-mRNA (Behrens and Luhrmann, 1991), leaving the spliceosome poised for the first transesterification reaction (Sander et al., 2006). During this stage U6 snRNP binds to the intronic 5' splice site nucleotides, replacing U1 snRNP binding at the 5' splice site and causing its displacement (Kandels-lewis and Seraphin, 1993; Lesser and Guthrie, 1993; Murray and Jarrell, 1999). U4 snRNP destabilization and release from U6 snRNP allows U6 snRNP to integrate into the active site of the spliceosome and form contacts with U2 snRNP bound at the branch-point (Staley and Guthrie, 1998). These shifting interactions transfer the premature B complex to a catalytically active B^{act} complex (activated spliceosome) (Bessonov et al., 2010) and allow the first catalytic step to occur (Figure 1.1. A).

The 2’ hydroxyl group of the branch-point adenosine nucleophillically attacks the 5’ splice site, producing a lariat intermediate containing a 2’-5’ phosphodiester branch and a free 5’ exon (Staley and Guthrie, 1998). Further rearrangement of the catalytic centre of the spliceosome, involving an alteration in U6 snRNP binding, allows for progression forwards to C complex (catalytic step 1 spliceosome) (Konarska et al., 2006). At this point U5 snRNP is also associated with exonic nucleotides in the 5’ and 3’ splice sites, which now play an important role in the second transesterification reaction (Figure 1.1. A). U5 snRNP holds the 5’ and 3’ exons in close proximity, enabling the second transesterification reaction to occur (Newman and Norman, 1992; Wyatt et al., 1992; Sontheimer and Steitzt, 1993; Newman, 1997). The 3’ hydroxyl group of the 5’ exon nucleophillically attacks the phosphodiester bond at the 3’ splice site, joining the two exons and resulting in complete excision of the lariat intron. The final post-spliceosomal complex is then formed, which breaks down to release the processed mRNA, lariat and U2, U5 and U6 snRNP (Staley and Guthrie, 1998).

In addition to the major spliceosome which is used for pre-mRNA splicing in the majority mammalian cells, the minor spliceosome is also used for splicing in a small fraction of mammalian cells. The minor spliceosome differs from the major through the use of alternative snRNPs and alternative splicing sequences. In the minor spliceosome U11, U12 and U4atac/U6atac snRNP are analogous to and used instead of U1, U2 and U4/U5 snRNPs respectively (Hall and Padgett, 1996).

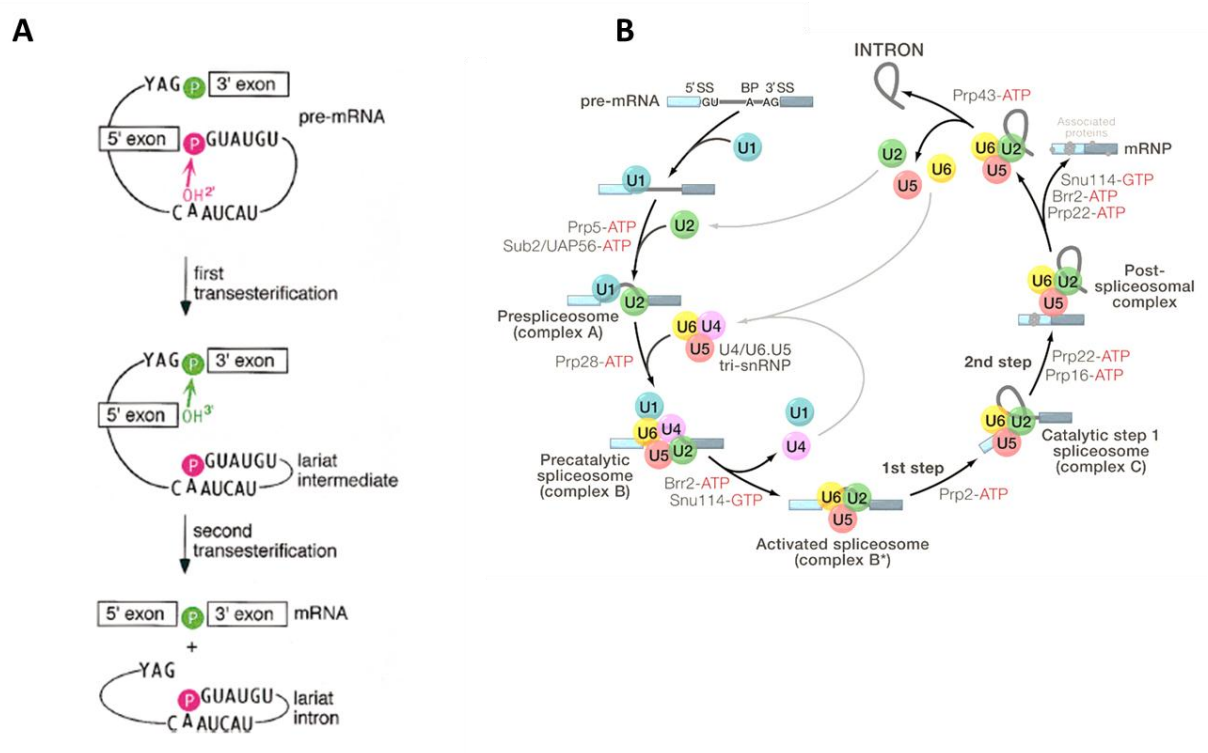

Figure 1.1. (A) The two catalytic steps of splicing are shown. Pink shows products of the first transesterification reaction, green shows products of the second transesterification reaction. Boxes = Exons, Introns = Lines, S. cerevisiae intron sequences have been used, Y = pyrimidine base (Wahl et al., 2009). **(B)** The spliceosomal complex is assembled on pre-mRNA Exons (blue), introns (grey), modified and disassembled. Here splicing is shown to initiate across an intron. snRNP's are shown as colored circles and enzymes required to execute the changes throughout splicing are shown as un-highlighted text. Many steps require ATP. Exons = boxes, Introns = lines (Staley and Guthrie, 1998).

1.2. Splicing Regulation

1.2.1. Splicing: An Interlinked Process

The synthesis of the correct mRNA isoform through alternative splicing is a highly complicated process, in which the obvious choice is not always the choice of the spliceosome. The regulation of alternative splicing within mammalian cells is achieved through a number of mechanisms, including differentiation (Boutz et al., 2007; Makeyev et al., 2007), external stimuli (Xie and Black, 2001) and signalling cascades (Shin and Manley, 2004).

Splicing has been shown to be interlinked with a variety of RNA processing mechanisms within the nucleus, in particular with transcription (Tennyson et al., 1995; Kornblihtt et al., 2004). Firstly, a gene's promoter has been shown to affect its splicing pattern, with the promoter structure altering the activity of splicing regulatory proteins (Cramer et al. 1997; Cramer et al. 1999). Chromatin structure and epigenetic modifications of DNA have also been shown to play a role in controlling transcription and so splicing of pre-mRNA. Histone modifications have been shown to regulate splicing, with several modifications being enriched within exons in comparison to flanking introns (Andersson et al., 2009; Kolasinska-Zwierz et al., 2009; Schwartz et al., 2009; Spies et al., 2009) and different modifications being present between alternatively and constitutively spliced exons (Andersson et al., 2009). It was also found that the higher the density of nucleosomes within a particular exon, the higher the probability of that exon splicing. For instance, nucleosomes have been found to be specifically enriched within exons that have long flanking introns or weak splice sites (Spies et al., 2009; Tilgner et al., 2009). Splicing has also been found to initially occur

co-transcriptionally (Tennyson et al., 1995; Kornblihtt et al., 2004), starting with U1 snRNP recruitment to the 5' splice site (Görnemann et al., 2005; Lacadie et al., 2005). Whether the spliceosome is then fully assembled and splicing is completed either before or after transcription is then determined by the length of the downstream exon (Tardiff et al., 2006). It has been also thought that pausing of RNA polymerase in exons due to nucleosome abundance induces exon definition and encourages splicing (Hodges et al., 2009; Nahkuri et al., 2009; Chodavarapu et al., 2010).

1.2.2. Enhancer and Silencer Elements

Whether the spliceosome successfully identifies an exon depends only partly on the binding of the core spliceosomal factors to the 5'and 3' splice sites and branch-point sequence. To enhance and control these basic spliceosomal interactions, *cis*-regulatory elements present in both exons and introns act as enhancers (ESE/ISE) and silencers (ESS/ISS) of splicing. Binding of regulatory proteins to these elements in pre-mRNA has been shown to influence the pattern of splicing, inducing skipping or inclusion of constitutive and alternatively spliced exons (Black, 2003; House and Lynch, 2008). In comparison with constitutively spliced exons, alternatively spliced exons often have diminished splice site signal strengths or suboptimal lengths (Stamm et al., 1994; Romano et al., 2001). Therefore the pattern of regulatory protein binding on any particular gene is highly context-dependent, allowing for either inclusion or exclusion of exons and so the production of a specific isoform in line with demand. There have been many studies looking at the distribution of regulatory elements on pre-mRNA (Wang and Burge, 2008). It has been found that ESE elements are enriched within

authentic exons containing weak splice sites (Fairbrother et al., 2002) and act to promote recognition of the flanking 3' and 5' splice sites (Shen and Green, 2004, 2006; Shen, Kan, and Green, 2004). On the other hand, ESS elements are commonly not present in authentic exons (Zhang and Chasin, 2004) and inhibition is commonly stimulated through factors binding to intronic regions (Ashiya and Grabowski, 1997; Singh et al., 2006). In addition, splicing stimulatory elements are not commonly present in introns and often have an inhibitory effect on splicing if located here (Kanopka et al., 1996; Ibrahim et al., 2005).

There are also a number of regulatory proteins that are expressed in a tissue-specific manner, including nPTB (Markovtsov et al., 2000; Polydorides et al., 2000), NOVA (Buckanovich et al., 1993) and FOX 1/2 (Jin et al., 2003; Underwood et al., 2005). These factors act to regulate splicing of transcripts specific to the tissue type in which they are expressed. One study identified the presence of a vertebrate-specific and nervous system-restricted SR protein, nSR100. They identified that this SR protein plays an integral role in approximately 11 % of brain-specific alternative splicing events. This study speculated that nSR100 acts as part of a regulatory complex with nPTB to overpower the inhibitory effect of PTB on exons and stimulate their inclusion (Calarco et al., 2009). This brain-specific splicing regulatory mechanism is an example of the fundamental way in which splicing is controlled through the combined activity of both enhancers and silencers. An additional interesting example of combinational regulation is *Fas* exon 6 splicing regulation by TIA-1 and PTB. Interestingly these proteins act with U1 snRNP to achieve either stimulation or inhibition of splicing. *Fas* exon 6 splicing is stimulated through the binding of TIA-1 and U1 snRNP to the 5' splice site of this exon, allowing for spliceosomal complex formation at the 3' splice site

and inclusion of exon 6. However, PTB binding to an ESS in exon 6 inhibits formation of the 3' splice site complex, in a mechanism that is also dependent on U1 snRNP binding at the 5' splice site of *Fas* exon 6 (Izquierdo et al., 2005). An additional well-studied relationship is that between SRSF1 and hnRNP A1 in U1 snRNP binding to 5' splice sites. It has been shown that SRSF1 and hnRNP A1 act in an antagonistic manner, enhanced and inhibiting U1 snRNP binding respectively (Eperon et al., 2000).

1.2.3. SR Proteins

SR proteins contain a C-terminal serine-arginine (RS) domain and either one or two N-terminal RNA recognition motifs (RRM) (Tacke et al., 1997; Mayeda et al., 1999). SR protein activity is regulated by phosphorylation of serine residues in the protein's RS domain, which is carried out by SR-specific protein kinase 1 (SRPK1) and cdc2-like kinases (CLK). Phosphorylation regulates SR protein entry into the nucleus, nuclear localization and so activity (Ghosh and Adams, 2011). For example, SRSF1 phosphorylation has been shown to allow for a contact to be formed with U1-70K (Cho, Hoang, et al., 2011), an interaction which has previously been shown to enhance 5' splice site selection (Eperon et al., 1993, 2000).

SR protein RS and RRM domains exhibit independent and interchangeable activity. RRM domains are able to bind RNA independently of RS domains and also maintain activity when coupled with RS domains originating from other SR proteins (Caceres and Krainer, 1993; Chandler et al., 1997; Mayeda et al., 1999; Sanford et al., 2008). Conversely, RS domains also maintain activity when coupled with RRM domains from other SR proteins (Chandler et al., 1997; Wang et al., 1998).

There are three distinct models relating to the activity of SR proteins (Figure 1.2.). Firstly it is thought that SR proteins could connect and stabilize spliceosomal formation across both exons and introns. It has been suggested that ESE associated SR proteins support exon definition, by connecting 5' and 3' splice sites across exons (Figure 1.2. AB) (Hoffman and Grabowski, 1992; Wu and Maniatis, 1993; Staknis and Reed, 1994a) and ISE associated SR proteins connect these splice sites across introns (Figure 1.2. C) (Kennedy et al., 1998).

In addition to stabilizing contacts between splicing factors, SR proteins have also been shown to stimulate the association of spliceosomal factors with RNA. They have been shown to stabilizes complex formation through the enhancement of U snRNA-pre-mRNA base pairing, through increasing the stability of this RNA-RNA duplex (Shen and Green, 2006). It has been shown that the RS domain of U2AF65 makes contacts with the branch-point early in spliceosomal complex formation (Shen, Kan, and Green, 2004), stimulating U2 snRNP binding (Shen and Green, 2006). Following this, the RS domain of SR proteins bound at ESEs have been shown to contact both the branch-point and 5' splice site directly, promoting assembly of the spliceosome and its conversion from a pre- to mature-spliceosome (Shen and Green, 2004). The SR protein SRSF1 has been implicated both in 5' splice site selection, through enhancement of U1 snRNP binding (Eperon et al., 1993; Kohtz et al., 1994; Zuo and Manley, 1994) and also 3' splice site activation, through the promotion of U2 snRNP and U2AF binding (Selvakumar and Helfman, 1999; Martins de Araújo et al., 2009). In addition to promoting formation of the commitment complex, SR proteins have also been shown to act later in the splicing reaction. They have been seen to stabilize the association of U6 and U5

snRNP with the 5' splice site during the first step and second step of splicing respectively (Shen and Green, 2007).

Conversely to studies that show SR proteins mediating their effect on splicing through their RS domain, it has also been argued that SR proteins can still maintain their effect on splicing when the RS domain is deleted (Zuo and Manley, 1993; Shaw et al., 2007). Recently a study showed that SRSF1 only contacts U1 snRNP through its RRM and that its RS domain has implications only in the regulation of this contact (Cho, Hoang, et al., 2011). In addition to the exon-mediated effect of SR proteins on splicing, SR proteins can also bind within introns and in these instances they sometimes exhibit inhibitory effects on splicing (Ibrahim et al., 2005).

SR proteins may also prevent the propagation and so the splicing inhibitory effect of negative regulators of splicing. This would occur through a physical block of binding of the negative regulators to RNA (Eperon et al., 2000; Zhu et al., 2001; Okunola and Krainer, 2009).

1.2.4. hnRNP Proteins

hnRNP proteins contain an RNA binding domain that varies in structure and also an auxiliary domain, responsible for protein-protein interactions. The auxiliary domain is often rich in a particular amino acid, such as glycine, proline or an acidic amino acid (Smith and Valcárcel, 2000; Dreyfuss et al., 2002). Like SR proteins, hnRNPs have a diverse role in RNA biogenesis in the cell and in addition to pre-mRNA splicing, have been associated with transcription, mRNA trafficking and translation regulation (Han et al., 2010).

Two well characterised hnRNPs are hnRNPA1 (Mayeda and Krainer, 1992; Eperon et al., 2000) and polypyrimidine tract binding protein (PTB, hnRNP I) (Shen, Kan, Ghigna, et al., 2004; Cherny et al., 2010). There are two models of how these proteins and others bring about splicing inhibition. Recent work by Sharma et al. (2011) has identified an interesting mechanism through which PTB inhibits splicing of the *c-src* N1 exon. They showed that PTB, in addition to interacting with CU rich pre-mRNA sequences, jointly interacts with the SL4 pyrimidine-rich internal loop of U1 snRNP. This both locks the 5' splice site into an unproductive complex and prevents binding of spliceosomal factors to the 3' splice site (Figure 1.2. D) (Sharma et al., 2011). Another example is the regulation of *Fas* exon 6 by PTB and RBM5. As with the *c-src* N1 exon, PTB was shown to inhibit recognition of the 3' splice site by U2 snRNP and U2AF, in a mechanism that was dependent on the binding of U1 snRNP to the downstream 5' splice site (Izquierdo et al., 2005). RBM5 is also thought to act at the 3' splice site, by preventing conversion of the pre-spliceosomal exon-defined complex to a mature spliceosomal intron-defined complex through the inhibition of Tri-snRNP recruitment (Bonnal et al., 2008). This inhibitory mechanism is echoed again in inhibition of *CD45* exon 4 splicing, where hnRNP L and E2 stall the spliceosome following U1 and U2 snRNP recruitment. Here hnRNPs hold the exon in A complex and prevent its progression through to B; the authors suggest that a ternary U1 and U2 snRNP-hnRNP complex is forming across the exon, making progression to B unfavourable (House and Lynch, 2006). In addition, a study has shown that hnRNP A1 may also act through inhibition of the U1 and U2 snRNP interaction, which has been shown to be required for splicing commitment (Dönmez et al., 2007; Yu et al., 2008).

In addition to splicing inhibition through stalling at a complex, hnRNPs have also been shown to simply prevent recognition of splice site signals through steric hindrance. PTB for example commonly inhibits recognition of 3' splice signals through the prevention of U2AF65 binding to the polypyrimidine tract (Figure 1.2. D) (Lin and Patton, 1995; Singh et al., 1995; Ashiya and Grabowski, 1997). Propagation of hnRNP binding along RNA is also a shown mechanism of splicing inhibition (Figure 1.2. E). Co-operative binding of hnRNP A1 to an ESS in exon 3 of the human immunodeficiency virus type 1 (HIV-1) has been shown to inhibit SR protein binding to this exon and prevent splicesomal complex formation at its 3' splice site (Okunola and Krainer, 2009). hnRNPs have also been shown to interact across RNA when bound at distant sites. This causes intervening RNA to loop out and exons within this region to be 'missed' by the spliceosome (Figure 1.2. F) (Nasim et al., 2002; Okunola and Krainer, 2009). In relation to the looping model, recently Cherny et al., (2010) used single molecule methods to look at the mechanism of inhibition of *α-tropomyosin* exon 3 splicing by PTB. This study indicated that five or six molecules of PTB were involved in the suppression of exon 3 inhibition. It suggested that PTB folds the intronic regions flanking exon 3 into a primary loop structure, allowing for binding of other proteins that then connect these two primary loops to form a secondary inhibitory loop occluding exon 3 (Cherny et al., 2010).

On top of the negative effect that hnRNPs have on exon inclusion, it has also been found that in some cases hnRNPs and other splicing regulatory factors have positional-dependent and gene-dependent effects on splicing. For example, hnRNP H inhibits splicing of the *fibroblast growth factor receptor 2* Exon IIIc when bound to an exonic element in this exon (Mauger et al., 2008), whereas it stimulates splicing of the *c-src* N1 exon when bound to

an intronic element in the downstream intron (Chou et al., 1999). Commonly, it appears that the binding of these factors to downstream introns stimulates exon inclusion (Chou et al., 1999), whereas binding to upstream introns inhibits exon exclusion (Carstens et al., 2000).

1.2.5. Additional Regulatory Factors

Splicing is not regulated only by SR and hnRNP proteins, it is also controlled by other classes of protein factors, that like hnRNP proteins, act in a positional-dependent manner. Examples of these include cell-specific factors such as NOVA (Ule et al., 2006), Star proteins such as Sam68 (Valacca et al., 2010), RBM factors such as FOX1 and 2 (Sun et al., 2012) and other RNA-binding proteins such as TIA-1 (Singh et al., 2011).

1.2.6. 5’ Splice Site Selection

U1 snRNP has been shown to bind pre-mRNA during assembly of the pre-catalytic spliceosome in E complex and is seen as the pathfinder of spliceosomal formation (Seraphin et al. 1988; Siliciano & Guthrie 1988). U1 snRNP binding to the 5’ splice site is mediated through the U1C auxiliary protein and its snRNA’s 5’ end (Heinrichs et al., 1990; Du and Rosbash, 2002; Pomeranz Krummel et al., 2009). Often the U1 snRNP-5’ splice site interaction is not highly complementary, with 5’ splice sites often not matching the 5’ splice site consensus sequence (Carmel, 2004; Sheth et al., 2006; Roca et al., 2008; Roca and Krainer, 2009). Hence, in most cases SR proteins are therefore required to stimulate U1 snRNP binding to these less than optimum sites. However, recently a study did showed that shifted base pairing of U1 snRNA to 5’ splice site sequences may allow more effective

binding of U1 snRNP to non-consensus 5' splice sites. This suggests that U1 snRNP may naturally be able to accommodate for alternative 5' splice site sequences (Roca and Krainer, 2009).

The mechanisms of U1 snRNP 5' splice site choice has been researched *in vitro* using RNase H protection assays. These experiments studied U1 snRNP binding using pre-mRNA substrates with two alternative consensus 5' splices sites in tandem, allowing for the patterns and rules of basic alternative 5' splice site selection to be understood. However, the rule of selection of one 5' splice site over another is still a contended matter. It is thought that when both upstream and downstream 5' splice sites are occupied by U1 snRNP use of the downstream 5' splice site always favoured, unless the sites are within 40 nucleotides of each other (Reed and Maniatis, 1986; Eperon et al., 1993; Hicks et al., 2010). However, this pattern of 5' splice site selection has been found to not apply in all cases (Mayeda & Ohshima 1988; Nelson & M R Green 1988). 5' splice site use has also been shown to be dependent on the rate of U1 snRNP binding at the critical point in splice site selection (O'Mullane and Eperon, 1998). So 5' splice site binding by U1 snRNP does not always correlate with 5' splice site use, and the rate of binding, position and strength of a 5' splice sites plays an important role in its function.

U6 snRNP is also an important determinant of 5' splice site choice (Kandels-lewis and Seraphin, 1993; Lesser and Guthrie, 1993) and it has been shown that U1 and U6 snRNP communicate to productively select and use a 5' splice site. U1 snRNP has been shown to enhance the U6 snRNP-5' splice site interaction and so stimulate the first transesterification

reaction (Cohen et al., 1994; Hwang and Cohen, 1996). U5 snRNP has also been shown to contribute to 5' splice site selection and use (Newman and Norman, 1991; Cortes et al., 1993).

SR and hnRNP proteins have been shown to play a significant role in 5' splice site selection (Fu et al., 1992; Zahler et al., 1993; Eperon et al., 2000). Hicks et al., (2010) showed that tethering an SR protein upstream of a 5' splice site enhanced the use of that splice site. When the SR protein was tethered in between two competing splice sites it slightly enhanced splicing to the dominant downstream site and further inhibited splicing to the upstream (Hicks et al., 2010). The effect of SRSF1 on 5' splice site binding by U1 snRNP has been thoroughly studied. The interaction between U1 snRNP and the 5' splice site is mediated between the RRM of U1-70K (an auxiliary protein of U1 snRNP) and the RRM of SRSF1, and is controlled by phosphorylation of the SRSF1 RS domain. In a hyper-phosphorylated form the RS domain allows the RRM of SRSF1 to interact with U1 snRNP, as when not phosphorylated the RS domain sequesters the RRM preventing it from binding (Cho, Hoang, et al., 2011). SRSF1 was shown to enhance U1 snRNP association simultaneously to two 5' splice sites in tandem, favouring the downstream (proximal) site for splicing in a manner dependent on the presence of the SR protein (Eperon et al., 1993, 2000; Cáceres et al., 1994). In addition to stimulation from SRSF1, Hicks et al., (2010) also observed an upstream 5' splice site acting as an enhancer of downstream 5' splice site use (Hicks et al., 2010). hnRNP A1 has also been shown to compete with SRSF1 to bind RNA (Eperon et al., 2000) and through this enhance use of the upstream (distal) site (Cáceres et al., 1994; Wang et al., 2006). hnRNP A1 disrupts the U1 snRNP-5' splice site association and therefore in this circumstance 5' splice site choice is determined by U1 snRNP affinity (Eperon et al., 2000).

hnRNP A1 and H have also been proposed to collaborate to promote 5' splice site choice. In this example, hnRNP A1 and H have been shown interact from their binding sites on RNA, bringing distant 5' and 3' splice sites into closer proximity and causing skipping of the intervening RNA. In this way hnRNP factors can be seen to both stimulate selection of splice sites and through doing so inhibit the use of others (Fisette et al., 2010).

The secondary structure of the 5' splice site has also been shown to regulate alternative 5' splice site choice. For instance, secondary structure of the 5' splice site in *SMN2* exon 7 has been shown to be a limiting factor of exon 7 splicing (Singh et al., 2007).

1.2.7. 3' Splice Site Selection

The 3' splice site of mammalian genes consists of three units: the branch-point sequence, located 18-40 nucleotides upstream of the intron/exon boundary, which contains the adenosine required for the first transesterification reaction; a polypyrimidine tract, directly downstream of the branch-point sequence; and the 3' splice site dinucleotide AG at the intron/exon boundary (Reed, 1989).

Recognition of the 3' splice site is initiated by the auxiliary protein U2AF. U2AF is composed of a large subunit U2AF65, which binds the polypyrimidine tract and a small subunit U2AF35, which binds the 3' splice site AG (Zamore and Green, 1989; Wu et al., 1999). U2AF65 contains an N-terminal RS domain and three C-terminal RRMs, two of which are thought to contact the RNA at the polypyrimidine tract (Zamore et al., 1992; Banerjee, 2003). U2AF65 has been found to be highly influential and limiting in assembly of the spliceosome, with the requirement for SR proteins for splicing of ESE dependent exons being

substituted through enhancement of U2AF65 binding to the polypyrimidine tract (Tian and Maniatis, 1994; Lorson and Androphy, 2000; Graveley et al., 2001). Conversely however some experiments have shown that pre-spliceosomal assembly is not limited by U2AF65 binding to the polypyrimidine tract (Kan and Green, 1999; Li and Blencowe, 1999). U2AF65 has been shown to bend the RNA, bringing the branch-point and the 3' splice within proximity of each other (Kent et al., 2003) and allowing for formation of a complex at the 3' splice site. In some instances, but not others, a complex of U2AF, SF1 and SF3 has been shown to be essential for the interaction of U2 snRNP with the branch-point during A complex assembly (Ruskin et al., 1988; Kramer and Utans, 1991; Huang et al., 2002; Tanackovic and Kra, 2005) and in particular U2 snRNP binding to the branch-point is encouraged by the RS domain of U2AF65 (Valcárcel et al., 1996). It is thought that the binding of U2AF65 to a polypyrimidine tract shifts the conformation of its RRM domains from a closed to an open state, allowing RNA binding and also the recruitment of U2 snRNP. This polypyrimidine tract-induced conformational change allows for regulation of the recognition and use of a polypyrimidine tract, with stronger polypyrimidine tracts enhancing the occurrence of the open conformation and so stimulating 3' splice site selection (Mackereth et al., 2011). The RRM3 of U2AF65 contacts SF1 (Selenko et al., 2003), which enables SF1-branchpoint binding prior to U2 snRNP association (Berglund et al., 1998; Liu et al., 2001). The U2 snRNP protein SF3b155 then displaces SF1 binding to U2AF65 and U2 snRNP is therefore recruited (Gozani et al., 1998). U2AF65 has been shown to be destabilized before the formation of A complex (Staknis and Reed, 1994b) and so the link between U2AF65 and U2 snRNP recruitment is still being elucidated. In some cases U2 snRNP recruitment has been seen to not be directly connected

with U2AF65 activity (Martins de Araújo et al., 2009). It has also been predicted that a protein homologous to U2AF65, PUF60, may replace U2AF65 binding to SF1 on the RNA before U2 snRNP binding. The PUF60-SF1 complex may then recruit SF3b155 and so U2 snRNP (Hastings et al., 2007).

U2AF35 binds to the 3' splice site AG (Wu et al., 1999) and competing 3' splice site AGs have been shown to be irreversibly selected at the second step of splicing (Crotti and Horowitz, 2009). U2AF35 has been found to have an important role in the assembly of the spliceosome across an exon (exon-definition) and has also been seen to interact with SR proteins bound within the exon (Wu and Maniatis, 1993; Zuo and Maniatis, 1996). It has been shown that U2AF35 encourages pre-spliceosomal assembly on weak splice sites and enhances the binding of U2AF65 to the polypyrimidine tract and so the rate of pre-spliceosomal arrangement (Wu et al., 1999; Graveley et al., 2001; Guth et al., 2001; Romfo et al., 2001). In some cases when an intron contains a weak polypyrimidine tract, the AG dinucleotide is required for initial 3' splice site recognition and pre-spliceosomal arrangement (AG-dependent). Conversely, when the polypyrimidine tract is strong, the AG dinucleotide is seen to not be required for assembly and step 1 (Reed, 1989).

1.2.8. Exon and Intron Definition

In vitro it has been shown that the length of both introns and exons can determine the pathway through which initial spliceosomal formation occurs, either across an exon or intron (exon and intron definition respectively) (Figure 1.2. G). Exon definition is favoured in substrates containing short exons and long introns (Fox-walsh et al., 2005) and conversely

intron definition is favoured in a system with short introns and long exons (Sterner et al., 1996).

Pre-spliceosomal assembly on metazoan RNA splicing occurs more commonly via exon definition (Robberson et al., 1990; Berget, 1995), as most exons are short and introns long in these pre-mRNAs. In exon definition, splicing components bound at exon-flanking 5' and 3' splice site interact, bridging across the exon. Exon definition has been studied and confirmed using a series of experiments whereby splice site strength was seen to affect the splicing efficiency of upstream or downstream introns *in vitro* (Talerico and Berget, 1990; Grabowski et al., 1991; Kuo et al., 1991) and *in vivo* (Carothers et al., 1993; Tsukahara et al., 1994). The exact mechanism by which the 5' and 3' splice sites communicate across an exon is thought to occur through an interaction between U1 snRNP, U2AF65 (Hoffman and Grabowski, 1992) and U2AF35 in E complex (Fu, 1993; Wu and Maniatis, 1993; Staknis and Reed, 1994a). Following initial spliceosome assembly across an exon, the exon defined spliceosome then transfers to form future complexes upon the intron only and allowing for its eventual excision (Sharma et al., 2008).

1.2.9. Post-assembly Regulation

On top of splicing regulation during the early stages of spliceosome formation, the splicing process has also been found to be regulated in the latter stages, following initial splice site recognition. Importantly the pairing of splice sites and the commitment to splice are two separate events, indicating that splice site pairing does not necessarily mean splicing will occur (Lim and Hertel, 2004). For instance, the protein RBM5 stimulates skipping of *Fas* exon

6 following recognition of both the 5' and 3' splice sites of exon 6 by U1 and U2 snRNP. This protein allows for the formation of an inhibitory complex across the exon and also facilitates skipping through the promotion of distal splice site pairing (Bonnal et al., 2008). A similar mechanism of action has also been found for the regulation of *CD45* exon 4 splicing. In this example hnRNPs bound to an ESS in exon 4 require both U1 and U2 snRNP to be bound to the splice sites flanking the exon for inhibition of splicing to occur (House and Lynch, 2006). PTB is a well characterised splicing regulatory protein that has been found to act both in the early (Izquierdo et al., 2005; Sharma et al., 2005) and later stages of splicing assembly. For instance, PTB has been found to inhibit conversion of an exon defined spliceosome to an intron defined spliceosome and hence through this mechanism inhibit splicing of the *c-src* N1 exon (Sharma et al., 2008).

In addition to the inhibition of splicing at later stages, splicing can also be stimulated during these stages. For instance, during the second step of exon 3 splicing in Drosophila sex-lethal pre-mRNA, the protein SPF45 has been found to stimulate the second catalytic step (Lallena et al., 2002).

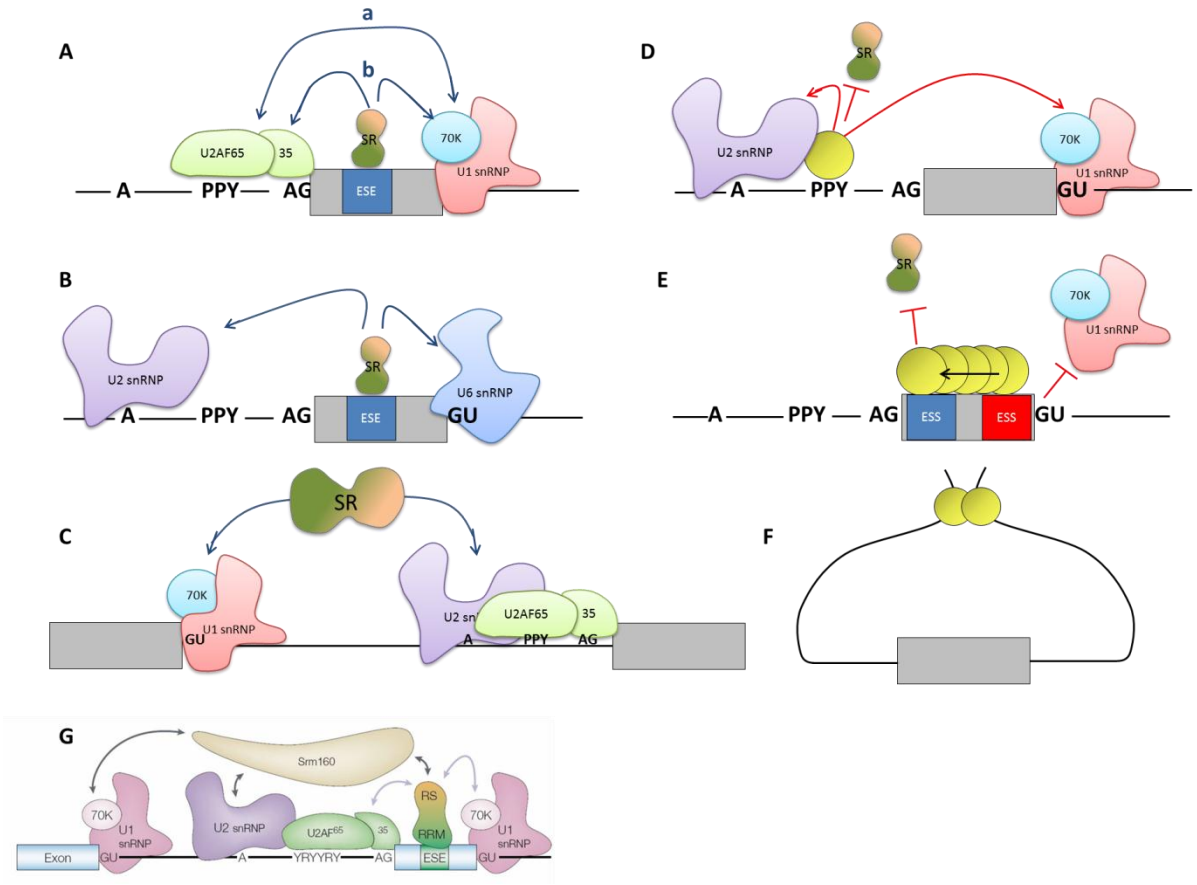

Figure 1.2. Splicing regulation by SR and hnRNP proteins. **(A)** a) SR protein binding to an ESE can stimulate the binding of splicing factors at the 3' and 5' ss. b) SR protein binding to an ESE can provide a connection between the 3' and 5' ss across an exon. **(B)** SR protein can stabilize the binding of U2 and U6 snRNP to RNA later in the splicing reaction. **(C)** SR proteins act as a bridge across an intron, connecting the 5' and 3' ss. **(D)** hnRNPs can bind to RNA and sterically inhibit the binding of spliceosomal factors. In some cases, once bound they are able to form non-progressive complexes with spliceosomal factors and stall splicing. **(E)** hnRNP's are able to bind to RNA and then propagate along RNA covering splicing sequences and inhibiting the binding of splicing factors. **(F)** hnRNPs can bind RNA and interact with other hnRNPs bound at distant sites on the RNA. This loops out the intervening RNA and inhibits the recognition of those elements located within the loop. **(G)** Exon definition shows assembly of the pre-spliceosomal complex across the exon, with interactions with U2AF35, factors bound at the ESE and U170K. Intron definition shows assembly of the pre-spliceosomal complex across the intron, with interactions stabilized by srn160. Blue boxes represent exons, lines represent introns and coloured circles represent U snRNPs and auxiliary proteins. Cartegni et al., (2002).

1.3. Alternative Splicing and Disease

Alternative splicing is a major contributor to the development and progression of disease. The development of therapies that alter alternative splicing patterns would target the foundations of these diseases and therefore have the potential to be very effective.

1.3.1. Small Molecule Inhibitors

Small molecule inhibitors have been able to regulate splicing through controlling the activity of SR proteins. For example, the small molecule pladienolide, FR901464 and methylated derivative spliceostatin A (SSA), all act by interacting with the U2 snRNP-associated factor SF3b and inhibiting pre-mRNA splicing (Kaida et al., 2007; Kotake et al., 2007). Small molecule inhibitors have been also found to be able to regulate phosphorylation of SR proteins. For instance, pseudocantharidins inhibit the activity of a protein phosphatase, that when active dephosphorylates and inactivates tra2-β1 (Zhang et al., 2011), an SR protein fundamental in exon 7 inclusion in *SMN1/2* (Hofmann et al., 2000). Indole derived compounds have also been used to induce changes in splicing through altering the activity of an SR protein, such as SRSF1. These compounds have been shown to compromise formation of complete HIV pre-mRNA and so viral complex formation (Bakkour et al., 2007), disrupt murine leukemia virus (MLV) replication, through alteration of the splicing-dependent synthesis of the retroviral envelope glycoprotein (Keriel et al., 2009) and reverse a pro-metastatic splicing event in the RON proto-oncogene, that has been found to occur in some forms of epithelial cell cancer (Ghigna et al., 2010) .

1.3.2. Oligonucleotides

Oligonucleotides are a very versatile therapeutic tool, as fundamentally they can be designed to complement any target. In comparison with small molecule inhibitors that act commonly through altering the activity of SR proteins in some way chemically or physically, oligonucleotides act through either altering the activity of spliceosomal factors or RNA secondary structure.

1.3.2.1. Oligonucleotide Chemistry

Traditional antisense oligonucleotides (ASOs) are synthesized from DNA and if left unmodified are able to induce RNase H-mediated digestion of their target RNA. ASOs that have been developed around their inherent RNase H activity are currently in clinical trials, an example being an oligonucleotide targeted to knockdown TGF-β2 in giloma (Bogdahn et al., 2011). However, generally this class of oligonucleotide is not significantly effective. Oligonucleotides designed to alter pre-mRNA splicing do not require RNase H activity, as the mRNA transcript must be preserved for translation. Therefore these oligonucleotides are chemical modified, firstly to inhibit RNase H activity and secondly to enhance other properties, such as cellular stability and binding affinity (Figure 1.3.).

Common oligonucleotide modifications include those to the 2’ position on the ribose moiety, which inhibits RNase H activity (Manoharan, 1999); these include 2’-*O*-methyl (2’-*O*-Me) (Dunckley et al., 1998; Wilton et al., 1999), 2’-*O*-methoxyethyl (MOE) (Hua et al., 2010), 2’-*O*-aminopropyl (Griffey et al., 1996) and locked or bridged bases, where the 2’-*O* and 4’ positions are connected through a methylene group (Teplova et al., 1999). The 2’-*O*-Me

modification was the first base modification to arise and generates a less soluble, but more stable oligonucleotide. In addition to modifications of the ribose ring, oligonucleotides also often contain a modified backbone. An example of this is the phosphorothioate (Ps) modification (Lu et al., 2003, 2005; Skordis et al., 2003; Hua et al., 2010), where the backbone phosphodiester is modified through addition of a sulphur atom. This modification enhances both cellular stability and solubility, but allows the oligonucleotide to retain its RNase H activity (Dias and Stein, 2002).

Often combinations of ribose and backbone modification are used in oligonucleotide synthesis. Examples of this include 2'-*O*-MePs/MOEPs and morpholino phosphorodiamidate (PMO) oligonucleotides all of which have proven to be very successful at altering pre-mRNA splicing (Skordis et al., 2003; Alter et al., 2006; Hua et al., 2010). In PMO oligonucleotides a phosphorodiamidate linkage replaces the phosphodiester bond and a morpholino moiety replaces the ribose. These modifications enhance the affinity of the oligonucleotide for its target sequence and provide greater cellular stability.

Oligonucleotides have also been synthesized to have varying modifications throughout, for instance the bifunctional oligonucleotide used to alter exon 7 splicing in *SMN2*. This oligonucleotide contains both 2'-*O*-Me and 2'-*O*-MePs modifications in its annealing region, and unmodified RNA which is protected by Ps groups at its 5' end in its tail (Skordis et al., 2003).

Peptide nucleic acid (PNA) oligonucleotides are composed of nucleobases anchored to the polyamide backbone of N-(2-aminoethyl)glycine units via methylene carbonyl linkers (Egholm et al., 1993) and Locked nucleic acid (LNA) oligonucleotides are composed of joined

2'-*O*,4'-C-methylene linked bicyclic ribofuranosyl nucleosides (Singh et al., 1998; Petersen et al., 2000). These have also been used in pre-mRNA splicing alteration and both bind efficiently to both RNA and DNA (Jensen et al., 1997; Singh et al., 1998).

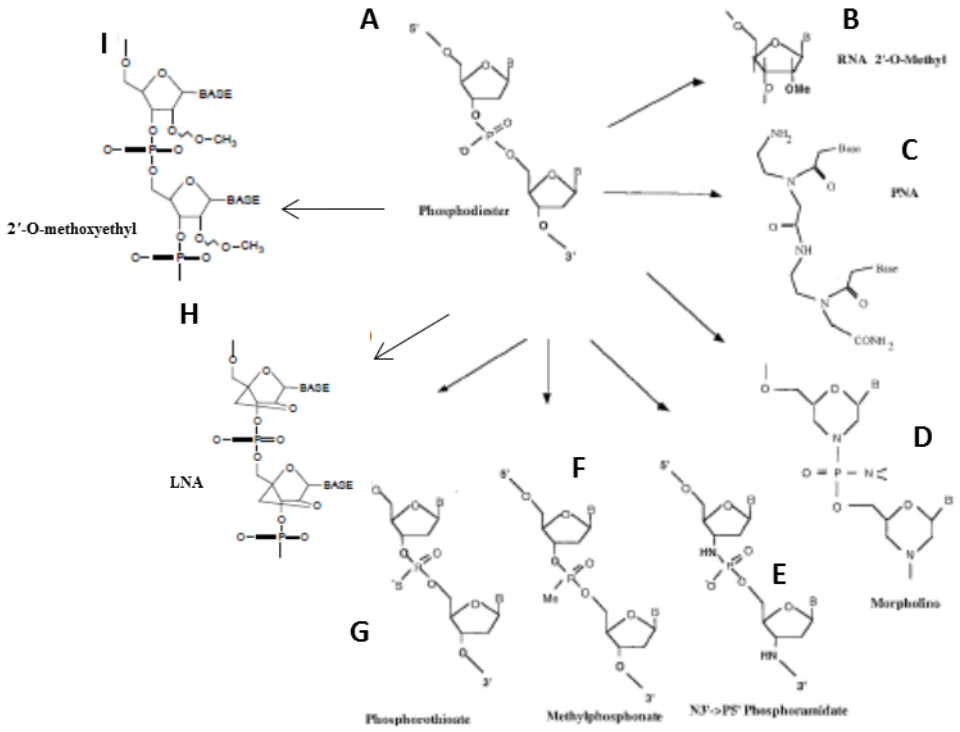

Figure 1.3. Chemical structures of RNA oligonucleotides used to alter pre-mRNA splicing. **(A)** Unmodified phosphodiester oligonucleotide. **(B)** 2'-*O*-Methyl (2'-*O*-Me - methyl group at position 2' of the ribose ring) **(C)** Peptide Nucleic Acid (PNA - non-charged polyamide backbone). **(D)** Morpholino (PMO - morpholine groups linked through phosphorodiamidate linkages). **(E)** N3′-P5′ phosphoramidate (contains N3′-P5′ phosphoramidate linkages in place of a bridging oxygen atom). **(F)** Methylphosphonate (methyl groups inplace of a non-bridging oxygen on each backbone phosphorous). **(G)** Phosphorothioate (Ps - Sulphur in place of a non-bridging oxygen atom on each backbone phosphorous). **(H)** Locked Nulcleic Acid (LNA - joined 2'-*O*,4'-C-methylene linked ribose ring). **(I)** 2′-O-methoxyethyl (MOE - 2' Methoxyethyl addition on to the ribose ring). Figure adapted from (Estibeiro and Godfray, 2001; Dias and Stein, 2002).

1.3.2.2. Oligonucleotide Targets

Oligonucleotides have been developed that are able to stimulate either exon inclusion or exclusion depending on their target RNA. ASOs have been used to stimulate skipping of exons in dystrophin in Duchenne Muscular Dystrophy (DMD), Lamin A in Hutchinson-Gilford progeria syndrome (Scaffidi and Misteli, 2005), Bcl-x in lung metastases (Taylor et al., 1999; Bauman et al., 2010), Mcl-1 in Basal cell carcinoma (Shieh et al., 2009) and β-globin in β-thalassemia (Sierakowska et al., 1996) They have also been developed to stimulate exon inclusion in RNAs including *SMN2* in SMA (Skordis et al., 2003), and *RON* Δ165 in gastric carcinoma (Ghigna et al., 2010).

1.3.2.2.1. DMD ASOs Stimulating Exon Skipping

ASOs are designed to block binding of splicing factors to either splice signals or regulatory sites and they often exert their effect by annealing directly over the binding site (Figure 1.4. B) (Dominski and Kole, 1993; Sierakowska et al., 1996). Blocking splicing signals in this way has proven to be an effective way of developing oligonucleotides for treatment of disease, including DMD.

DMD is an X-linked disease affecting 1 in 3500-6000 male births. This condition sees gradual muscle deterioration, with boys becoming wheelchair-dependent at 12 years of age and mortality occurring at approximately 19 years, from respiratory and cardiac failure. DMD is caused by a deficiency in the protein dystrophin (Hoffman et al., 1987), the longest gene in the human genome comprising 79 exons. Dystrophin forms an integral part of the trans-membrane complex connecting the muscle cytoskeleton with the extracellular protein matrix

and is vital for membrane stability during muscle contraction. DMD commonly arises due to deletion mutations in dystrophin (exons 3-7 and 45-55), which generates premature termination codons (PTCs) and so inhibits its expression. With the loss of dystrophin the muscle cell membrane is unable to maintain the correct ionic balance required for muscle contraction control and therefore over time the muscle degrades. In some cases mutations do not disrupt the reading-frame and so a mutated, but functional dystrophin protein is expressed and the milder Becker Muscular Dystrophy (BMD) is seen (Yeung et al., 2005; Nakamura and Takeda, 2009).

Glucocorticoids slow muscle wastage, and are currently the only available medication for DMD (Bushby et al., 2010; Moulton and Moulton, 2010). Hence, there is an unmet need for more effective treatments. The concept behind treatment of DMD with oligonucleotides is that if skipping of exons containing PTCs could be achieved, a shorter but functional form of dystrophin would be produced (Koenig et al., 1989). Thus this would artificially shift DMD to the milder BMD, which has reduced but sufficient dystrophin function. The benefit of using oligonucleotides for treatment of DMD is that a series of oligonucleotides can applied in each individual case to suit their specific mutational profile (Yokota et al., 2009).

The first DMD oligonucleotide studies used the *mdx* mouse, which contains a nonsense mutation in exon 23 and inhibits dystrophin expression. 2'-*O*-Me oligonucleotides targeted to the 3' and 5' splice site of exon 23 were seen to cause skipping of exon 23 in transfected *mdx* myotubes (Dunckley et al., 1998; Wilton et al., 1999). Following this a 2'-*O*-MePs oligonucleotide, directed toward the 5' splice site of exon 23, was tested for its effect on dystrophin expression in *mdx* mice. This oligonucleotide enhanced body-wide dystrophin

levels, but not to a high enough level to be translated to the clinic (Lu et al., 2003, 2005). To address this, this oligonucleotide was resynthesized containing the PMO modification and following intramuscular injection in to *mdx* mice, induction of body-wide skeletal dystrophin expression was again seen. However, dystrophin expression in cardiac muscle was unchanged (Alter et al., 2006). Cardiac muscle expression of dystrophin is key to the treatment of DMD. Therefore an increase in skeletal muscle dystrophin levels, with no simultaneous increase in cardiac muscle, does not treat the condition sufficiently and may actually compound the disease (McNally, 2007; Townsend et al., 2008). Many studies have struggled to achieve dystrophin expression in cardiac muscle, even when ASOs are conjugated to a delivery enhancing cell-penetrating peptide (CPP) carrier molecule (Fletcher et al., 2007). Therefore a number of studies were undertaken to address this and finally the PMO oligonucleotide effect reached cardiac muscle in the *mdx* mouse, through its conjugation to modified cell penetrating peptides (CPPs) ($(RXR)_4XB$ R = L-arginine, X = 6-aminohexanoic acid, B = β-alanine) (Yin et al., 2008).

DMD oligonucleotides that stimulate skipping of human exon 51 have been taken into clinical trials. Abdominal subcutaneous injections of an unconjugated 2'-*O*-MePs oligonucleotide (PRO051) induced dystrophin expression in muscle to approximately 15.6 % of the control tissue (Goemans et al., 2011). In addition, the intra-muscular injection of an unconjugated phosphorodiamidate PMO (AVI-4658) oligonucleotide has been seen to stimulate dystrophin exon 51 skipping in humans. This oligonucleotide increased dystrophin expression in muscle to approximately 27 % of the control tissue (Kinali et al., 2009) - the suggested percentage of dystrophin required for adequate muscular function (Neri et al.,

2007). More recently the exon 51 splicing and toxicity characteristics of the AVI-4658 oligonucleotide administered via IV were assessed in a phase two clinical trial. This oligonucleotide was seen to be non-toxic and induce expression of dystrophin-fibers in patients by up to 55 % (Cirak et al., 2011).

Oligonucleotide chemistry has also been found to have an effect on the activity of splice altering oligonucleotides. For instance, oligonucleotides modified with varying chemistries have also been used to enhance *SMN2* exon 7 inclusion and have shown varied activities, with some studies favoring the use of 2'-*O*-MePs (Skordis et al., 2003) 2'-*O*-Me (Williams et al., 2009) 2'-*O*-MOE (Hua et al., 2010) or PNA (Cartegni and Krainer, 2003) modifications.

1.3.2.2.2. Bifunctional Oligonucleotides to Stimulate Exon Inclusion

Oligonucleotides have also been developed to not only sterically block splicing signals, but also to recruit or replace regulatory proteins to stimulate splicing (Figure 1.4. C). Bifunctional oligonucleotides were initially designed to alter the splicing of exon 7 in *SMN2* (Cartegni and Krainer, 2003; Skordis et al., 2003), exon 18 in BRCA1 (Cartegni and Krainer, 2003) and the ratio of Bcl-xL and Bcl-xS (Villemaire et al., 2003). These oligonucleotides contain both an RNA binding domain and a functional domain. The bifunctional oligonucleotides have been designed to either recruit splicing regulatory proteins (TOES) (Skordis et al., 2003; Villemaire et al., 2003) or to contain RS domains to provide artificial enhancer capabilities (ESSENCE) (Cartegni and Krainer, 2003). The idea that oligonucleotides could be used to stimulate splicing and so inclusion of an exon was, up until

this point, seen as quite a challenge. It was a great success when it was achieved in 2003 and demonstrated that oligonucleotides could be used in a more sophisticated way than simply in the blocking of splicing signals to induce exon skipping.

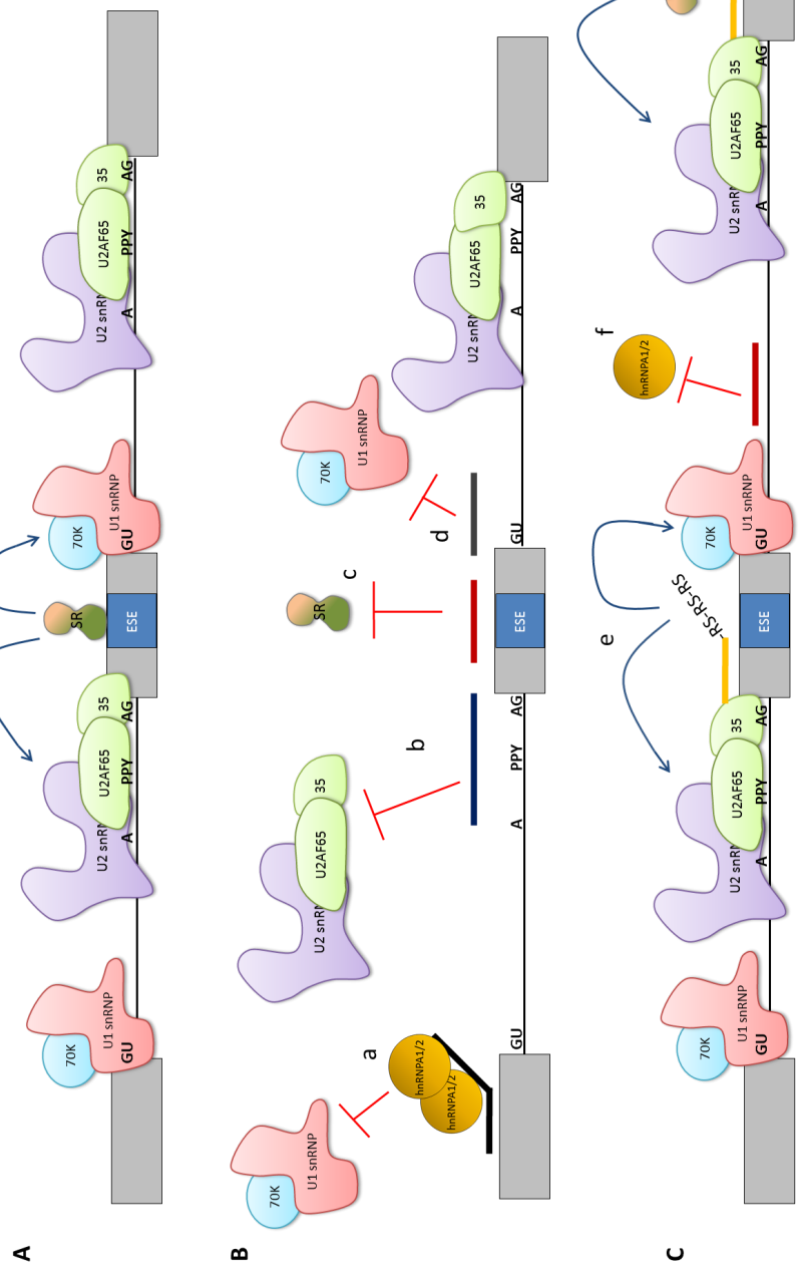

Figure 1.4. Pre-mRNA splice altering therapeutic oligonucleotides. **(A)** Normal splicesomal assembly. **(B)** Oligonucleotides inhibiting splicing. a) Tailed oligonucleotide inhibiting recruitment of U1 snRNP to the 5' splice site through the binding of hnRNP A1/2 to its tail domain. b) ASO blocking spliceosomal assembly on the 3' ss. c) ASO blocking the binding of SR proteins to ESE and so inhibiting their positive effect in spliceosomal assembly. d) ASO blocking spliceosomal assembly at the 5' ss. **(C)** Oligonucleotides stimulating splicing. e) ESSENCE oligonucleotide containing an RS tail that stimulates splicing through artificially acting as an SR protein. f) ASO that blocks the binding of negative regulators of splicing to splicing silencer elements and allowing for splicing through the removal of their inhibitory effect. g) TOES/bifunctional oligonucleotide that recruits SR proteins via its tail domain and this stimulates splicing.

1.3.2.3. Delivery

To exert their effect, oligonucleotides must be delivered efficiently to their target cells *in vivo*. Oligonucleotides have been shown to be transported across the cell membrane via endocytosis, mainly either bound or unbound to carrier molecules. Once within the cell, they must then escape from the endosome in order to reach their site of action (Richard et al., 2003; Juliano et al., 2009). The release of internalized oligonucleotides from endosomes appears to be the major factor limiting oligonucleotide activity.

DMD oligonucleotides were able to stimulate dystrophin expression only in skeletal muscle (Alter et al., 2006) and as the success of DMD treatment with oligonucleotides is measured against the level of dystrophin recovery in cardiac muscle (McNally, 2007; Townsend et al., 2008), this had to be addressed for these oligonucleotides to be a viable therapeutic. CPPs were first used to enhance the delivery of a PMO oligonucleotide into the *mdx* mouse (Fletcher et al., 2007). The selected CPP was $(RXR)_4$ (X = 6-aminohexanoic acid, R = Arginine) and the resulting PMO-$(RXR)_4$ conjugate has been commonly used since to study the effect of the exon 23 skipping in *mdx* mice. Interestingly, further studies have shown that oligonucleotide-dependent expression of dystrophin in cardiac muscle appears to be related to the method of administration of this oligonucleotide, with IV injection giving better results that either IP or subcutaneous injection (Yin et al., 2008; Goyenvalle et al., 2010).

Modification of the $(RXR)_4$ CPP carrier through the replacement of two 6-aminohexanoic acid groups with β-alanine ($(RXRRBR)_2$), also generated a less toxic (Wu et al., 2007) and more effective oligonucleotide conjugate. Oligonucleotides conjugated to the

$(RXRRBR)_2$ carrier and delivered by IV injection almost completely recovered dystrophin levels in both cardiac and skeletal muscle of *mdx* mice (Wu et al., 2008).

Additional CPPs that have been developed for conjugation onto DMD oligonucleotides include R6-Penetratin (R6Pen), that together with the selected PNA oligonucleotide forms the PIP-PNA conjugate (Abes et al., 2007). This modification has been shown to increase the skipping of exon 23 ~3-fold in *mdx* mouse models, compared to that of either the naked oligonucleotide or this oligonucleotide conjugated to $(RXR)_4$ (Ivanova et al., 2008). However, recent clinical trials studying the characteristics of the exon 51 skipping unconjugated PMO ASO (AVI-4658) in DMD patients has indicated that IV injection of this ASO was able to stimulate exon 51 skipping and enhance dystrophin expression (Cirak et al., 2011). The success of this naked ASO indicates that the use of carrier peptides to enhance ASO delivery is not always required for their successful action.

Further studies into the use of CPPs for delivery into other cell types have been undertaken. For example, a positive ASO effect was seen with a PMO-$(RXR)_4$ oligonucleotide targeted towards genes involved in T cell function in primary leukocytes (Marshall et al., 2007). Modification of oligonucleotides with cell-specific markers also allows for their delivery directly to their target cells. An example of this was conjugation of the DMD oligonucleotide, PMO-23, to a muscle-specific peptide (MSP) that enhanced the activity of this oligonucleotide in *mdx* mice. This effect was then increased further through the addition of the $(RXRRBR)_2$ CPP, generating a $(RXRRBR)_2$-MSP-PMO oligonucleotide (Yin et al., 2009).

Oligonucleotides have also been delivered to cells via nanoparticle carriers that range from 50-200 nm. Nanoparticles are often used to aid uptake of oligonucleotides that have also been conjugated to CPPs. One example of this is the use of cationic lipids and CPPs to aid the delivery of a PMO oligonucleotide into to HeLa cells, to alter β-globin pre-mRNA splicing. The cationic lipids enabled escape of the oligonucleotide from endolytic vesicle and the CPPs promoted initial uptake (Trabulo et al., 2010). Nanoparticles have also been formed using a polycation such as polymethylmethacrylate (PMMA) conjugated with 2′-*O*-MePS oligonucleotides. In this example the oligonucleotides were delivered successfully to block the 5' splice site of exon 23 in *mdx* mouse dystrophin, enabling restoration of dystrophin expression in striated muscle tissue (Rimessi et al., 2009). Gold nanoparticles have recently been used to deliver DNA oligonucleotides to the nuclei of mammalian cells and mice. DNA oligonucleotides conjugated to these carriers were targeted toward a number of factors involved in cancer formation and in each case they had positive effects at reducing tumour progression, indicating successful nuclear delivery (Kim et al., 2011). As with oligonucleotides, targeting nanoparticles to specific tissues has also become possible. For instance, nanoparticles modified with the transferrin receptor and conjugated to DNA-Ps modified oligonucleotides aimed at knocking down Bcl-2, have been highly successful at inducing apoptosis in leukemia cell lines (Yang et al., 2008). Oligonucleotides conjugated to carriers that allow for on-demand triggered release via an enzymatic or physical trigger have also been developed (Venkatesh et al., 2009).

Delivery of modified RNA oligonucleotides in to the CNS is a major hurdle for their use in disorders such as SMA and Alzheimer's disease. Research in this area is still relatively

premature, but there have been successful studies where SMA oligonucleotides have been delivered using a micro-osmotic pump directly into the CNS, as well as embryonic or neonatal intracerebroventricular injection (Hua et al., 2010). One draw-back is that these methods are highly invasive and so the use of a delivery agent would be more favorable. For instance, it is possible to target siRNA to the brain through conjugation to a 29 amino acid peptide modified from the rabies virus glycoprotein. siRNA conjugation to this carrier permitted selective gene silencing in the brains of mice (Kumar et al., 2007). An additional way to transfer oligonucleotides across the blood brain barrier (BBB) is to use a nanogel of poly(ethylene glycol) and polyethylenimine that encapsulates negatively charged oligonucleotides and escorts them across the BBB. This method has been shown to allow for uptake of oligonucleotides in to bovine brain micro-vessel endothelial cells (Vinogradov et al., 2004). Adeno-associated virus (AAV) vectors are also a potential way of transporting oligonucleotides in to the brain in SMA (Foust et al., 2010; Passini et al., 2010) and muscle in DMD (Blankinship et al., 2006; Gregorevic et al., 2006). The expression of ASOs linked to U7 snRNA has also been shown to be successful (Goyenvalle et al., 2004; Meyer et al., 2009).

1.4. SMN1/2 and SMA

The success of oligonucleotide therapy for the treatment of DMD paved the way for the development of oligonucleotides to combat other diseases. Developing oligonucleotides to treat SMA was an obvious next step, as oligonucleotide-dependent reversal of the exon 7 skipping event in *SMN2* would allow for direct recovery of SMN expression and treatment of SMA. In addition, using oligonucleotides to stimulate exon inclusion, instead of skipping as in DMD, would take the capabilities of splice altering oligonucleotides to the next level. Hence, a great understanding of the splicing characteristics of the target exon was achieved and many diverse approaches used to induce exon inclusion.

1.4.1. SMA Genotype and Phenotype

SMA is a degenerative muscular disorder resulting from progressive degradation of anterior horn cells, located within the brain stem nuclei and spinal cord (Dubowitz 1989). It is an autosomal recessive disorder, with an occurrence rate of 1 in 6,000/10,000 live births and a carrier frequency of 1 in 35 (Roberts et al. 1970; Pearn 1973; Pearn 1978; Czeizel & Hamula 1990; Emery 1991; Feldkötter et al. 2002; Cusin et al. 2011). The disease state is characterized by time of onset and severity: type I, also known as Werdnig-Hoffman disease, induces severe symptoms which become apparent before 6 months of age (Werdnig 1894; Hoffmann 1893; Munsat 1992); type II has intermediate severity and delayed onset, becoming apparent up to 18 months of age (Fried 1971; Munsat 1992); type III, also known as Kugelberg-Welander disease, induces mild symptoms, becoming apparent after 18 months of age (Kugelberg and Welander, 1956; Munsat and Davies, 1992). SMA patients typically have significant and

progressive muscle wastage and weakness (Munsat and Davies, 1992), with death normally occurring due to ineffective respiratory musculature (Yuan et al., 2007).

The onset of SMA is due to loss of the spinal motor neuron (SMN) protein, through loss of expression from both alleles of the *survival of motor neuron 1* (*SMN1*) gene (Lefebvre et al., 1995). The *SMN1* gene is located at position 5q13 (Lefebvre et al. 1995; Nicole et al. 2002; Melki et al. 1994) and mapping of this gene has identified 8 exons, 7 of which form the genes coding region (Burglen, 1995). In humans the *SMN1* gene has been duplicated, generating *SMN2* (Lefebvre et al., 1995). The severity of SMA is dictated by the copy number of *SMN2* (Lefebvre et al., 1995; Elsheikh et al., 2009): type I SMA patients have two copies, type II have three and type III have four. *SMN2* generates an SMN protein with variable activity and so compensates for the loss of *SMN1* in some cases more than others (Le et al., 2005; Prior et al., 2009; Vezain et al., 2010).

The protein product of *SMN1* mediates the correct assembly of Sm proteins on snRNA, which are fundamental in the correct functioning of snRNPs during splicing. The loss of SMN function as seen in SMA has been shown to induce widespread splicing alterations in a number of tissues, in addition to those of the nervous system (Zhang, Lotti, et al., 2008; Fox-Walsh and Hertel, 2009).The SMN protein complex comprises the SMN protein together with SIP1 and Gemins 2-8 (Fischer et al., 1997; Liu et al., 1997; Meister et al., 2001; Will and Lührmann, 2001; Pellizzoni et al., 2002) and functions through an unknown mechanism. However, analysis of SMA mutations is gradually helping to unravel the mechanism of SMN function. For instance, a recent study identified that a common SMA causing mutation in

SMN1 (Wirth et al., 2006) disrupts the SMN/Gemin 2 interaction, which is important in blocking RNA binding to the assembling Sm pentamer (Zhang, So, et al., 2011).

1.4.2. SMN1/2 Splicing Regulation

The regulation of exon 7 splicing in *SMN2* has been analysed extensively, as the development of oligonucleotides to re-introduce exon 7 into *SMN2* mRNA requires a detailed understanding of exon 7 regulatory characteristics (Figure 1.5). Systematic mutagenesis and *in vivo* selection of individual nucleotides across *SMN2* exon 7 has showed that this exon is divided into three distinct regions: an inhibitory cluster at the 5'end (SE1), a conserved central region (SE2) and an inhibitory cluster at the 3' end (SE3) (Lorson and Androphy, 2000; Singh, Androphy, and Singh, 2004a).

SMN2 exon 7 skipping has been linked with its poor 3' splice site sequence (Lim and Hertel, 2001). *SMN2* has a poor polypyrimidine tract sequence and studies where this sequence was strengthened, in the presence of Tra 2β, have seen more *SMN2* exon 7 inclusion (Hofmann et al., 2000; Lorson and Androphy, 2000). In addition, an inhibitory hnRNP A1 binding site has been identified that spans the 3' splice site of intron 6 and part of the SE1 region of exon 7 (Doktor et al., 2011). Binding of hnRNP A1 to this region has been implicated in the disruption of this region's positive effect on *SMN2* exon 7 splicing and has been shown to inhibit U2 snRNP binding to the 3' splice site of *SMN2* intron 6 (Martins de Araújo et al., 2009). This region's G8 residue is normally incorporated within a stem loop structure (TSL-1), which allows communication between positive regulatory proteins bound at the central SE2 region and U2AF35 bound at the 3' splice site of intron 6 (Singh, Androphy,

and Singh, 2004a, 2004b). Also located in the SE1 region of *SMN2* exon 7 is a C6U transition (Lorson et al., 1999), which sees both the creation of an additional inhibitory hnRNP A1 binding site (Kashima and Manley, 2003; Cartegni et al., 2006) and the loss of a stimulatory SRSF1 binding site. SRSF1 binding to this region has previously been shown to be necessary and essential for exon 7 inclusion in *SMN1* (Cartegni and Krainer, 2002) and has been shown to enhance binding of U2 snRNP and U2AF65 to the 3' splicie site of SMN2 intron 6 (Martins de Araújo et al., 2009). hnRNP A1 binding to the site created through the C6U transition in *SMN2* may be synergistic with Sam68 binding, as this protein has been shown to also bind this region and induce *SMN2* exon 7 skipping (Pedrotti et al., 2010).

The central SE2 region (Lorson and Androphy, 2000) has been shown to be a binding site for the splicing enhancer proteins Tra2β (Hofmann et al., 2000; Cléry et al., 2011), hnRNP G (Hofmann and Wirth, 2002), hnRNP Q (Chen et al., 2008) and SRSF9 (Young et al., 2002), which collaborate together to stimulate exon 7 inclusion. Of these regulatory proteins however, Tra2β has proven to be vital for the stimulatory activity of exon 7 in both *SMN1* and *2* (Hofmann et al., 2000). In addition, an hnRNP A1 binding site in the SE2 region that overlaps with the Tra2β binding site has also been implicated in *SMN2* exon 7 skipping. A select number of SMA patients found to have a point mutation in this site exhibited a higher level of *SMN2* exon 7 splicing, which was attributed to disruption of hnRNP A1 binding (Vezain et al., 2010).

It has also been suggested that U1 snRNP binding to the 5' splice site of *SMN2* exon 7 may act as a rate-limiting factor of exon 7 splicing (Singh, Androphy, and Singh, 2004a). Part of the SE3 inhibitory region has been shown to form a hairpin-loop structure (TSL2), which

sequesters the GU of the *SMN2* intron 7 5' splice site and potentially inhibits U1 snRNP binding (Singh et al., 2007).

As well as the role that exonic sequences play in the regulation of *SMN2* exon 7 splicing, *SMN2* introns 6 and 7 also play a significant role in this. *SMN2* introns 6 and 7 have been shown to contain regulatory regions known as elements 1 and 2, located at positions -112 to -68 and +59 to +124 respectively (Miyajima et al., 2002). Element 1 has been shown to inhibit *SMN2* exon 7 splicing and bind the inhibitory protein PTB (Baughan et al., 2009). Whereas element 2 has been shown to fold into a functionally dependent stem-loop structure, that when folded stimulates *SMN2* exon 7 splicing (Miyaso et al., 2003).

Intron 7 also plays a role in exon 7 splicing regulation through hnRNP A1. In addition to the hnRNP A1 binding sites in exon 7, there are an additional two inhibitory hnRNPA1 binding sites in *SMN2* intron 7. The first is located within an inhibitory region designated ISS-N1, between positions 10-24 of intron 7 (Singh et al., 2006); and the second is located +100 nucleotides downstream of exon 7 (Kashima et al., 2007). ISS-N1 also shares a GC rich sequence that has been shown to be inhibitory, as blocking this region alone with the 3UP8 ASO fully rescues *SMN2* exon 7 splicing (Singh et al., 2009). Downstream of the ISS-N1 sequence there are also URC1/URC2 motifs which form binding sites for the T-cell-restricted intracellular antigen-1 (TIA 1) and TIA 1-related (TIAR) proteins. Binding TIA 1 to these motifs inhibits the hnRNP A1/ISS-N1 interaction, so stimulating recruitment of U1 snRNP to the 5' splice site of intron 7 and so enhancing splicing of *SMN2* exon 7 (Singh et al., 2011).

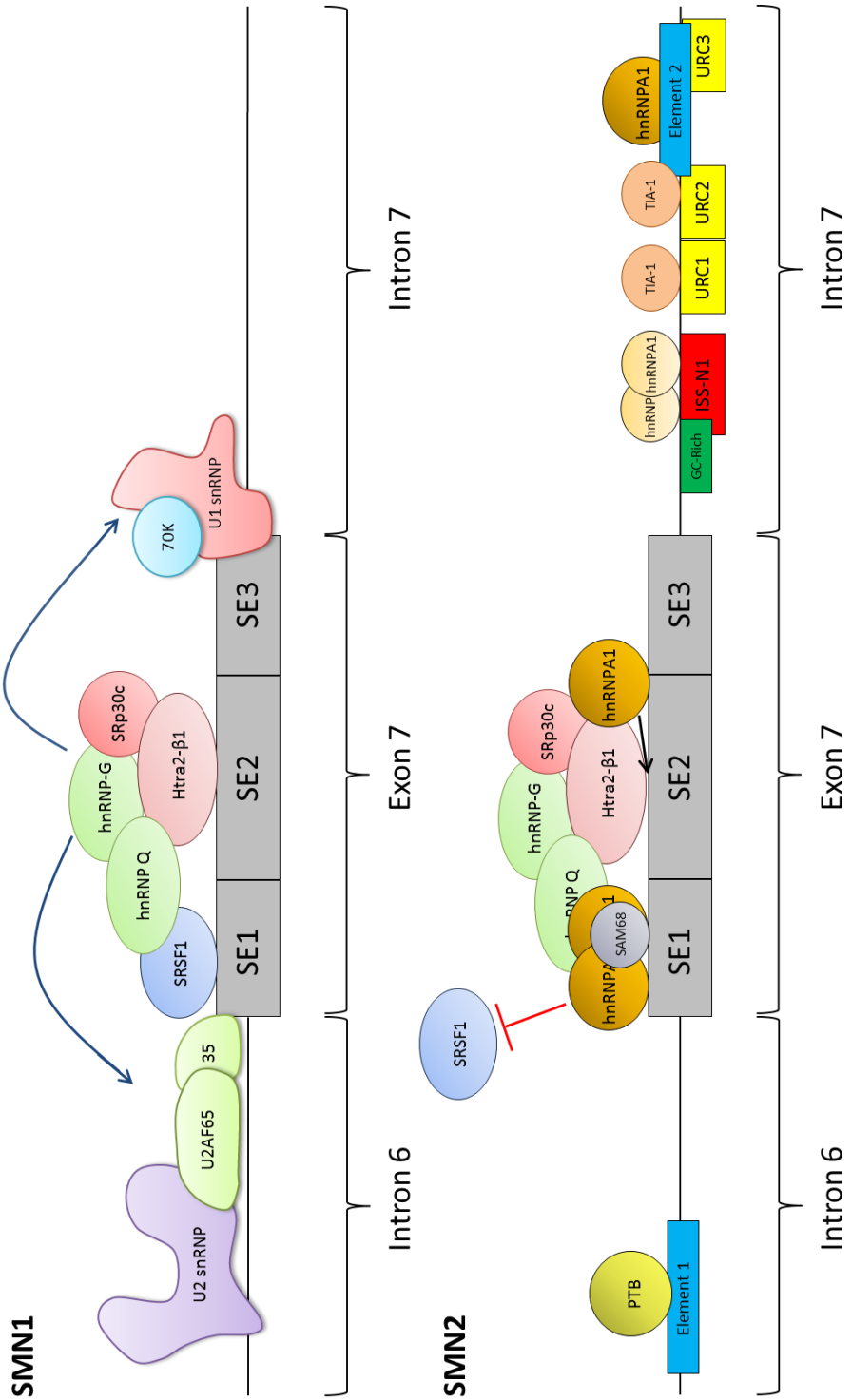

Figure 1.5. Protein binding to *SMN1/2*. Introns are shown as lines and exons as grey boxes. Proteins are shown as coloured circles and regions of RNA are shown as colored rectangles. Stimulatory interactions are shown by blue arrows.

1.4.3. SMA Therapy

1.4.3.1. Small Molecules

Attempts to enhance SMN expression have used histone deacetylase (HDAC) inhibitors, which aim to increase expression of *SMN2* and therefore potentially the amount of active SMN expressed (Andreassi et al., 2004; Avila et al., 2007). Studies investigating compounds able to increase the stability of SMN (Burnett et al., 2009; Mattis et al., 2009) and also prevent damage to neurons, have also been investigated for their potential application in SMA treatment (Nizzardo et al., 2011).

1.4.3.2. Oligonucleotides

1.4.3.2.1. Mouse Models

There has been extensive research into the use of oligonucleotides to alter the pre-mRNA splicing of *SMN2 in vitro,* in patient fibroblasts and in mouse models (Figure 1.6.). Mice contain only one *SMN* gene and its knockout results in embryonic lethality (Schrank et al., 1997). The replacement of this gene with two copies of human *SMN2* allows for viable off spring and the severity of the SMA condition seen is, as with SMA in infants, related to the *SMN2* copy number. Two *SMN2* copies generates a severe (type I) SMA mouse, four generate a mild (type II) SMA mouse and eight rescue the mouse almost entirely (type III) (Hsieh-li et al., 2000). In some cases a mouse expressing *SMN2* Δ7 together with two copies of *SMN2* (*SMN2* Δ7 mouse) has also been used for the assessment of oligonucleotide action. This

combination of a severe SMA phenotype together with a more viable background, extends the life span of the mice and increases experimental viability (Le et al., 2005).

1.4.3.2.2. Assessment

The first oligonucleotides shown to efficiently activate *SMN2* splicing were bifunctional oligonucleotides. The bifunctional (TOES) oligonucleotide incorporates an RNA binding region complementary to a target sequence in *SMN2* exon 7 and a 5' non-complementary RNA tail consisting of six GGA repeats, designed to bind SRSF1 (Skordis et al., 2003). This oligonucleotide was shown to generate full length *SMN2* mRNA, containing exon 7 to approximately the same level as that of wild type *SMN1* both *in vitro* and in type II SMA patient fibroblasts. This oligonucleotide also demonstrated a long-term effect, maintaining SMN protein expression in patient fibroblasts for up to 28 days following two consecutive transfections (Skordis et al., 2003; Owen et al., 2011). A similar 2'-*O*-Me bifunctional oligonucleotide was also developed to stimulate recognition of *SMN2* exon 7 through inhibition of *SMN2* exon 8 splicing. This oligonucleotide was designed to recruit hnRNP A1 to exon 8, slowing splicing of exon 8 and allowing exon 7 to be recognized and spliced. This oligonucleotide increased the level of exon 7 inclusion and SMN protein expression in SMA type I fibroblasts and in the CNS of *SMN2* Δ7 mice (Dickson et al., 2008). Finally, an oligonucleotide known as 'ESSENCE' (PNA) also targeted to *SMN2* exon 7, was seen to stimulate splicing of this exon *in vitro*. This oligonucleotide acted to promote exon 7 splicing through the action of its conjugated RS domain, that in theory acts as an SR protein's RS domain to stimulate splicing (Cartegni and Krainer, 2003).

As the understanding of the regulation of *SMN2* exon 7 splicing was developed, ASOs that block binding of repressor proteins, instead of recruiting positive regulators, were developed to stimulate exon 7 splicing. Administration of a 2'-*O*-MePs ASO targeted to the ISS-N1 element in *SMN2* intron 7 was found to effectively stimulate exon 7 inclusion both *in vitro* and *in vivo* (Singh et al., 2006; Williams et al., 2009). Postnatal intracerebroventricular (ICV) injection of this ASO into *SMN2* Δ7 mice, at different time points, stimulated SMN expression in the CNS, and mice exhibited increased body weight and movement. Surprisingly this study saw more activity from an unconjugated naked ASO than a lipid-conjugated ASO (Williams et al., 2009). A further antisense micro-walk next identified that the shortest ASO with the highest *SMN2* exon 7 stimulatory effect was the 3UP8 oligonucleotide, located at positions 7-14 in *SMN2* intron 7 (Singh et al., 2009).

In parallel studies, an ASO walk along *SMN2* exon 7 and flanking introns was used to identify the optimum ASO position for *SMN2* exon 7 splicing stimulation (Hua et al., 2007, 2008). The most successful *SMN2* exon 7 ASO were found to be targeted to positions 09-23 and 10-27 of intron 7, and were modified MOE oligonucleotides with either phosphodiester (mammalian cell culture) or phosphorothioate (Mice) backbones. These oligonucleotides successfully induced *SMN2* exon 7 inclusion *in vitro*. However, they were unable to cross the BBB when injected into the tail vein of mice (type III) and *SMN2* exon 7 splicing was therefore only stimulated in non-neuronal tissue and left unaltered in neural tissue (Hua et al., 2010). Therefore, as in Williams et al. (2009), direct injection of this ASO into the neural tissue was used to ensure its successful delivery across the BBB. The MOE-Ps ASO targeted to positions 10-27 of *SMN2* intron 7 was injected at embryonic day 15 into the cerebral lateral

ventricles of SMA mice with four copies of *SMN2* (Hsieh-li et al., 2000). This ASO increased motor neuron number and lengthened survival of treated SMA mice (Hua et al., 2010). Hua et al. (2010) also used an osmotic pump to deliver this oligonucleotide directly into the lateral cerebral ventricle of adult SMA mice (as above), inducing both stimulation of *SMN2* exon 7 splicing and expression of SMN protein in the spinal cord. Importantly the effect of this oligonucleotide was long lasting, with a 7 day ICV injection of 50 µg into SMA adult mice maintaining ~ 90 % *SMN2* exon 7 inclusion for up to 6 months. In addition, this oligonucleotide was also shown to not induce an immune response (Hua et al., 2010). Recently, the therapeutically effective dose of this oligonucleotide (8 µg/g tissue) was identified through tests in *SMN2* Δ7 SMA mouse models. Delivery of 3 mg of this oligonucleotide to cynomolgus monkeys, via an intrathecal injection, confirmed that this oligonucleotide could reach the required active dose in the spinal cord via this administration method into larger mammals (Passini et al., 2011).

Oligonucleotides to enhance *SMN2* exon 7 splicing have also been conjugated to U7 snRNA, allowing it to be expressed from a gene and enhancing its stability. U7 snRNA conjugation to a bifunctional oligonucleotide targeted to the 5' region of exon 7 caused prolonged *SMN2* exon 7 inclusion in SMA type I fibroblasts, but had little effect on SMN protein level (Marquis et al., 2007). The genetic introduction of this U7 snRNA-conjugated oligonucleotide in to *SMN2* Δ7 SMA mice via germline transgenesis, saw the recovery of a severe SMA phenotype (Meyer et al., 2009). In addition, the effect of an oligonucleotide targeted to bind sites flanking element 1, and inhibit binding of PTB/FUSE-BP via looping out of this region, was initially pioloted conjugated to U7 snRNA. Following this oligonucleotides

demonstrated success, it was then developed without U7 conjugation and containing the 2'-*O*-Me modification. ICV injection of this modified oligonucleotide into SMA mice induced SMN protein expression and extended life span (Baughan et al., 2009).

As previously discussed oligonucleotide delivery to the nucleus limits and inhibits their action. SMA is a developmental disease and as successful embryonic development depends on the presence of SMN, it would appear that the earlier SMA treatment is applied the more successful the outcome. Due to this, direct injection of oligonucleotides into the brain of embryonic (Hua et al., 2010) and adult (Passini et al., 2011) SMA mice has proven to be the most successful method of enhancing SMN expression. However, this method of oligonucleotide delivery is highly invasive, so it has been favorable to develop non-invasive methods such as the use of oligonucleotides incorporated into AAV vectors. For instance, AAV vectors have been used to deliver a U7-conjugated ASO targeted to the intron7/exon8 boundary. Transduction of SMA type I fibroblasts with this construct stimulated both production of *SMN2* mRNA containing exon 7 and expression of the SMN protein to levels seen in healthy cells (Madocsai et al., 2005; Geib and Hertel, 2009). Viral vectors containing the sequence of the bifunctional oligonucleotide targeted to *SMN2* exon 7, from the work of Skordis et al. (2003), was also transduced into SMA type I patient fibroblasts and increased SMN protein expression in these cells (Baughan et al., 2006).

Gene therapy, whereby *hSMN1* CDNA is expressed within an AAV construct, has also been injected into the CNS of *SMN2* Δ7 SMA mice. This resulted in SMN expression throughout the spinal cord and an improved phenotype (Passini et al., 2010).

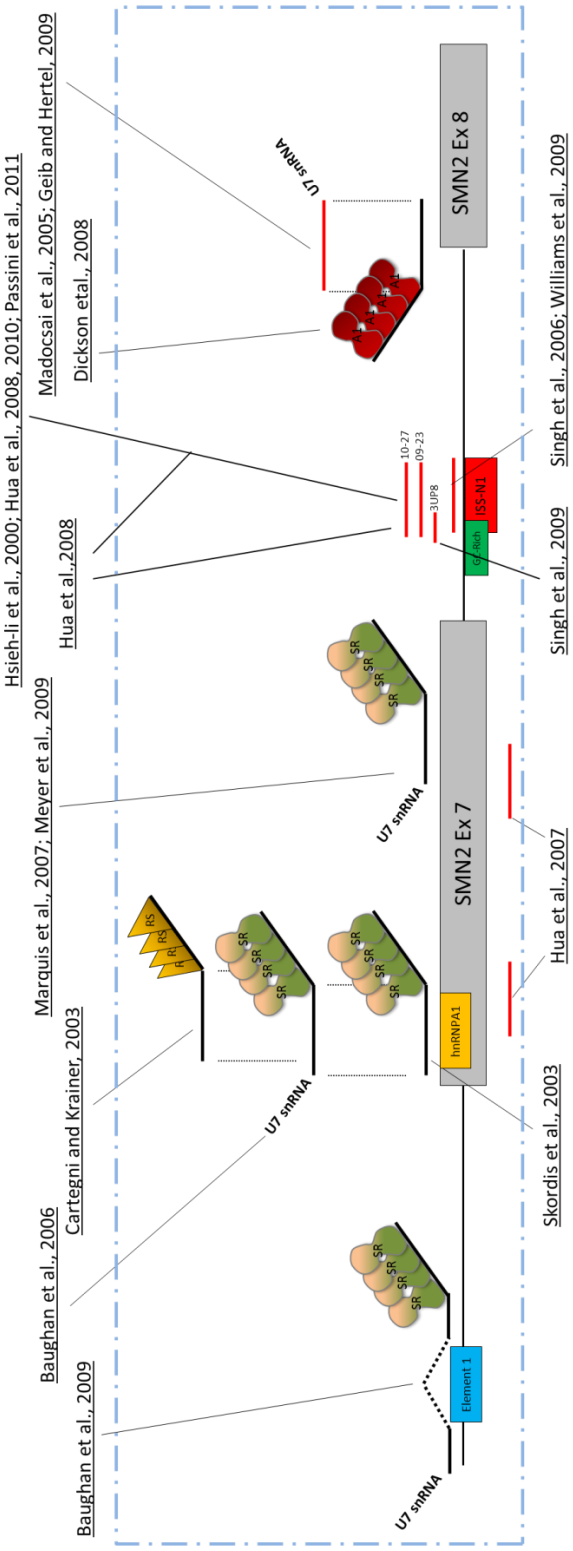

Figure 1.6. Diagram showing the position of RNA oligonucleotides used to artificially stimulate inclusion of *SMN2* exon 7. ASOs are shown in red and bifunctional oligonucleotides are shown in black. SR and hnRNP factors that bind to the non-complementary tail regions of bifunctional oligonucleotides are shown as green and red shapes and are labelled respectively. RS domains are shown as orange triangles labelled RS. *SMN2* exons 7 and 8 are shown as grey boxes and introns 6 and 7 are shown as black lines. Fundamental regions blocked by ASOs are indicated by blue (Element 1), Green (GC-rich and red (ISS-N1) boxes.

1.5. RON Tyrosine Kinase

The potential of ASOs to alter splicing in disease and therefore be used as a successful form of disease therapy was initially made evident through the studies on oligonucleotide treatment of DMD and SMA. As ASOs were now able to both inhibit and stimulate splicing of exons, it was clear that oligonucleotides could be developed to alter many other disease-related splicing changes, such as those commonly seen in cancer.

1.5.1. RON and Cancer

Receptor d'origine nantais (RON) is a receptor tyrosine kinase expressed universally in many tissue types (Waltz et al., 1998). It is a heterodimeric protein which is initially processed from a 180 KDa precursor, generating both a transmembrane (α:35 KDa) and catalytic (β:150 KDa) chain, which are then joined by several disulfide bonds and expressed at the cell membrane (Figure 1.7. B). The extracellular α chain binds to the receptors ligand, the macrophage-stimulating protein (MSP), activating the catalytic tyrosine kinase domain, which is located in the cytoplasmic region of the β chain (Gaudino et al., 1994; Wang et al., 1995). MSP dependent activation of RON stimulates RON homodimerization and autophosphorylation of specific tyrosine residues within its catalytic domain. This series of phosphorylation events in the RON catalytic domain define it as a multi-functional docking site, allowing for the activation of downstream signaling pathways including PI-3K, JNK, Ras and NF-κβ (Wang et al., 1995, 2003; Waltz et al., 2001; Park et al., 2011).

The downstream effects of RON signaling include wound healing, liver regeneration, bone resorption, embryogenesis and the immune response (Bezerra et al., 1994; Wang et al.,

1994, 1996; Kurihara et al., 1996; Waltz et al., 2001; Leonis et al., 2002). Importantly RON signaling has also been shown to activate the epithelial to mesenchymal transition (EMT), which has been linked to the development of metastasis in epithelial cell cancer, a process also referred to as invasive growth (Trusolino and Comoglio, 2002; Wang et al., 2003; Conrotto et al., 2004; Camp et al., 2005). The activation of RON signaling has been shown to result in the break-down of cell-cell contacts, allowing for cell mobility and matrix invasion. The RON dependent phosphorylation of β-catenin, which normally acts with E-cadherin to form cell-cell adherens junctions, induces the break-down of these cell junctions and sees the release of β-catenin. β-catenin can then shuttle to the cell nucleus, where it acts as a signaling molecule stimulating cell growth through the up-regulation of cyclin D1 and myc (Wijnhoven et al., 2000; Wagh et al., 2011).

There are eight known variants of RON including Δ170, Δ165, Δ160, Δ155, Δ110, Δ55, Δ85 and Δ90 (Figure 1.7. B). These variants are derived from splicing alterations that cause changes in the structure and activity of RON. Some RON isoforms demonstrate constitutive activation, stimulating transformation and progression of tumours (Lu et al., 2007; Eckerich et al., 2009). To this end RON signaling has been implicated in pancreatic (Thomas et al., 2007), brain (Eckerich et al., 2009), colorectal (Zhou et al., 2003), mammary (Ghigna et al., 2005), gastric (Zhou et al., 2008), ovarian (Maggiora, 2003), hepatocellular (Chen et al., 1997), prostate (Thobe et al., 2010), urinary (Cheng et al., 2005) and renal (Rampino et al., 2003) carcinomas.

RON signaling has been directly linked to the onset of metastasis in cancer. For instance, Ghigna et al. (2005), showed that constitutive RON activation through expression of

the RON Δ165 isoform was directly linked to the induction of cell migration in gastric carcinoma cells (Collesi et al., 1996; Ghigna et al., 2005). In other studies, siRNA mediated knock-down of RON in both hepatocellular and gastric carcinoma cell lines, saw the inhibition of cell migration and so the induction of apoptosis (Park et al., 2010; Cho, Park, et al., 2011). In prostate cancer cell lines, knockdown of RON indicated a connection between RON activation and angiogenic chemokine overexpression. This identified that prostate tumour progression is directly linked to RON overexpression and identified how RON acts to enhance tumour growth through the promotion of endothelial cell chemotaxis and angiogenesis (Thobe et al., 2010).

It has been seen that RON is able to heterodimerize with other tyrosine kinase receptors, in particular the erythropoietin receptor, Met, EGFR, GM-CSF and the common β-signal transducer receptor for interleukins 3 and 5 (Mera et al., 1999; Follenzi et al., 2000; Peace et al., 2003; Ney et al., 2011). Interestingly, RON transphosphorylation has also been shown to be essential for the sustained and dramatic effect of signaling via the MET receptor in cancer of epithelial cell origin. In this study the knock-down of RON reduced MET-dependent cell proliferation and tumorigenicity (Benvenuti et al., 2011).

1.5.2. RON Δ165

Expression of *RON* Δ165 mRNA has been found in breast and gastric carcinoma tumours and has been linked with the development of an invasive phenotype in these tissues (Ghigna et al., 2005). This isoform lacks *RON* exon 11, which codes for a 49-amino acid trans-membrane region in the β chain (Figure 1.7. A). The loss of this region means that the

receptor is unable to be held at the cell membrane and instead is expressed in the cytoplasm. Loss of *RON* exon 11 also results in loss of three cysteine residues from the β chain. Loss of these residues, which are normally involved in intramolecular disulphide bond formation, leaves an uneven number of cysteine residues that can then form intermolecular disulphide bonds with other RON Δ165 monomers. This disulfide bond formation between two RON Δ165 monomers then generates stable intracellular oligomers, which causes constitutive activation of RON signaling via trans-phosphorylation between the bound receptor pair (Collesi et al., 1996; Wang et al., 2010).

A study has found that binding of SRSF1 to *RON* exon 12 induces skipping of *RON* exon 11 and increases expression of *RON* Δ165 mRNA. This study showed that when cells were induced to over-express SRSF1 they took on a spindle-shaped morphology, akin to the morphology of cells in EMT and were stimulated to migrate. Knock-down of SRSF1 in KATO III gastric carcinoma cells reduced *RON* Δ165 expression and accordingly reduced cell motility. Conversely, when *RON* Δ165 was knocked down in KATO III cells the same effect on cell motility was seen as in the SRSF1 knockdown. This consolidates the link between SRSF1 concentration, *RON* Δ165 mRNA expression and cell motility (Ghigna et al., 2005). These findings are highly sensical given that SRSF1 has been identified as proto-oncogene, with its expression often being up-regulated in tumours. SRSF1 has been found to alter the expression of certain mRNAs, that have been shown to consequently lead to cancer development and propagation (Karni et al., 2007; Sinha et al., 2010).

A recent study has also implicated Sam68 in the regulation of *RON* splicing and *RON* Δ165 mRNA expression through its effect on an SRSF1 negative feed-back loop (Valacca et

al., 2010). SRSF1 modulates its own concentration, through the synthesis of unproductive shorter SRSF1 isoforms. It does this by splicing within its 3' UTR and producing shorter unproductive mRNA transcripts (Sun et al., 2010). Phosphorylation of Sam68 by ERK 1/2 kinase, a kinase that stimulates processes commonly seen to be induced by RON signaling (Thiery and Sleeman, 2006), promoted Sam68 binding to the 3' UTR of SRSF1. Sam68 binding inhibited SRSF1-mediated splicing of its own transcript's 3' UTR and led to inhibition of the SRSF1 negative feed-back loop. The following increase in SRSF1 concentration then stimulated expression of *RON* Δ165 mRNA, which then in turn would further stimulate ERK 1/2 kinase activity (Valacca et al., 2010).

As well as SRFSF1, hnRNP H has also been implicated in the regulation of *RON* Δ165 expression. hnRNP H binding to *RON* exon 11 has been shown to inhibit exon 11 inclusion and promote the expression of *RON* Δ165 mRNA. Knock-down of hnRNP H was seen to inhibit production of the *RON* Δ165 isoform and so reduce cell mobility and invasion. Conversely, coupling the hnRNP H knock-down with stimulation of *RON* Δ165 mRNA expression recovered cell motility, confirming the link between hnRNP H and *RON* Δ165 expression (Lefave et al., 2011).

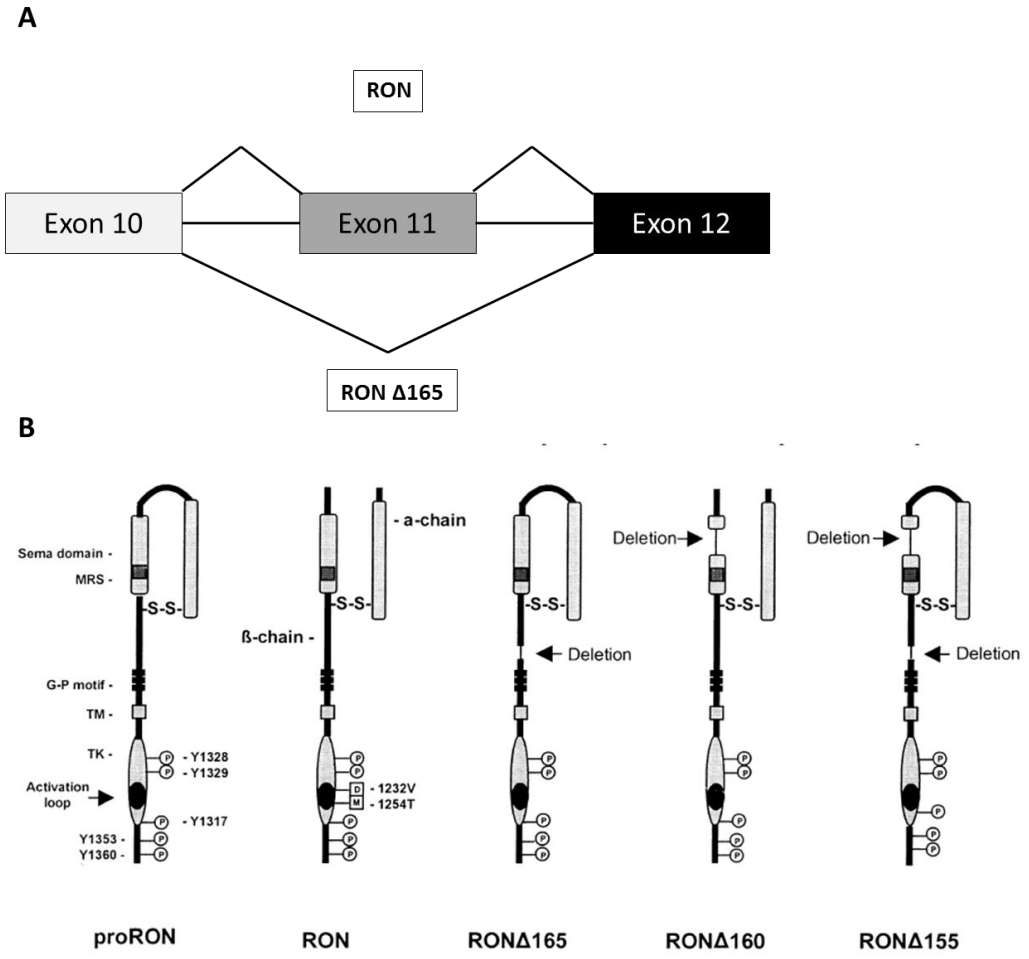

Figure 1.7. Schematic representation of *RFL*$^{1-692}$ pre-mRNA and the RON isoforms most commonly expressed in cancer. **(A)** *RFL*$^{1-692}$ pre-mRNA is processed by the spliceosome generating either full length *RON* mRNA, where exon 11 has been spliced or *RON* Δ165 mRNA, where exon 11 has been skipped. The sequence of this construct can be found in the appendix (7.2.1.). **(B)** During maturation pro-RON is cleaved to separate the 40 kDa α and 150 kDa β chains to produce RON. The α chain is extracellular and anchored to the membrane via a disulphide bridge with the membrane spanning β chain. In addition to the membrane spanning region, the β chain also contains an extracellular domain and cytoplasmic tyrosine kinase domain. On activation through MSP binding autophosphorylation then occurs within the β chain ,eventually resulting in the activation of downstream signaling pathways (Wang et al., 2003).

1.5.3. Potential Therapies

The activation of RON has been seen to be inhibited through the action of a five amino acid peptide from the v6-CD44 co-receptor. Transfection of a plasmid containing this peptide in to mammalian colon and pancreatic cancer cell lines saw a reduction in cell migration. This peptide acts by binding and blocking the activity dependent association of RON with the full length CD44 v6 co-receptor, thus inhibiting signaling (Matzke et al., 2005). In a similar way the antagonistic RON isoforms, RON Δ85 and Δ90, inhibit RON signaling through binding and sequestering MSP, thus preventing it binding to and activating RON (Eckerich et al., 2009; Ma et al., 2010). RON Δ170 has also been seen to inhibit the tumorigenic activity of RON Δ160 in colorectal cancer cell lines. RON Δ170 forms an inactive complex with RON Δ160, preventing MSP-induced cell signaling pathways and reducing the tumorigenic effect of RON Δ160 (Wang et al., 2007).

The use of indole compounds has also been implicated in the reduction of RON signaling. IDC92 was seen to specifically alter splicing of *RON* Δ165 and re-induce inclusion of *RON* exon 11 in a breast cancer cell line stably expressing *RON* Δ165 and SRSF1 (Ghigna et al., 2010). Additional small molecule inhibitors that target both RON and Met have been developed. AMG 458, a quinolone-derived compound, was seen to both inhibit signaling through Met and RON and reduce cell mobility in a selection of epithelial cancer cell lines and mouse xenograft models (Liu et al., 2008; Zhang, Kaplan-Lefko, et al., 2008). The Met inhibitor BMS-777607, a pyridine derived compound, has also been shown to be active towards a gastric carcinoma xenograft model and is being taken into clinical trials (Schroeder et al., 2009). In addition to this, two pyridine-based compounds have also recently been

identified that bind specifically and selectively to RON, with one having a significant inhibitory effect on RON phosphorylation and so signaling (Raeppel et al., 2010).

Antibodies targeted toward RON have also been developed. IMC-41A10 is a monoclonal antibody that blocks the interaction of MSP with the RON receptor. This antibody was successful at antagonizing the RON induced downstream signaling cascade and so cell migration and tumorigenic effect (O'Toole et al., 2006). In addition, an antibody (Zt/f2) targeting the catalytic domain of the β chain has been shown to induce RON receptor internalization and inhibition of downstream signaling (Yao et al., 2011). Recently, this antibody has been used as a carrier and internalization catalyst for a chemotherapeutic agent. When conjugated to doxorubicin-immunoliposomes this antibody induced internalization of the receptor bound therapeutic and so selectively reduced viability of the target cells (Padhye et al., 2011).

A bifunctional oligonucleotide to combat the expression of *RON* Δ165 mRNA expression has recently been tested for its effect in gastric carcinoma cells. This oligonucleotide re-stimulated *RON* exon 11 inclusion, but its effect was overshadowed both by the low level of *RON* background splicing and the amount of oligonucleotide required to stimulate the splice change (Ghigna et al., 2010).

1.6. Immunoglobulin M

The use of ASOs to alter splicing by sterically blocking splice sites was highly successful at inducing exon skipping in DMD. Therefore the same approach could potentially be successful when applied to stimulate exon skipping in *IgM* pre-mRNA. This would see the development of a therapy for B-cell lymphocytic leukemia. In addition, the nature of this disease, which affects B-cells present in the blood, could potentially rule-out the problems of oligonucleotide delivery seen with other ASO treatments.

1.6.1. B-Cell Lymphocytic Leukaemia

B-CLL is characterised by circulating monoclonal B cells that express surface molecules usually found on mature lymphocytic cells. It results from deletions or translocations at 13q (Caligaris-Cappio and Hamblin, 1999). B-CLL can be divided into two groups, dependent on whether the B-CLL cells have undergone V_H mutations. Originally it was thought that B-CLL cells circulated the body in the resting/G^o phase of the cell cycle (Fais et al., 1998). However, Damle et al. (2002), showed that circulating B-CLL cells, with both mutated and unmutated V_H genes, express the surface phenotype of antigen-experienced B lymphocytes which varies from that of the resting antigen-naive B cells (Damle, 2002). Therefore this indicates that B-CLL cells have undergone antigen-induced activation through the B-cell receptor (BCR), as with antigen stimulated B cells (Reth, 1992).

1.6.2. The B Cell Receptor

The BCR complex on the surface of B-CLL cells is composed of IgM and a heterodimer of Igα/Igβ (CD79a/CD79b) (Reth, 1992). There are two contradictory views of the effect of signalling through the IgM-BCR in B-CLL cells. In one case B-CLL cells are thought to down-regulate expression of the IgM-BCR, as signals delivered through these receptors have been shown to induce apoptosis (Zupo et al., 2000). This supports the work of Damel et al. (2002), as BCR down-regulation occurs normally in antigen-experienced B-cells, perhaps intentionally to reduce apoptotic-inducing signals through the BCR and B-CLL death (Alfarano et al., 1999). It has been shown that B-CLL cells down-regulate the expression of the BCR through a change in the alternative splicing pattern of Igα/Igβ. Igα/Igβ has been found to play a principal role in the transportation of IgM to the surface of the B cell. Hence, splice variants of Igα/Igβ in B-CLL cells cause loss of this transportation, loss of expression of the BCR (Indraccolo et al., 2002) and so loss of its apoptotic effect (Zupo et al., 2000). Contradictory to this, Bernal and colleagues showed that induction of NF-κB and expression of bcl-2, mcl-1 and bfl-1, stimulated through cross-linking of the BCR, inhibits apoptosis and so promotes survival of the cancer cell (Bernal, 2001). On top of this it was found that sustained signalling through the BCR by immobilized anti-IgM induced a typical BCR signal, which is characterised through sustained Akt and ERK activation and an increase in the concentration of the anti-apoptotic protein Mcl-1. Whereas BCR cross-linking to soluble anti-IgM induced apoptosis, via down-regulation of Mcl-1 (Petlickovski et al., 2005). A high Mcl-1 concentration has also been shown to be related to ineffective chemotherapy (Bellosillo et al., 1999), with fludarabine and chlorambucil for instance (Kitada et al., 1998) and studies

have shown that a decrease in Mcl-1 concentration must precede successful chemotherapy (Lømo et al., 1996; Bellosillo et al., 1999). In addition to this, an investigation by King et al. (1999), showed that signalling through the BCR in immature B-cells induces apoptosis, whereas in mature B-cells it signals for proliferation and differentiation (King et al., 1999). This would suggest that the proliferation of those B-CLL cells with a mature B-cell phenotype (Alfarano et al., 1999) would be induced by BCR signalling, not apoptosis.

1.6.3. Expression Regulation of Membrane bound IgM/secreted IgM

The regulatory mechanisms that determine the levels of membrane bound IgM (μ_m)/secreted IgM (μ_s) in B-cells has been widely studied. In mice the inclusion of the two IgM membrane binding domains (M1 and M2) has been shown to be regulated by an enhancer and inhibitor located in the second membrane binding domain, M2 (Kan and Green, 1999). A study by Shen and colleagues identified that binding of PTB to one of the two PTB binding domains in the inhibitor, is enough to inhibit splicing of both M1 and M2. They also showed that an enhancer-bound RS domain was enough to antagonise this inhibitory effect of PTB binding on splicing (Shen, Kan, Ghigna, et al., 2004).

Peterson et al. (1989) have studied the regulatory mechanisms of IgM μ_m/μ_s expression in detail and initially suggested two models; the poly(A) site model and the μ_s site-splice model. The poly(A) site model suggests that cleavage-polyadenylation of the pre-mRNA of μ_m and μ_s are in competition; the splice-site model suggests there is simple competition between cleavage-polyadenylation at the μ_s poly(A) site and splicing of Cμ4-M1. After investigation it was found that the relative abundance of μ_m to μ_s IgM is in fact dependent on competition

between cleavage-polyadenylation at the μ_s poly(A) site (shown as pA in Figure 1.8.) and splicing of Cμ4-M1 (shown as SS in Figure 1.8.) (Peterson and Perry, 1989). The idea that 'competition control' regulates the expression of IgM μ_m and μ_s is supported by the fact that both μ_m and μ_s are expressed in naive B-cells or plasma cells in balance, and that 'competition control' and not specific *cis*-regulatory elements in the gene determine the ratio of the variant of IgM produced (Peterson et al., 1991, 1994; Peterson, 2007). Another study supporting these results shows that as the concentration of the cleavage specificity factor (CstF-64) increase in cells, so too does the concentration of μ_s. This shows that as cleavage and polyadenylation of μ_s increases the splicing and polyadenylation of μ_m decreases, indicating further the competitive nature of the control of μ_m/μ_s production (Takagaki et al., 1996).

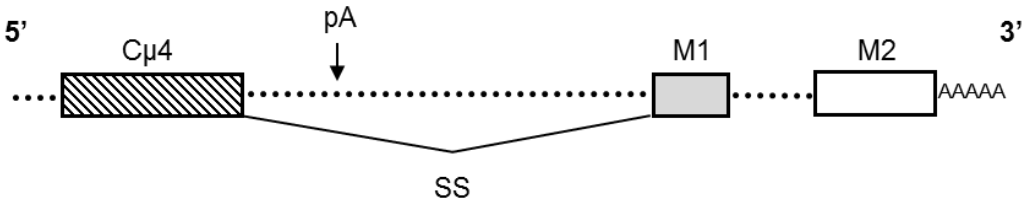

Figure 1.8. Diagrammatic representation of the membrane binding domain of Immunoglobulin M. Exon Cμ4 = Hatched box, Exon M1 = Grey box, Exon M2 = White box, Dotted lines = Intron. The competitive polyadenylation site is labeled pA.

1.7. Summary

Splicing is a vital process required to increase the complexity of an organism. It is highly regulated with many variables that accumulate to result in the production of mRNA. Commonly however, mutation and expression changes alter this complex regulatory network and splicing is altered accordingly. This unchecked spicing regulation change is a key factor in the development and progression of disease.

ASOs have been developed and successfully used to alter the splicing pattern of disease dependent RNAs, for instance ASOs to treat DMD are currently going through clinical trials. Following their use in DMD, ASOs have also been developed to target other diseases, including SMA and cancer. In each case however, ASO development is highly complex with oligonucleotide sequence, modification and delivery all requiring optimization.

There have been many different oligonucleotides developed to stimulate *SMN2* exon 7 splicing as a treatment for SMA. These include bifunctional oligonucleotides that act through the recruitment of either SR or hnRNP proteins, ESSENCE oligonucleotides containing active RS domains, and ASOs that sterically block elements that suppress exon 7 splicing. Both *in vitro* and *in vivo* assessment of these oligonucleotides has unequivocally demonstrated that they are effective at combating the SMA disease state; however, the ease of their delivery to their site of action in the CNS poses a problem for their progression into trials in humans.

Skipping of exon 11 in the RON proto-oncogene leads to the expression of the RON Δ165 isoform that has been shown to stimulate metastasis in several epithelial cell cancers. In the same way as the *SMN2* bifunctional oligonucleotide, a *RON* bifunctional oligonucleotide was developed to stimulate re-inclusion of *RON* exon 11 and preventing the onset of

metastasis. However, when tested *in vivo* this *RON* oligonucleotide demonstrated a limited effect.

As the challenge of ASO delivery has been shown to reduce their effectiveness as a therapy, developing ASOs to a disease where cells are more easily accessed could be more effective. B-CLL affects B-cells present in the circulatory system and therefore poses as a potential target. In B-CLL, signaling through the BCR present at the membrane of cancerous B-cells stimulates these cells to be resistant to apoptosis and so chemotherapy. IgM is able to exist either as a secreted soluble protein (μ_s) or at the B-cell membrane (μ_m) as part of the BCR. Regulation of IgM location is determined by competition between polyadenylation after the last exon of the constant region (Cμ4) and splicing of this exon to the first membrane binding exon (M1).

1.8. Aims

The initial purpose of this investigation is to uncover the mechanism through which the *SMN2* bifunctional oligonucleotide stimulates *SMN2* exon 7 inclusion. Once this is known, it may then offer an insight into why the *RON* bifunctional oligonucleotide was not significantly effective (Ghigna et al., 2010). Knowledge of the *SMN2* oligonucleotide mechanism would then allow a new *RON* oligonucleotide to be designed and tested. RON full length ($RFL^{1\text{-}692}$) pre-mRNA has also been shown to be inherently poor at splicing and so identifying the reasons for this could also aid in the development of a more effective *RON* oligonucleotide.

ASOs targeted to switch expression of IgM from μ_m to μ_s in B-CLL cells through inhibition of pre-mRNA splicing will also be developed. Importantly, the characteristics of B-CLL could allow for easy oligonucleotide delivery and so effect. Here ASOs will aim to promote use of the polyadenylation site between exons Cμ4 and M1 and dually inhibit splicing of exons M1 and M2. This may result in a reduction of μ_m expression and so reduce the number of positive cell survival signals transmitted through the BCR. Loss of these positive signals could potentially make B-CLL cells more sensitive to the effects of chemotherapy.

1.9. Objectives

Phase A – Mechanistic analysis of *SMN2* bifunctional oligonucleotide action

1. Investigate *in vitro* the effect of the *SMN2* oligonucleotide on the splicing of two exon constructs, with *SMN2* exon 7 either upstream or downstream. Identify which intron the oligonucleotide is stimulating to be spliced.
2. Use *in vitro* assays including immunoprecipitation, psoralen cross-linking and native gel analysis to investigate whether the *SMN2* oligonucleotide stimulates binding of U1 snRNP to the 5' splice site of *SMN2* intron 7 (as previously predicted (Skordis et al., 2003; Owen et al., 2011)).
3. Investigate the effect of the *SMN2* oligonucleotide on spliceosomal complex formation on *SMN2* exon 7 using native gel analysis.
4. Use UV cross-linking and western blots to identify protein factors whose binding could be stimulated by the *SMN2* oligonucleotide.

Phase B – Analysis of the *RON* Δ165 pro-metastatic splice

1. Investigate *in vitro* the effect of the *RON* oligonucleotide on the splicing of *RON* exon 11 centered in a three exon construct.
2. Investigate *in vitro* the effect of the *RON* oligonucleotide on the splicing of two exon constructs, with *RON* exon 11 either upstream or downstream. Identify which intron the oligonucleotide is stimulating to be spliced.
3. Use a series of two and three exon constructs of RON and RON/β-globin hybrid to systematically identify where the inherent weakness in *RON* exon 11 splicing lies. Use

UV cross-linking to identify whether a protein is binding to this identified region which could be having an inhibitory role in exon 11 splicing.

4. Design a new *RON* bifunctional oligonucleotide to stimulate splicing of *RON* exon 11, base its design on what is found to be inherently inhibitory for *RON* exon 11 splicing and what is known about the mechanism of the *SMN2* oligonucleotide.

Phase C- Switching splicing of *IgM* pre-mRNA using oligonucleotides

1. Design three sterically blocking ASOs: two targeted to the 5' and 3' splice sites of exon M1 and one to an ESE in exon M1. Also, design one bifunctional oligonucleotide to stimulate polyadenylation through the recruitment of polyadenylation factor Cstf-64.
2. Test the effectiveness of *IgM* oligonucleotides *in vivo* through transfection into a B-CLL cell line and analysis of the resulting mRNA changes using real-time PCR.

2. Methods

2.1. Construct Synthesis Methods

2.2. Cell Culture Methods

2.3. *In vitro* RNA Methods

2.4. *In vitro* Protein Methods

2.1. Construct Synthesis Methods

2.1.1. Genomic DNA Extraction

Mec-1 cells at $8x10^5$ cells/ml were pelleted in 15 ml falcon tubes by centrifugation and washed twice in PBS. The pellet was re-suspended in 900 µl digestion buffer (100 mM NaCl, 10 mM Tris HCl pH8, 25 mM EDTA pH 8, 0.5 % SDS). Protein was removed by treating with 50 µl PNK buffer containing Proteinase K (0.4 mg/ml) (Roche) at 60 ºC for 30 minutes and then 37ºC for 30 minutes, followed by phenol chloroform extraction and ethanol precipitation. The pellet was re-suspended in 20 µl TE.1 (10 mM Tris pH 7.5, 0.1 mM EDTA pH 8). The DNA concentration was measured using a nanodrop and a sample was electrophoresed on a 2 % agarose gel containing ethidium bromide (0.5 mg/ml) to check DNA integrity.

2.1.2. PCR

All PCR reactions were carried out in a Storm PCR machine. Phusion Hot Start High-Fidelity DNA Polymerase (NEB) was used to generate PCR products for cloning. Red Taq DNA Polymerase (Sigma), Crimson Taq DNA Polymerase (NEB) and GoTaq Hot start Polymerase (Promega) were used to optimize PCR conditions and to generate production of templates for transcription. On completion all reactions were analyzed on 1 % agarose gels containing ethidium bromide (0.5 mg/ml) before further processing.

2.1.3. Site Directed Mutagenesis

Primers were designed that are approximately 20 nucleotides in length, have a similar melting temperature and overlap the required alteration in the template. In a final volume of 50 µl, 10x Pfu Turbo buffer (Stratagene), 0.2 mM dNTP and 2.5 µM primers were mixed on ice. A concentration range of template DNA was used i.e. 5 ng, 10 ng, 20 ng and each sample was duplicated (plus and minus enzyme). 1 µl of Pfu turbo (Stratagene) was added to half the samples and water to the others. The reactions were put through cycling conditions of 95 ºC 30 seconds (step 1), 95 ºC 35 seconds (step 2), 50 ºC 1 minute (step 3) and 68 ºC 2 minute elongation per kb (step 4). The reaction was cycled through steps 2 to 4 12x. Following PCR all reactions were digested with 1 µl DpnI (NEB) for 1 hour at 37 ºC. Products were checked on a 1.5 % agarose gel containing ethidium bromide (0.5 mg/ml) and transformed into DN5α cells. Successful colonies were identified through colony PCR and sequencing by PNACL sequencing services, University of Leicester.

2.1.4. Isolating Competent Cells

A 5 ml LB overnight culture was inoculated with the cell line to be isolated and grown overnight at 37 ºC, 200 rpm. 200 µl of the overnight culture was used to inoculate 100 ml of LB which was incubated until OD ≈ 0.5. Cells were collected by centrifugation, re-suspended in 0.1 mM $CaCl_2$ and incubated on ice for 30 minutes. Cells were collected by centrifugation and the pellet was re-suspended in 4 ml of 0.1 mM $CaCl_2$ 15% glycerol, aliquoted into 50µl, snap frozen and stored at -80ºC.

2.1.5. Transformation

100 ng of PCR product was transformed into the relevant TOPO vector (Invitrogen). The pCR™4-TOPO® TA Vector was used for transformation of PCR products containing 3'A overhangs, generated from PCR with Red Taq, GoTaq and Crimson Taq polymerases. The pCR®-Blunt II-TOPO® or pCR™4Blunt-TOPO® vectors were used for transformation of PCR products containing blunt ends, generated from PCR with Phusion polymerase. In each case 50-100 µl of the transformed cells were aseptically spread on LB agar plates containing the appropriate antibiotic (30 µg/ml). Plates were incubated overnight at 37 ºC and successful colonies were analysed by colony PCR.

2.1.6. Colony PCR

Successful colonies were selected, streaked onto an agar plate containing the appropriate antibiotic (30 µg/ml) and the remainder used to inoculate a 10 µl crimson Taq (NEB) or red Taq (Sigma) PCR reaction. The streaked plate was incubated at 37 ºC overnight and the reaction was analyzed on a 1 % agarose gel containing ethidium bromide (0.5 mg). Successful colonies were grown up and DNA isolated (see 2.1.7.).

2.1.7. Plasmid Isolation

Colonies were cultured overnight individually in 5 ml of LB supplemented with the required antibiotic (30 µg/ml). Cells were collected by centrifugation and the pellet was re-suspended in 200 µl of Solution 1 (50 mM Glucose, 25 mM Tris HCl pH 8, 10 mM EDTA supplemented with 6 µl/ml of RNase A (10 mg/ml)). 400 µl of Solution 2 (0.2 mM NaOH, 1

% SDS) was added, the samples were vortexed briefly and incubated on ice for 5 minutes. 300 µl of Solution 3 (KAc 3M, pH 4.8) was added and samples were vortexed briefly and incubated on ice for 10 minutes. Samples were centrifuged for 10 minutes at 13 K and 4 ºC. 400 µl of the supernatant was ethanol precipitated; the pellet was dried and then purified further by phenol chloroform extraction and ethanol precipitation. Once dried, the pellet was re-suspended in 20 µl TE.1. The DNA concentration was measured using a nanodrop and 500 ng was analysed on a 1 % agarose gel containing ethidium bromide (0.5 mg).

2.1.8. Cloning

2.1.8.1. DsRed-eGFP Cloning

The DsRed-eGFP vector was constructed through cloning of eGFP into the pDsRed-Express-1 vector (Invitrogen), using *BamHI* and *XbaI* restriction sites.

2.1.8.2. Plasmid Preparation for DsRed-eGFP Cloning

5x 500 ng of the DsRed-eGFP plasmid was digested in a stepwise manner with *BamHI* and *XhoI*. The plasmid was digested with 4 units of *XhoI* for 3 hours at 37 ºC with buffer 3 and 1x BSA. 10 µl of the digest was run on a 0.8% agarose gel containing ethidium bromide (0.5 mg) to check digestion. The plasmid was digested further with 2 units of *BamHI* for 3 hours at 37 ºC. The enzymes were denatured by incubation at 70 ºC for 10 minutes. The reactions were combined and the digestion was treated with 3.5 units of antarctic phosphatase (NEB) for 30 minutes at 37 ºC and inactivated by incubation for 15 minutes at 65 ºC.

2.1.8.3. Insert Isolation and Purification

The Cμ4M1 region of IgM was isolated from genomic DNA via Phusion PCR (NEB) and cloned into the pCR®-Blunt II-TOPO® Vector (Invitrogen). 10 μg of the TOPO-Cμ4-M1-TOPO plasmid was double digested for 2 hours at 37 ºC with 20 units of *BamHI* and 40 units of *XhoI* in buffer 3 with 1x BSA (NEB). The Cμ4-M1 insert was purified from an LMP gel stained with crystal violet (Quiagen gel extraction kit).

2.1.8.4. Ligation

The insert was cloned in to the DsRed-eGFP vector between DsRed and GFP using *XhoI* and *BamHI* restriction sites. Digested vector and purified insert were ligated at a ratio of 1:3 respectively in a final volume of 10 μl with 0.3 μl T4 DNA Ligase (Promega) and 1x supplied buffer overnight at 4 ºC. 5 μl of the ligation reaction was transformed into TOP10 cells as normal (see 2.1.5.). Colonies were selected and DNA isolated (see 2.1.7.). Successful clones were identified using a double digest with *BamHI* and *XhoI* as described previously and those containing the insert were verified via DNA sequencing (PNACL).

2.1.8.5. RON Cloning

PCR reactions were carried out on either the β-globin (Ex2-Ex3) or RON (Ex10-Ex11-Ex12) templates generating overlapping PCR products amplified by Phusion polymerase (NEB). PCR reactions were checked on 1 % agarose gels containing ethidium bromide (0.5 mg/ml) alongside hyperladder IV and V (Bioline). Parental plasmid was digested with 10 units per 10 μl PCR reaction of DpnI for 30 minutes at 37ºC and then 80ºC for 20 minutes. A

second Phusion polymerase PCR reaction was used to fuse 1 µl of the relevant PCR reactions together. The resulting PCR product was checked on an agarose gel and transformed directly into the Zero blunt pCR™4Blunt-TOPO® vector or the pCR®-Blunt II-TOPO® Vector (Invitrogen).

2.1.9. Sequence Analysis

Plasmid DNA concentration was measured on a nanodrop and DNA integrity was checked on a 1.5 % agarose gel containing ethidium bromide (0.5 mg/ml). 500 ng of plasmid DNA was used per sequencing reaction. The M13F and M13R primers (Invitrogen) were used for all sequencing reactions. Plasmids were cleaned up using DyeEx columns and the sequence is analyzed using a 3730 automated sequencer (PNACL sequencing services, University of Leicester). Sequences were analyzed using Clustal software (NCBI, online).

2.2. Cell Culture Methods

2.2.1. Establishing Cell Line from a Frozen Stock

Cells were removed from a liquid nitrogen store and warmed immediately in hands. Cells were transferred to a 10 ml tissue culture flask and supplemented with 9 ml of complete media. The flask was incubated vertically at 37 ºC, 0.5 % $C0_2$. Following 24 hours, cell growth was assessed (Olympus Tokyo 10x magnification) and the flask replaced horizontally in the incubator. Cell growth was assessed regularly. When cells reached confluence, the cell number was measured using a heamocytometer and cells were split. Cells reached confluence on average between 2-4 days following cracking open.

2.2.2. Mec-1 B-CLL Cells

Mec-1 cells were cultured in RPMI media (Gibco) supplemented with 10 % FBS (Invitrogen). Cells were cultured in 20 ml (75 cm^3 flask) or 40 ml (150 cm^3) of supplemented media. Cell number was measured using a haemocytometer, at $1.6x10^6$ cells/ml cells were split to 2 $x10^5$ cells/ml. Cells were split every 2-3 days.

2.2.3. HeLa and HEK 293T Cells

Cells were cultured in DMEM media (Gibco) supplemented with 10 % FBS and 1x PenStrep. Cells were cultured in 15 ml of media in 75 cm^3 flasks and 25 ml of media in 150 cm^3 flasks. Once cells were at 1.6 x 10^6, HeLa but not HEK 293T cells were washed with 10 ml hanks phosphate buffered saline. Both cell types were released from the flask surface by

incubation with 5 ml of trypsin. Cells were collected by centrifugation and the pellet was re-suspended in 10 ml of media. Cells were counted using a haemocytometer and either plated for transfection or diluted 1:8 in to culture flasks. Cells were split ever 2-3 days.

2.2.4. KATO III Cells

Kato III cells were cultured in Ham F12 medium (Gibco) supplemented with 10 % FBS, 5 % PenStrep and 2 mM L-Glutamine. Cells were cultured as HeLa and 293t cells. Cells grew partly adhered to the flask base and partly in suspension. Before centrifugation adhered cells were released from the flask base using a sterile cell scrapper. The cell pellet was re-suspended in 10 mls of media and split as HeLa and 293t.

2.2.5. Cell Counting

Cells were counted using a 5x5 grid haemocytometer. Two readings were taken for each count and the average was multiplied by 1×10^4, so calculating the number of cells per milliliter.

2.2.6. Plating Adherent Cells for Transfection

HeLa and HEK 293T cells were counted using the haemocytometer and plated at a final cell number of 5×10^4 cells per well in a 12 well plate, 1×10^5 cells per well in a 6 well plate and 5×10^6 cells in a 15 cm^3 plate.

2.2.7. Transfection

2.2.7.1. Nucleofection Transfection.

For each transfection $2x10^6$ Mec-1 cells were transfected via Nucleofection (Amaxa Biosystems) using Kit L and program C-05. In each case cells were transfected before reaching passage 20. Oligonucleotides were transfected at 50 nM, 100 nM, 250 nM, 500 nM and 1000 nM and RNA was harvested after 24 hours, 48 hours and 72 hours. All transfections were done in triplicate. RNA was extracted from transfected cells using RNaeasy kits (Quiagen).

2.2.7.2. Calcium Chloride Transfection

24 hours post-seeding media was replaced and cells were incubated for 4 hours. 100 µl of ice cold $CaCl_2$ solution (1 mM Tris-HCL pH 7.5, 0.1 mM EDTA, 300 mM $CaCl_2$) was mixed on ice with a specified amount of the plasmid to be transfected. All transfected plasmids were purified from E.Coli using an endofree midi-prep kit (Quiagen). 100 µl ice cold HBS solution (342.23 mM NaCl, 12.41 mM KCl, 1.76 mM Na_2HPO_4 (anhydrous), 13.88 mM Glucose, 52.45 mM Hepes pH 7.5) was added to the DNA:$CaCl_2$ mix and incubated on ice for 10 minutes. The DNA:$CaCl_2$:HBS mix was gently added to the plate of cells. After 24 hours cells were shocked for 3 minutes by incubation with pre-warmed DMEM:DMSO solution (75% DMEM:25% DMSO). Cells were then washed twice with DMEM before a further 24-48 hours of incubation.

2.2.7.2. Fugene Transfection

Optimum and Fugene (Roche) reagent were mixed 3:1 and incubated at room temperature for 5 minutes. DNA was added to the mixture and the reaction was incubated for 30 minutes. The reaction was added directly to cells and incubated overnight at 37 ºC, 0.5 % $C0_2$.

2.2.8. Transfection Efficiency Analysis

To assess the transfection efficiency of oligonucleotides into Mec-1 cells, cells were transfected as in 2.2.7.1. with an oligonucleotide labeled with Alexa 488 (emission: 520 nm) (250 nM). After 24 hours, transfection efficiency was analyzed utilizing the FITC channel on a BD FACS Canto III (BD Biosciences). The PE channel was used to detect the R-phycoerythrin (RPE) emission signal (575 nm) from mIgM immunostaining.

2.2.9. Fluorescence Microscopy

Fluorescence was detected from transfected constructs using a Nikon Eclipse TS100 microscope at 40x and 20x magnification. A eGFP filter 460 nm-500 nm was used to detect eGFP fluorophores and a Tx red filter 540 nm-580 nm was used to detect DsRed fluorophores.

2.3. In vitro RNA Methods

2.3.1. *In vitro* Transcription

2.3.1.1. Transcription Reaction

10x Hot Transcription Buffer (200 mM Tris HCL pH 7.5, 30 mM $MgCl_2$, 10 mM spermidine HCl, 50 mM NaCl), 1 µl Low GTP mix (GTP $1/10^{th}$ of ATP, CTP, GTP), 1 mM diguanosine triphosphate Sodium [G(5')ppp(5')G] (GE Healthcare), 5 mM DTT, 1 µl 50 ng/µl DNA template, 20 units RNaseOUT (Invitrogen), 10 µCi α^{32}P-GTP (PerkinElmer), 0.5 µl T7 Polymerase (1:50 dilution) in a total volume of 10 µl was mixed at ambient temperature. The reaction was incubated at 37 ºC for 1-2 hours, mixed with 10µl formamide dyes and loaded onto a 5 % polyacrylamide gel. The gel was run according to the transcript size. Transcripts were visualized using x-ray film and excised. RNA was eluted overnight at 4 ºC in 300 µl RNA Elution Buffer (0.5 M NaCl pH 5, 0.2 % SDS, 1 mM EDTA 0.5 M pH 8). Following elution, RNA was purified by ethanol precipitation, re-suspended in 20 µl TE.1 and stored at -80ºC.

2.3.1.2. Cold transcription

In a total volume of 100 µl 1x Cold Transcription Buffer (10x: 400 mM Tris pH 7.5, 200 mM $MgCl_2$, 100 mM NaCl, 20 mM spermidine HCl), 10 mM DTT, 4 mM NTP, 1 µg DNA template, 5µl T7 polymerase (1:50) and 200 units RNaseOUT were mixed at ambient temperature. The reaction was incubated at 37 ºC for 4 hours, divided into two 50 µl aliquots

and treated with 5 µl of DNase (Promega) for 30 minutes at 37 ºC in a final volume of 100 µl. 10 µl stop solution was added and the reaction was incubated for 10 minutes at 65 ºC. The transcription was passed through the appropriate spin column according to the transcript size (G-50 or S-300 (GE healthcare)) and purified by phenol chloroform extraction and ethanol precipitation. The pellet was dried and re-suspended in 20µl TE.1. The concentration of RNA was measured using a nanodrop and 500 ng was run on a 6% polyacrylamide gel to check RNA synthesis. The RNA stored at -80ºC.

2.3.1.3. Biotinylated Transcription

A cold transcription reaction was set up as 2.3.1.2., with 5 µg DNA template and 5 µl T7 polymerase (1:20). The reaction was supplemented with Bio-16-UTP (Ambion) to a final concentration of 100 nM and 25 µCi α^{32}P-GTP (Perkin Elmer). The reaction was incubated at 37 ºC for 4 hours. The reaction was divided into two 50 µl aliquots and treated with 10 µl DNase for 30 minutes at 37 ºC in a final volume of 100 µl. 10 µl stop solution was added and the reaction was incubated at 65 ºC for 10 minutes. The reaction was mixed 1:1 with formamide dyes and loaded onto a 6 % polyacrylamide gel. The products were visualized using X-ray film and excised and purified as described for a hot transcription (2.3.1.1.). The transcription was quantified using a nanodrop and the concentration calculated using the formula: A_{260} = L x Ɛ x Concentration (M) (where A_{260} = measured absorbance at 260 nM, L = length by default 1 cm, Ɛ = extinction coefficient, calculated using - http://biophysics.idtdna.com/UVSpectrum.html).

2.3.2. RNA Purification

2.3.2.1. RNA/DNA Shadowing

RNA or DNA to be purified was mixed 1:1 with formamide dyes, pre-heated for 20 seconds at 80 ºC and loaded onto a 6 % polyacrylamide gel. Once run, the gel plates were separated and the gel transferred onto saran wrap. The wrapped gel was placed on a piece of thin layer chromatography paper. The RNA was visualized using a UV wand that emitted long wave UV and was seen as a black shadow against the paper. The RNA band was excised and the RNA eluted in 300 µl H_2O overnight at 4ºC.

2.3.2.2. RNA Purification from Polyacrylamide Gel

RNA eluted overnight at 4 ºC in RNA elution buffer was separated from the excised gel fragment and supplemented with 900 µl ethanol. The RNA was ethanol precipitated, re-suspended in 20 µl TE.1 and stored at -80°C. Shorter RNA/DNA molecules purified through shadowing were eluted in H_2O. This elutant was supplemented with $1/10^{th}$ v/v sodium acetate (3 M) and ethanol precipitated at 4 ºC. The pellet was re-suspended and stored as normal.

2.3.3. *In vitro* Splicing

In a final volume of 10 µl 1 µl radiolabelled transcript was mixed on ice with 9 µl of a splicing-competent master mix (1.5 mM ATP, 20 mM creatine phosphate, 3.2 mM $MgCl_2$, 50 mM potassium glutamate, 20 mM Hepes (pH 7.5), 5 % NP40 (1 %), 20 units RNaseOUT (Invitrogen) and 50 % splicing competent nuclear extract (Cilbiotec). The reaction was

incubated at 30 ºC. 2 µl or 1.5 µl samples were taken at specific time points into a microtitre plate on dry ice. Time points were treated with 50 µl Proteinase K buffer (100 mM Tris-HCL pH 7.5, 12.5 mM 0.5 M EDTA, 150 mM NaCl, 1 % SDS) containing proteinase k (0.4 mg/ml) (Roche) for 15 minutes at 37 °C. The samples were then ethanol precipitated and re-suspended in 10 µl of formamide dyes. *In vitro* splicing reactions were run on 6 % denaturing polyacrylamide gels containing 25% formamide. Gels were fixed in 10 % IMS and 10 % acetic acid for 15 minutes before drying and exposing to a phosphorimager screen. Optiquant software was used to analyse results.

2.3.4. Stalling the *in vitro* Splicing Reaction

When stalling at A complex, a 2'-*O*-methyl modified anti-U6 oligonucleotide was used (5'-CUCUGUAUCGUUCCAAUUUU-3') to inhibit U6 snRNP activity (Dönmez et al., 2007). This oligonucleotide was incubated at a final concentration of 3 µM in nuclear extract for 15 minutes at 30 °C before addition to the splicing reaction. To stall at E complex ATP and creatine phosphate were left out of the splicing master mix and the nuclear extract was pre-incubated at 30 ºC for 30 minutes (Das and Reed, 1999).

2.3.5. 5' End Labeling Oligonucleotides

In 20 µl 100 pmoles of RNA oligonucleotide was added to 4 units polynucleotide kinase (Promega), 10 x polynucleotide kinase buffer and 5 µCi [γ -^{32}P]ATP (Perkin Elmer). The reaction was incubated at 37 °C for 1 hour, passed through a G-25 spin column (GE Healthcare) and stored at -80°C.

2.3.6. Modified Oligonucleotides

The sequences of splice altering modified RNA oligonucleotides' are shown in Table 2.1. Oligonucleotides 1-9 were synthesised by Eurogentec and 10-13 by integrated DNA technologies. Oligonucleotides 8 and 9 were a gift from Claudia Ghigna, Istituto di Genetica Molecolare - Consiglio Nazionale delle Ricerche (IGM-CNR), Pavia, Italy. Oligonucleotide abbreviations: s = phosphorothioate, o = 2'-*O*-methyl, L = LNA.

2.3.7. Oligonucleotide Test Reaction

The effect of oligonucleotides on splicing of pre-mRNA substrates was carried out in a final volume of 10 µl (1 x). 1 µl of radio labelled RNA, 100 mM potassium glutamate, 20 mM Hepes pH 7.5 and the desired amount of chemically modified RNA oligonucleotide was mixed on ice in a final volume of 5 µl. The reaction was annealed in a PCR machine (program: 80 °C 5 min, 70 °C 5 min, 60 °C 5 min, 50 °C 5 min, 40 °C 5 min, 30 °C 5 min) and then mixed with 5 µl of 1.5 mM ATP, 20 mM creatine phosphate, 3.2 mM $MgCl_2$ and 40 % nuclear extract (Cilbiotech). The reaction was incubated at 30 °C and time points were taken and processed in the same way as described in *in vitro* splicing (2.3.2.). Where E complex was isolated, ATP and creatine phosphate were excluded and the extract was pre- incubated at 30 °C for 30 minutes to remove ATP (Das and Reed, 1999).

2.3.8. Synthesis of Radioactive Ladder

2 µg of the commercial plasmid pBR322 (Fermentas) was mixed with 10 units HPA II and 10 x buffer 1 in a final volume of 10 µl and incubated at 37 ºC for 30 minutes. The

reaction was mixed in a final volume of 20 µl with 10 units of antarctic phosphatase (NEB) and 10 x antarctic phosphatase buffer and incubated at 37 ºC for 15 minutes. The reaction was stopped by incubation at 65 ºC for 15 minutes. In a total volume of 10 µl, 2 µl digested plasmid, 10 x T4 kinase buffer, 2 units of T4 polynucleotide kinase (Promega) and 2 µCi [γ-^{32}P]ATP (Perkin Elmer) were mixed and the reaction incubated for 30 minutes at 37 ºC. The reaction was passed through a G50 spin column (GE healthcare). The ladder was diluted in formamide dyes and stored -80ºC.

2.3.9. RNase H Assays

2.3.9.1. Assessing Binding Affinity of Different Oligonucleotide Chemistries

An annealing reaction (1 x) containing *SMN2* oligonucleotides 1 (GGA-b), 4 (GGA-O) and 7 (GGAL/O) (50 nM, 100 nM, 250 nM, 500 nM) was set up and incubated at 30 ºC for 30 minutes. 50 pmoles of a DNA oligonucleotide (MWG eurofins) seq: 5'-GATTTTGTCTAAAAC-3' and 2.5 U RNase H (NEB) was added and the reaction was incubated at 30 ºC for 30 minutes. Reactions were treated with 50 µl of PNK buffer containing Proteinase K (0.4 mg/ml) (Roche) for 15 minutes at 37 ºC, ethanol precipitated and re-suspended in 10 µl formamide dyes. 5 µl of each sample was incubated at 80 ºC for 20 seconds and loaded onto a 6 % denaturing polyacrylamide gel containing 25 % formamide. The gel was run for 1.5 hours at 18 watts, fixed in 10 % IMS:10 % acetic acid and dried. Results were visualized using a phosphoimager screen (Eperon et al., 2000).

2.3.9.2. Assessing RNA Binding of the *SMN2* Bifunctional Oligonucleotide throughout Splicing

To investigate the binding of the oligonucleotide in E or A complex the splicing reaction was stalled at these complexes (Das and Reed, 1999). A 1 x oligonucleotide test reaction containing 250 nM oligonucleotide 1 in the annealing reaction and 1.5 units of RNase H (NEB) in the splicing reaction was set up. The annealing and splicing master mixes were kept separately on ice for the duration of the experiment. The 2 hour time point was initiated first and as each time point was reached 2.5 µl of the splicing reaction and 2.5 µl of the annealing reaction were combined and the plate sealed and incubated upside down in a 30 ºC oven. 50 pmoles of a DNA oligonucleotide (MWG Eurofins) seq: 5'-GATTTTGTCTAAAAC-3' was added to each relevant 5 µl time point and the plate was re-incubated for 10 minutes at 30 ºC. Samples were treated with 50 µl of PNK buffer containing Proteinase K (0.4 mg/ml) (Roche) for 15 minutes at 37 ºC, ethanol precipitated and re-suspended in 10 µl formamide dyes. Each time point was incubated at 80 ºC for 20 seconds and 5 µl was run on a 6% denaturing polyacrylamide gel containing 25 % formamide for 1.5 hours at 18 watts. The gel was fixed in 10 % acetic acid:10 % IMS, dried and exposed to a phosphorimager screen (Eperon et al., 2000).

2.3.10. Psoralen Cross-linking

A 0.5 x oligonucleotide test reaction was set up for each condition containing 250 nM oligonucleotide 1. The reaction was supplemented with $1/60^{th}$ v/v Trioxsalen 4'amino methyl, hydrochloride (2 mg/ml) (Calbiochem). Two time points were used, t = 0 and t = 5 minutes,

each of which were 2.5 µl. The 0.5 x oligonucleotide test reaction was divided in the t = 0 samples were directly cross-linked through a glass plate with long wave UV peak 365 nm (UVP Bio-lite) and the t = 5 samples were sealed and incubated upside down in a 30 ºC oven for 5 minutes. The 5 minute plate was cross-linked in the same manner. Following cross-linking, samples were treated with 50 µl of PNK buffer containing Proteinase K (0.4 mg/ml) (Roche) for 15 minutes at 37 ºC and ethanol precipitated. Following re-suspension in 10 µl of formamide dyes, the samples were pre-incubated at 80 ºC for 20 seconds and 5 µl was loaded on to a 5 % denaturing polyacrylamide gel containing 25% formamide. The gel was run for 1.5 hours at 18 W and fixed for 15 minutes in 10 % acetic acid, 10 % IMS solution. The gel was exposed to a phopshorimager screen and quantified using optiquant software (Eperon et al., 2000).

2.3.11. Real-Time PCR

Synthesis of CDNA was done using 500 ng of RNA in the presence Superscript III (Invitrogen). Q-PCR (Rotor-Gene 3000, Corbett Research) was carried out using a Sybr Green detection method (Quantace). PCR reactions were done in a final volume of 20 µl and RNA was diluted 1:10 before analysis. PCR primers were used that could selectively detect the polyadenylated (μ_S) and spliced isoform (μ_m). μ_S primers were used at a final concentration of 300 nM and μ_m primers at 150 nM. A plasmid standard of a known concentration containing the μ_S and μ_m PCR products was used to quantify all qPCR reactions. A threshold value was determined and used uniformly between comparable samples to calculate the expression

levels. The ratio of μ_S/μ_m expression was plotted. All transfections and qPCR reactions were done in triplicate.

2.4. *In vitro* Protein Methods

2.4.1. Native Gel Complex Analysis of Spliceosomal Complex Formation

2.4.1.1. ABC Complex Gels

Splicing reactions were set up and time points taken as described for *in vitro* splicing (2.3.2.). Before loading, samples were treated with 0.8 mg/ml heparin for 30 minutes at ambient temperature. 2.5 µl of tris:glycine loading dyes were added and samples were loaded onto 2 % native LMP agarose gel. The running buffer was 50mMTris:50mM Glycine. Gels were run at 100 V at 4 °C for 4.5hours (Das and Reed, 1999). To stall the splicing reaction at A complex the anti-U6 oligonucleotide (Dönmez et al., 2007) was used as in 2.3.4.. To identify A complex containing U2 snRNP two RNase H compatible DNA oligonucleotides were used to cleave U2 snRNA and inhibit U2 snRNP activity in nuclear extract seq: E15) AGGCCGAGAAGCGAT, L15) CACATACTACAGTTG (Black et al., 1985). Nuclear extract was pre-incubated with 50 pmoles of each oligonucleotide for 30 minutes at 30 °C with 15 units of RNase H (NEB) per 50 µl nuclear extract.

2.4.1.2. E Complex Gels

To isolate E complex, ATP, creatine phosphate and $MgCl_2$ were excluded from the splicing mix and nuclear extract was pre-incubated at 30 °C for 30 minutes. Samples were not treated with heparin before loading. To confirm the presence of E complex, an anti-U1 2'-*O*-

methyl oligonucleotide ($^{5'}$TGCCAGGTAAGTAT$^{3'}$) was used. 80 pmoles of oligonucleotide was added per 10 µl of nuclear extract and incubated at 30 °C for 30 minutes.

2.4.2. Immunostaining

Following transfection with the ESE-blocking oligonucleotide, $1x10^6$ cells were collected and washed twice in PBS at 4 ºC. The cell pellet was re-suspended in RPE labeled mouse anti-IgM:RPE antibody (1:200) (Serotec UK) and incubated in the dark at 4 °C for 15 minutes. Cells were washed and re-suspended in PBS before analysis. All experiments were done in triplicate.

2.4.3. UV Cross-linking

A 5 µl (1/2 splicing reaction) was set up containing the required radiolabelled substrate and incubated in a 30 °C oven, upside down in a sealed microtiter plate for 15 minutes. Samples for the zero time-point were not incubated. Samples were cross-linked using the 254 nm Spotcure for 5 minutes. Samples were digested with 0.25 µl RNase A (NEB) and T1 (Fermentas) for 10 minutes at 37 °C before being mixed with 5 µl SDS dyes. Samples were pre-heated at 80 °C for 1 minute before resolving on a 10 % SDS gel. The resolved proteins were then transferred to a nitrocellulose membrane, before drying and exposing to a phosphoimager screen.

2.4.4. UV Cross-link-Immunoprecipitation

1 µl of hnRNP H/F antibody (abcam: ab10689) and 0.34 µl Living Colors full-length A.v. polyclonal antibody (Clonetech: 632460) were used per immunoprecipitation. The antibody was pre-bound to 37.5 µl of protein G agarose beads (Pierce) per reaction in 9 µl BSA (10 mg/ml) and 900 µl PBS for 2 hours rotating at 4 ºC. The beads were washed 3 x in PBS. 4 x splicing reaction containing [α^{32}P]-GTP labeled substrates were set up for each sample. The reactions were divided into 10 µl aliquots in a microtitre plate, sealed and incubated upside down in a 30 ºC oven for 15 minutes. Samples were cross-linked for 5 minutes using a 254 nm Spotcure, before being pooled and centrifugated at 13 K for 1 minute. The cross-linked splicing reactions were pre-cleared rotating at 4 ºC for 2 hours through addition of 50 µl protein G agarose beads (Pierce) and 300 µl IP buffer (20 mM Hepes pH 8, 1.5 mM $MgCl_2$, 0.05 % NP40, 200 mM NaCl). The beads were removed from by settling for 15 minutes on ice and the reaction was added to the washed beads bound to antibody. The combined reactions were incubated rotating at 4 ºC for 2 hours. The samples were added to a column (Biorad) and the beads were washed with 10 ml of ice cold IP buffer each. The columns were pulsed in the centrifuge to remove excess buffer and 25 µl SDS dyes were added to each. Columns were incubated in eppendorfs at 90 ºC for 5 minutes and proteins eluted by pulsing in a centrifuge. Samples were resolved on a 12 % SDS gel, transferred onto nitrocellulose and visualized using a phophorimager screen.

2.4.5. Immunoprecipitation of Radioactive RNA

2 µl of an U1A antibody (abcam (ab55751)) was pre-bound to 15 µl of protein G agarose beads (Pierce) in 900 µl PBS and 0.1 mg/ml BSA rotating for 2 hours at 4 ºC. Antibody bound protein G beads were washed 3 x in PBS at 4ºC. An 8 x oligonucleotide test reaction, that satisfies E complex conditions only (Das and Reed, 1999), was set up containing 250 nM oligonucleotide 1. Three RNA's of different sizes were precipitated together in the same IP, allowing for quantification of the effect of the oligonucleotide 1 on U1snRNP binding and immunoprecipitation of the *SMN2* Ex7 -defined substrate. Hot RNA substrates were quantified using cherenkov detection on a scintillation counter (LS 6500 multipurpose scintillation counter, Beckman Coulter) and the number of moles of each was calculated making the reading relative to the number of G in each. An equal number of moles of each radiolabelled substrate were used. The splicing reaction was incubated for 15 minutes at 30 ºC and then pre-cleared by rotating at 4 ºC for 2 hours with 50 µl of protein G bead slurry and 300 µl IP buffer (20 mM Hepes pH 8, 1.5 mM $MgCl_2$, 0.05 % NP40, 200 mM NaCl). The beads were removed from the splicing reaction by settling and the reaction was added to the antibody bound protein G beads. The reaction was rotated at 4 ºC for 2 hours. The beads were allowed to settle on ice for 10 minutes and the supernatant was discarded. The beads were washed 5 x in IP buffer at 4 ºC, allowing the beads to settle for 10 minutes in between each wash. The RNA was eluted by incubation with 50 µl of PNK buffer containing Proteinase K (0.4 mg/ml) (Roche) for 15 minutes at 37 ºC. The reaction was centrifugated and the supernatant ethanol precipitated. The pellet was re-suspended in 10 µl formamide dyes, incubated at 80 ºC for 20 seconds and loaded on to a 6 % denaturing polyacrylamide gel. The

gel was dried and radioactivity detected using a phosphorimager screen, which was quantified using image quant software.

2.4.6. Western Blot Analysis

Protein samples were heated at 80 ºC for two minutes and resolved on SDS gels. The gel was run at 80 V through the stacking and 150 V through the separating gel, until the bromophenol blue had run off. Samples were transferred to nitrocellulose membrane. The blot was blocked overnight at 4 ºC in 5 % milk, 1 x TBS (20 mM Tris-HCL pH 7.5, 150 mM NaCl) and 0.1 % Tween-20. All further steps were carried out rocking at ambient temperature. The blot was washed in 1 x TBS and 0.1% Tween-20 for 10 minutes. The blot was incubated with the correct dilution of primary antibody in 1 % milk, 1 x TBS and 0.1 % tween for 1 hour. The blot was washed again with 1 x TBS and 0.1 % Tween-20 for 15 minutes, changing the wash buffer 3 times. The blot was incubated with a 1:1000 dilution of protein A/G (Peirce), diluted in 1 % milk, 1 x TBS and 0.1 % Tween-20 for one hour and then it was washed in 1 x TBS and 0.1 % Tween-20 for 30 minutes, changing the buffer 3 times. The protein A/G signal was detected using ECL solution (Peirce) as per the protocol provided, and the signal detected using x-ray film.

2.4.7. Biotin Affinity Purification

Biotinylated RNA (250 nM) was annealed to oligonucleotide (250 nM) in a 10 x oligonucleotide test reaction. The nuclear extract used was pre-cleared by centrifugation at 13 000 rpm for 30 seconds before addition to the splicing reaction. The reaction was incubated at

30 ºC for 20 minutes. 30 µl NeutrAvidin agarose resin (ThermoScientific) (10:3, splicing reaction:bead slurry) was washed once in 1 ml wash buffer (100 mM Tris HCL pH 7.5, 1 % SDS, 10 mM DTT) and 3 x in buffer D (20 mM Hepes pH 8, 10 % v/v Glycerol, 0.2 mM EDTA, 100 mM KCL). The splicing reaction and beads were mixed and incubated rotating at 4 ºC for 2 hours. The reaction was added to a column (BioRad) and washed with 20 ml salt containing sodium phosphate buffer (100 mM sodium phosphate pH 7.2, 150 mM sodium chloride, 0.05 % NP40) and 10 ml salt lacking sodium phosphate buffer (100mM sodium phosphate pH 7.2, 0.05 % NP40). The columns were briefly centrifuge to remove excess buffer. 25 µl of SDS dyes were added and the column was incubated at 90 ºC for 5 minutes. To elute protein the column was briefly centrifuged. The entire reaction was loaded onto a 10 % SDS gel and proteins were visualized by silver staining.

2.4.8. Silver Staining

Gels were soaked in 50 % acetone, 0.1 % 37 % formaldehyde and 20 µl TCA. Gels were washed in H_20, 50 % acetone and then again in H_20. Gels were incubated with 85 µl 6.4 % $Na_2S_2O_3$ in a total volume of 50 ml and then washed in H_2O. This was followed by an 8 minute wash in 0.14 g $AgNO_3$, 2 % 37(38) % formaldehyde and a wash in water. The gel was submerged in 1 g Na_2CO_3, 21 µl 6.4% $Na_2S_2O_3$, 21 µl 37(38) % formaldehyde for ≈ 10 seconds. The reaction was stopped with 1 % acetic acid, 50 % acetone and the gel was dried (Promega).

2.4.9. Nuclear Extraction

Cells were harvested and washed once in PBS. The cell pellet was re-suspended in 1 packed cell volume of buffer A (10 mM Hepes pH 8, 1.5 mM $MgCl_2$, 10 mM KCl, 1 mM DTT, 25 µl per 400 µl 1% NP40) and left to swell on ice for 15 minutes. Cells were lysed by vortexing and pelleted by centrifugation. The pellet was re-suspended in 2/3 of the original packed cell volume of buffer C (20 mM Hepes pH 8, 25 % v/v glycerol, 420 mM NaCl, 0.2 mM EDTA, 1 mM DTT) and incubated on ice for 30 minutes stirring. The debris was removed by centrifugation and the supernatant was dialyzed (25 mm Millipore filters pore size 0.025 µm) against buffer D (20 mM Hepes pH 8, 10% v/v glycerol, 100 mM KCl, 0.2 mM EDTA, 1 mM DTT) at 4 ºC for 2 hours, before snap freezing and storing at -80º.

Table 2.1. Splice altering RNA oligonucleotides. (Abbreviations see Methods 2.8.8.)

	Name	Number	Cap	Tail	Annealing	Sequence
SMN2	SMN2-GGA	1	pS	RNA	pS/2'OMe	AsGsGsAsGsGACGGAGGACGGAGGACA-GoAoUosUosUosUosGosUoCoUoAoAosAosAosCo
	NT	2	/	/	pS/2'OMe	GoAoUosUosUosUosGosUoCoUoAoAosAosAosCo
	TO	3	pS	RNA	/	AsGsGsAsGsGACGGAGGACGGAGGACA
	SMN2-GGAO	4	2'OMe	2'OMe	2'OMe	AoGoGoAoGoGoAoAoCoGoGoAoGoGoAoCoGoGoAoGoAoCoAoGoAoUoUoUoUoGoUoCoUo AoAoAoAoCo
	ONT	5			2'OMe	GoAoUoUoUoUoGoUoCoUoAoAoAoAoCo
	OTO	6	2'OMe	2'OMe	/	AoGoGoAoGoGoAoAoCoGoGoAoGoGoAoGoAoCoAo
	GGA-L/O	7	LNA	RNA	LNA/2'OMe	ALGLGLALGLGACGGAGGACGGAGGACAGLAOULUOULUOGLUOCLUOALAOALAOCO
RON	RON-GGA	8	2'OMe	2'OMe	2'OMe	AoGoGoAoGoGoAoAoCoGoGoAoGoAoCoGoGoAoGoGoAoAoCoAoCoCoAoAoUoGoUoCoCoCoCoC oCoGoGoAoAoAoCo
	RON-NT	9			2'OMe	CoCoAoUoGoUoCoCoCoCoCoCoGoGoAoAoAoCo
IGM	Cstf-64 Recruiter	10	2'OMe	2'OMe	2'OMe	GoGoUoCoCoCoCoCoAoAoGoUoGoUoUoUoUoGoCoGoCoAoGoCoAoCoAoGoCoCoGoGoCoC oAoCoCoCoCoCoAo
	3'ss Block	11	/	/	2'OMe	GoCoGoGoCoUoCoAoCoCoUoCoCoCoCoCoUoCoUoGoCoAoGoGoGoAoGoAoCoAoCoAo
	5'ss Block	12	/	/	2'OMe	AoCoAoCoGoGoUoUoGoUoAoCoAoGoGoGoGoUoGoUoUoUoAoCoCoGoGoGoUoGoGo
	ESE Block	13	/	/	2'OMe	GoCoCoCoCoAoCoAoGoGoUoUoCoUoCoAoAoAoGoGoCoCoCoUoUoCoGoUoCoGo

Table 2.2. General Oligonucleotides.

Name	Oligonucleotide Sequence	Number
T7 Exon 2 βB	AAATTAATACGACTCACTATAGGGCTGCTGGTTGTCTACCCA	**1A**
βG Exon 3-U1	AACTTACCTGCCAAAATGATGA	**2A**
T7 βG(2)40XLF	AAATTAATACGACTCACTATAGGGTAGTCGCCTGCTTTTCTGCC	**3A**
END βG(2)40XL R	TGCCCCCTCCATATAACATG	**4A**
βG 40nt Frag F	AAATTAATACGACTCACTATAGGGCTCTGCTAACCATGTTCATGCCTTCTTCTTTTTCCTACAG	**5A**
βG 40nt Frag R	CTGTAGGAAAAAGAAGAAGGCATGAACATGGTTAGCAGAG-CCCTATAGTGAGTCGTATTAATTT	**6A**

Table 2.3. Chapter 3 Oligonucleotides.

Name	Oligonucleotide Sequence	Number
T7 MidInt 6 *SMN2*	AAATTAATACGACTCACTATAGGGAATAAAATAAGTAAAATGTC	**1B**
MidInt 7 *SMN2*	AACTTAC-TAATAGTTTTGGCATCAAAA	**2B**
T7 *SMN2* Exon 7	AAATTAATACGACTCACTATAGGGGGTTTTAGACAAAATCAAAA	**3B**
End *SMN2* Exon7 U1	AACTTACTCCTGATTTAAGGAATGTGA	**4B**
***SMN2*midint7redA**	TAATAGTTTTGGCAT	**5B**
***SMN2*midint7redC**	TACATTAACCTTTCA	**6B**
***SMN2*midint7redD**	CTAACATCTGAACTT	**7B**
***SMN2*midint7redE**	ATGTTCAAAAACATT	**8B**
***SMN2*midint7redF**	TCCACAAACCATAAA	**9B**
***SMN2*midint7redH**	CATAATGCTGGCAGA	**10B**
T7 SMN(7)40XLF	AAATTAATACGACTCACTATAGGGATATAGCTATTTTTTTTAAC	**11B**

END SMN(7) 40XLR	ACAAAAGTAAGATTCACTTT	**12B**

Table 2.4. Chapter 4 Oligonucleotides.

Name	Oligonucleotide Sequence	Number
T7 Exon 10	AAATTAATACGACTATAGGGTGTGAGAGGCAGCTTCCAGA	1C
T7 Exon 11	AAATTAATACGACTATAGGGCTGGGCGCTGTGGCTGA	2C
Blunt Exon 11	TATATTGGGCTGGGCGC	3C
End Ex11 Blunt R	TCCAGCTGGGCTGCCTACCTGCAATGGGGCACCATC	4C
EX11-INT11	TGCCTACCTGCAATGGGGCACCATCCT	5C
EX11-U1	AACTTACCTGCTGCAATGGGGCACCATCCT	6C
END EXON 12	CTAGCTGCTTCCTCCGCCA	7C
End Exon 12 Intron 12	AACTCACCTAGCTGCTTCCTCCGCCA	8C
Exon 12-U1	AACTTACCTAGCTGCTTCCTCCGCCA	9C
T7 MID Int βG	AAATTAATACGACTCACTATAGGGTTATATGGTCGACTCTGCT	10C

End Int βG Rev	CTGTAGGAAAAAGAAGA	11C
βG Int – Ex11 Rev	AGCGCCCAGCCCAATATACTGTAGGAAAAAGAAGAA	12C
MIDINT10-MIDβG	AGCAGAGTCGACCATATAATTTCA-GATCCCCAACTGT	13C
MID INTRON βG	TTATATGGTCGACTCTGCT	14C
MIDβG-MIDINT10B	AGCAGTAGGCTGGCCCCTACCATGAATTTTACAATAGCGAA	15C
MID INT11-MID βG	AGCATAGTCGACCATATAACTGCCCGTGTTTCCCAGGGA	16C
MID βG – MID INT11	AGGCCCAGCCTGTAGGCCCTCATGCCTTTTACAATAGCGAA	17C
MID INTRON 10	GTAGGGGCCAGCCTACTGCT	18C
MID INTRON 11	AGGGCCTACAGGCTGGGCCT	19C
EX10–βG INTRON	AGCATGCCATTAAGTTTGAGGTGAGTTTGGGGACCCTT	20C
EX10 – βG INT REV	AAGGGTCCCCAAACTCACCTCAAACTTAATGGCATGCT	21C
βG INTRON –	TTCTTCTTTTTCCTACAGTATATTGGGCTGGGCGCT	22C

EX11		
EXON 11 – βG INT	AGGATGGTGCCCCATTGCAGGTGAGTTTGGGGACCCTT	23C
EX11 – βG INT REV	AAGGGTCCCCAAACTCACCTGCAATGGGGCACCATCCT	24C
βG INTRON – EX 12	TTCTTCTTTTTCCTACAGGTCTGCGTAGATGGTGAATGTCA	25C
βG INT – EX12 REV	TGACATTCACCATCTACGCAGACCTGTAGGAAAAAGAAGAA	26C
Int10 βG3 Fw	TCATGACCCTCTCTGCAGCTCCTGGGCAACGTGCTGGT	27C
INT10 – βG3 Rw	ACCAGCACGTTGCCCAGGAGCTGCAGAGAGGGTCATGA	28C
Int11 – βG3 Fw	AGTTGCCACCTGCCCCCAGCTCCTGGGCAACGTGCTGGT	29C
INT11 – βG3 Rw	ACCAGCACGTTGCCCAGGAGCTGGGGGCAGGTGGCAACT	30C
βG2 Int10 Fw	TGGATCCTGAGAACTTCAGGGTAAGTGTAAGGGATAGGGGCA	31C
βG2 Int10 Rev	TGCCCCTATCCCTTACACTTACCCTGAAGTTCTCAGGATCCA	32C
βG2 Int11 Fw	TGGATCCTGAGAACTTCAGGGTAGGCAGCCCAGCTGGACCT	33C

βG2 Int11 Rev	AGGTCCAGCTGGGCTGCCTACCCTGAAGTTCTCAGGATCCA	34C
T7 Mid Int βG	AAATTAATACGACTCACTATAGGGCTCTGCTAACCATGTTCAT	35C
End βG Int Rev	CTGTAGGAAAAAGAAGAA	36C
Gradually Replacing Intron inhibitory region Oligonucleotides		
INT10A RON R11	ATGAGGACCAGCCAGTAGGCGACCATATAACATGAATTT	37C
INT10B RON R11	TGCAGAGAGGGTCATGAGGACGTTAGCAGAGTCGACCATAT	38C
INT10CRON R11(B)	TTGCCCAGGAGCTGCAGAGAGGGCATGAACATGGTTAGCAGA	39C
βG – RONInt10 AF	CCTCATGGCTGGTCCTCAT	40C
βG – RONInt10 BF (B)	GTCCTCATGACCCTCTCTGCA	41C
βG – RONInt10 CF (B)	CCTCTCTGCAGCTCCTGGGCAA	42C
βG Int11RON AF	TTATATGGTCGACGGCTGGGCCTGAGTT	43C
βG Int11RON AR	GTCGACCATATAA	44C

βG Int11RON BF	TCTGCTAACCATGGAGTTGCCACCTGCC	45C
βG Int11RON BR	CATGGTTAGCAGA	46C
βG Int11RON CF	TTCATGCCTTCTTCTGCCCCCAGCTCCT	47C
βG Int11RON CR	AAGAAGGCATGAA	48C
Mutagenesis Oligonucleotides		
RON Int10bpF	CCAGCCTACTG	49C
βG RON Int10bpR	CAGTAGGCTGGGTCGACCATATAACA	50C
RON Int11bpF	GGGCCTGAGTT	51C
βG RON Int11bpR	AACTCAGGCCCGTCGACCATATAACA	52C
Int10βG BP R	CATGAACATGGTTAGGCTGGCCCCTACTTT	53C
Int11βG Bp R	CATGAACATGGTTAGGCCCAGCCTGTAGGC	54C
βG BP F	CTAACCATGTTCATG	55C
BranP Int 10AF	GGATCTGAAAGTAGGGGCCATACTAACTGGCTGGTCCTCATGACCCT	56C

BranP Int10AR	AGGGTCATGAGGACCAGCCAGTTAGTATGGCCCCTACTTTCAGATCC	57C
BranP Int10BF	GCCAGCCTACTGGCTGGTCCTACTAACCCTCTCTGCAGTATATTGGG	58C
BranP Int10BR	CCCAATATACTGCAGAGAGGGTTAGTAGGACCAGCCAGTAGGCTGGC	59C
BranP Int11AF	CTGGGAAACACGGGCAGAGGTACTACAGGCTGGGCCTGAGTTGCCA	60C
BranP Int11AR	TGGCAACTCAGGCCCAGCCTGTAGTACCTCTGCCCGTGTTTCCCAG	61C
BranP Int11BF	GCAGAGGGCCTACAGGCTGGTACTAACTTGCCACCTGCCCCCAGGTC	62C
BranP Int11BR	GACCTGGGGGCAGGTGGCAAGTTACTACCAGCCTGTAGGCCCTCTGC	63C
Int11 5'SS F	AGGATGGTGCCCCATTGCAGGTAAGTAGCCCAGCTGGACCTCCCTGG	64C
Int11 5'SS R	CCAGGGAGGTCCAGCTGGGCTACTTACCTGCAATGGGGCACCATCCT	65C

Cross-linking Substrate Oligonucleotides		
T7 3' Int10	AAATTAATACGACTCACTATAGGGGTAGGGGCCAGCCTACTGGCT	66C
T7 3' Int11	AATTAATACGACTCACTATAGGGAGGGCCTACAGGCTGGGCCT	67C
End Int10	CTGCAGAGAGGGTCATGAGGA	68C
End Int11	CTGGGGGCAGGTGGCAACTCA	69C
Int10/11inhibRF	AAATTAATACGACTCACTATAG	70C
Int10 inhibRR	CTGCAGAGAGGGTCATGAGGACCAGCCAGTAGGCTATAGTGAGTCGTATTAATTT	71C
Int11 inhibRR	CTGGGGGCAGGTGGCAACTCCTATAGTGAGTCGTATTAATTT	72C
T7 RON(11)40B	AAATTAATACGACTCACTATAGGGCCAGCCTACTGGCTGGT	73C
ENDRON(11)40XLR	CTGCCCGTGTTTCCCAGGGA	74C
Lengthening Intron Oligonucleotides		
Int10 Length F	GGACAGTTGGGGATCTGAAAAAAATTCATGTTATATGGTCGTA	75C

	GGGGCCAGCCTACTGGC	
Int10 Length R	GCCAGTAGGCTGGCCCCTACGACCATATAACATGAATTTTTTT CAGATCCCCAACTGTCC	76C
Int11 Length F	TCCCTGGGAAACACGGGCAGAAAATTCATGTTATATGGTCAGG GCCTACAGGCTGGGCCT	77C
Int11 Length R	AGGCCCAGCCTGTAGGCCCTGACCATATAACATGAATTTTCTG CCCGTGTTTCCCAGGGA	78C

Table 2.5. Chapter 5 Oligonucleotides.

Name	Oligonucleotide Sequence
1A	ATTCTCGAGCTGGAGGCGGTTCAGCCCTGCACAGGCCCGATGT
1B	TAGGATCCGCTCCCTCCACCTACCTTGAACAAGGTGACGGTGGTAC
Ex4A Realtime	CCTGCACAGGCCCGATGTC
Ex4M1 Realtime	GGCGCTCACCTCCCCCTCGGTG
Ex3Ex4 Realtime	CATCTCCCGGCCCAAGGGGGT
EX4B Realtime	CACACACAGAGCGGCCAGCC

Table 2.6. Site-Directed Mutagenesis Oligonucleotides.

Name	Oligonucleotide Sequence
Construct 2F	TAAAATTCATGGTAGGGGCCAGCCTACTGGCTGGTCCTCA
Construct 2R	TGAGGACCAGCCAGTAGGCTGGCCCCTACCATGAATTTTA
SD Int11 BPAF	AACACGGGCAGAGGTACTAACGGCTGGGCCTGAGTTGCCA
SD Int BPAR	TGGCAACTCAGGCCCAGCCGTTAGTACCTCTGCCCGTGTT

3. Analysis of *SMN2* Bifunctional Oligonucleotide Action

3.1. Introduction

There have been a number of studies into the use of oligonucleotides to alter the pre-mRNA splicing of *SMN2* exon 7 in SMA (reviewed in Burghes and McGovern, 2010). The current study investigates the mechanism of action of the *SMN2* bifunctional oligonucleotide (Oligonucleotide 1; Table 2.1), which has been shown to induce inclusion of *SMN2* exon 7 (Skordis et al., 2003; Owen et al., 2011). A greater understanding of the mechanism of action of this oligonucleotide will allow for the targeted development of new bifunctional oligonucleotides to alter similar mis-splicing events in other diseases.

3.2. Analysis of RNA Binding Affinity and Chemical Composition of the *SMN2* Bifunctional Oligonucleotide

Owen et al. (2010) recently identified that oligonucleotide 1 is firstly targeted to the optimum place to stimulate *SMN2* exon 7 inclusion and that secondly the activity of this oligonucleotide is dependent on its chemical composition (Owen et al., 2011). In the current investigation, an RNase H protection assay was used to assess the RNA binding capacity of oligonucleotide 1 in specific splicing conditions (Figure 3.2. and 3.3.). Using an RNase H compatible DNA oligonucleotide (500 nM) of the same sequence as the annealing region of oligonucleotide 1, it was possible to identify whether oligonucleotide 1 protects RNA from digestion and hence determine its RNA binding activity during splicing. Throughout this study, a construct composed of *SMN2* exon 7 with flanking intronic regions between exons 2 and 3 of rabbit β-globin was used to assess oligonucleotide 1 action (Figure 3.1.). This

construct has been used previously to study the effect of oligonucleotide 1 on *SMN2* exon 7 splicing *in vitro* (Skordis et al., 2003).

Oligonucleotide 1 (GGA*) (250 nM) was annealed to the *SMN2* transcript and a splicing reaction carried out, following which the RNase H compatible DNA oligonucleotide was added and the RNA substrate digested accordingly. It was seen that oligonucleotide 1 remained bound to the *SMN2* transcript throughout a splicing time-course (Figure 3.2. A) and that after 2 hours the oligonucleotide maintained protection of exon 7 containing mRNA. Oligonucleotide 1 was also shown to be functional as it increased the amount of exon 7 included mRNA. The affinity of oligonucleotide 1 for RNA was also investigated in conditions known to block assembly at E and A complex. Oligonucleotide 1 protected RNA from digestion in each case and so is still bound to the *SMN2* transcript in both of the conditions tested (Figure 3.2. B and C).

Selection of chemical modification is an integral part of oligonucleotide design, as oligonucleotide chemistry has been shown to effect oligonucleotide activity (Owen et al., 2011). In the current study, an RNase H protection assay was carried out in the presence of increasing concentrations of oligonucleotides 1, 4 and 7 (Table 2.1.) (50 nM, 100 nM, 250 nM, 500 nM) (Figure 3.3.). Oligonucleotide 1 was seen to exhibit a lower RNA binding affinity than both 4 and 7 (Binding stability = 1<4<7). However, the batch of oligonucleotide 1 (GGA-b) used in this experiment was later shown to be less active at stimulating exon 7 splicing than oligonucleotide 4 and other batches of oligonucleotide 1 (Figure 3.4. A). Therefore a conclusion on the relationship between RNA binding affinity and activity of oligonucleotide 1 cannot be made here. Owen et al. (2010) showed that oligonucleotide 4 had

a greater effect on *SMN2* exon 7 splicing and SMN protein expression than 7. This indicates that in the case of oligonucleotide 4 and 7, RNA binding affinity is inversely proportional to the success of that oligonucleotide at stimulating *SMN2* exon 7 splicing and SMN protein expression (Owen et al., 2011). However, results shown here indicate that the diminished effect on splicing and protein expression seen with oligonucleotide 4 and 7, in comparison with 1 (Owen et al., 2011), is not due to the failure of these oligonucleotides to anneal to the pre-mRNA, but due to another factor, for example oligonucleotide rigidity or secondary structure.

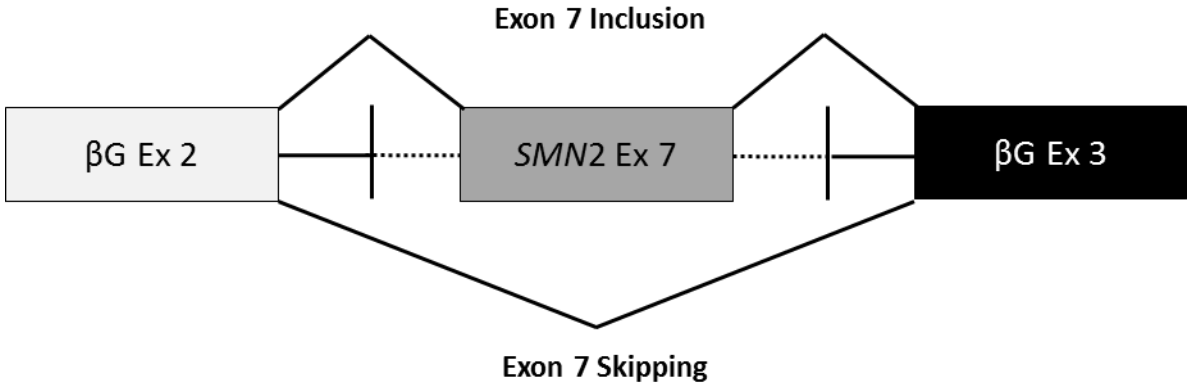

Figure 3.1. Diagram of the *SMN2*/β-globin construct. Composed of *SMN2* exon 7 flanked by sections of *SMN2* introns 6 and 7 and inserted within β-globin intron 2. The upstream exon is β-Globin exon 2 and the downstream exon is β-globin exon 3. Light grey box = β-globin exon 2, dark grey box = *SMN2* exon 7, black horizontal lines = β-globin introns, dashed horizontal lines = *SMN2* introns 6 and 7, black vertical lines = join between β-globin intron and *SMN2* intron 6 and 7 respectively. The sequence of this construct can be found in the appendix (7.2.3.).

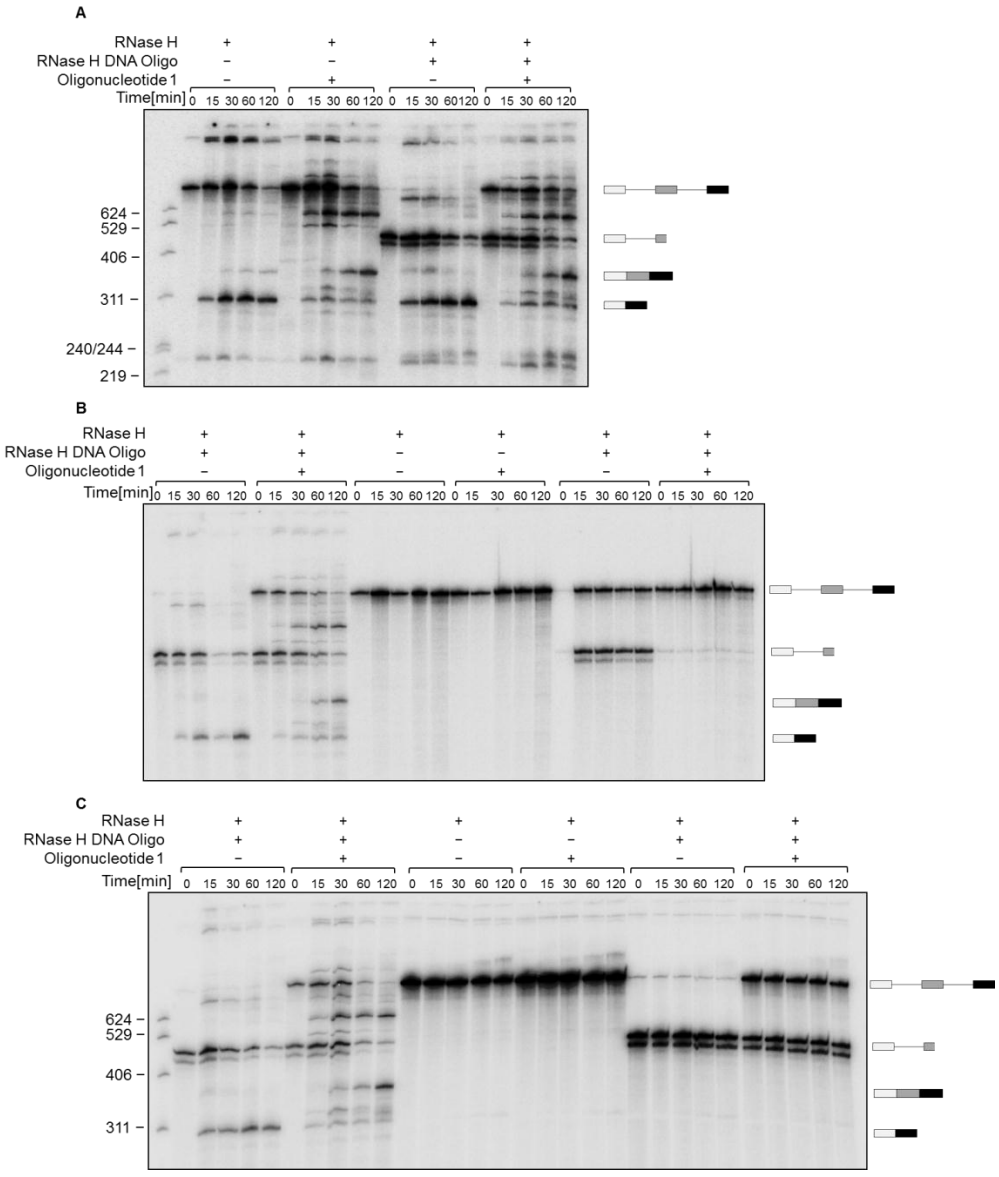

Figure 3.2. Oligonucleotide 1 is bound to its target site in exon 7 throughout a splicing time-course. **(A)** The annealing properties of oligonucleotide 1 (GGA*), throughout an *in vitro* splicing time-course, were assessed through digestion of unbound *SMN2* RNA using RNase H and a DNA oligonucleotide complementary to the target RNA region of oligonucleotide 1. **(B)** The annealing properties of oligonucleotide 1 to *SMN2* RNA were assessed under conditions thought to stall splicing at E complex. The same digestion procedure was used as in (a). **(C)** The annealing properties of oligonucleotide 1 to *SMN2* RNA were assessed under conditions thought to stall splicing at A complex. The same digestion procedure was used as in (a and b).

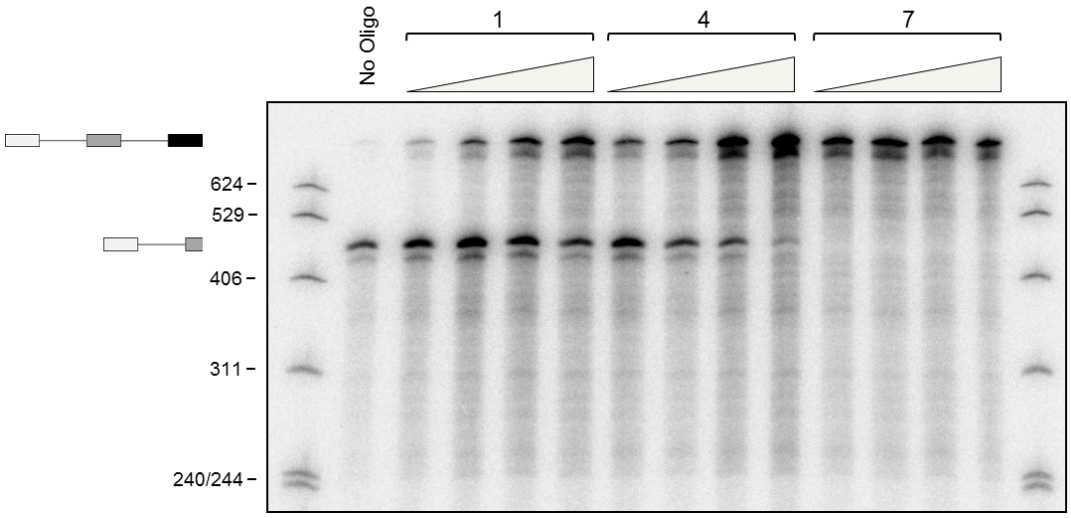

Figure 3.3. Oligonucleotide modification affects the binding of oligonucleotides to their target RNA. Oligonucleotides 1 (GGA-b), 4 and 7 were annealed to the *SMN2*/β-globin transcript in nuclear extract and the extent of RNA protection they provided was assessed using RNase H digestion. An RNase H compatible DNA oligonucleotide, complementary to the target RNA sequence of oligonucleotide 1, 4 and 7, was able to digest any RNA left unbound and so unprotected. The undigested *SMN2* transcript and the 5' digestion products are identified on the left, the 3' digestion product has been degraded.

3.3. Analysis of *SMN2* Bifunctional Oligonucleotide Action

There is an indication that the long-term storage of modified RNA oligonucleotides may alter their concentration and viability, as in initial experiments, oligonucleotide 1 failed to produce the expected effect. For this reason, the activity of four oligonucleotide stocks of oligonucleotide 1, together with oligonucleotides 2-6, were assayed for their effect on inclusion of *SMN2* exon 7 (Figure 3.4.). All oligonucleotides had a significant stimulatory effect on exon 7 inclusion. The GGA* batch of oligonucleotide 1 induced the greatest fold increase in *SMN2* exon 7 inclusion (18.3-fold), stimulating it above that seen with oligonucleotide 4 (9-fold) and control oligonucleotide 2 (3.8-fold) (Figure 3.4. A). The GGA* batch of oligonucleotide 1 was used in all future *SMN2* oligonucleotide experiments.

It was possible that the activity of oligonucleotide 1 might be affected by the concentration of regulatory proteins and splicing factors in the splicing reaction. However, there was no significant change in the level of *SMN2* exon 7 inclusion when the effect of oligonucleotide 1 was tested in a splicing reaction containing 30 % nuclear extract (Figure 3.4. B) instead of 40 % (Figure 3.4. A).

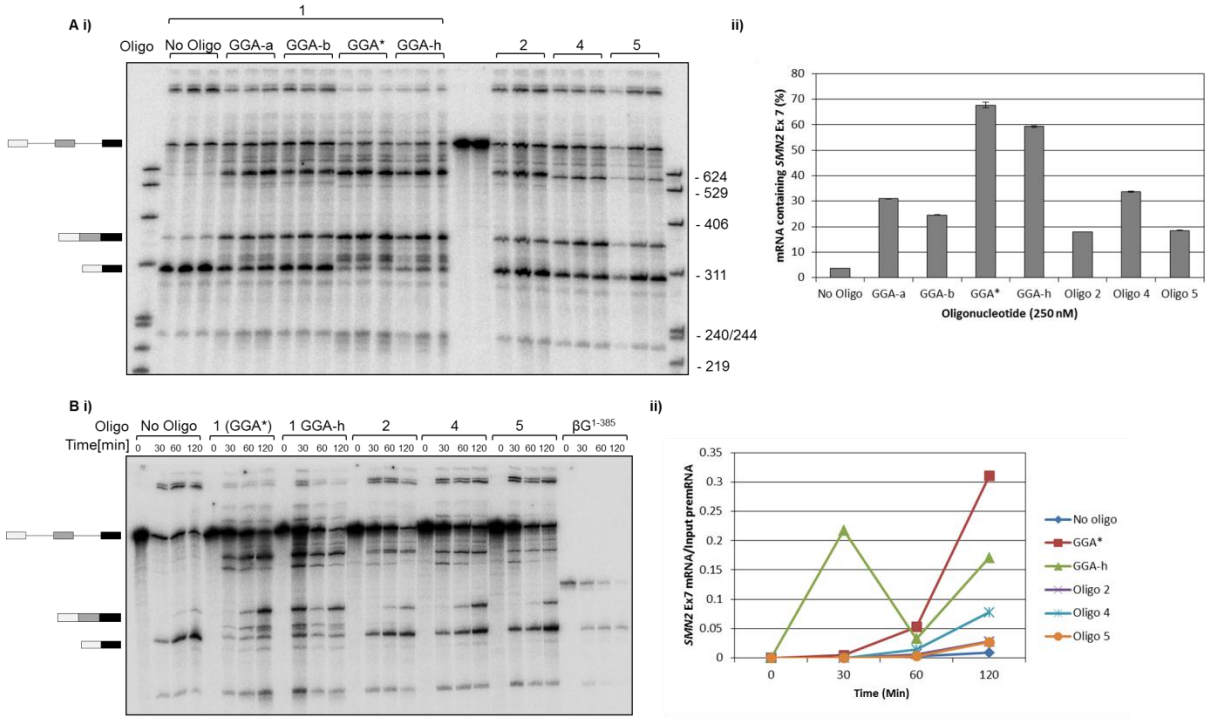

Figure 3.4. Different batches of oligonucleotide 1 exhibit different levels of activity. Oligonucleotide 1 demonstrates greater exon 7 inclusion activity than oligonucleotide 4 and control oligonucleotides 2, 3, 5 and 6. **(A)** i) A comparison of the effect of four batches of oligonucleotide 1 (GGA-a, GGA-b, GGA* and GGA-h) and oligonucleotides 2-6 on *SMN2*/β-globin splicing. Each lane represents one 2 hr time-point from an independent splicing and annealing reaction. Each condition was done in triplicate. ii) Histogram showing the percentage of *SMN2* exon 7 included mRNA produced for each sample. Values were calculated using [Inclusion mRNA/(Inclusion mRNA + Exclusion mRNA + pre-mRNA)]. Standard deviation values have also been plotted. **(B)** (i) A comparison of the effect of oligonucleotides 1 (GGA* and GGA-h), 4, 2 and 5 on *SMN2*/β-globin splicing in 30% nuclear extract. An *in vitro* splicing reaction was established as normal containing a reduced concentration of extract. (ii) A graph showing the proportion of input *SMN2*/β-globin pre-mRNA that was spliced to generate the *SMN2* exon 7 mRNA product for each sample. Values were calculated using [*SMN2* Exon 7 mRNA/Input pre-mRNA].

3.4. Analysis of the Effect of the *SMN2* Bifunctional Oligonucleotide on Splicing of Constructs Derived from the *SMN2*/β-globin construct

As it had been previously predicted that oligonucleotide 1 stimulated splicing of *SMN2* intron 7 (Skordis et al., 2003), the effect of oligonucleotide 1 (GGA*) on the splicing efficiency of $SMN2^{1\text{-}503}$ and $SMN2^{451\text{-}878}$ pre-mRNA (Figure 3.5. A) was assessed. These constructs contained either *SMN*2 intron 6 ($SMN2^{1\text{-}503}$) or intron 7 ($SMN2^{451\text{-}878}$) between flanking exons (*SMN2*/β-globin construct). Oligonucleotide 1 did not significantly promote splicing of either $SMN2^{1\text{-}503}$ or $SMN2^{451\text{-}878}$ pre-mRNA, enhancing mRNA production by only 1.2- and 1.1-fold respectively after 2 hours (Figure 3.5. B). Oligonucleotide 1 may be having a marginal effect on the splicing efficiency of $SMN2^{1\text{-}503}$ and $SMN2^{451\text{-}878}$as these constructs have a high level of background splicing, making the effect of the oligonucleotide difficult to detect. Therefore both $SMN2^{1\text{-}503}$ and $SMN2^{451\text{-}878}$ constructs were extended, until background splicing was reduced. In addition, the stimulatory effect seen with control oligonucleotides 2 and 3 on splicing of $SMN2^{1\text{-}503}$ and $SMN2^{451\text{-}878}$ was negligible.

Six constructs were synthesized by extending the 3' end of the $SMN2^{1\text{-}503}$ construct into intron 7 by 20, 60, 80, 100, 120 and 160 nucleotides (synthesis oligonucleotides 1A and 10B, 9B, 8B, 7B, 6B, 5B respectively). As the constructs 3' end was extended, the level of background splicing decreased and the effect of oligonucleotide 1 on splicing efficiency increased (Figure 3.6. A). In each case the effect of oligonucleotide 1 on stimulation of mRNA production was significant. At a 3' extension length of 160 nucleotides splicing was inhibited and recovered through addition of oligonucleotide 1 (250 nM). Splicing of constructs with oligonucleotide 2 showed that the annealing region of oligonucleotide 1 is playing a small role

in the enhancement of splicing of these constructs (Figure 3.6. B). However, as shown in Figure 3.6. C, the tail of oligonucleotide 1 is stimulating splicing above that seen with oligonucleotide 2 in each case.

The *SMN2*$^{1\text{-}503}$ + 80 nt construct was selected for further analysis of oligonucleotide action. It was previously suggested that oligonucleotide 1 acts by enhancing splicing of the downstream intron (intron 7), perhaps through stimulating U1 snRNP binding to the 5' splice site of intron 7 (Skordis et al., 2003; Owen et al., 2011). Firstly, the effect of oligonucleotide 1 on spliceosomal complex formation under conditions known to stall assembly at E complex was assessed on *SMN2*$^{1\text{-}503}$ + 80 nt pre-mRNA using native gels (Das and Reed, 1999). U1 snRNP is a major component of E complex, and therefore assessment of E complex formation in the presence of oligonucleotide 1 could indicate whether E complex and hence U1 snRNP association is being stimulated by the oligonucleotide. Oligonucleotide 1 (250 nM) appears to increase the yield of a complex formed on this transcript at earlier time-points, but this complex cannot be confidently labeled as E, as the control lane to identify E complex via a U1 snRNP knock-down was not clearly resolved (Figure 3.7. A). Hence, it is not clear whether E complex formation is enhanced via the oligonucleotide. For completeness, the effect of oligonucleotide 1 (250 nM) on the assembly of higher complexes on this transcript was also investigated. As expected, this oligonucleotide enhanced formation of A, B and C complexes (Figure 3.7. B).

The effect of oligonucleotide 1 on splicing of the downstream intron was then studied, the 5' end of the *SMN2*$^{451\text{-}878}$ construct was extended by 122 nucleotides into *SMN2* intron 6 (*SMN2*$^{329\text{-}878}$, synthesis oligonucleotides: 1B and 2A). Oligonucleotide 1 increased the splicing

efficiency of this construct by 1.4-fold after 2 hours (Figure 3.8. A). The band apparent only in the presence of oligonucleotides 1, 2 and 3 was identified as intron 7 by RNase H-DNA oligonucleotide-dependent digestion (Figure 3.8. B) and bands above the pre-mRNA were identified as lariat intermediates (Figure 3.8. C). It is clear that oligonucleotide 1 is not stimulating splicing of the downstream intron, intron 7.

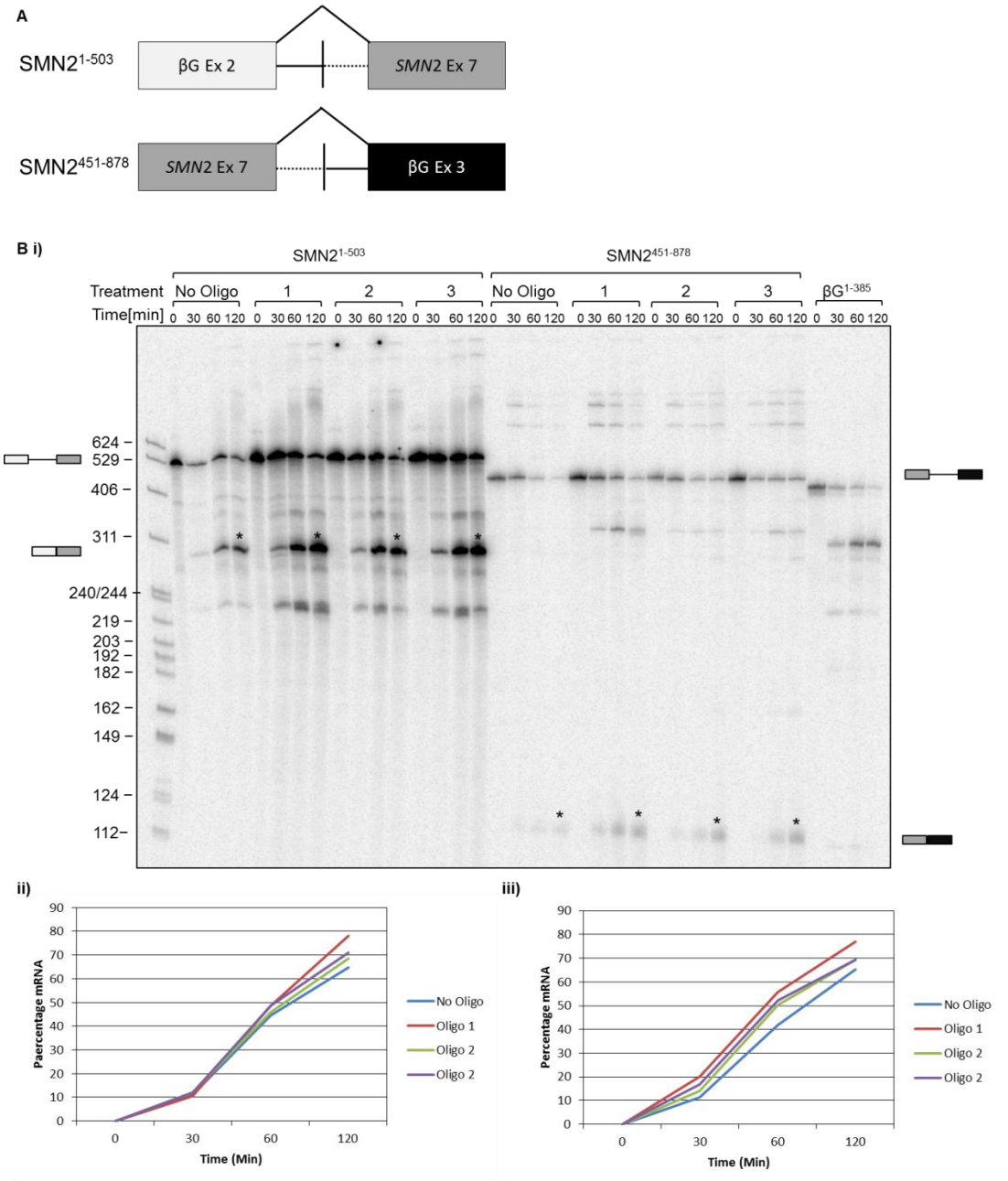

Figure 3.5. Oligonucleotides 1, 2 and 3 have no effect on the splicing efficiency of *SMN2*$^{1\text{-}503}$ and *SMN2*$^{451\text{-}878}$ pre-mRNA. **(A)** Constructs used in this figure. **(B)** (i) The effect of oligonucleotides 1, 2 and 3 on *SMN2*$^{1\text{-}503}$ and *SMN2*$^{451\text{-}878}$ pre-mRNA splicing. Diagrams showing pre-mRNA and mRNA are shown on the left for *SMN2*$^{1\text{-}503}$ and right for *SMN2*$^{451\text{-}878}$. (ii) Time-course of *SMN2*$^{1\text{-}503}$ splicing. iii) Time-course of *SMN2*$^{451\text{-}878}$ splicing. Asterisk = identifies mRNA

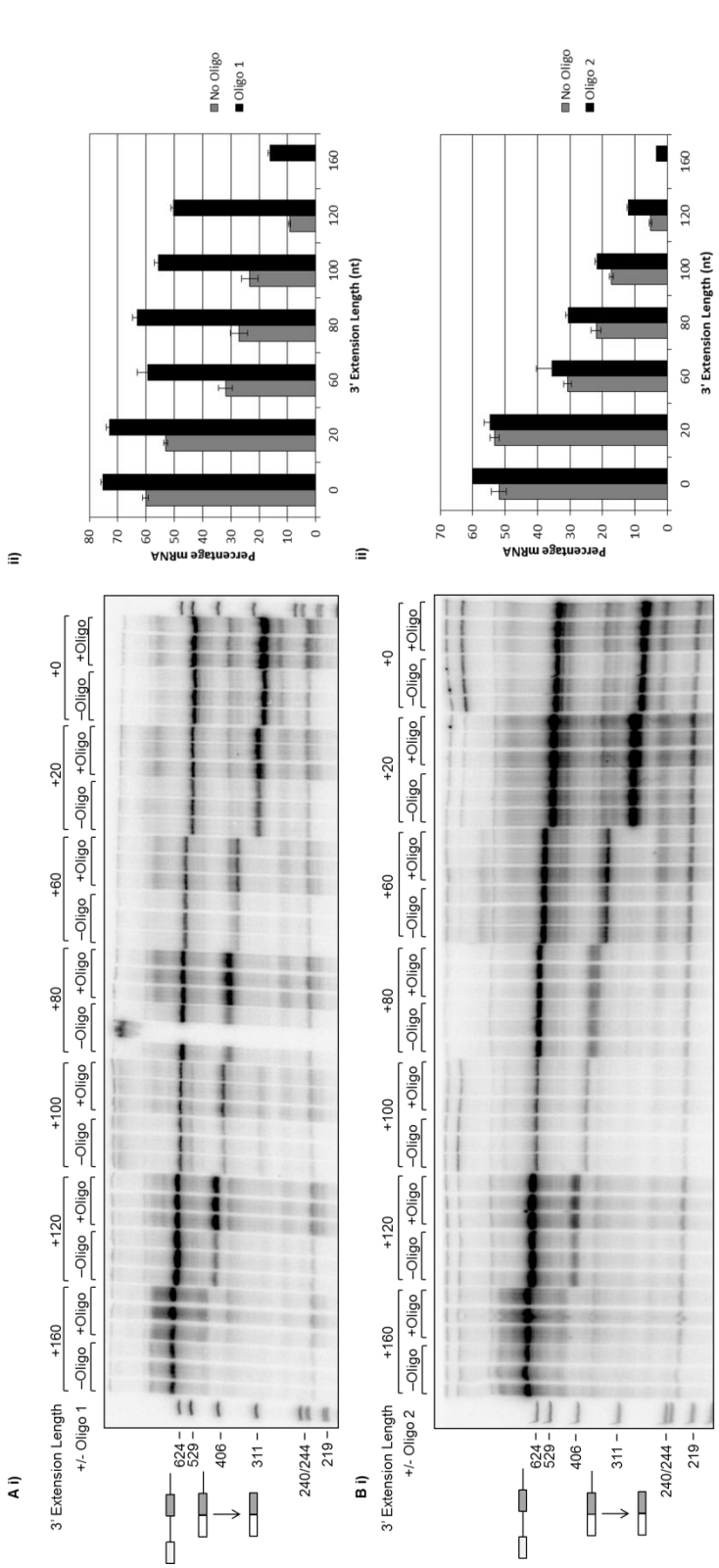

Figure 3.6. Oligonucleotide 1 enhances the splicing efficiency of *SMN2*$^{1\text{-}503}$ constructs with gradually increasing 3' extensions. **(A)** i) A splicing assay investigating the effect of oligonucleotide 1 (250 nM) on the splicing efficiency of the *SMN2*$^{1\text{-}503}$ 3' extension constructs. Each annealing and splicing reaction was handled independently and all reactions were done in triplicate. Reactions were incubated for 2 hrs. ii) Histogram showing the percentage mRNA produced +/- Oligo 1 for each extension length. **(B)** i) A splicing assay showing the effect of oligonucleotide 2 on the splicing efficiency of the *SMN2*$^{1\text{-}503}$ 3' extension constructs. The reactions were carried out as in (a). ii) Histogram showing the percentage mRNA produced +/- Oligo 2 for each extension length tested. C) Fold increase in mRNA for each construct with oligo 1 (ai) and oligo 2 (bi) relative to no oligo.

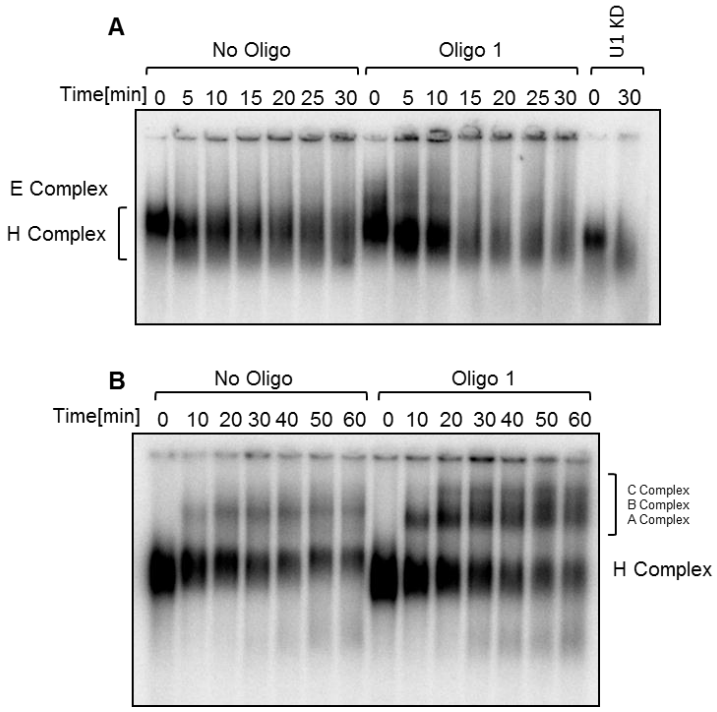

Figure 3.7. Oligonucleotide 1 does not enhance E complex formation, but does enhance A, B and C complex formation on *SMN2*$^{1\text{-}503}$ + 80 nt pre-mRNA. **(A)** A splicing reaction was stalled at E complex, through depletion of ATP and CrPi. Samples were taken and complexes resolved on a 1.5 % LMP native gel. **(B)** To assess the effect of oligonucleotide 1 on A, B and C complex formation samples were taken from an unstalled splicing reaction, pre-treated with heparin and resolved on a 2 % LMP native gel.

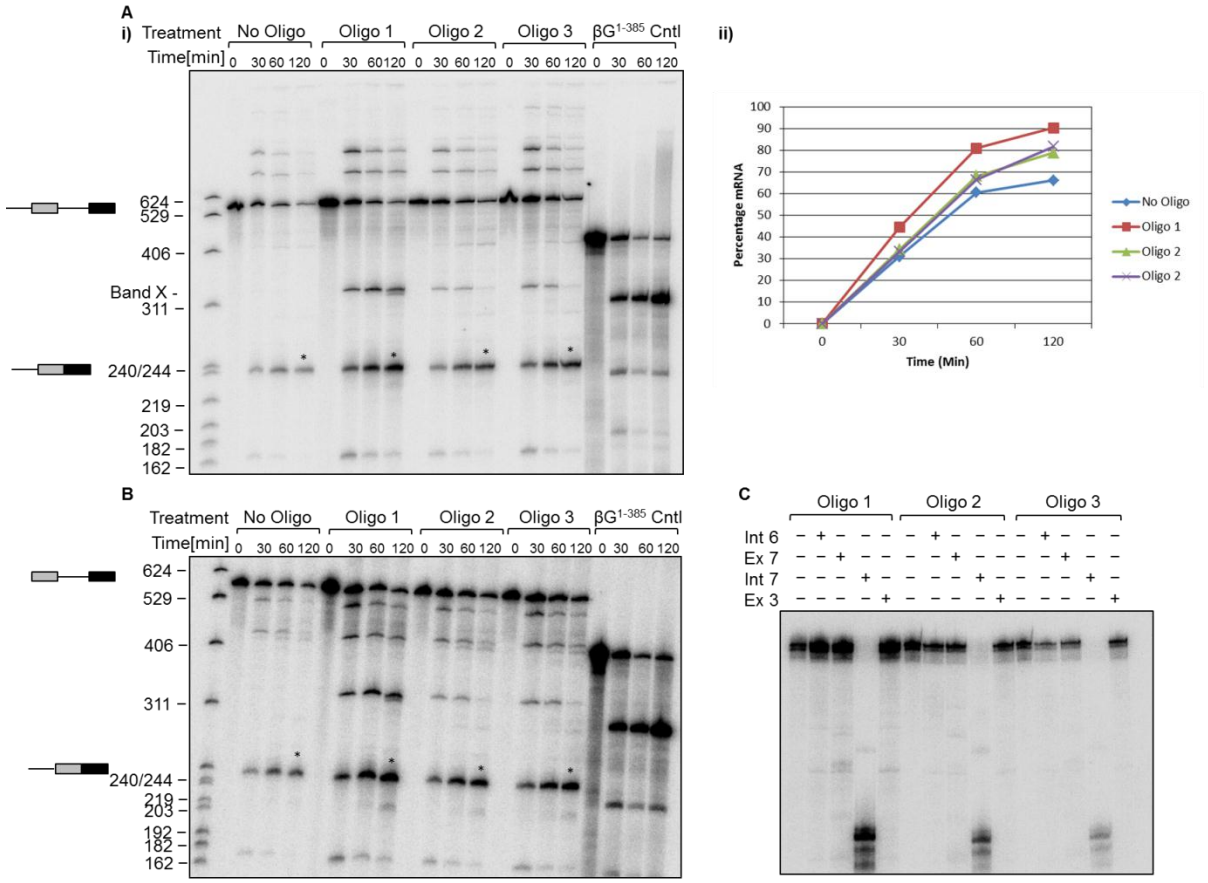

Figure 3.8. Oligonucleotides 1, 2 and 3 have no effect on the splicing of *SMN2*$^{329\text{-}878}$ pre-mRNA. **(A)** i) A splicing reaction was carried out in the presence of oligonucleotides 1, 2 and 3. The pre-mRNA and mRNA are labeled on the left of the figure. ii) A time-course showing the effect of oligonucleotides 1, 2 and 3 on the percentage of mRNA produced after 2 hours of *SMN2*$^{329\text{-}878}$ pre-mRNA splicing. **(B)** Splicing of *SMN2*$^{329\text{-}878}$ resolved on a 4% denaturing polyacrylamide gel containing formamide. Shifting of RNA bands located above the pre-mRNA in (a) identifies them as splicing lariat intermediates. **(C)** Identification of the oligonucleotide dependent band (band X) using sequence specific RNase H digestion via four DNA oligonucleotides targeted to *SMN2*$^{329\text{-}878}$ pre-mRNA (intron 6, exon 7, intron 7 and *β*-globin exon 3). Band X was excised from the gel shown in (a), the RNA extracted, purified and digested by the RNase H activity supported by each DNA oligonucleotide. Samples were mixed with formamide loading dyes, pre-heated at 80 °C for 20 seconds and resolved on a 6 % formamide gel.

3.5. Identification of the Molecular Action of the *SMN2* Bifunctional Oligonucleotide

As earlier studies predicted that oligonucleotide 1 stimulates splicing of intron 7 (Skordis et al., 2003; Owen et al., 2011), and U1 snRNP association with the 5' splice site of intron 7 was thought to be a limiting factor for splicing of *SMN2* exon 7 (Singh et al., 2007), U1 snRNP binding to this site was next investigated. Psoralen cross-linking was carried out on the *SMN2*$^{1\text{-}503}$ + 80 nt transcript **(**Figure 3.9. A) and a U1 snRNP knockdown was used to identify the U1 snRNP crosslink. U1 snRNP cross-linking was detected, but was not enhanced by the presence of oligonucleotide 1 (250 nM). The cross-link detected may have been cross-linking of U1 snRNP to the 5' splice site of intron 6 and not intron 7, therefore not allowing the effect of oligonucleotide 1 on U1 snRNP binding to the 5' splice site of intron 7 to be analysed. This may have been due to U1 snRNP having a low binding efficiency to the 5' splice site of intron 7 due to secondary structure (Singh et al., 2007), thus preventing the formation of efficient crosslinks. To check this U1 snRNP binding to *SMN2* exon 7 with flanking intronic regions (*SMN2* exon 7-defined construct, 41 nt upstream and 58 nt downstream, synthesis oligonucleotides: 11B and 12B) was investigated using U1A immunoprecipitation. This construct contained only the 5' splice site of intron 7, unlike *SMN2*$^{1\text{-}503}$ + 80 nt, allowing for assessment of U1 snRNP binding to this site alone (Figure 3.9. B). This construct was immunoprecipitated using an antibody to U1A in the presence of oligonucleotide 1 (250 nM) and the immunoprecipitation of RNA was not enhanced by the oligonucleotide (Figure 3.9. C). Also, oligonucleotide 1 (250 nM) did not enhance complex assembly on the *SMN2* exon 7-defined construct under conditions thought to stall complex

assembly at E (Figure 3.9. D). RNase H protection assays were also used to investigate U1 snRNP binding to the 5' splice site of intron 7, but these were unsuccessful.

As oligonucleotide 1 did not enhance binding of U1 snRNP to the 5'splice site of intron 7, the investigation turned to look at whether the oligonucleotide was enhancing assembly of spliceosomal factors at the 3' splice site, polypyrimidine tract and branch-point of intron 6. As oligonucleotide 1 is targeted toward the 5' end of *SMN2* exon 7, it would seem feasible that this could be the case. The assembly of ATP-dependent complexes on the *SMN2* exon 7-defined construct, used for the experiment in Figure 3.9. C and D, was investigated in the presence of oligonucleotide 1 (250 nM) and their formation was seen to be enhanced by the oligonucleotide (Figure 3.10. A lanes 5-8). Complexes on the transcript alone and in the presence of oligonucleotide 2 did form, but did not accumulate to the level seen with oligonucleotide 1 (Figure 3.10. A, lanes 1-4 and 9-12 respectively). U2 snRNP is shown to be vital for the integrity of the oligonucleotide 1-dependent complex (Figure 3.10. B, lanes 13-16), whereas knock-down of U1 and U6 snRNP does not dramatically affect the accumulation of this core U2 snRNP-dependent complex (Figure 3.10. C, lanes 9-12 and 13-16 respectively). However, an intermediate band (Figure 3.10.7 C, lanes 5-8) does disappear with the knock-down of U1 and U6 snRNP. Further to this, psoralen cross-linking was carried out on the *SMN2* exon 7-defined construct to identify whether U2 snRNP binding to the RNA (intron 6 branch-point) is being directly affected by the presence of oligonucleotide 1. U2 snRNP cross-linking to the RNA was detected and increased 1.8-fold in the presence of oligonucleotide 1 (250 nM) **(**Figure 3.10. D).

U2 snRNP base-pairing to the pre-mRNA is indicative of productive recognition of a 3' splice site. Other splicing factors including U2AF65 and 35, that bind to and around the 3' splice site, aid in the definition of the 3' splice site and together recruit U2 snRNP (Valcárcel et al., 1996). It may be the case that oligonucleotide 1 is acting via these factors to enhance U2 snRNP binding. To test this, the *SMN2* exon 7-defined construct was cross-linked at 254 nm to proteins in the presence of oligonucleotide 1 (250 nM), in both HeLa and HEK 293T nuclear extract. Cross-linking of a protein (protein X: mw 50-75) in the presence of the oligonucleotide increased 2-fold in HeLa and 2.4-fold in HEK 293T nuclear extract (Figure 3.11. A). 'Protein X'-cross-linking in the presence of oligonucleotide 1 was also detected in a biotin affinity purification of the *SMN2* exon 7-defined construct (250 nM) (Figure 3.11. B). In addition, UV cross-linking of this construct in nuclear extracts expressing U2AF65-GFP (92 KDa) and U2AF35-mCherry (63.8 KDa) fusion proteins gave rise to an additional band, indicating that oligonucleotide 1 induces binding of U2AF65-GFP to the RNA (Figure 3.11. C). To confirm that 'protein X' was U2AF65 a western blot was carried out on cross-linking samples utilizing a U2AF65 antibody (Gama-Carvalho et al., 1997) and successfully identified 'protein X' as U2AF65 (Figure 3.11. D). Therefore, U2AF65 cross-linking is enhanced with both oligonucleotide 1 and 2, which increase cross-linking of this protein to RNA by 1.4- and 1.5-fold respectively.

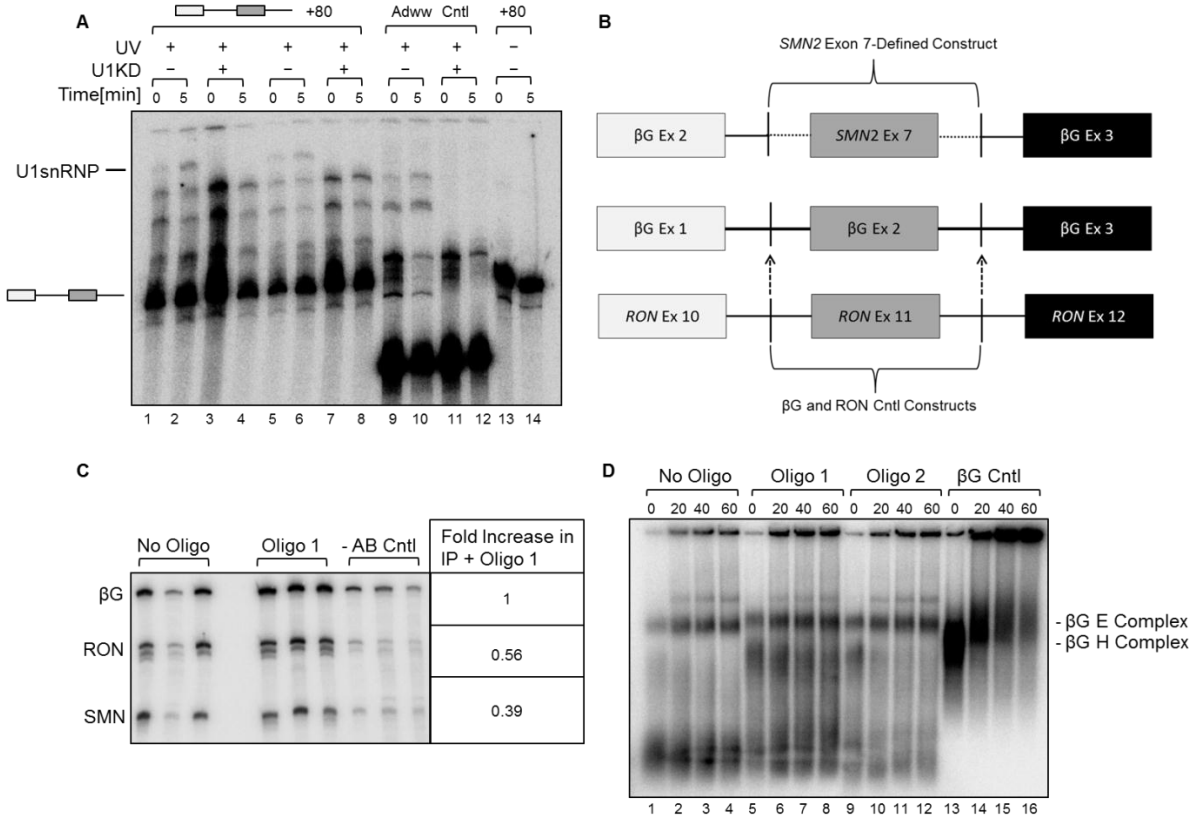

Figure 3.9. Oligonucleotide 1 does not enhance U1 snRNP binding or E complex formation on an *SMN2* exon 7-defined RNA substrate, containing *SMN2* exon 7 and flanking *SMN2* intronic regions. **(A)** Alteration of U1 snRNP binding to the 5' ss of *SMN2* intron 7, in the presence of oligonucleotide 1, was investigated using psoralen cross-linking. Splicing reactions supplemented with psoralen were incubated and then cross-linked for 5 mins via long wave UV. Samples were treated with proteinase k, re-suspended in formamide dyes, pre-heated and resolved on a 5 % polyacrylamide gel containing formamide. The U1 snRNP crosslink was identified via a U1 snRNP knock-down (lanes 13 and 14) and is labeled on the left of the figure. **(B)** A Diagram showing the *SMN2* exon 7-defined construct and β-globin exon 2- and *RON* exon 11-defined control constructs. **(C)** Immunoprecipitation of *SMN2* exon 7 -defined RNA via an antibody to U1A was used to ascertain the effect of oligonucleotide 1 on U1 snRNP binding to the 5' splice site of *SMN2* intron 7. Immunoprecipitation of the β-globin exon 2- and *RON* exon 11-defined RNA substrates were used as internal controls, allowing for quantification of the effect of the oligonucleotide on *SMN2* RNA immunoprecipitation. The fold increase in RNA immunoprecipitation with oligonucleotide 1 is shown on the right of the figure. **(D)** The effect of oligonucleotide 1 on E complex formation on *SMN2* exon 7 -defined RNA was assessed. The *SMN2* exon 7-defined RNA construct is unable to splice, however ATP and CrPi were depleted as normal and complexes allowed to form. Samples were resolved on a 1.5 % LMP native gel.

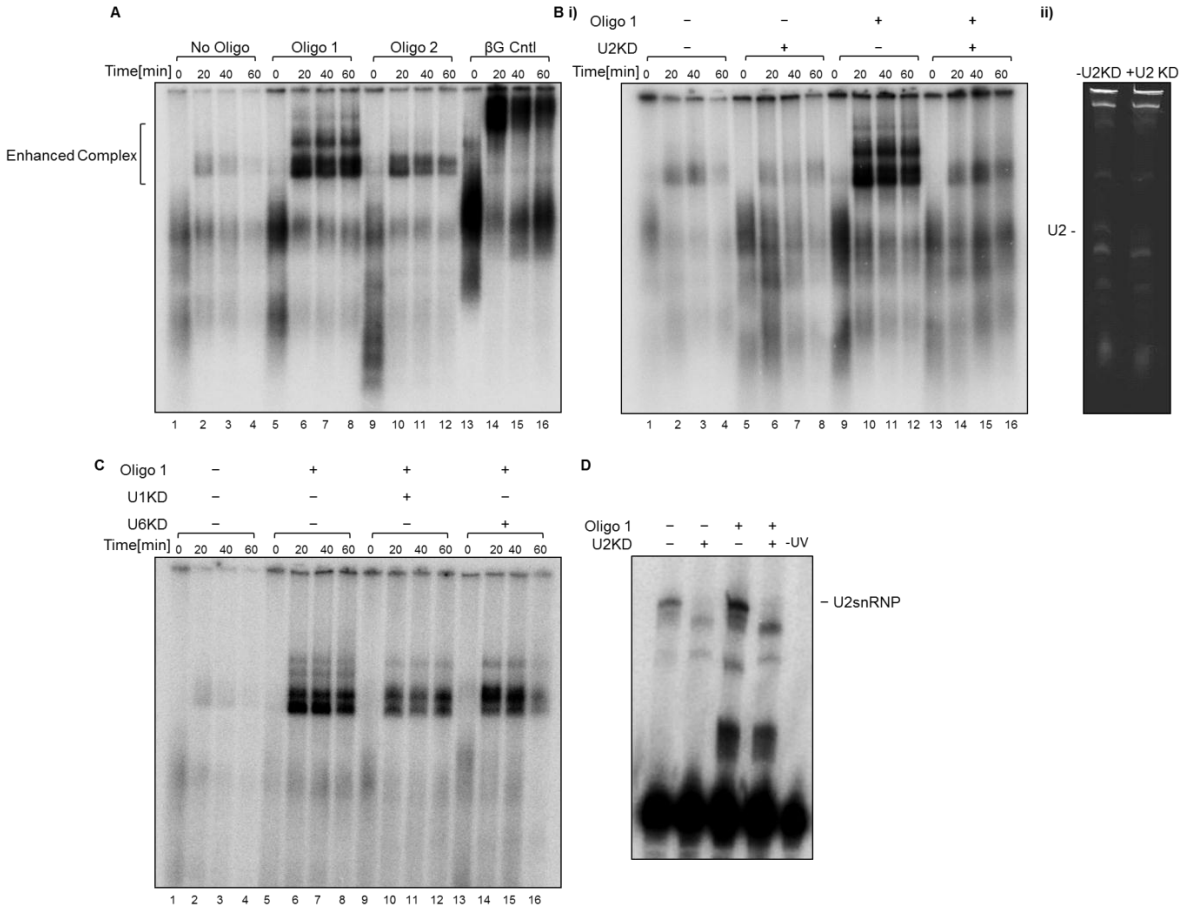

Figure 3.10. Oligonucleotide 1 stimulates formation of a U2 snRNP dependent complex and enhances binding of U2 snRNP to *SMN2* exon 7-defined RNA. **(A)** A splicing reaction was set up in the presence of oliognucleotide 1 and 2. Time-point samples were taken, treated with heparin and resolved on a 2 % LMP agarose gel. **(B)** i) The importance of U2 snRNP on oligonucleotide 1-dependent complex formation was shown via a U2 snRNP knock down (lanes 12-16). U2 snRNP was knocked down by cleavage of U2 snRNA via two RNase H compatible DNA oligonucleotides. Splicing reactions were set up containing nuclear extract with and without U2 snRNP, time-points were taken, treated with heparin and spliceosomal complexes were resolved on a 2 % LMP gel. ii) 5 µl of nuclear extract, with and without U2 snRNP knocked down from (i), was treated with proteinase K, re-suspened in formamide dyes, pre-heated at 80 °C and resolved on a 6 % polyacrylamide gel. snRNA was visualized through post-staining with ethidium bromide (1:10,000). The knock-down is highlighted through loss of a band in the knock-down lane (labelled U2). **(C)** The requirement of U1 and U6 snRNP for oligonucleotide 1-dependent complex formation was investigated. U1 and U6 snRNP were knocked down in nuclear extract and the effect of this was assessed as in Bi, U1 snRNP (lanes 9-12) and U6 snRNP (lanes 13-16). **(D)** Psoralen cross-linking was used to assess the effect of oligonucleotide 1 on binding of U2 snRNP to the RNA substrate. Splicing reactions, suplemented with psoralen, were incubated and crosslinked via long-wave UV. The samples were treated with proteinase K, re-suspended in formamimide dyes, pre-heated and resolved on a 5 % polyacrylamide gel containing formamide.

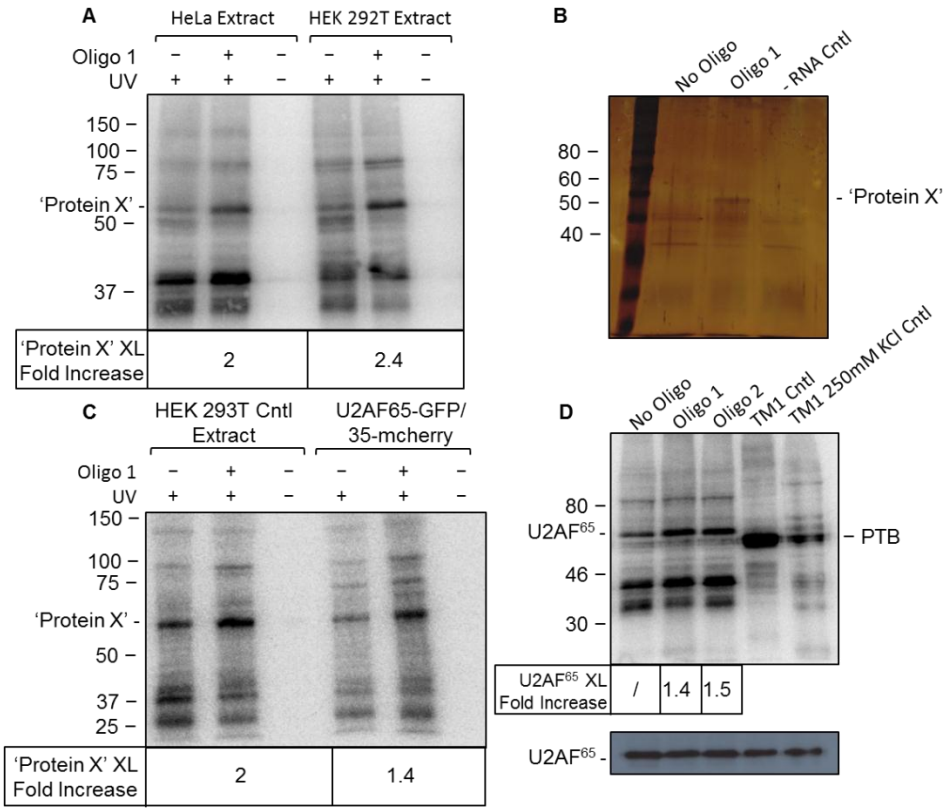

Figure 3.11. Oligonucleotide 1 enhances the binding of U2AF65 to the *SMN2* exon 7-defined RNA substrate. Following cross-linking via short-wave UV (≈ 254**)**, all samples were digested with RNase A and T1, resolved on 10 % non-denaturing polyacrylamide gels and transferred to nitrocellulose, before being exposed to a phosphorimager screen. **(A)** Cross-linking in both HeLa and HEK 293T extract was assessed. The fold increase in cross-linking of the major band with oligonucleotide 1 is shown at the bottom on the image. **(B)** Biotin affinity purification of *SMN2* exon 7-defined RNA in the presence of oligonucleotide 1. Splicing reactions containing HeLa extract and the biotinylated RNA substrate were set up. The reactions were incubated before purification of RNA via neutravadin beads. The RNA was eluted, resolved on a polyacrylamide gel and proteins were visualized via silver staining. **(C)** Cross-links were identified as U2AF65 via UV cross-linking in a splicing reaction containing nuclear extract expressing U2AF65-GFP and U2AF35-mcherry fusion proteins. Modified extracts were produced through calcium chloride transfection of HEK 293T cells with 4 µg of the relevant expression plasmids. U2AF65/U2AF65-GFP expression was 50:50. The fold increase in cross-linking of the major band with oligonucleotide 1 is shown at the bottom on the image. **(D)** A western blot utilizing a U2AF65 antibody identified the major crosslink as U2AF65. A standard UV cross-linking experiment was carried out (transcript labeled with a [α-32P] UTP) and the cross-linked proteins were analyzed via western blot. The fold increase in cross-linking of the major band with oligonucleotide 1 is shown at the bottom on the cross-linking gel. The western blot gel is shown at the bottom of this panel. When the cross-linking and the western blot were overlaid the major cross-linked band aligns with the band identified as U2AF65 by the western blot. A PTB cross-linking control was used to act as a size marker.

3.6. Summary

Oligonucleotide 1 does not enhance U1 snRNP binding to the 5' splice site of *SMN2* intron 7. It does however stimulate binding of U2 snRNP and U2AF65 to the 3' splice site of *SMN2* intron 6. The oligonucleotide's non-complementary tail stimulates formation of a U2 snRNP-dependent complex on *SMN2* exon 7, while the annealing region of the oligonucleotide does not. The annealing region (Oligonucleotide 2) stimulates cross-linking of U2AF65 to the polypyrimidine tract of *SMN2* exon 7.

There is a long-range 'zone of inhibition' formed across *SMN2* exon 7, which is formed between a factor binding downstream in *SMN2* intron 7 and upstream in *SMN2* intron 6.

4. Analysis of the *RON* Δ165 Pro-Metastatic Splice

4.1. Introduction

4.2. Basic Analysis of the Effect of the *RON* Bifunctional Oligonucleotide on *RON* pre-mRNA Splicing

4.3. Basic Analysis of *RON* Exon 11 Splicing

4.4. Detailed Analysis of Splicing Signals

4.5. Identifying the Specific Inhibitory Sequence in the Downstream Region of *RON* Introns 10 and 11

4.6. Identification of RNA Binding Proteins

4.7. Summary

4.1. Introduction

Skipping of *RON* exon 11 generates the RON Δ165 isoform that has been connected with the development and progression of some forms of epithelial cell cancer (Collesi et al., 1996; Zhou et al., 2003; Ghigna et al., 2005). The RON Δ165 isoform is generated through skipping of *RON* exon 11, that has previously been shown to be stimulated by the binding of SRSF1 to *RON* exon 12 (Ghigna et al., 2005). In addition, hnRNP H has also been found to stimulate *RON* exon 11 skipping, via a binding site located on exon 11 (Lefave et al., 2011).

A bifunctional oligonucleotide (oligonucleotide 8, Table 1) targeted to *RON* exon 11 has been tested for its ability to stimulate re-inclusion of this exon and so prevent expression of the RON Δ165 isoform *in vivo* (Ghigna et al., 2010). However, the exon inclusion effect seen with this oligonucleotide was relatively much weaker than that observed following *SMN2* bifunctional oligonucleotide stimulation of *SMN2* exon 7 splicing (chapter 3). Developing both an understanding of the mechanism behind the action of the *SMN2* bifunctional oligonucleotide and the factors limiting *RON* exon 11 splicing, may enable the development of a more effective oligonucleotide to stimulate *RON* exon 11 inclusion in target cancers.

4.2. Basic Analysis of the Effect of the *RON* Bifunctional Oligonucleotide on *RON* pre-mRNA Splicing

In vitro assays were used to determine the mechanism through which oligonucleotide 8 induces *RON* exon 11 inclusion (Ghigna et al., 2010). Constructs containing *RON* pre-mRNA from exon 10 to exon 12 (*RFL*$^{1\text{-}692}$, Figure 4.1. A) were annealed to increasing concentrations

of oligonucleotide 8 (250 nM) (Figure 4.1. B) and spliced *in vitro* (Figure 4.1. C). *RFL*$^{1\text{-}692}$ did not splice and oligonucleotide 8 did not stimulate its splicing.

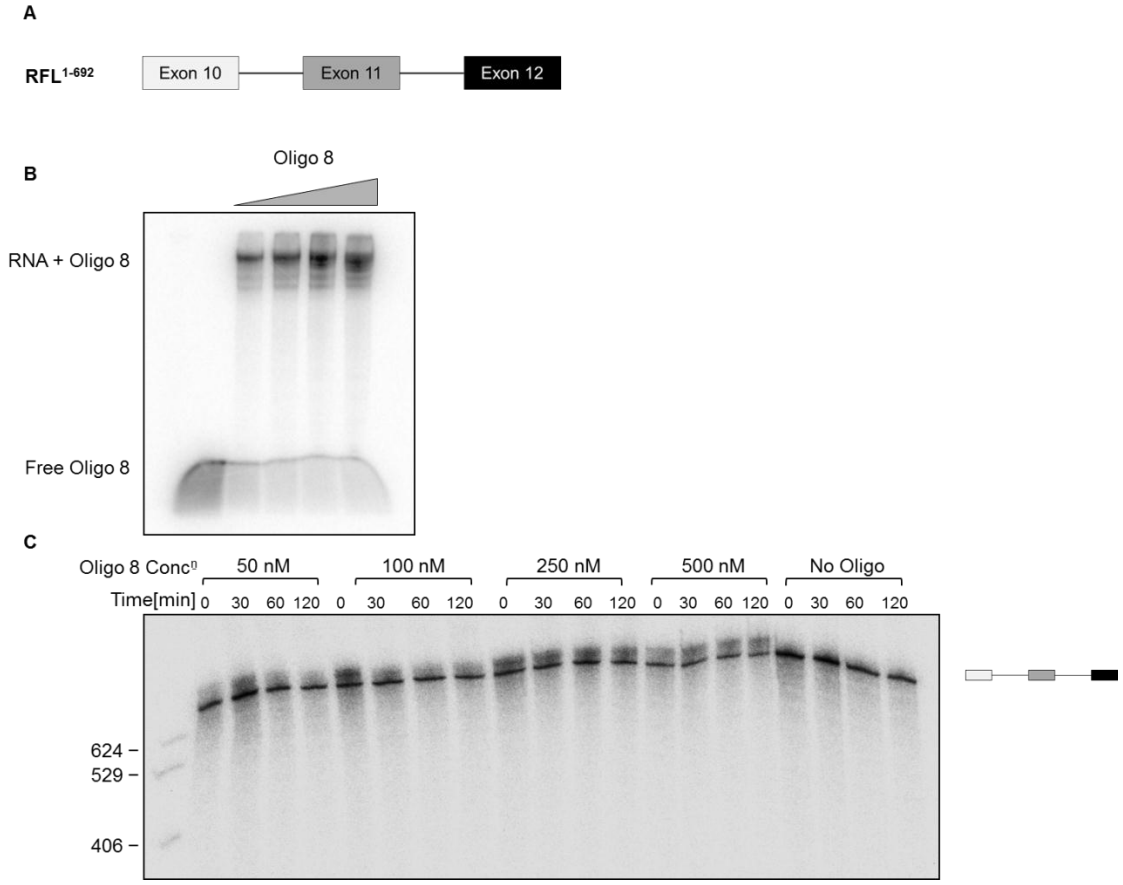

Figure 4.1. Oligonucleotide 8 anneals to *RFL*[1-692] pre-mRNA and does not enhance its splicing *in vitro.* **(A)** Diagram of *RFL*[1-692] pre-mRNA. **(B)** 5' end labeled Oligonucleotide 8 anneals to cold *RFL*[1-692] RNA. RNA and oligonucleotide were annealed by exposure to a temperature gradient of 80 °C to 30 °C. They were mixed with formamide dyes and resolved on a 6 % polyacrylamide gel. The free and annealed oligonucleotide is labeled on the left of the figure. **(C)** *RFL*[1-692] pre-RNA does not splice and increasing concentrations of oligonucleotide 8 does not stimulate its splicing. Pre-mRNA is labelled on the right of the image. (White = *RON* exon 10, Light Grey = *RON* exon 11, Dark Grey = *RON* exon 12, Thin lines = *RON* introns.)

4.3. Basic Analysis of *RON* Exon 11 Splicing

As *RFL*$^{1\text{-}692}$ pre-mRNA did not splice *in* vitro and oligonucleotide 8 did not stimulate inclusion of *RON* exon 11 or *RFL*$^{1\text{-}692}$ splicing (Figure 4.1.), the under-lying mechanisms of *RFL*$^{1\text{-}692}$ splicing were investigated. Identification of the reasons why *RFL*$^{1\text{-}692}$ pre-mRNA does not splice *in vitro* might allow for the design of a more effective *RON* bifunctional oligonucleotide that can compensate for this weakness and so stimulate *RON* exon 11 splicing, consequently also reducing RON Δ165 expression in target cancers. Factors relating to the composition of *RFL*$^{1\text{-}692}$ pre-mRNA that could be promoting skipping of *RON* exon 11 include the short length of introns 10 and 11, the presence of G tracts which could allow for splicing regulation by hnRNP H/F (Lefave et al., 2011), the weak polypyrimidine tract and branch-point sequences in both introns 10 and 11, and the weak 5' splice site in intron 11.

Splicing assays showed that neither full length pre-mRNA (*RFL*$^{1\text{-}692}$, Figure 4.2. A) nor pre-mRNA containing one intron (*R*$^{1\text{-}444}$, *R*$^{1\text{-}444(U1)}$ and *R*$^{296\text{-}692}$ and *R*$^{296\text{-}692(U1)}$, Figure 4.2. A) spliced in HeLa nuclear extract (Figure 4.2. B and C). Following this spliceosomal complex formation on R$^{1\text{-}444(U1)}$ and *R*$^{296\text{-}692(U1)}$ was investigated, as identification of the complex at which splicing is stalled could indicate which spliceosomal factor is limiting for the progression of splicing. Complexes were seen to assemble on pre-mRNA containing only one intron (R$^{1\text{-}444(U1)}$ and R$^{296\text{-}692(U1)}$) **(**Figure 4.2. D). The complex formed on R$^{1\text{-}444(U1)}$ was confirmed to be E complex, through treatment of samples with heparin and a U1 snRNP knock-down. The complex formed on *R*$^{296\text{-}692(U1)}$ was resistant to U1 snRNP knock-down, but not to heparin, indicating that a U1-independent complex is forming on *R*$^{296\text{-}692(U1)}$. A, B and C complexes were not seen to assemble on either substrate (Figure 4.2. E). Complex analysis

therefore indicates that splicing of $R^{1\text{-}444(U1)}$ stalls between E and A complex assembly and $R^{296\text{-}692(U1)}$ splicing stalls before E complex assembly. For completeness, the effect of oligonucleotide 8 and the non-tailed *RON* bifunctional oligonucleotide (oligonucleotide 9) (250 nM) on splicing and complex formation on $R^{1\text{-}444(U1)}$ and $R^{296\text{-}692(U1)}$ was assessed. Neither oligonucleotide stimulated splicing or complex formation on either construct (Figure 4.3. A and B).

Previous studies on the regulation of RON Δ165 expression were carried out in KATO III cells (gastric carcinoma), as RON Δ165 is endogenously expressed in these cells (Ghigna et al., 2005). Splicing competent nuclear extract was prepared from this cell-line to assess whether this could stimulate $RFL^{1\text{-}692(U1)}$ splicing. $RFL^{1\text{-}692(U1)}$ did not splice in KATO III extract (Figure 4.4. A), indicating that there is no essential splicing factor or condition present in KATO III cells, that is not present in HeLa extract, that is required to stimulate $RFL^{1\text{-}692}$ splicing. This finding validated the use of HeLa nuclear extract in future experiments investigating $RFL^{1\text{-}692(U1)}$ splicing regulation.

Comparison of splicing sequences in the $RFL^{1\text{-}692(U1)}$ region with the consensus splicing sequences indicated that *RON* introns 10 and 11 both contain weak polypyrimidine tract sequences, which may restrict U2AF65 binding. In addition, weak U2AF65 binding has been shown to stimulate skipping of other exons in disease (Frappaz et al., 2002; Martins de Araújo et al., 2009), hence poor U2AF65 binding could be contributing to exon 11 skipping and $RFL^{1\text{-}692(U1)}$ splicing inhibition. To test this $RFL^{1\text{-}692(U1)}$ was spliced in nuclear extracts enriched in U2AF65/35 and U2AF65 (Figure 4.4. B), as it has been shown that U2AF35 is required for recognition of weak polypyrimidine tract sequences and acts in a heterodimer with U2AF65

(Pacheco et al., 2006). These nuclear extracts expressed U2AF65/35 and U2AF65 at two times the concentration of control extracts (Mark. J. Hodson, personal communication) and so may enhance polypyrimidine tract recognition. However, this was not the case and extracts enriched in U2AF65/35 did not induce splicing of *RFL*$^{1\text{-}692(U1)}$. This indicates that either the polypyrimidine tracts of intron 10 and 11 bind U2AF65 so weakly that increased concentration has no effect on splicing or that U2AF65 binding does not limit splicing of these introns.

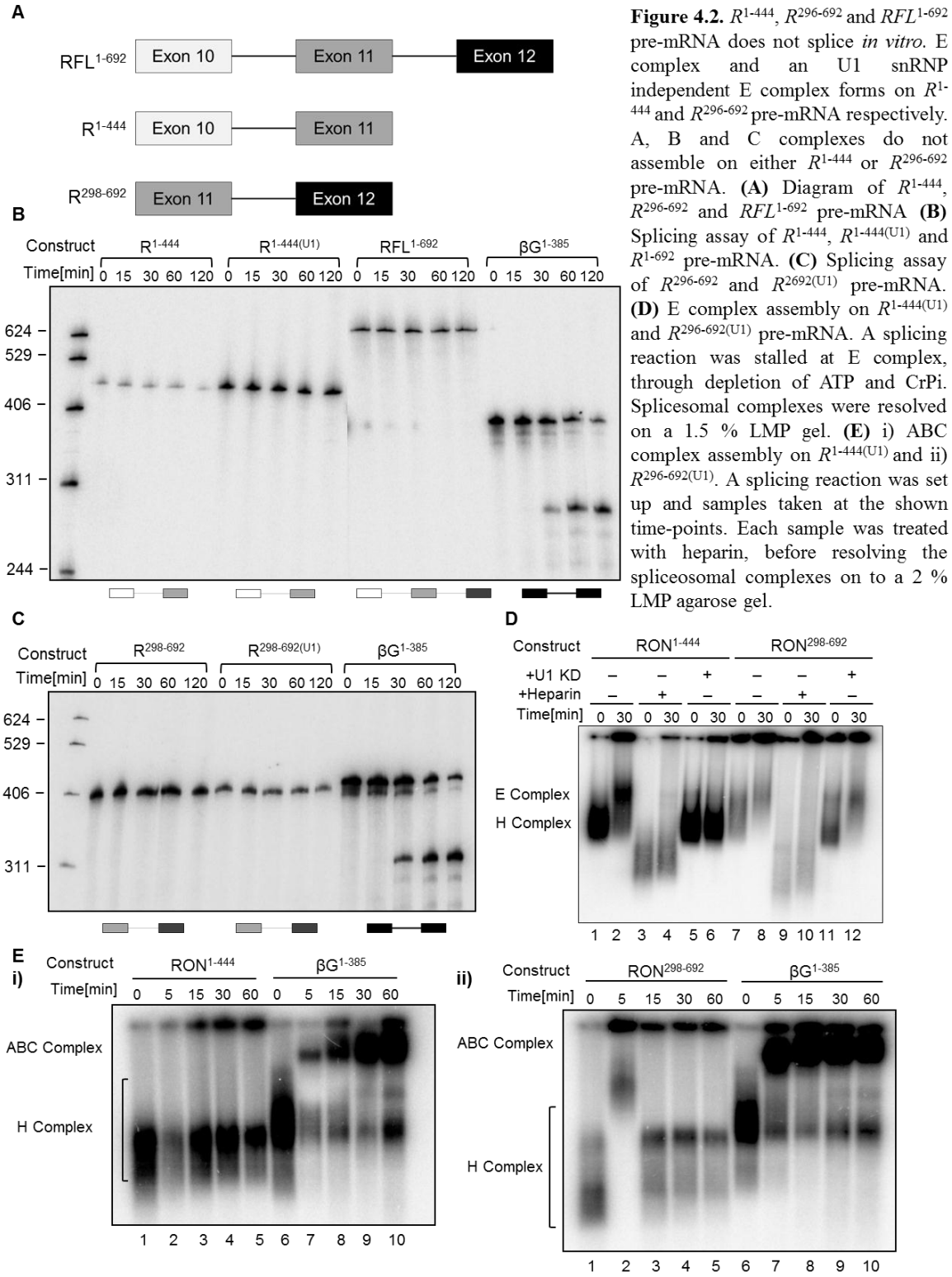

Figure 4.2. $R^{1\text{-}444}$, $R^{296\text{-}692}$ and $RFL^{1\text{-}692}$ pre-mRNA does not splice *in vitro*. E complex and an U1 snRNP independent E complex forms on $R^{1\text{-}444}$ and $R^{296\text{-}692}$ pre-mRNA respectively. A, B and C complexes do not assemble on either $R^{1\text{-}444}$ or $R^{296\text{-}692}$ pre-mRNA. **(A)** Diagram of $R^{1\text{-}444}$, $R^{296\text{-}692}$ and $RFL^{1\text{-}692}$ pre-mRNA **(B)** Splicing assay of $R^{1\text{-}444}$, $R^{1\text{-}444(U1)}$ and $R^{1\text{-}692}$ pre-mRNA. **(C)** Splicing assay of $R^{296\text{-}692}$ and $R^{2692(U1)}$ pre-mRNA. **(D)** E complex assembly on $R^{1\text{-}444(U1)}$ and $R^{296\text{-}692(U1)}$ pre-mRNA. A splicing reaction was stalled at E complex, through depletion of ATP and CrPi. Splicesomal complexes were resolved on a 1.5 % LMP gel. **(E)** i) ABC complex assembly on $R^{1\text{-}444(U1)}$ and ii) $R^{296\text{-}692(U1)}$. A splicing reaction was set up and samples taken at the shown time-points. Each sample was treated with heparin, before resolving the spliceosomal complexes on to a 2 % LMP agarose gel.

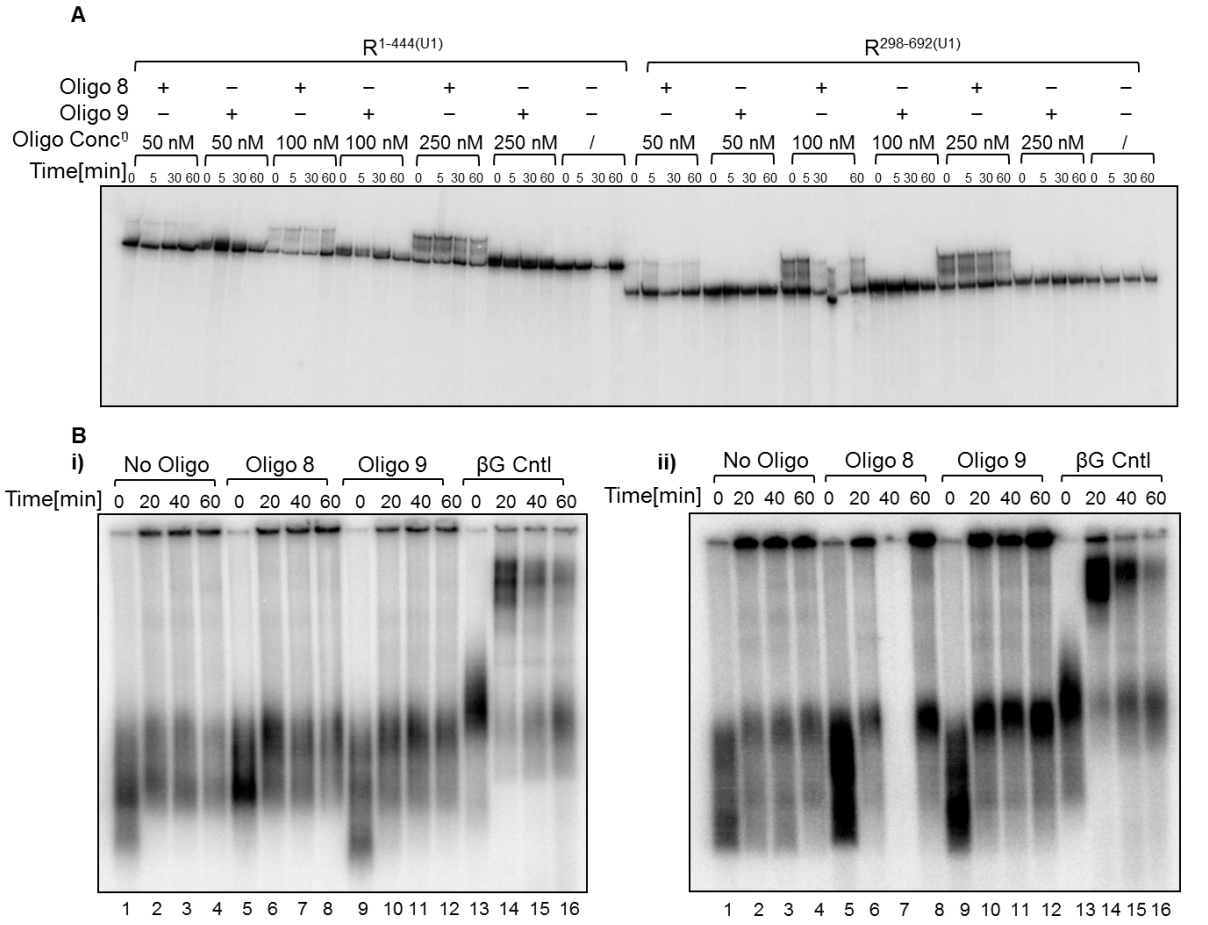

Figure 4.3. Oligonucleotide 8 does not stimulate splicing or spliceosomal complex formation on $R^{1\text{-}444}$ and $R^{298\text{-}690}$ pre-mRNA. **(A)** Oligonucleotide 8 was annealed to $R^{1\text{-}444}$ and $R^{298\text{-}692}$ and its effect on the splicing of these pre-mRNAs was assessed. **(B)** Oligonucleotide 8 was annealed to i) $R^{1\text{-}444}$ and ii) $R^{298\text{-}692}$ pre-mRNA and spliceosomal complex formation was investigated. A splicing reaction was set up containing oligonucleotide 8 annealed to either $R^{1\text{-}444}$ or $R^{298\text{-}690}$ pre-mRNA and time-points were taken. Samples were treated with heparin and complexes were resolved on a 2 % LMP gel.

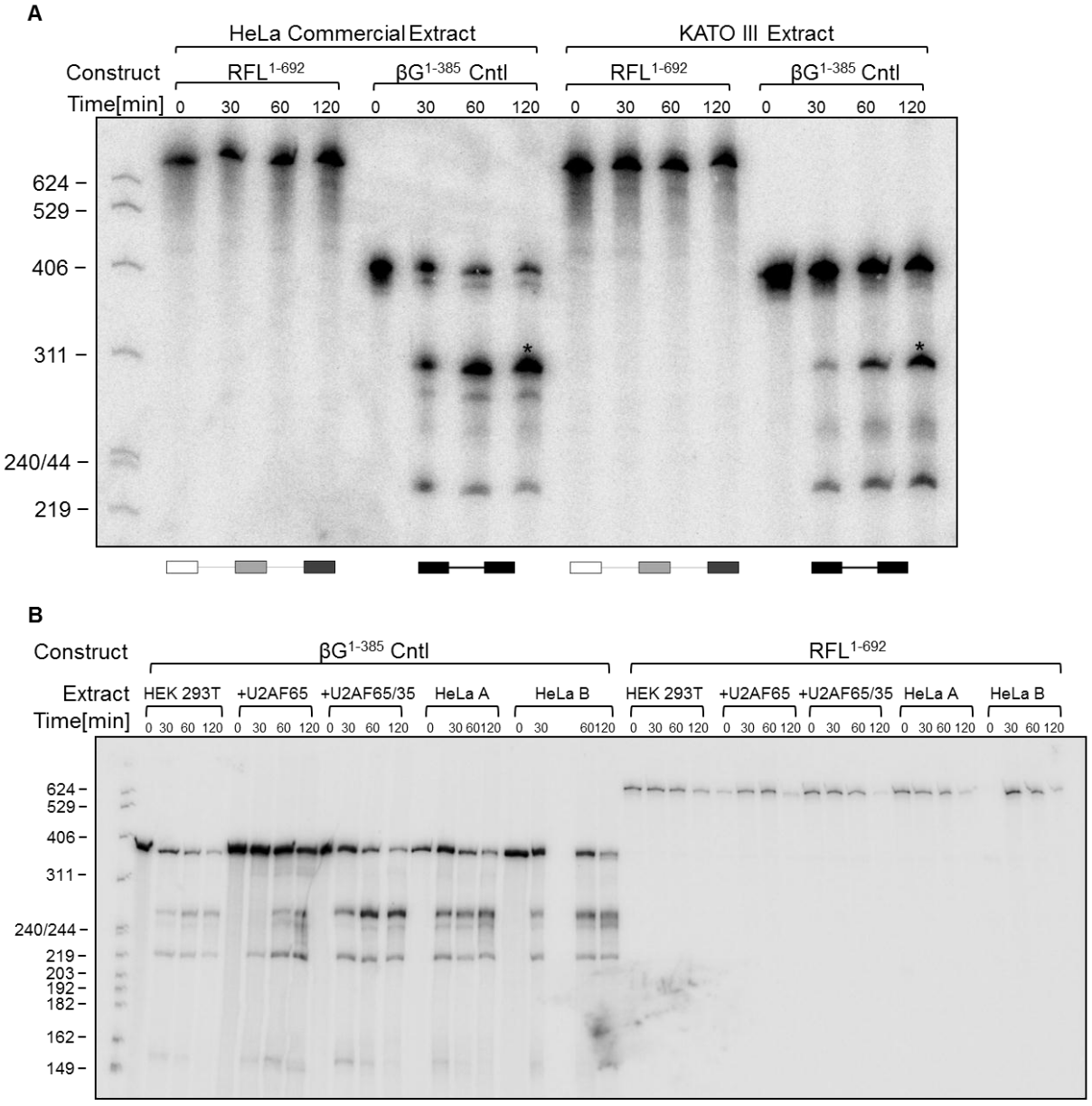

Figure 4.4. *In vitro* splicing of *RFL*[1-692] pre-mRNA in KATO III cell nuclear extract or HEK 293T cell nuclear extract with overexpression of U2AF65/35 does not stimulate splicing. **(A)** Splicing of *RFL*[1-692] in KATO III cell nuclear extract. **(B)** Splicing of *RFL*[1-692] in HEK 293T cell nuclear extract with overexpressed U2AF65 and U2AF65/35. (White = *RON* exon 10, Light Grey = *RON* exon 11, Dark Grey = *RON* exon 12, Thin lines = *RON* introns. Asterisks = mRNA)

4.4. Detailed Analysis of Splicing Signals

To identify the reason as to why *RFL*$^{1-692}$ does not splice *in vitro*, the splicing characteristics of a series of *RFL*$^{1-692}$/β-globin pre-mRNA constructs were analysed (Table 4.1. and 4.2.). Previously the regions in *RFL*$^{1-692}$ pre-mRNA that could potentially inhibit its splicing were identified and subsequently the effect of these on splicing was tested.

RFL$^{1-692}$/β-Globin constructs were synthesized with increased intron length, through the insertion of 20 nucleotides from the center of the β-globin intron into the center of each *RON* intron. The splicing characteristics of constructs with either one (RFL/INT10βG$^{44-63}$, RFL/INT11βG$^{44-63}$) or two (RFL/INT10+11βG$^{44-63}$) introns lengthened were assessed (Figure 4.5. A). The additional length did not induce splicing (Figure 4.5. B).

To identify where the splicing inhibitory region is located in *RFL*$^{1-692}$ pre-mRNA, the splicing of substrates fusing upstream and downstream regions of *R*$^{1-444(U1)}$/*R*$^{296-692(U1)}$ and β-globin was assessed (Figure 4.6. A). Splicing of these *RON*/β-Globin constructs showed that the downstream half of both introns 10 and 11 coupled with exon 11 and 12 respectively, were inhibitory for splicing (βG$^{1-279}$/R$^{254-444}$ and βG$^{1-279}$/R$^{485-692}$) (Figure 4.6. B). To identify whether specifically the exonic or intronic components of βG$^{1-279}$/R$^{254-444}$ and βG$^{1-279}$/R$^{485-692}$ were responsible for splicing inhibition, the splicing of additional constructs containing isolated exons and introns in a β-globin background was assessed. It was identified that that introns (Figure 4.6. D, R$^{1-444}$/βGINT$^{226-331}$, R$^{298-692}$/βGINT$^{226-331}$, βG$^{1-385}$/RINT$^{211-297}$ and βG$^{1-385}$/RINT$^{445-526}$), but not exons (Figure 4.6. C, R$^{1-210}$/βG$^{226-385}$, βG$^{1-331}$/R$^{298-444}$, R$^{298-444}$/βG$^{226-385}$, βG$^{1-331}$/R$^{525-692}$) contain the necessary sequences for inhibition of *RFL*$^{1-692}$ splicing. This was confirmed by the inhibitory effect of the downstream half of each *RON* intron on the

splicing of β-globin (βG$^{1\text{-}385}$/3'INTR$^{254\text{-}297}$ and βG$^{1\text{-}385}$/3'INTR$^{485\text{-}526}$) (Figure 4.6. E). Splicing of $R^{1\text{-}444(U1)}$ and $R^{296\text{-}692(U1)}$ was also stimulated through replacement of their inhibitory downstream intron segments by the complementary region from the β-globin intron (R$^{1\text{-}444}$/ 3'INTβG$^{280\text{-}331}$ and R$^{298\text{-}692}$/3'INTβG$^{280\text{-}331}$) (Figure 4.6. E).

Splicing of the R$^{298\text{-}484}$/βG$^{280\text{-}385}$ construct was also repeated in the presence of oligonucleotide 8 (250 nM) in order to assess whether this oligonucleotide could enhance splicing of a substrate that already partially splices. However, the oligonucleotide did not enhance splicing of this substrate (Figure 4.7. B).

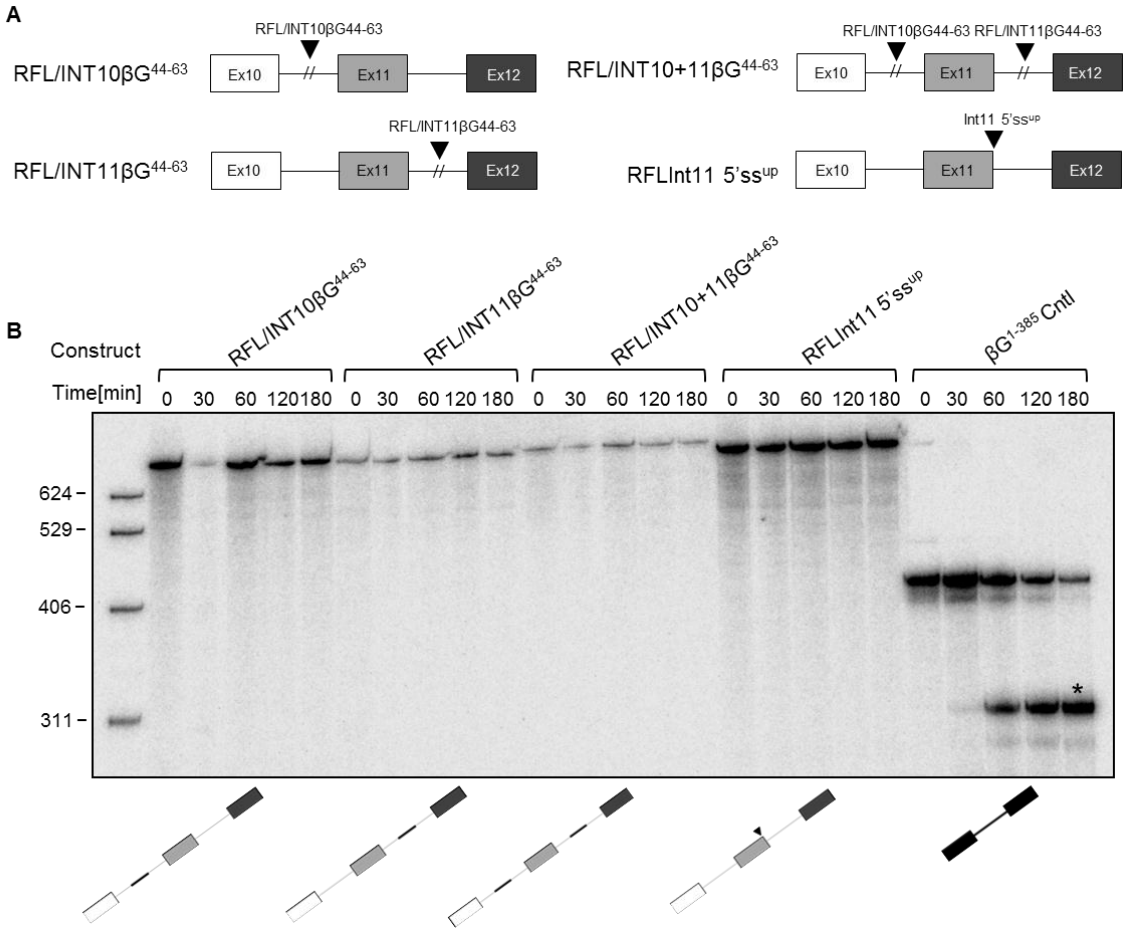

Figure 4.5. Increasing the length of *RON* introns 10 and 11 and up-regulating the 5' splice site of intron 11 does not stimulate splicing of *RFL*$^{1-692}$. Intron 10 and 11 were lengthened by 20 nucleotides, either individually (RFL/INT10βG$^{44-63}$, RFL/INT11βG$^{44-63}$) or together (RFL/INT10+11βG$^{44-63}$). The 5'splice site of intron 11 was up-regulated to the consensus sequence (Int11 5'ss^{up}). A schematic of each construct is shown below its pre-mRNA splicing. **(A)** Constructs used in this figure. **(B)** *In vitro* splicing assay of constructs shown in (A). (White = *RON* exon 10, Light Grey = *RON* exon 11, Dark Grey = *RON* exon 12, Thin lines = *RON* introns. Asterisks = mRNA)

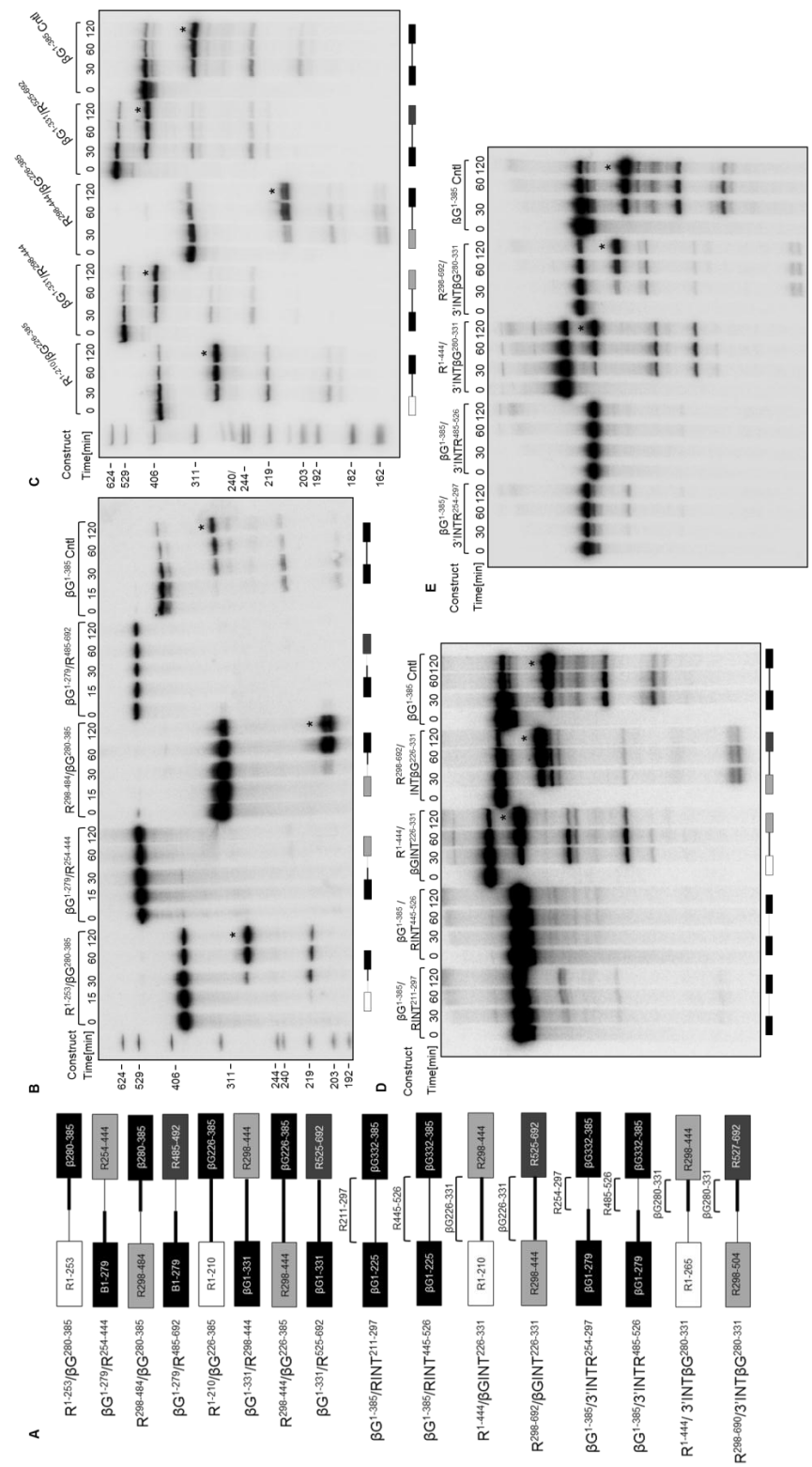

Figure 4.6. The downstream half of both *RON* introns 10 and 11 inhibit *RON* splicing. **(A)** Constructs used in this figure. **(B)** *In vitro* splicing assay of constructs combining the upstream and downstream halves of *RFL*$^{1\text{-}692}$ with the opposite half of $\beta G^{1\text{-}385}$. **(C)** *In vitro* splicing assay testing whether exons are inhibitory for splicing. Constructs contain a β-globin background with individual *RON* exons. **(D)** *In vitro* splicing assay testing whether introns 10 and 11 are inhibitory for *RON* splicing. Constructs contain either β-globin or *RON* exons separated by either intron 10 or 11 of *RON* or the β-globin intron, respectively. **(E)** *In vitro* splicing assays testing whether the downstream half of RON introns 10 and 11 are inhibitory. Constructs contain a β-globin background, with the downstream half of the β-globin intron replaced with either *RON* intron 10 or 11. (White = *RON* exon 10, Light Grey = *RON* exon 11, Dark Grey = *RON* exon 12, Black = β-globin, Thin lines = *RON* introns, Thick lines = β-globin introns).

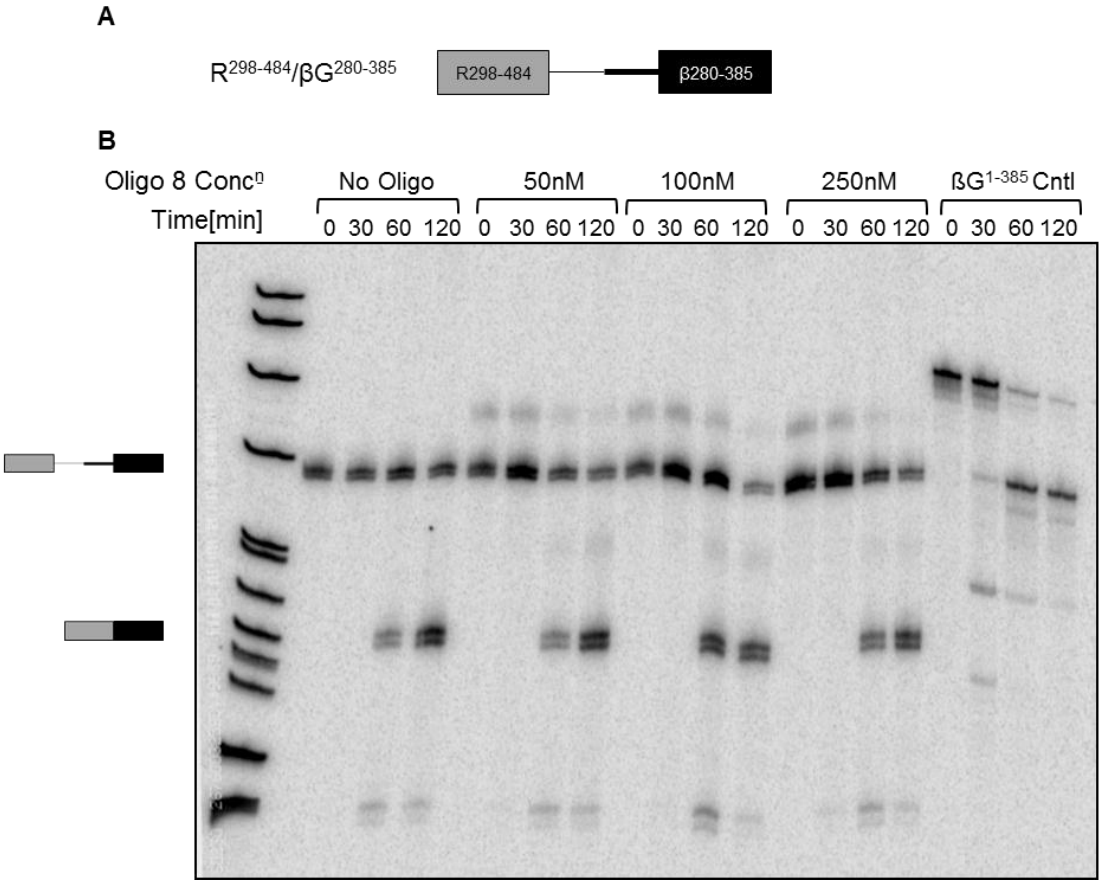

Figure 4.7. Oligonucleotide 8 does not enhance splicing of $R^{298-484}/\beta G^{280-385}$ pre-mRNA. **(A)** Construct used in this figure. **(B)** An *in vitro* splicing assay was carried out on $R^{298-484}/\beta G^{280-385}$ pre-mRNA in the presence of an increasing concentration of oligonucleotide 8, this construct splices *in vitro*. Oligonucleotide 8 was annealed to the RNA and a splicing time-course was carried out. Samples were resolved on a 6 % polyacrylamide gel containing formamide. The pre-mRNA and mRNA is labeled on the left of the image. (Grey box = *RON* Exon 11, Black box = β-globin, thin line = *RON* intron 11, thick line = β-globin intron)

4.5. Identifying the Specific Inhibitory Sequence in the Downstream Regions of *RON* Introns 10 and 11

Both *RON* intronic regions in constructs $\beta G^{1-385}/3'INTR^{254-297}$ and $\beta G^{1-385}/3'INTR^{485-526}$ were gradually replaced by intronic β-globin sequence (5'-3') in order to identify the minimal sequence required to inhibit β-globin splicing. Three constructs for intron 10 (Figure 4.8. A, $\beta G^{1-290}/R^{265-297}/\beta G^{332-385}$, $\beta G^{1-301}/R^{276-297}/\beta G^{332-385}$, $\beta G^{1-312}/R^{287-297}/\beta G^{332-385}$**)** and intron 11 **(**Figure 4.8. A, $\beta G^{1-292}/R^{495-524}/\ \beta G^{332-385}$, $\beta G^{1-305}/R^{505-524}/\beta G^{332-385}$, $\beta G^{1-318}/R^{515-524}/\beta G^{332-385}$) were synthesized. These constructs showed that the last 32 nucleotides in intron 10 and the last 20 nts in intron 11 ($R^{264-297}$ and $R^{504-524}$ respectively) are the minimal sequences required to inhibit splicing of β-globin (Figure 4.8. B and C). These minimal inhibitory regions contain the *RON* branch-point and polypyrimidine tract sequences and when both these sequences were replaced by the corresponding β-globin sequences in a *RON* background (Figure 4.8. A, R^{1-444}/βG297-331 BP PY and $R^{298-692}/\beta$G297-331 BP PY) splicing was induced (Figure 4.8. D and E).

To distinguish whether *RON* splicing inhibition is due specifically to either the branch-point or polypyrimidine tract sequences in the identified inhibitory regions, firstly the branch-points were mutated to the branch-point consensus sequence (Zhuang et al., 1989) and the effect of this on *RON* splicing was assayed. Two potential sites were up-regulated in both introns, one of which in both instances stimulated a low level of splicing of single intron constructs (Figure 4.9. A, R^{1-444}/264-269BP^{up} and $R^{298-692}$R501-507BP^{up}) (Figure 4.9. B and C). The observed low efficiency of splicing stimulated by branch-point up-regulation indicates that the branch-point must not be the only determining factor of *RON* splicing inhibition.

The effect of the *RON* intron 10 branch-point mutation, *RON* 264-269BP^{up}, was also tested for its effect on β-globin splicing. Two constructs were synthesised containing β-globin exon 2 as the upstream exon, *RON* intron 10 containing the branch-point mutation and either *RON* exon 11 or β-globin exon 3 as the downstream exon (Figure 4.9. A, βG$^{1-225}$/R$^{211-297}$R264-269BP^{up}/βG$^{332-385}$ and βG$^{1-225}$/R$^{211-444}$/R264-269BP^{up}). Splicing of these constructs indicated that *RON* exon 11 is a more well-defined exon than β-globin exon 3 as the efficiency of βG$^{1-225}$/R$^{211-297}$R264-269BP^{up}/βG$^{332-385}$ splicing was lower than βG$^{1-225}$/R$^{211-444}$/R264-269BP^{up} (Table 4.1.) (Figure 4.9. D). Thus, this strengthens the conclusion that *RON* exon 11 does not contribute to inhibition of RON splicing and that the last nucleotides of intron 10 contain the elements essential for splicing inhibition.

The weak 5' splice site of *RON* exon 11 could also be limiting *RFL*$^{1-692}$ splicing through poor U1 snRNP binding, as suggested for the 5' splice site of SMN2 intron 7 (Singh, Androphy, and Singh, 2004a). Therefore the effect of mutating the 5' splice site of intron 11 to the consensus 5' splice site sequence was also assessed (Figure 4.5. and 4.9. A, RFLInt11 5'ss^{up} and Int 11 5'ss^{up}). This modification did not enhance splicing of *RFL*$^{1-692}$ and also did not induce splicing of intron 11 in a single and double intron construct (Figure 4.5. B and 4.9. E). This again confirms that the 3' end of intron 10 and 11 contain the key inhibitory components for *RFL*$^{1-692}$ splicing (Figure 4.10.).

It was possible to assess the effect of oligonucleotide 8 on *RFL*$^{1-692}$ splicing *in vitro* if this construct was firstly stimulated to splice through mutation and then demonstrated increased exon 11 skipping in response to SRSF1 (Ghigna et al., 2005). This construct would then be a physiologically relevant testing system for studying oligonucleotide 8 action, and may reveal

other characteristics of *RFL*$^{1-692}$ pre-mRNA splicing regulation. To stimulate splicing intron 10 and 11 branch-point mutations (Figure 4.9. B and C) were applied to the *RFL*$^{1-692}$ two intron construct (Figure 4.11. A, RFL264-269BP^{up}, RFL280-286BP^{up}, RFL488-494BP^{up} and RFL501-407BP^{up}). A low level of *RON* Δ165 mRNA was produced with the R501-507BP^{up} mutation to intron 11, which was confirmed to be generated through splicing via a U6 snRNP knock-down (Dönmez et al., 2007). The 264-269BP^{up} mutation of intron 10 also stimulated a low level of splicing intermediates to be produced (Figure 4.11. B). To stimulate production of *RON* Δ165 mRNA splicing, a series of constructs coupling mutations of the branch-point in introns 10 and 11 and the 5' splice site of intron 11 were synthesized (Figure 4.11. A, RFL$^{1-692}$/264-269BP^{up}/Int115'ss^{up}, RFL$^{1-692}$/264-269BP^{up}/R501-407BP^{up} and RFL$^{1-692}$/264-269BP^{up}/Int115'ss^{up}/R501-407BP^{up}). Combining the 264-269BP^{up} branch-point mutation with the intron 11 5' splice site mutation did not generate spliced products, but did induce production of a splicing intermediate, as was seen in Figure 4.11. B (Figure 4.11. C). When coupled, the 264-269BP^{up} and 501-507BP^{up} branch-point mutations did induce splicing and the generation of a low level of both *RON* 10/11/12 and *RON* Δ165 mRNA (Figure 4.11. D and G). The following addition of the intron 11 5' splice site mutation to these stimulatory branch-point mutations did not significantly stimulate these mRNAs (Figure 4.11. D, E). Splicing of *RFL*$^{1-692}$ was further improved through the replacement of whole RON introns by the β-globin intron, and additional branch-point mutations in the remaining *RON* intron (Figure 4.11. E, F and G) (Figure 4.11. A, RFL$^{1-692}$/Int11βG$^{226-331}$, RFL$^{1-692}$/Int 1 βG 226-331/R501-407BP^{up} and RFL$^{1-692}$/264269BP^{up}/Int 2 βG 226-331).

Overall the splicing charcateristics of these constructs indicates that both *RON* introns are able to stall splicing at an intermediate or reduce splicing efficiency, when coupled in *RFL*$^{1\text{-}692}$ with a more defined intron such as β-globin (Figure 4.12.).

Finally the effect of oligonucleotide 8 on the splicing of *RFL*$^{1\text{-}692}$ constructs stimulated to splice through mutation was assessed. It was seen that this oligonucleotide had no effect on the splicing efficiency of any of the tested *RFL*$^{1\text{-}692}$ constructs (Figure 4.13. B) (Figure 4.13. A, RFL/264-269BP^{up}/501-507BP^{up}, RFL/264-269BP^{up}/Int115'ss^{up}/R501-507BP^{up}, RFL/Int 1 βG$^{226\text{-}331}$/R501-407BP^{up} and RFL/264-269BP^{up}/Int 2 βG$^{226\text{-}331}$).

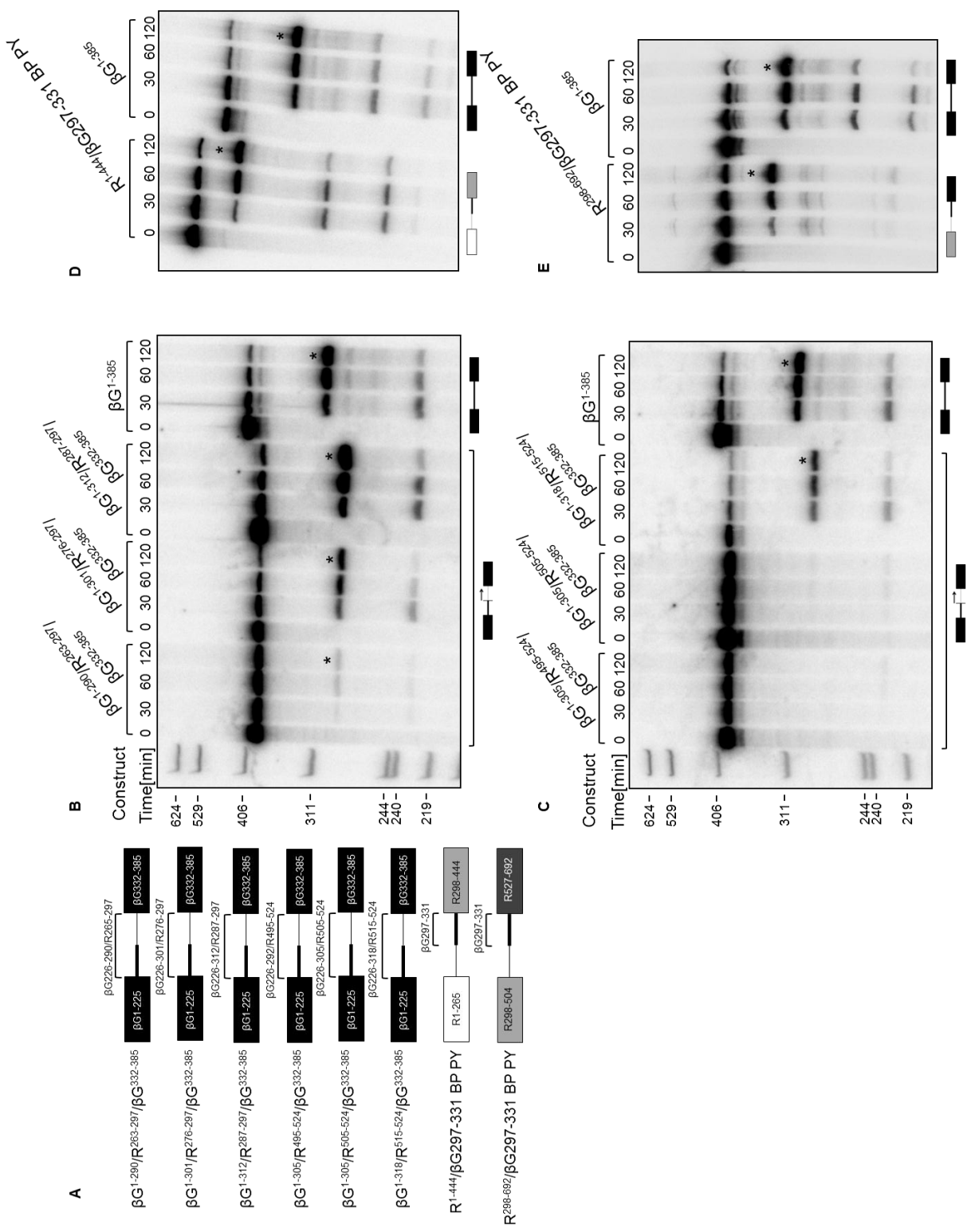
A
βG1-290/R263-297/βG332-385
βG1-301/R276-297/βG332-385
βG1-312/R287-297/βG332-385
βG1-305/R495-524/βG332-385
βG1-305/R505-524/βG332-385
βG1-318/R515-524/βG332-385
R1-444/βG297-331 BP PY
R298-692/βG297-331 BP PY
βG1-225
βG332-385
R1-265
R298-504
R527-692
βG226-290/R265-297
βG226-301/R276-297
βG226-312/R287-297
βG226-292/R495-524
βG226-305/R505-524
βG226-318/R515-524
βG297-331
B
C
D
E
Construct
Time[min]
0 30 60 120
βG1-385
R1-444/βG297-331 BP PY
R298-692/βG297-331 BP PY
624
529
406
311
244
240
219

[Figure 4.8.]

Figure 4.8. The minimal sequence required to inhibit *RON* spicing is the last 32 nucleotides of intron 10 ($R^{264-297}$) and the last 20 nucleotides of intron 11 ($R^{504-524}$). **(A)** Constructs used in this figure. **(B/C)** *In vitro* splicing assays were carried on pre-mRNA constructs consisting of the downstream inhibitory regions from *RON* (B) intron 10 and (C) 11, in a β-globin background. The *RON* intronic regions were gradually replaced by β-globin until splicing was stimulated and the inhibitory sequences identified. **(D/E)** Replacement of the bps and ppt of *RON* (D) introns 10 and (E) 11 with the corresponding β-globin sequence stimulates splicing of R^{1-444} and $R^{298-692}$ pre-mRNA. (White box = *RON* exon 10, Light grey box = *RON* exon 11, Dark grey box = *RON* exon 12, Black box = β-globin, Thin lines = *RON* introns, Thick lines = β-globin introns, Asterisk = mRNA).

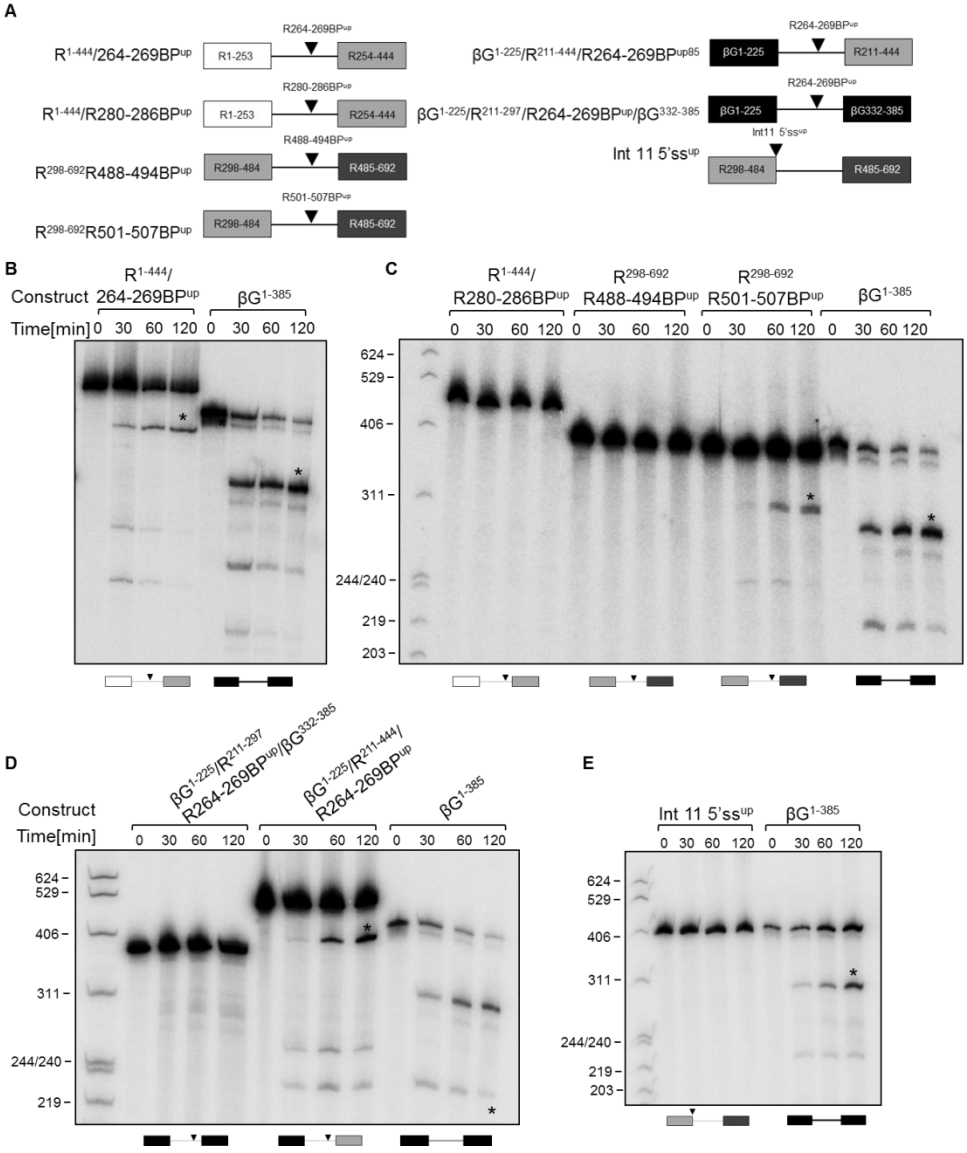

Figure 4.9. Mutation of both branch-points in *RON* introns 10 and 11 to the branch-point consensus sequence stimulates splicing of a single intron construct, but mutation of the 5' splice site of intron 11 to the 5' splice site consensus sequence does not. **(A)** Constructs used in this figure. **(B/C)** An *in vitro* splicing assay looking at the effect of the 264-269, 280-285, 488-494 and 501-507 branch-point mutations on $R^{1\text{-}444}$ and $R^{298\text{-}692}$ splicing. **(D)** An *in vitro* splicing assay on *RON* intron 10 containing the 264-269 branch point mutation, within β-globin exons 2 and 3 and the same intron within β-globin exon 2 and *RON* exon 11. **(E)** An *in vitro* splicing assay looking at the effect of up-regulation of the intron 11 5' splice site on splicing of $R^{298\text{-}692}$. (White = *RON* exon 10, Light Grey = *RON* exon 11, Dark Grey = *RON* exon 12, Black = β-globin, Thin lines = *RON* introns, Thick lines = β-globin introns).

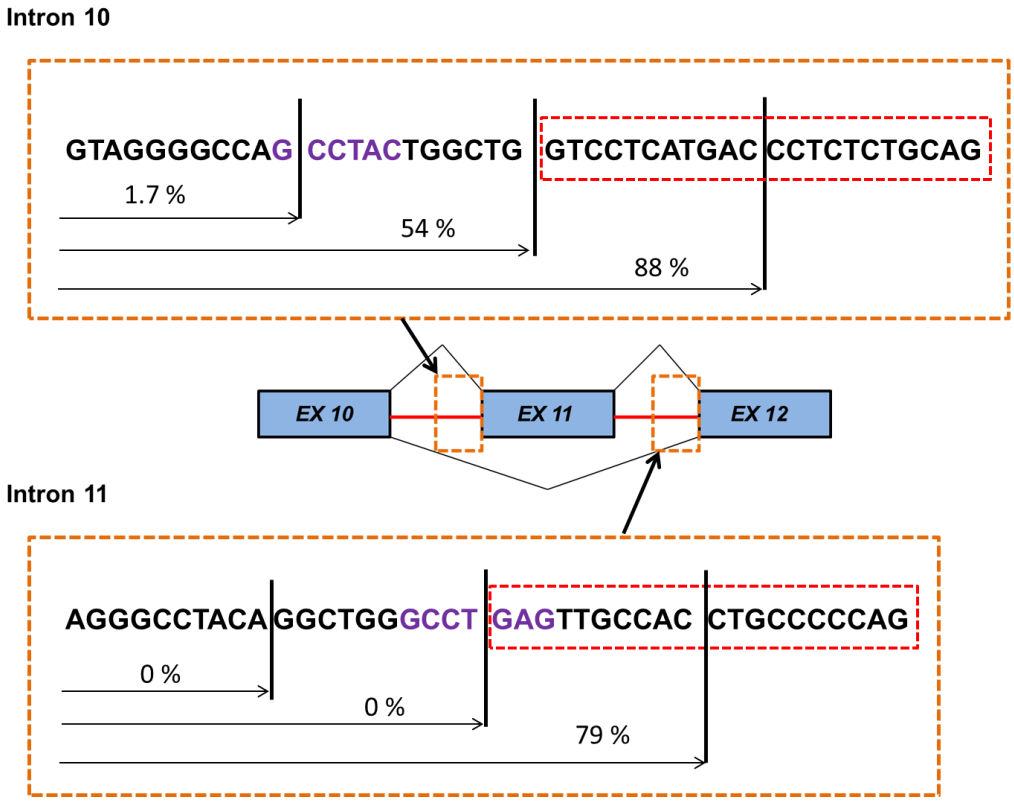

Figure 4.10. The inhibitory regions of *RFL*$^{1\text{-}692}$. The inhibitory downstream half of introns 10 and 11 (*RON* Int10$^{254\text{-}297}$ and Int11$^{485\text{-}526}$) are highlighted with orange dashed boxes. The black lined divisions shows the boundary to which RON was replaced by β-globin and the resulting percentage of mRNA production is shown. The 32 nt inhibitory region of intron 10 and the 20 nt inhibitory region of intron 11 are highlighted by red dashed boxes. The bp sequences are highlighted in purple font.

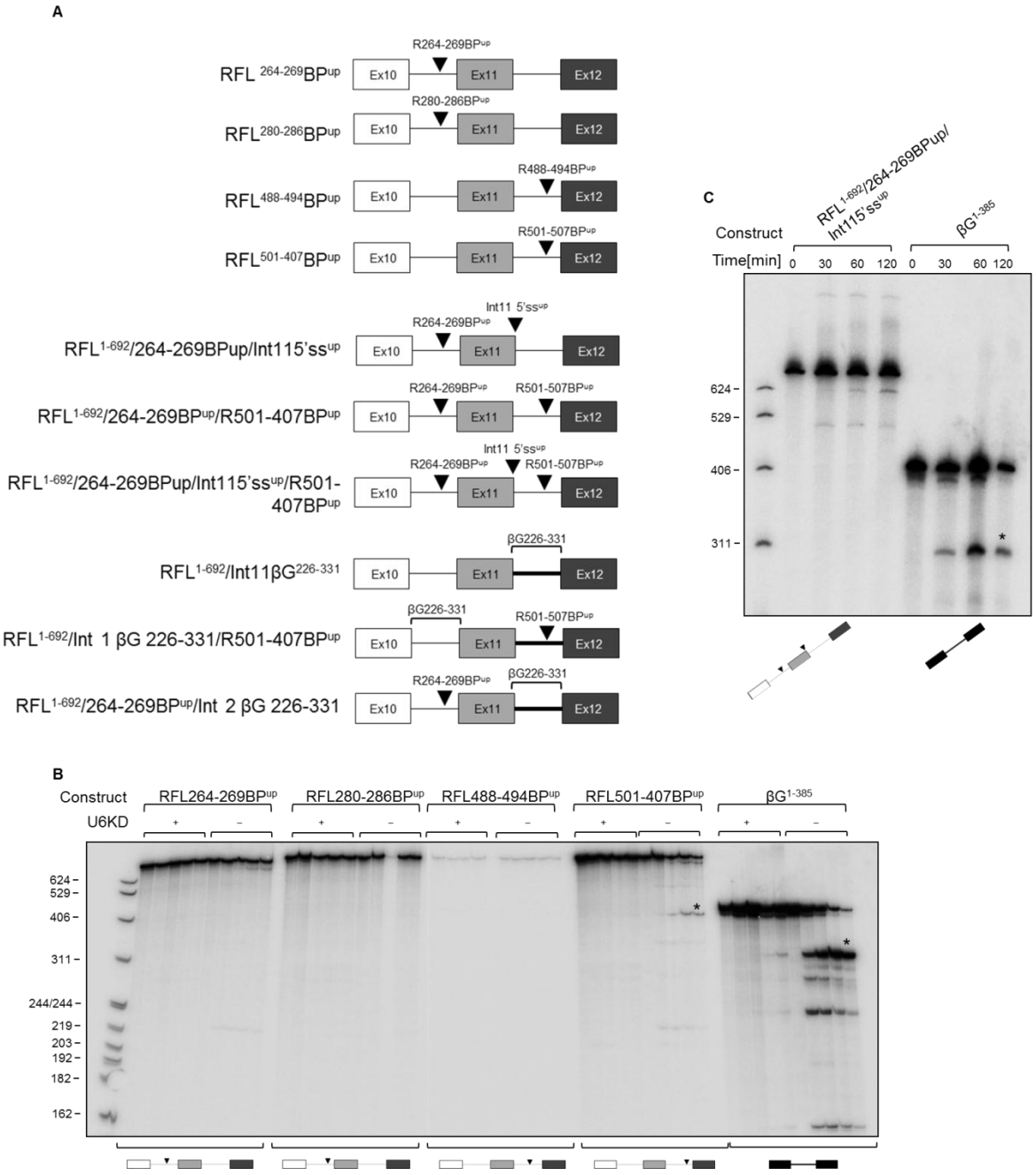
A
RFL 264-269BPup
R264-269BPup
RFL280-286BPup
R280-286BPup
RFL488-494BPup
R488-494BPup
RFL501-407BPup
R501-507BPup
RFL1-692/264-269BPup/Int115'ssup
Int11 5'ssup
RFL1-692/264-269BPup/R501-407BPup
RFL1-692/264-269BPup/Int115'ssup/R501-407BPup
RFL1-692/Int11βG226-331
βG226-331
RFL1-692/Int 1 βG 226-331/R501-407BPup
RFL1-692/264-269BPup/Int 2 βG 226-331
Ex10
Ex11
Ex12
C
Construct
RFL1-692/264-269BPup/Int115'ssup
βG1-385
Time[min]
0 30 60 120 0 30 60 120
624
529
406
311
B
Construct
RFL264-269BPup
RFL280-286BPup
RFL488-494BPup
RFL501-407BPup
βG1-385
U6KD
624
529
406
311
244/244
219
203
192
182
162

[Figure 4.11.]

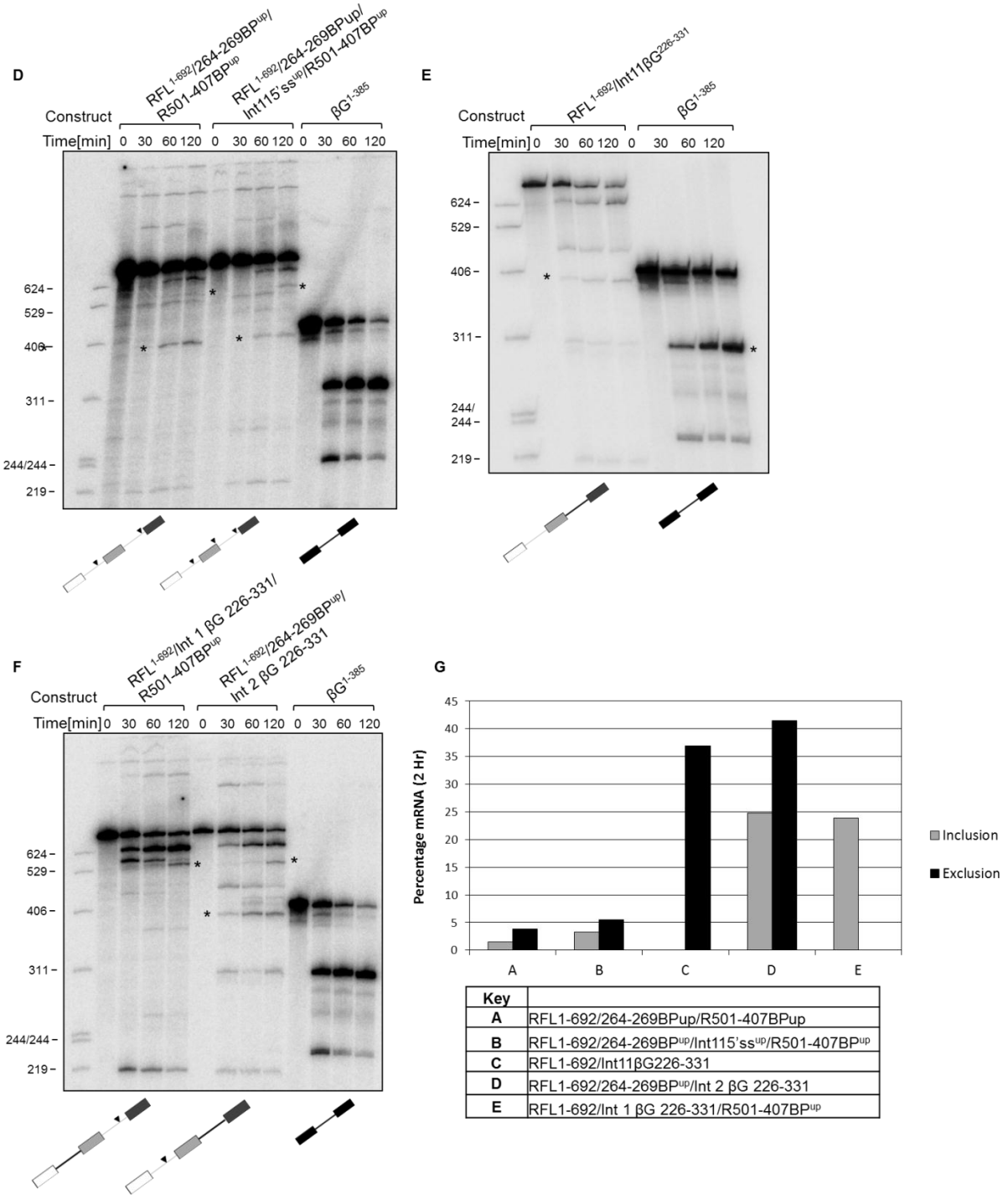
D
Construct
RFL1-692/264-269BPup/ R501-407BPup
RFL1-692/264-269BPup/ Int115'ssup/R501-407BPup
βG1-385
Time[min] 0 30 60 120 0 30 60 120 0 30 60 120
624
529
406
311
244/244
219
E
Construct
RFL1-692/Int11βG226-331
βG1-385
Time[min] 0 30 60 120 0 30 60 120
624
529
406
311
244/ 244
219
F
Construct
RFL1-692/Int 1 βG 226-331/ R501-407BPup
RFL1-692/264-269BPup/ Int 2 βG 226-331
βG1-385
Time[min] 0 30 60 120 0 30 60 120 0 30 60 120
624
529
406
311
244/244
219
G
Percentage mRNA (2 Hr)
45
40
35
30
25
20
15
10
5
0
A
B
C
D
E
Inclusion
Exclusion
Key
A RFL1-692/264-269BPup/R501-407BPup
B RFL1-692/264-269BPup/Int115'ssup/R501-407BPup
C RFL1-692/Int11βG226-331
D RFL1-692/264-269BPup/Int 2 βG 226-331
E RFL1-692/Int 1 βG 226-331/R501-407BPup

[Figure 4.11.]

Figure 4.11. Branch-point and 5' splice site mutations to consensus sequences in the *RFL*$^{1-692}$ construct stimulates splicing. **(A)** Constructs used in this figure. **(B)** An *in vitro* splicing assay testing the effect of single bp mutation on splicing of *RFL*$^{1-692}$. **(C)** An *in vitro* splicing assay assessing the effect of coupling the intron 10 bp mutation and the intron 11 5' ss mutation on the splicing of *RFL*$^{1-692}$. **(D)** An *in vitro* splicing assay testing the effect of coupled bp mutations, with and without the intron 11 5' ss mutation, on the splicing of *RFL*$^{1-692}$. **(E/F)** The effect of replacing individual *RON* introns with the β-globin intron, with and without mutation of the opposing *RON* bp **(G)** A histogram showing the percentage of mRNA (either exon 11included or excluded) produced after 2 hrs of splicing constructs shown in A-E. (White box= *RON* exon 10, Light Grey box = *RON* exon 11, Dark grey box = *RON* exon 12, Black box = β-globin, Thin lines = *RON* introns, Thick lines = β-globin introns, Asterisk = mRNA).

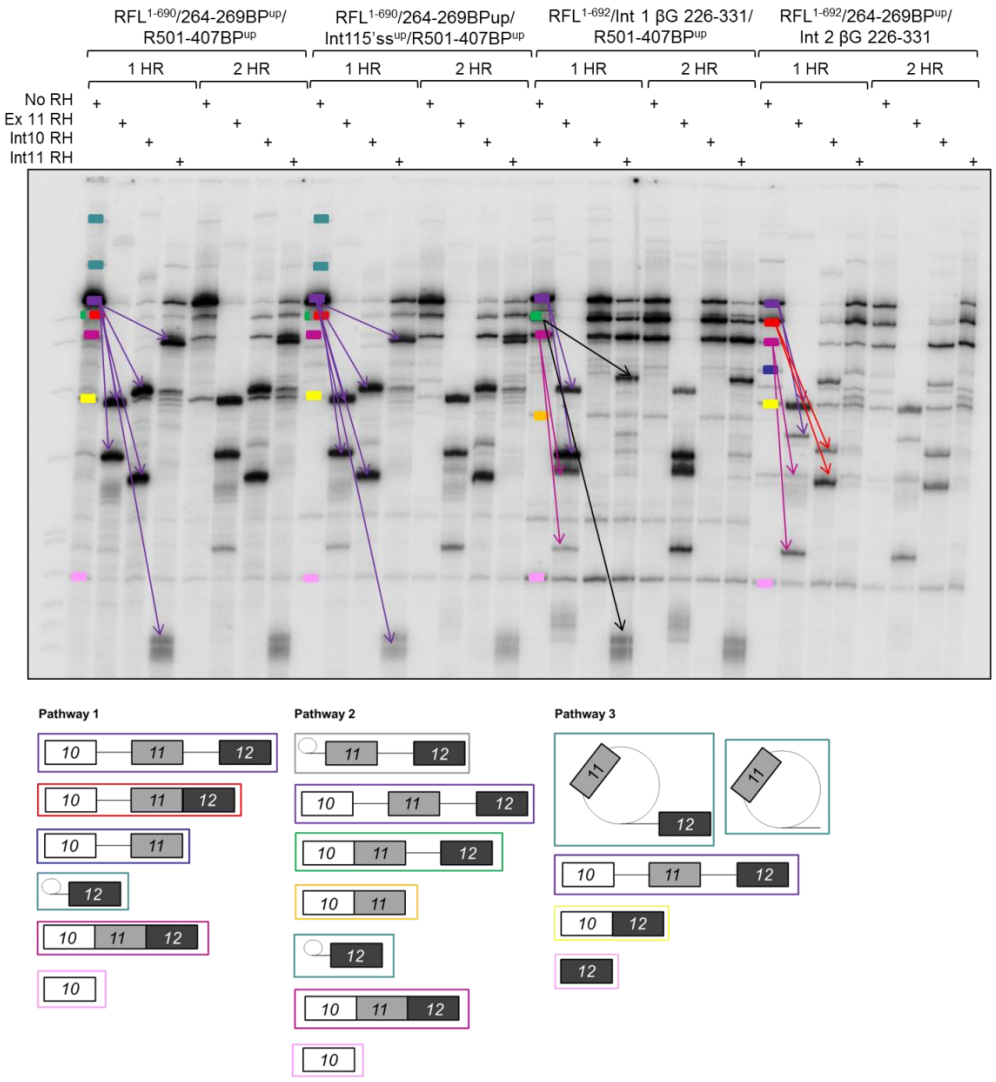

Figure 4.12. RNase H-compatible DNA oligonucleotides targeted to *RON* exon 11 and intron 10 and 11 were used to identify splicing intermediates, products and pathways for each contruct tested. Coloured arrows show RNA bands resulting from digestion of an original RNA product shown at the arrows origin. Splicing intermediates and products are contained in coloured boxes that correspond to the coloured boxes shown on the splicing gel. RFL$^{1\text{-}692}$/264-269BP^{up}/R501-407BP^{up} and RFL$^{1\text{-}692}$/264-269BP^{up}/Int115'ss^{up}/R501-407BP^{up} splice successfully thorough pathway 3 to produce *RON* Δ165 mRNA. Intermediates of pathway 1 and 2 could also be present here, however splicing through pathway 1 and 2 is stalled in these constructs. RFL$^{1\text{-}692}$/Int 1 βG 226-331/R501-407BP^{up} splices through pathway 2, with the β-globin intron splicing before *RON* intron 11. RFL$^{1\text{-}692}$/264-269BP^{up}/Int 2 βG 226-331 splices through pathway 2, with the β-globin intron splicing before *RON* intron 10.

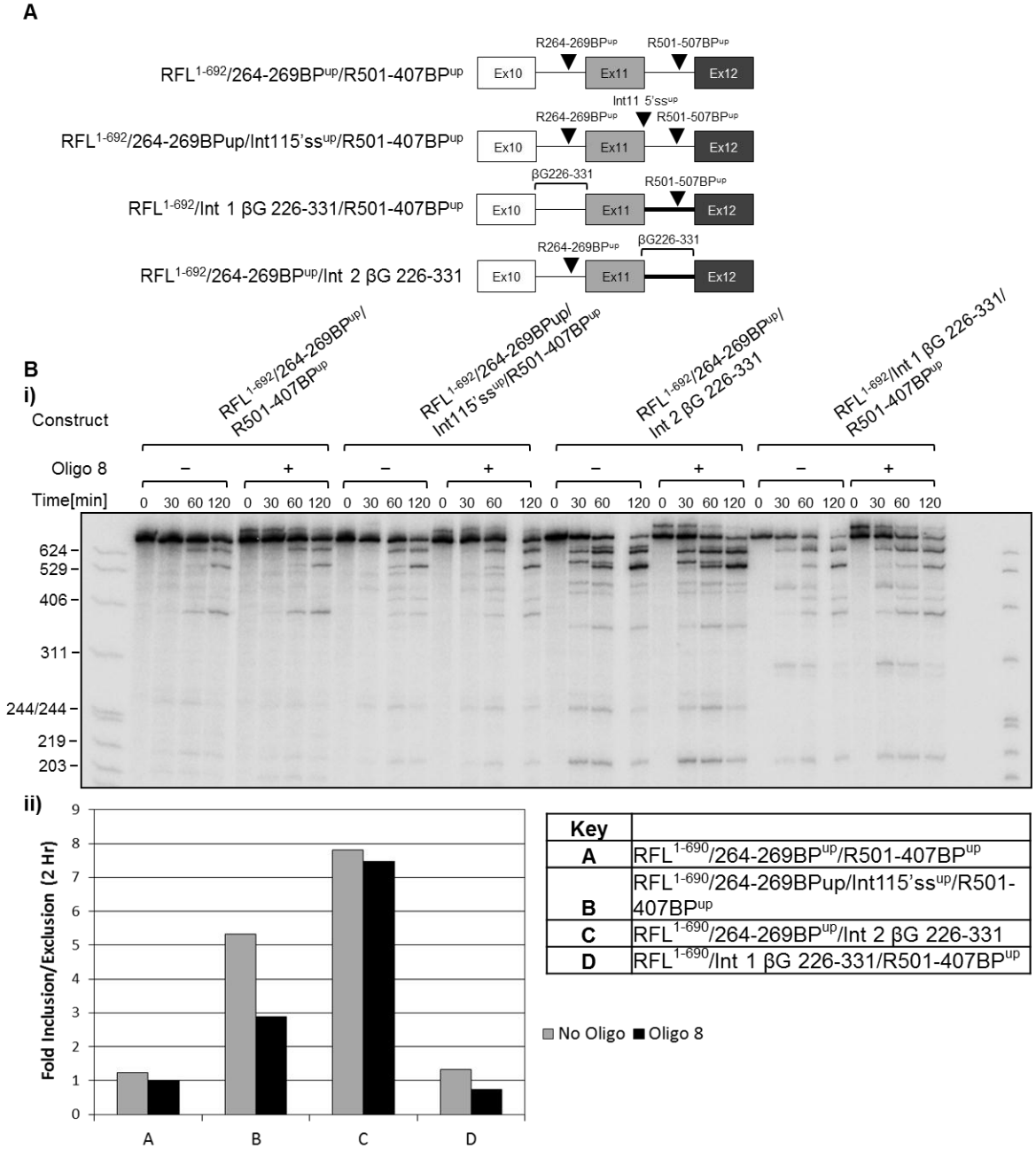

Figure 4.13. Oligonucleotide 8 has no effect on splicing of *RFL*$^{1\text{-}692}$ constructs that have been stimulated to splice through branch-point mutations, intron lengthening and and 5' splice site mutation. **(A)** Constructs used in this figure. **(B)** (i) In vitro splicing assay assessing the effect of oligonucleotide 8 on splicing of *RFL*$^{1\text{-}692}$ constructs. (ii) A histogram showing the effect of this oligonucleotide on the splicing of these constructs after 2 hrs.

4.6. Identification of RNA Binding Proteins

As mutation of branch-point sequences to the consensus sequence does not stimulate efficient *RFL*$^{1-692}$ splicing (Figure 4.9. B and C, Figure 4.11., Table 4.1. and 4.2.), but replacement of the downstream intronic region of both RON introns does (Figure 4.6. E, Figure 4.8.), indicates that another factor in addition to the weak branch-point sequences is inhibiting *RON* splicing. The polypyrimidine tract sequence of both *RON* introns 10 and 11 is weak, and it is a possibility that U2AF65 binding to this region is being inhibited by the binding of a protein factor. Protein binding to the inhibitory regions, *RON* Int10$^{254-297}$ and Int11$^{485-526}$ (Figure 4.14.), was assessed using the web tool 'splice aid' and this indicated that proteins hnRNP H/F/L and A1 could be binding to this region (Figure 4.14.).

UV cross-linking of the *RON* Int10$^{254-297}$ and Int11$^{485-526}$ inhibitory regions (Figure 4.15. A) in HeLa nuclear extract was used to identify protein binding partners of this sequence. Two proteins at approximately 50 KDa were identified to cross-link to the inhibitory regions of *RFL*$^{1-692}$ (Figure 4.15. B), highlighting PTB (57-KDa) and hnRNP H/F (56/53-KDa) as potential binding partners. The cross-linked proteins were shown to not be PTB, by repeating the cross-linking in an extract expressing a PTB-eGFP fusion protein (gift from D Cherny) (Figure 4.15. C). However, binding of hnRNP H/F to both substrates was confirmed through cross-linking in nuclear extract expressing an hnRNP F-GFP fusion protein (Figure 4.15. D) and also through cross-linking to qRRM 1/2 and 3 of hnRNP F (gift from C Dominguez, (Dominguez and Allain, 2006) (Figure 7.1.). A crosslink-IP, utilizing an hnRNP H/F antibody, more precisely confirmed the association of this protein with these regions in *RON* (Figure 4.15. E).

Protein binding partners for the minimal splicing inhibitory regions in intron 10 and 11 ($R^{264-297}$ and $R^{504-524}$ respectively) were now investigated (Figure 4.16. A). The same pattern of cross-linking was seen (as in Figure 4.15. B) when UV cross-linking was carried out on the 32 nt *RON* intron 10 fragment, but not the 20 nt *RON* intron 11 fragment (Figure 4.16. B). To confirm that the cross-link on the 32 nucleotide inhibitory region of intron 10 was not PTB, cross-linking of this fragment was carried out alongside a PTB cross-link control (Figure 4.16. C). To analyse protein binding further a biotin affinity purification on both the 32 nt intron 10 fragment and the 20 nt intron 11 fragment was proposed. However, when attempted the biotin affinity purification showed no recovery of proteins, even though native gel analysis of complex formation on these RNA substrates indicated that complexes could stably form (Figure 4.16. D).

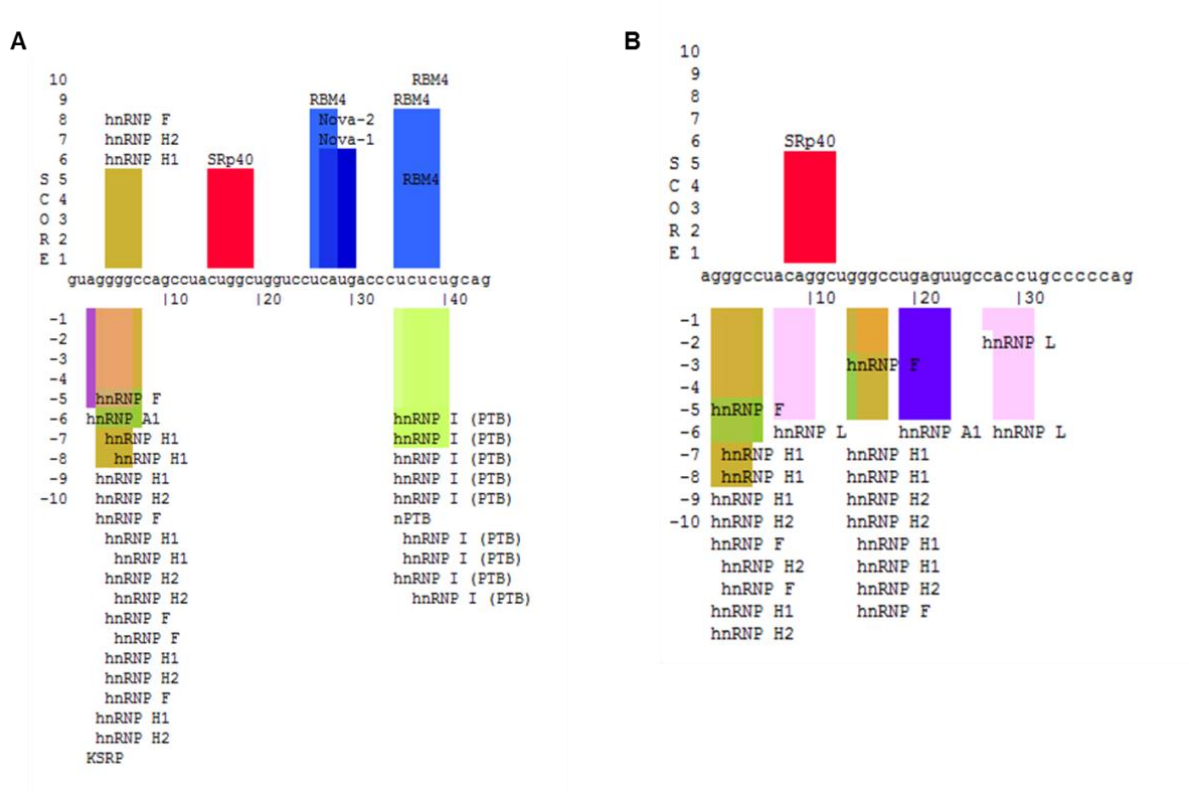

Figure 4.14. *In silico* prediction of protein binding to *RON* inhibitory regions. The 'SpliceAid' database (www.introni.it/splicing.html) was used to predict protein binding on **(A)** $R^{1\text{-}444}$ and **(B)** $R^{298\text{-}692}$**.** The sequences were analysed and the protein binding partners of both intron segments are labeled on the graphs. The height of the bar is an indication of the strength of protein binding, with the higher bars indicating greater binding affinity and vice versa. Positive bars indicate enhancers and negative bars indicate silencers.

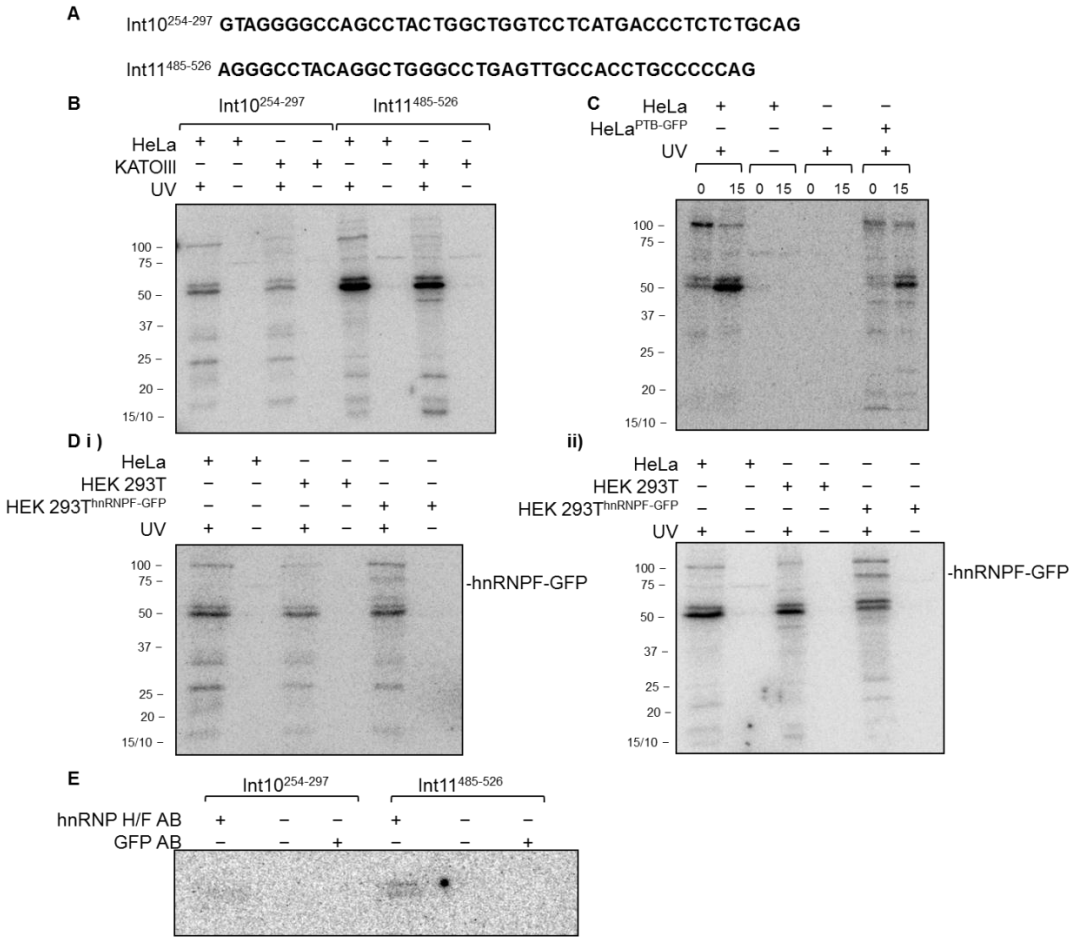

Figure 4.15. Analysis of UV cross-linking of *RON* Int10$^{254\text{-}297}$ and Int11$^{485\text{-}526}$ RNA identifies that hnRNP H/F is binding to this region. **(A)** Sequence of *RON* Int10$^{254\text{-}297}$ and Int11$^{485\text{-}526}$. **(B)** UV cross-linking of *RON* Int10$^{254\text{-}297}$ and Int11$^{485\text{-}526}$ RNA in the presence of either HeLa or KATO III nuclear extract was carried out. An *in vitro* splicing assay was set up, incubated at 30 °C for 15 minutes and then cross-linked using short wave UV. Samples were digested with RNase A and T1, before resolution on a 12 % non-denaturing polyacrylamide gel. Radioactive RNA was transferred to nitrocellulose and exposed to a phosphorimager screen. **(C)** UV cross-linking was carried out as in (a), in the presence of HeLa nuclear extract expressing a PTB-GFP fusion protein. **(D)** UV cross-linking was carried out as in (a) in the presence of HEK 293T nuclear extract expressing an hnRNP F-GFP fusion protein that enabled identification of hnRNP F cross-linking. The additional crosslink is labeled on the left. (i) RON Int10$^{254\text{-}297}$ and (ii) Int11$^{485\text{-}526}$. **(E)** To confirm the binding of hnRNP F/H a crosslink-IP was carried out using an hnRNP H/F AB. A UV cross-linking reaction was carried out as in (a), however the cross-linked samples were immunoprecipitated before resolution on a gel.

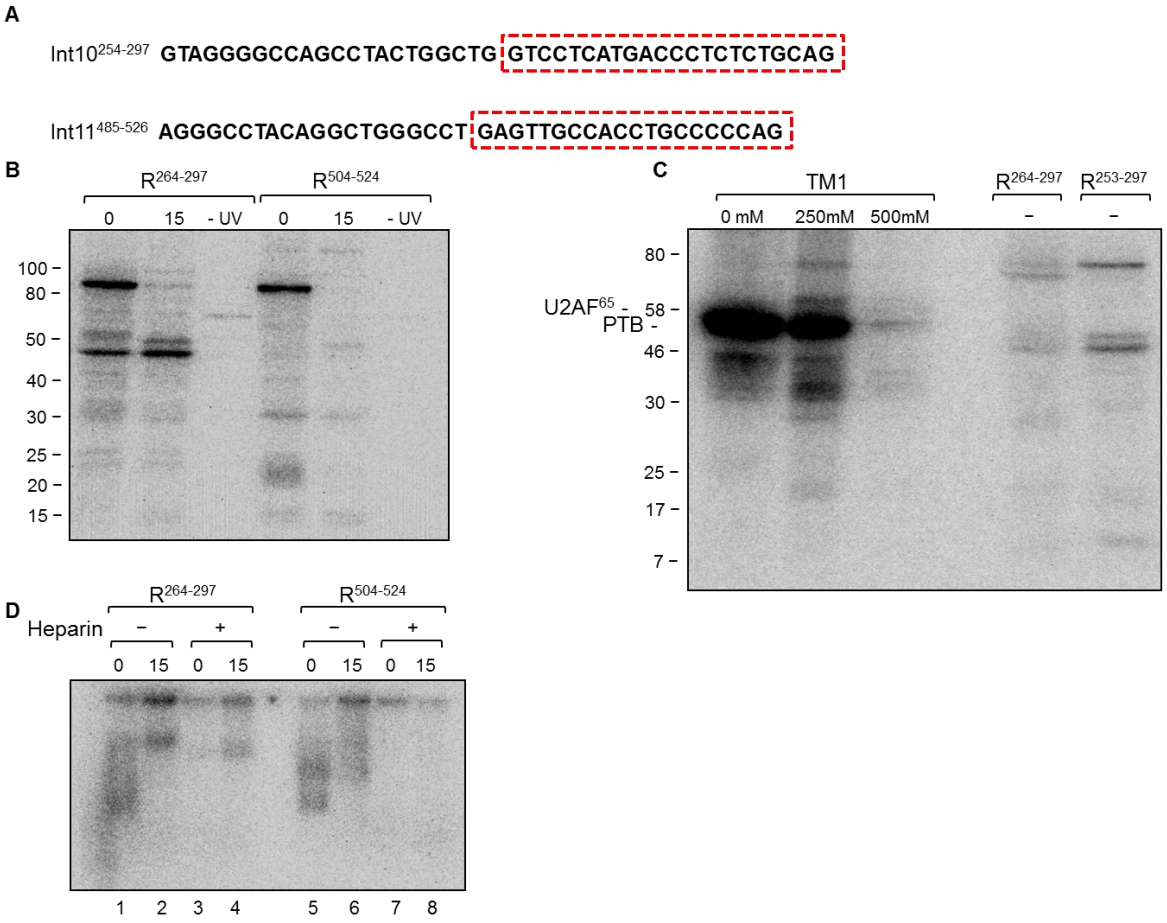

Figure 4.16. hnRNP F/H cross-linking is maintained to $R^{264-297}$ but not $R^{504-524}$ minimal *RON* inhibitory regions. **(A)** Sequence of *RON* $Int10^{264-297}$ and $Int11^{504-526}$ inhibitory regions highlighted by red dashed boxes. **(B)** Cross-linking of proteins to *RON* $Int10^{264-297}$ and $Int11^{504-526}$. An *in vitro* splicing reaction containing radiolabelled RNA fragments was set up and incubated at 30 °C for 15 minutes, cross-linked using short wave UV for 5 minutes and digested using RNase A and T1. Samples were resolved on a 12 % non-denaturing polyacrylamide gel, transferred to nitrocellulose and exposed to a phosphorimager screen. **(C)** Cross-linking was carried out as in (a), with $Int10^{254-297}$ and $Int10^{264-297}$. A PTB cross-linking control included to identify PTB cross-linking. **(D)** Protein complexes were shown to form on *RON* $Int10^{264-297}$ and $Int11^{504-526}$. A splicing reaction was set up and incubated as normal, time-points taken and samples treated with heparin before resolution of formed complexes on a 2 % LMP agarose gel.

4.7. Summary

Analysis of the splicing characteristics of *RFL*$^{1\text{-}692}$ pre-mRNA has shown that exons 10, 11 and 12, the 5 ‘ splice site of intron 11 and intron length do not inhibit splicing of this region. *RFL*$^{1\text{-}692}$ pre-mRNA does not splice *in vitro* in either a one intron or two intron context. RON nucleotides 264-297 and 504-524 in this region have been identified to be the minimal sequences required to inhibit *RFL*$^{1\text{-}692}$ splicing. Therefore the failure of *RFL*$^{1\text{-}692}$ to splice *in vitro* is a consequence of poor polypyrimidine tract sequences in *RON* introns 10 and 11, with weak branch-points possibly also having an inhibitory role. *RFL*$^{1\text{-}692}$ also splices via intron definition and a low level of splicing can be stimulated through double intron branch-point up-regulation, with or without intron 11 5’ splice site up-regulation.

hnRNP H/F cross-links to the inhibitory downstream half of *RON* introns 10 and 11 and this pattern of cross-linking is maintained to *RON* nucleotides 264-297, but not 504-524.

Table 4.1. Single Intron RON Constructs.

Construct	Schematic	Synthesis Oligos	% mRNA (2Hr)
$\mathbf{R^{1-253}/\beta G^{280-385}}$	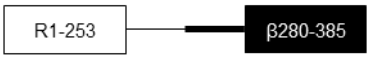	1C 2A 14C 13C	72
$\mathbf{\beta G^{1-279}/R^{254-444}}$	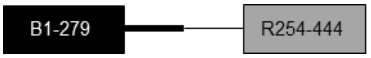	1A 6C 18C 15C	0
$\mathbf{R^{298-484}/\beta G^{280-385}}$	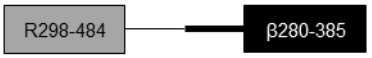	2C 2A 14C 16C	62
$\mathbf{\beta G^{1-279}/R^{485-692}}$	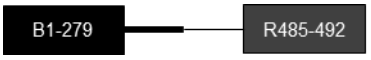	19C 9C 1A 17 C	0
$\mathbf{R^{1-210}/\beta G^{226-385}}$		1C 2A 20C 21C	96
$\mathbf{\beta G^{1-331}/R^{298-444}}$		1A 6C 22C 11C	91
$\mathbf{R^{298-444}/\beta G^{226-385}}$		2C 23C 24C 2A	85
$\mathbf{\beta G^{1-331}/R^{525-692}}$		1A 25C 26C 9C	94
$\mathbf{\beta G^{1-385}/INTR^{211-297}}$	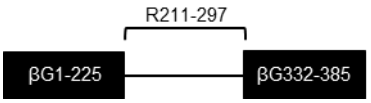	1A 28C 27C 2A 31C 32C	1.6
$\mathbf{\beta G^{1-385}\ /INTR^{445-526}}$	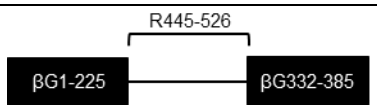	1A 2A 29C 30C 33C 34C	0
$\mathbf{R^{1-444}/INT\beta G^{226-331}}$	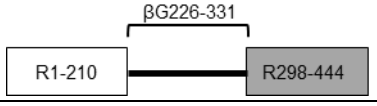	1C 6C 20C 21C 22C 12C	91
$\mathbf{R^{298-692}/INT\beta G^{226-331}}$	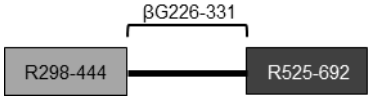	2C 23C 24C 9C 25C 26C	86

βG$^{1-385}$/3'INTR$^{254-297}$	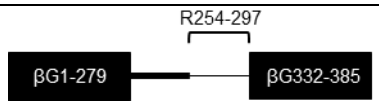	1A 18C 2A 15C	2.6
βG$^{1-385}$/3'INTR$^{485-526}$	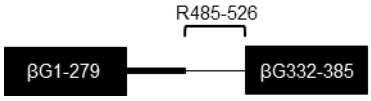	1A 19C 2A 17C	0
R$^{1-444}$/3'INTβG$^{280-331}$		1C 14C 6C 13C	72
R$^{298-692}$/3'INTβG$^{280-331}$		2C 14C 16C 9C	68
βG$^{1-290}$/R$^{265-297}$/βG$^{332-385}$	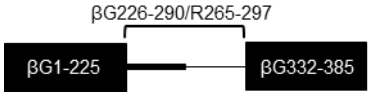	1A 2A 37C 40C	0
βG$^{1-301}$/R$^{276-297}$/βG$^{332-385}$	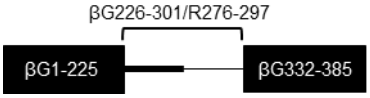	1A 2A 38C 41C	59
βG$^{1-312}$/R$^{287-297}$/βG$^{332-385}$	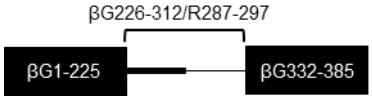	1A 2A 39C 42C	90
βG$^{1-292}$/R$^{495-524}$/ βG$^{332-385}$	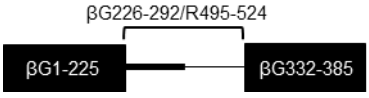	1A 2A 43C 44C	0
βG$^{1-305}$/R$^{505-524}$/βG$^{332-385}$	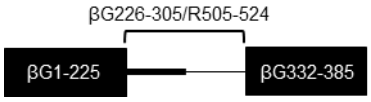	1A 2A 45C 46C	0
βG$^{1-318}$/R$^{515-524}$/βG$^{332-385}$	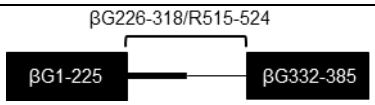	1A 2A 47C 48C	81
R$^{1-444}$/264-269BP^{up}	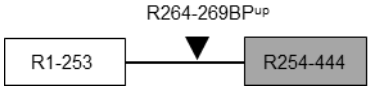	1C 56C 57C 6C	16
R$^{1-444}$/R280-286BP^{up}	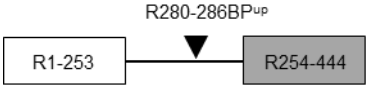	1C 58C 59C 6C	0
R$^{298-692}$R488-494BP^{up}	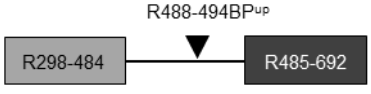	2C 60C 61C 9C	0

$R^{298-692}$R501-507BP^{up}	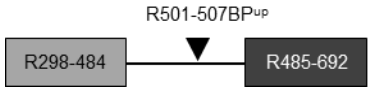	2C 62C 63C 9C	1.7
Int 11 5'ss^{up}		2C 64C 65C 7C	0
$\beta G^{1-225}/R^{211-444}$/R264-269$BP^{up}$	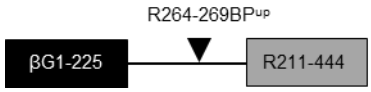	1A 6C 31C 32C	0
$\beta G^{1-225}/R^{211-297}$/R264-269$BP^{up}/\beta G^{332-385}$	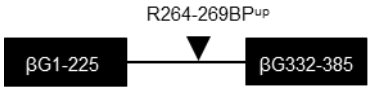	1A 2A 31C 32C 27C 28C	20
R^{1-444}/βG297-331 BP PY		1C 6C 53C 55C	89
$R^{298-692}/\beta$G297-331 BP PY	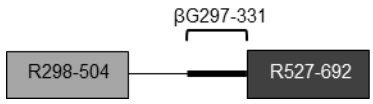	2C 9C 54C 55C	77

Table 4.2. Double Intron RON Constructs.

Construct	Schematic	Synthesis Oligos	% Incl (2 Hr)	% Excl (2 Hr)
***RFL*/INT10βG$^{44-63}$**	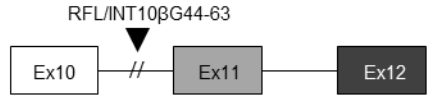	1C 9C 75C 76C	0	0
***RFL*/INT11βG$^{44-63}$**	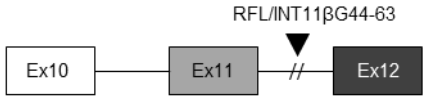	1C 9C 77C 78C	0	0
***RFL*/INT10+11βG$^{44-63}$**		1C 9C 75C 76C 77C 78C	0	0
***RFL* Int11 5'ss^{up}.**	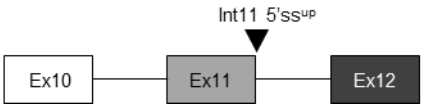	1C 9C 64C 65C	0	0
***RFL* 264-269BP^{up}**	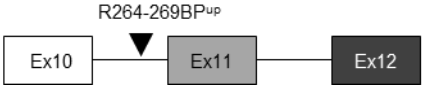	1C 9C 56C 57C	0	0
***RFL* 280-286BP^{up}**	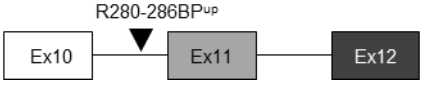	1C 9C 58C 59C	0	0
***RFL* 488-494BP^{up}**	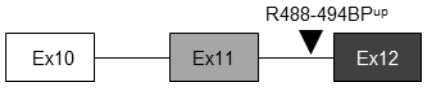	1C 9C 60C 61C	0	0
***RFL* 501-507BP^{up}.**	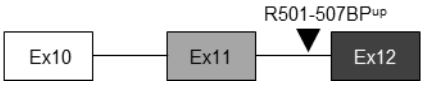	1C 9C 62C 63C	0	22
***RFL*/264-269BP^{up}/501-507BP^{up}**	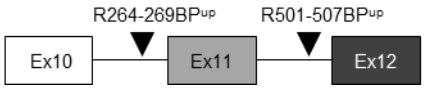	1C 9C 56C 57C 62C 63C	1.5	3.8

***RFL*/264-269BP^{up}/Int115'ss^{up}**	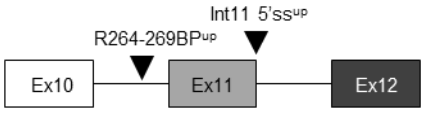	1C 9C 56C 57C 64C 65C	0	0
***RFL*/264-269BP^{up}/Int115'ss^{up}/R501-507BP^{up}**	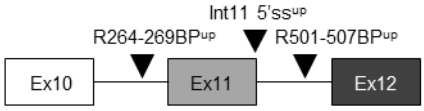	1C 9C 56C 57C 64C 65C 62C 63C	3.2	5.5
***RFL*/Int11βG$^{226-331}$**	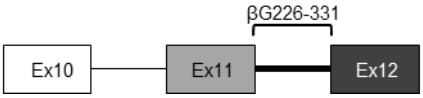	1C 9C 23C 24C	0	37
***RFL*/Int 1 βG$^{226-331}$/R501-407BP^{up}**	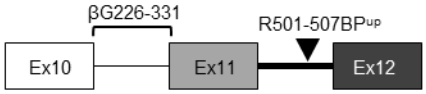	1C 9C 20C 21C 62C 63C	24	0
***RFL*/264-269BP^{up}/Int 2 βG$^{226-331}$**	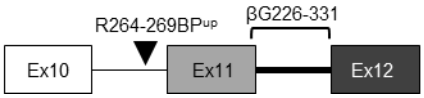	1C 9C 23C 24C 56C 57C	25	41

5. Inhibiting Splicing of *IgM* pre-mRNA Using Oligonucleotides

5.1. Introduction

The IgM receptor is a fundamental component of the BCR receptor, expressed at the cell membrane of premature B-cells. This receptor is important in the maturation of B-cells into memory and plasma B-cells, during the immune response. However, signaling through this receptor has also been implicated in the survival of B-CLL cells, with signaling through these receptors instilling resistance to apoptosis and hence resistance to chemotherapy.

ASOs have previously been used successfully to alter the characteristics of pre-mRNA splicing in disease and may be applied here to alter splicing and expression of IgM in B-CLL. ASO-mediated inhibition of IgM and so BCR expression at the cell membrane of B-CLL cells could potentially inhibit the transfer of positive survival signals to these cells alleviating apoptosis resistance and allowing for chemotherapeutically induced cell death.

5.2. An Artificial System to Assay *IgM* Oligonucleotides

To test the efficiency of exclusion of exons M1 and M2 from *IgM* mRNA through action of *IgM* oligonucleotides (Figure 5.1. A and C), an artificial red-green assay system was established. The aim of this was to establish a stable cell-line expressing the Cμ4-M1 region with the fluorescent DsRed-eGFP indicator to allow for quick assessment of potential ASOs.

A DsRed-eGFP vector containing the Cμ4-M1 region of IgM was synthesized (Figure 5.1. B). Previously it has been shown that HeLa cells can express both spliced (μ_m) and polyadenylated (μ_s) forms of IgM (Peterson 1994), therefore when the DsRed- Cμ4-M1-eGFP vector is expressed in these cells both eGFP and DsRed should be detected.

The DsRed-Cμ4M1-eGFP vector was transfected in to HeLa cells at increasing concentrations (500 ng, 375 ng, 250 ng, 187 ng, 125 ng) (Figure 5.2.) and fluorescence was assessed 24 hours following transfection. In some cases cells expressed only red fluorescent protein (sIgM) and some both red and green (mIgM) as predicted. The efficiency of transfection of the DsRed-Cμ4M1-eGFP construct was reduced compared to the empty DsRed-eGFP vector (Figure 5.2. A and B) and comparison of the BF and fluorescent images showed that the majority of cells transfected with the DsRed-Cμ4M1-eGFP expressing red and green fluorescence were dead (Figure 5.2. B-F).

The DsRed-Cμ4M1-eGFP construct was seen to be potentially toxic to HeLa cells and so was transfected into B-CLL cells using nucleofection. As the Cμ4-M1 junction is processed naturally in these cells to generate IgM, processing of the DsRed-Cμ4-M1-eGFP construct may not be toxic here. As shown in Figure 5.3., 24 hours post transfection, both red and green fluorescence was observed and these signals co-localized. In this case the DsRed-CμM1-eGFP construct does not appear to be toxic, although the transfection was very inefficiency. The toxicity demonstrated by the DsRed-CμM1-eGFP construct may therefore be limited to HeLa cells, however its inefficient transfection into B-CLL cells means its use to assess IgM ASO action is not viable.

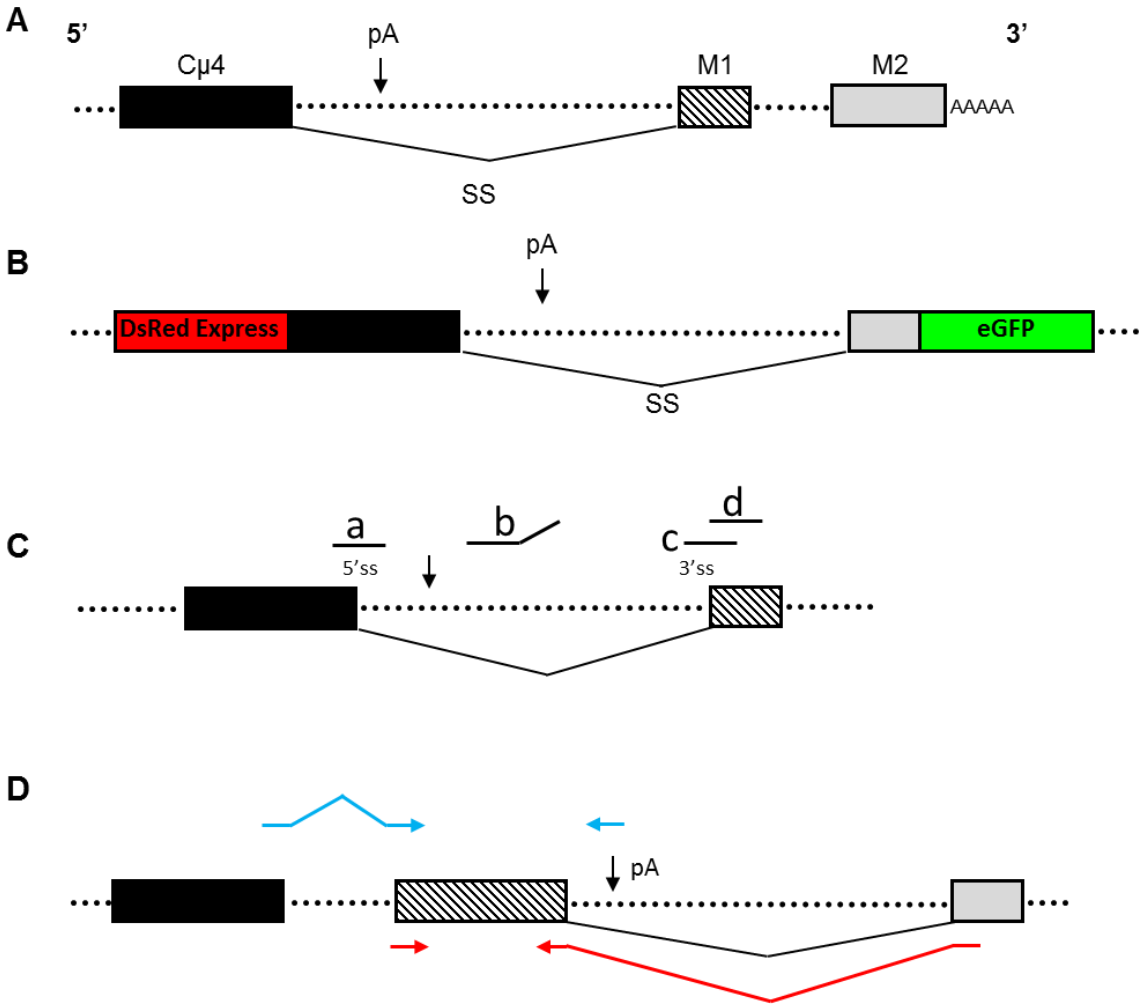

Figure 5.1. The constructs and oligonucleotides used for studying ASO induced pre-mRNA processing changes in the Cμ4-M1-M2 region of the IgM heavy chain. **(A)** The wild-type arrangement of Cμ4-M1-M2 pre-mRNA. **(B)** The Cμ4-M1 region as cloned into the DsRed-eGFP assay vector generating the DsRed-Cμ4M1-eGFP construct. **(C)** Position of ASOs aimed to inhibit splicing of Cμ4-M1 and stimulate polyadenylation following the Cμ4 exon. a) Oligo 12, b) Oligo 10, c) Oligo 11, e) Oligo 13 **(D)** Location of real-time PCR primers (DNA oligos) used to assay the effect of the ASOs on the production of μ_s and μ_m. Blue arrows indicate the location of forward and reverse oligos to detect mRNA polyadenylated following the Cμ4 exon (μ_s), red arrows indicate the location of forward and reverse oligos to detect spliced Cμ4-M1-M2 mRNA (μ_m). (Black box = Cμ4 exon, Hatched box = M1 exon, Grey box = M2 exon, dotted line = introns. 'pA' = polyadenylation site following the Cμ4 exon (μ_s), SS = splicing event between Cμ4-M1).

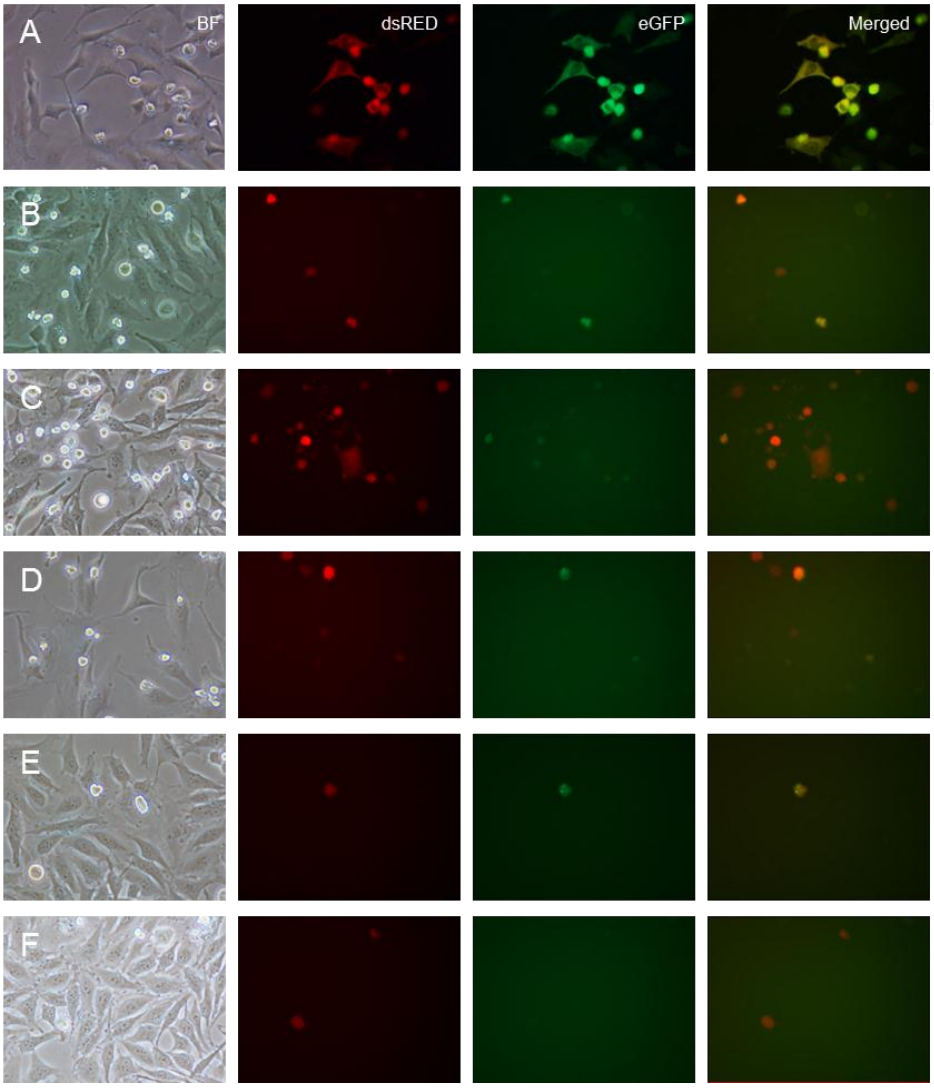

Figure 5.2. The DsRed-Cμ4-M1-eGFP construct is toxic in HeLa cells. **(A)** Control plasmid DsRed-eGFP 500 ng **(B)** DsRed-Cμ4-M1-eGFP 500 ng **(C)** DsRed-Cμ4-M1-eGFP 375 ng **(D)** DsRed-Cμ4-M1-eGFP 250 ng **(E)** DsRed-Cμ4-M1-eGFP 187 ng **(F)** DsRed-Cμ4-M1-eGFP 125 ng. Images were taken 24 hrs following transfection, at 40X.magnification. Images taken using the green channel (eGFP) and the red channel (DsRed) are labeled in panels A and apply for the rest of the figure. Co-localisation of the eGFP and DsRed signals are shown in the merged panels.

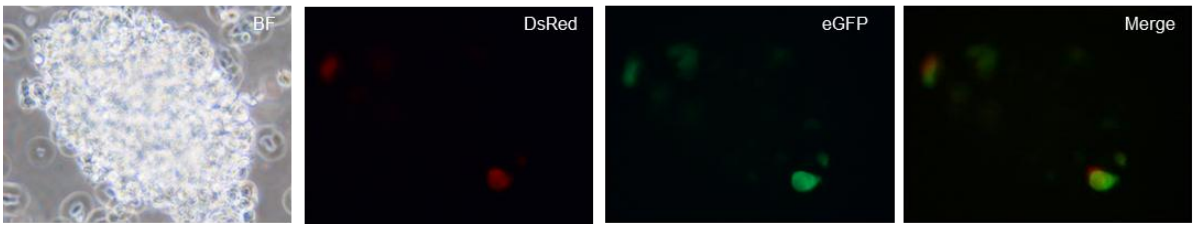

Figure 5.3. Transfection of 500 ng of the DsRed-Cμ4M1-GFP construct into Mec-1 cells is not toxic, but inefficient. Images were taken 24 hrs following transfection at 40X magnification. Images taken using the green channel (eGFP) and the red channel (DsRed) are labeled. Co-localisation of the eGFP and DsRed signals are shown in the merged panel.

5.3. Assaying Splice Switching IgM Oligonucleotides in a B-CLL Cell Line

The effect of oligonucleotides 10-13 (Table 2.1., Figure 5.1. C) on splicing of the Cμ4-M1 junction (Figure 5.1. A) was investigated in a B-CLL cell line using real-time PCR (qPCR) to detect the μ_s (polyadenylated) and μ_m (spliced) mRNA products (Figure 5.1. D). Oligonucleotides 11-13 (Figure 5.5. C) were designed to block the recognition of the 5' splice site of the Cμ4 exon (a, oligonucleotide 12), the 3' splice site of the M1 exon (c, oligonucleotide 11), the splicing enhancer in the M1 exon (d, oligonucleotide 13). Oligonucleotide 10 was designed to stimulate polyadenylation following the Cμ4 exon through the recruitment of polyadenylation factor CstF-64 to its tail sequence. CstF-64 has been shown previously to be present in higher concentrations in cells expressing the polyadenylated isoform (μ_m). Hense a bifunctional oligonucleotide recruiting this factor may enable the μ_s/μ_m competition to favour polyadenylation and so μ_s expression over splicing and μ_m expression (Takagaki and Manley, 1998).

The efficiency of transfection of oligonucleotides in to the Mec-1 B-CLL cell line using nucleofection was assayed. 250 nM of an oligonucleotide labeled with Alexa-488 was transfected in to cells and the efficiency of transfection was recorded. The transfection efficiency was shown to be 100 % (Figure 5.4.).

Oligonucleotide 10 was transfected into Mec-1 cells at increasing concentrations of 50 nM, 100 nM and 250 nM and RNA harvested after 24 hours (Figure 5.5. A). Results of a t-test (50 nM (0.3), 100 nM (0.46), 250 nM (0.43)) show that at these concentrations the oligonucleotide had no significant effect on the μ_m/μ_s ratio. When cells were transfected with 250 nM oligonucleotide and RNA harvested 42 and 72 hours later (Figure 5.5. B and C)

results of a t-test (0.49 and 0.27 respectively) again show that this ASO has no significant effect on this ratio. When the concentration of the oligonucleotide is increased to 500 nM and 1 μM and RNA harvested 72 hours later (Figure 5.5. D), results of the t-test (0.11 and 0.04 respectively) again show no significant effect of this ASO on this ratio.

When cells were transfected with oligonucleotide 11 (250 nM) and RNA harvested 24 hours later (Figure 5.6. A), results of a t-test (0.49) show that this ASO had no significant effect on the ratio of μ_m/μ_s. Similarly when a higher concentration of this oligonucleotide (500nM and 1000nM) was transfected into cells and RNA harvested 72 hours later (Figure 5.6. B), results of a t-test (0.21 and 0.11 respectively) also show no effect of this oligonucleotide on the μ_m/μ_s ratio.

When cells were transfected with oligonucleotide 12 (250 nM) and RNA harvested 24 hours later (Figure 5.7. A), results of a t-test (0.0017) show a significant effect of this oligonucleotide on the μ_m/μ_s ratio. However, this significant t-test result is generated through a decrease in the polyadenylated isoform (μ_s) and no change in the membrane-bound form (μ_m), which even though significant, is not the desired effect. Importantly, when a higher concentration of this ASO is transfected into cells (500 nM and 1000 nM) and RNA harvested 72 hours later (Figure 5.7. B), results of a t-test (0.1 and 0.19 respectively) show no significant effect on the μ_m/μ_s ratio.

When cells were transfected with oligonucleotide 13 (250 nM) (Figure 5.8. A) and RNA harvested 24 hours later, results of the t-test (0.4) show no significant effect on the μ_m/μ_s ratio. When the incubation time of this ASO following transfection was increased to 48

(Figure 5.8. B) and 72 hours (Figure 5.8. C) results of the t-test (0.38 and 0.14 respectively) also show no significant effect on the μ_m/μ_s ratio.

Expression of IgM on the surface of Mec-1 cells transfected with oligonucleotide 13 was investigated using immunostaining. First the correct dilution of labeled antibody to use for immunostaining of IgM expressed at the cell membrane (mIgM) was determined (Figure 5.8. D). Cells transfected with oligonucleotide 13 (250 nM) were stained with an RPE labeled antibody to mIgM and the level of staining was analyzed. Figure 5.8. E shows the results of a t-test on the mean number of stained cells transfected with and without oligonucleotide 13. There is no significant effect of the oligonucleotide on the expression level of mIgM 24, 48 or 72 hours post-transfection with 250 nM of oligonucleotide 13. In each case cells were co-transfected with the Alexa 488 oligonucleotide to control for transfection efficiency.

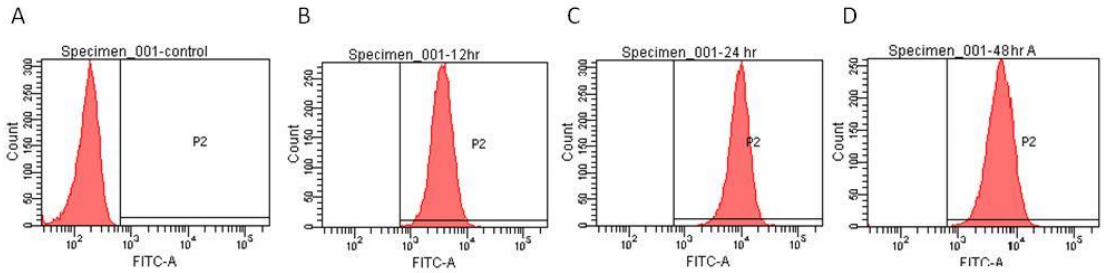

Figure 5.4. The transfection efficiency of a control oligonucleotide into a B-CLL cell line (Mec-1) using nucleofection is 100%. Measurement of transfection efficiency of an Alexa 488 labeled oligonucleotide into Mec-1 cells. Cells were transfected with 250 nM of an Alexa 488 labeled control oligonucleotide. After incubation cells were collected and the fluorescent signal analysed via FACS. **(A)** Mock transfection, **(B)** 12 hr, **(C)** 24hr, **(D)** 48hr. Transfected cells have an FITC signal above that of the control.

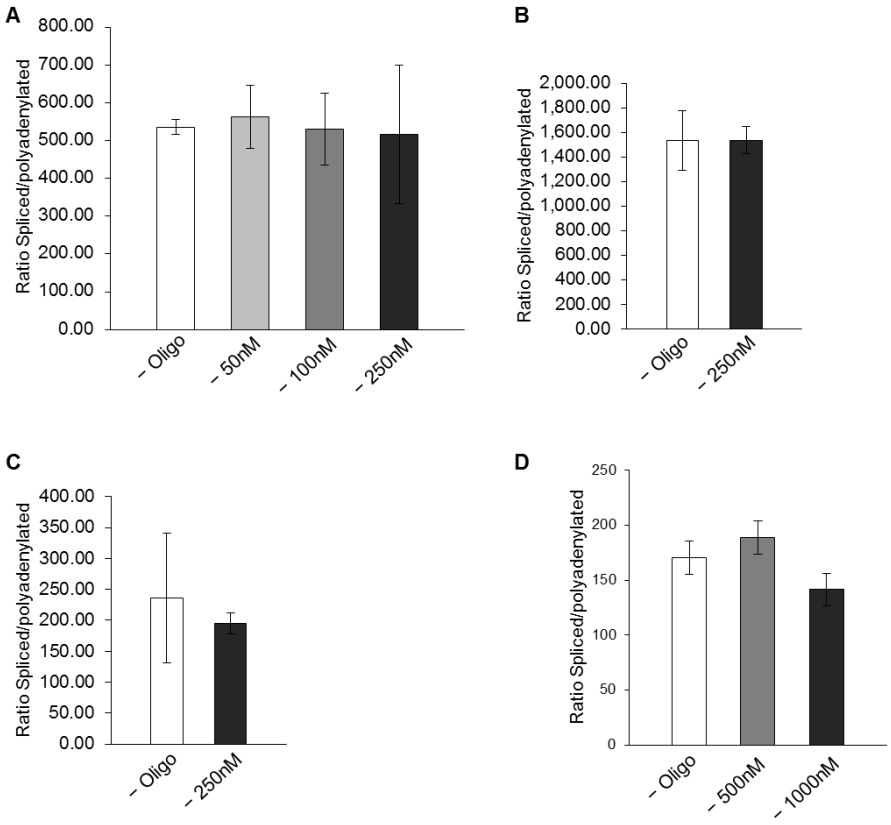

Figure 5.5. Oligonucleotide 10 has no effect on the μ_m/μ_s ratio. Cells were transfected with a bifunctional oligonucleotide containing a tail shown to recruit the polyadenylation factor Cstf-64. **(A-C)** 1/3 of the transfected cells were harvested at each time-point and replaced with media for further incubation. **(A)** 24 hrs. **(B)** 48 hrs. **(C)** 72 hrs. **(D)** Cells were transfected and split by 1:1 dilution in media after 24 and 48 hrs and cells were harvested after 72 hrs.

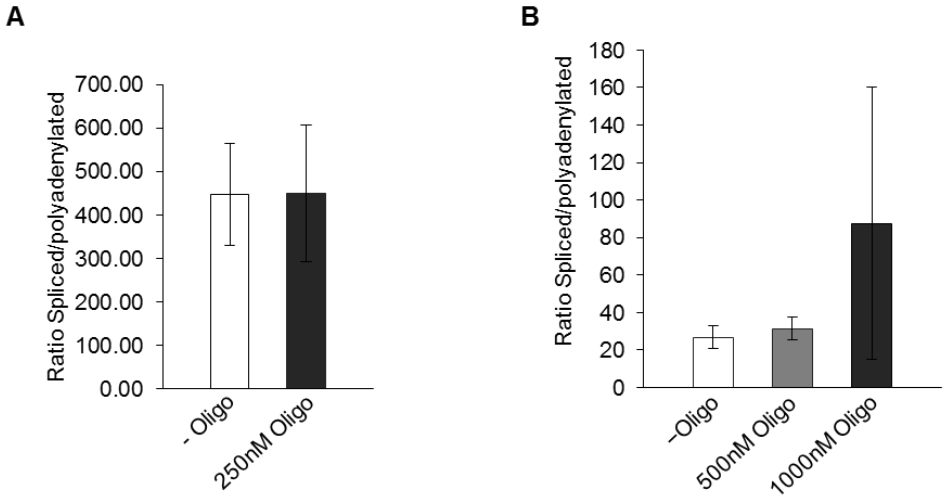

Figure 5.6. Oligonucleotide 11 has no effect on the μ_m/μ_s ratio. Cells were transfected with oligo 11 at the concentrations shown above and 1/3 of the transfected cells were harvested at each time-point and replaced with media for further incubation. **(A)** 24 hrs. **(B)** 72 hrs.

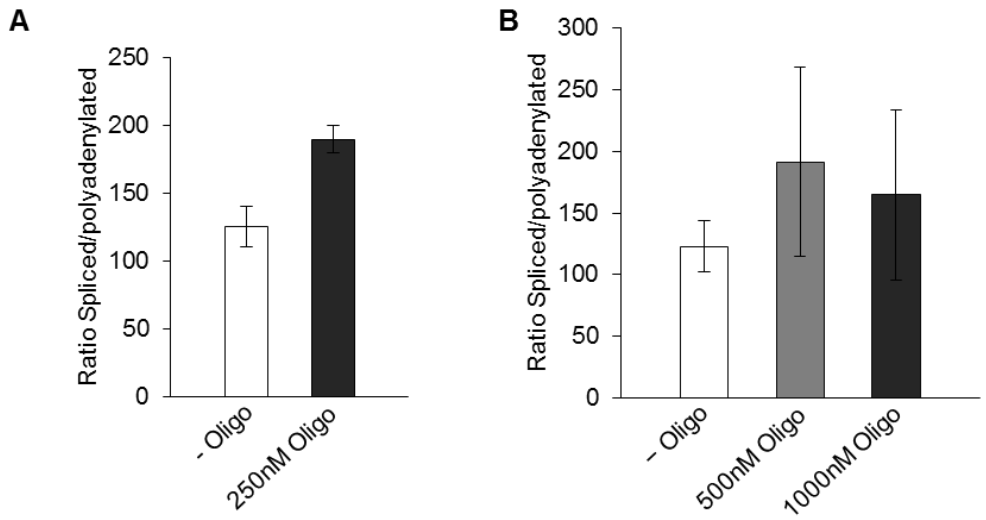

Figure 5.7. Oligonucleotide 12 has no effect on the μ_m/μ_s ratio. Cells were transfected with oligo 11 at the concentrations shown above and 1/3 of the transfected cells were harvested at each time-point and replaced with media for further incubation. **(A)** 24 hrs. **(B)** 72 hrs.

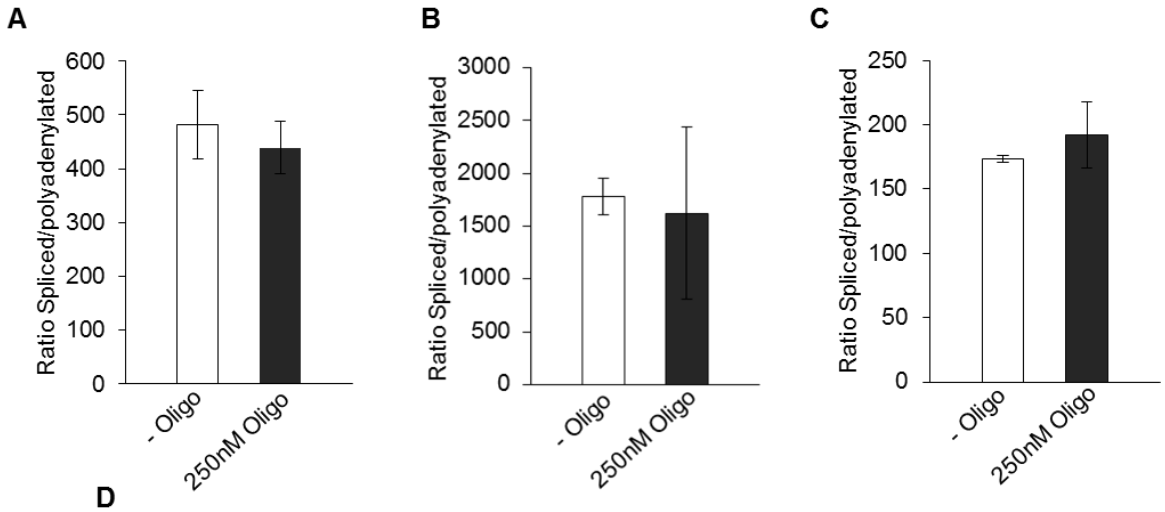

E

Time	T-Value
72	0.24
48	0.11
24	0.40

Figure 5.8. Oligonucleotide 13 has no effect on the μ_m/μ_s ratio. Cells were transfected in a staggered manner and harvested together, with individual transfections for each time-point. The transfection was divided into two, with $1x10^6$ cells being used for both RNA extraction (A-C) and anti-IgM staining (D,E). **(A-C)** The effect of oligo 13 on the μ_m/μ_s ratio **(A)** 24 hrs, **(B)** 48 hrs, **(C)** 72 hrs. **(D-E)** The effect of oligo 13 on IgM expression at the cell membrane**.** **(D)** $1x10^6$ un-transfected cells were collected and stained using an anti-IgM:RPE labeled antibody i) cells alone, ii) 1:100 AB dilution, iii) 2:100 AB dilution. The graph shifting to the right indicates staining. The 1:200 AB dilution was selected for use in oligo 13 transfected cells. **(E)** $1x10^6$ cells transfected with oligo 13 were collected and stained with the anti-IgM labeled antibody (2:100). The table shows the results of a t-test that was performed on the mean intensity of the RPE signal detected from the stained samples.

5.4. Summary

IgM ASOs targeted to sterically block use of the Cμ4 5' splice site, an ESE in exon M1 and this exons 3' splice site did not have the desired effect of inhibiting the Cμ4-M1 splicing event in IgM pre-mRNA. A bifunctional oligonucleotide aimed at recruiting Cstf-64 via its tail sequence to stimulate polyadenylation following the Cμ4 exon, and so inhibit the Cμ4-M1 splicing event, was also inactive.

6. DISCUSSION

6.1. Action of the *SMN2* Bifunctional Oligonucleotide

6.1.1. Chemical Modification of the *SMN2* Bifunctional Oligonucleotide and its Effect on Oligonucleotide Action

In this study *in vitro* assays have been used to identify the mechanism of action of a bifunctional oligonucleotide, shown previously to successfully induce exon 7 inclusion in *SMN2* (Skordis et al., 2003; Owen et al., 2011). Oligonucleotide 1 was shown to remain bound to the RNA throughout a 2 hour splicing assay and also bind the mRNA product (Figure 3.2.). Oligonucleotide modification was shown to have an effect on oligonucleotide binding affinity for RNA, with the 2'-*O*-MePs modified oligonucleotide (oligonucleotide 1) having lower affinity for RNA than the 2'-*O*-Me (oligonucleotide 4) and LNA (oligonucleotide 7) modified oligonucleotides respectively (Figure 3.3.). A definitive conclusion linking oligonucleotide modification, RNA affinity and so activity of oligonucleotide 1 is unable to be made here, as the RNA binding capacity was tested using the less active GGA-b oligonucleotide 1 batch (Figure 3.4. A). However, the RNA binding activity of oligonucleotides 4 and 7 do show that there may be a correlation between oligonucleotide RNA binding affinity and activity. The results indicate that the greater the RNA binding affinity of an oligonucleotide, the lower effect it has on splicing. Oligonucleotide 4 has been previously shown to stimulate *SMN2* exon 7 inclusion and SMN protein expression above that seen with oligonucleotide 7 (Owen et al., 2011). This implies that to act successfully the *SMN2* bifunctional oligonucleotide may have to bind and release the RNA or enable the RNA to bend and flex whilst it remains bound

throughout the splicing reaction (Kent et al., 2003) – something that the LNA modification may not allow (Singh et al., 1998; Petersen et al., 2000).

In vitro splicing assays also showed that the no-tail control oligonucleotides (oligonucleotides 2 and 5) partially enhanced *SMN2* exon 7 inclusion (Figure 3.4. and Figure 3.6. B). This effect may have be due to inhibition of hnRNP A1 binding to the ESS in exon 7, created by the C6U mutation (Lorson et al., 1999), as the bifunctional oligonucleotide anneals directly over this site.

6.1.2. Differential Activity of the RNA Annealing Region and Non-complementary Tail Region of the *SMN2* Bifunctional Oligonucleotide

Oligonucleotide 1 did not stimulate splicing of either *SMN2* intron 6 or 7 in single introns constructs (*SMN2*$^{1\text{-}503}$ and *SMN2*$^{451\text{-}878}$, Figure 3.5.). This may be due to the level of background splicing masking the effect of the oligonucleotide, as these constructs both splice efficiently.

Analysis of the effect of oligonucleotide 1 on splicing of the *SMN2*$^{1\text{-}503}$ transcript with incremental 3' end extensions, identified that the tail domain of oligonucleotide 1 stimulated splicing to a greater extent than the oligonucleotide's annealing domain alone (oligonucleotide 2) (Figure 3.6.). As previously stated, the annealing domain of oligonucleotide 1 binds over the *SMN2* specific hnRNP A1 site (Lorson et al., 1999) and as binding of hnRNP A1 to this site has been shown to induce skipping of exon 7 (Kashima and Manley, 2003; Cartegni et al., 2006), it would be expected that blocking this site could play a major role in oligonucleotide 1 action. However, splicing these constructs with oligonucleotide 2 did not stimulate splicing to

the same degree as oligonucleotide 1 (Figure 3.6. C) and therefore the tail domain is amplifying the effect demonstrated by the annealing domain. Interestingly, as the 3' end extension is lengthened from 80 to 120 nucleotides on this construct, background splicing is inhibited. Within the additional 40 nucleotides between +80 and +120 downstream of exon 7 there is a hnRNPA1 site, which previously has been shown to play a role in the inhibition of splicing of *SMN2* exon 7 (Kashima et al., 2007). Kashima et al. (2007) previously suggested that hnRNP A1 binding at the downstream site located in *SMN2* intron 7 may form an inhibitory interaction with hnRNP A1 bound to the SE1 region of *SMN2* exon 7. However, the results presented in the current study indicate that this interaction plays a small role in the inhibition of *SMN2* exon 7 splicing, as potentially preventing this interaction by oligonucleotide 2 did not stimulate exon 7 splicing to the same level as oligonucleotide 1. It may be that the tail domain of oligonucleotide 1 is having such a drastic stimulatory effect on *SMN2* exon 7 splicing, that the effect of the annealing domain/oligonucleotide 2 is under-represented. The results of the current study support the predication of Singh et al. (2011) that a long-range 'zone of inhibition' may be blocking recognition of *SMN2* exon 7 for splicing. Evidence from Figure 3.6. may indicate that hnRNP A1 binding downstream in intron 7 may be forming the 'zone of inhibition' with PTB bound at element 1 in *SMN2* intron 6 (Wagner and Garcia-Blanco, 2001; Kashima et al., 2007; Baughan et al., 2009; Singh et al., 2011).

Oligonucleotide 1 also stimulated the assembly of A, B and C complexes on *SMN2*$^{1\text{-}503}$ +80 nt pre-mRNA, but had no effect on the assembly of complexes when the reaction was stalled at E complex (Figure 3.7.). This indicates that oligonucleotide 1 may be acting through stimulation of the binding of a splicing component(s) present in A, B or/and C complex.

However, in order to separate the effect of the tail and annealing region of oligonucleotide 1 on complex assembly on this construct, complex assembly in the presence of oligonucleotide 2 should also be assessed.

Oligonucleotide 1 did not demonstrate any stimulatory effect on splicing of *SMN2*$^{329\text{-}878}$ with a 5' extension of 122 nucleotides into *SMN2* intron 6 (Figure 3.8. A). However, interestingly a splicing intermediate, identified as *SMN2* intron 7, is seen in the presence of oligonucleotides 1, 2 and 3 (Figure 3.8. A and C). The oligonucleotide dependence of this intermediate implies that oligonucleotides must be enhancing its stability, whereas without them it is degraded. The oligonucleotide-dependent stability of this intermediate could indicate another mechanism through which the oligonucleotide in enhancing *SMN2* exon 7 splicing, through increasing RNA stability and integrity.

6.1.3. The *SMN2* Bifunctional Oligonucleotide Stimulates Assembly of a Spliceosomal Complex at the 3' Splice Site of *SMN2* Intron 6

Previous studies have predicted that U1 snRNP binding to the 5' splice site of *SMN2* intron 7 is a limiting factor for *SMN2* exon 7 splicing (Singh, Androphy, and Singh, 2004a; Singh et al., 2007). It was originally predicted that oligonucleotide 1 stimulated *SMN2* exon 7 inclusion through the enhancement of U1 snRNP binding to this 5' splice site (Skordis et al., 2003; Owen et al., 2011). However, the findings of the current study instead implicate oligonucleotide 1 in the enhancement of spliceosomal complex formation at the 3' splice site of *SMN2* intron 6 (Figure.3.9. and 3.10.).

Oligonucleotide 1 was found to enhance formation of a U2 snRNP-dependent complex on an *SMN2* exon 7-defined construct (Figure 3.9. B), with a less stable complex being formed in the presence of oligonucleotide 2 (Figure 3.10. A and B). This indicates that the extent of formation of this U2 snRNP containing complex is dependent on the oligonucleotide tail. As previously discussed the tail domain of oligonucleotide 1 may be interrupting long-range inhibitory interactions between *SMN2* intron 6 and 7. The tail domain may be achieving this through the physical binding of bulky proteins. Alternatively, it may also stimulate U2 snRNP binding through the recruitment and action of positive regulators of splicing, such as SRSF1 and Tra2-β1 (Martins de Araújo et al., 2009; Owen et al., 2011). In both instances U2 snRNP binding to the 3' splice site of intron 6 would then enable a commitment complex to form across exon 7, stabilizing spliceosomal complex formation (Figure 6.1.) (Shen and Green, 2006). In addition, it has been shown previously that enhancing U2 snRNP binding to the branch-point of *SMN2* intron 6 stimulated exon 7 splicing (Scholl et al., 2007), which supports the conclusions of Figure 3.4. and Figure 3.10., that show oligonucleotide 1 stimulating splicing of exon 7 and also recruiting U2 snRNP.

As well as U2 snRNP, U2AF65 is also required for 3' splice site selection and has been shown to be linked to the recruitment of U2 snRNP to the branch-point (Valcárcel et al., 1996). Previous studies have predicted that U2AF65 binding to the 3' splice site of *SMN2* intron 6 is a limiting factor for *SMN2* exon 7 splicing, with the binding of U2AF65 to this site being outcompeted by its binding to the 3' splice site of exon 8 (Hastings et al. 2007; Lim & Hertel 2001). In the current study, both oligonucleotides 1 and 2 enhanced U2AF65 UV cross-linking to the *SMN2* exon 7-defined construct (Figure 3.11. D), implying that enhancement of

U2AF65 RNA binding is mediated by the annealing domain of oligonucleotide 1 and not the tail. Previously it has been shown that SRSF1 binding to exon 7 (Cartegni and Krainer, 2002) stimulates both U2AF65 and U2 snRNP cross-linking to the 3' splice site of *SMN2* intron 6 (Martins de Araújo et al., 2009), and also that hnRNP A1 binding to this site in inhibits the U2 snRNP-branch-point association, but has no effect on U2AF65 cross-linking (Martins de Araújo et al., 2009). The results of the current study contradict the latter findings of Martins de Araujo (2009). It appears that the annealing region of oligonucleotide 1 and 2 may inhibit hnRNP A1 binding within the SE1 region through steric hindrance (Kashima and Manley, 2003; Cartegni et al., 2006; Doktor et al., 2011), allowing U2AF65 binding to the 3' splice site of *SMN2* intron 6, which would then support splicing of *SMN2* exon 7 (Figure 6.1.).

Previous studies have shown that U2 snRNP association with the branch-point in A complex is dependent on U2AF, SF1 and SF3 (Ruskin et al., 1988; Kramer and Utans, 1991; Huang et al., 2002). However, the recruitment of U2 snRNP and U2AF65 to the 3' splice site of *SMN2* intron 6 has been previously shown to not always directly correlate (Martins de Araújo et al., 2009), and additional factors including PUF60 have also been predicted to play a vital role in U2 snRNP recruitment to the branch-point sequence of this intron (Hastings et al., 2007). As oligonucleotide 1, but not 2, stimulates U2 snRNP-dependent complex formation (Figure 3.10.), it may be the case that the tail and the annealing domains are acting separately or that the tail enhances the action of the annealing domain.

It can be concluded that the annealing domain of oligonucleotide 1 enhances U2AF65 binding to the polypyrimidine tract of *SMN2* intron 6; while the tail domain enhances U2 snRNP recruitment through a cumulative effect of U2AF65 binding as well as other factors,

which would therefore not necessarily involve a direct U2AF65-U2 snRNP interaction (Figure 6.1.). For instance, the oligonucleotides annealing domain may be enhancing SF1 association with the branch-point of intron 6, a factor that has been shown to be recruited to the 3' splice site in a complex with U2AF65 and whose binding is a pre-requisite for U2 snRNP-branch point association (Berglund et al., 1998; Liu et al., 2001; Selenko et al., 2003). In addition, as hnRNPA1 binding to the SE1 region of *SMN2* exon 7 has been shown to inhibit U2 snRNP binding to the branch-point of intron 6 (Martins de Araújo et al., 2009), inhibiting hnRNPA1 binding to this site via the annealing domain of the oligonucleotide would in theory allow for enhanced U2 snRNP binding perhaps through the ability of SF1 to bind the branch point in company with U2AF65. However, the results of the current study indicate that for U2 snRNP recruitment to follow SF1 binding additional conditions must be met, such as steric hindrance of inhibitory connections across exon 7 or the recruitment of positive regulators of splicing that directly stimulate U2 snRNP recruitment.

A previous study has shown that binding of Tra2-β1 to exon 7 enhanced U2 snRNP binding to the 3' splice site of intron 6 (Martins de Araújo et al., 2009), and that oligonucleotide 1 makes the required association of Tra2-β1 with the SE2 region of *SMN2* exon 7 redundant (Owen et al., 2011). As SRSF1 has been shown to associate with the tail of oligonucleotide 1 (Owen et al., 2011) it seems feasible that the oligonucleotide tail also stimulates U2 snRNP binding via the recruitment of Tra2-β1 or SRSF1, a pathway in which U2AF65 does not play a direct role.

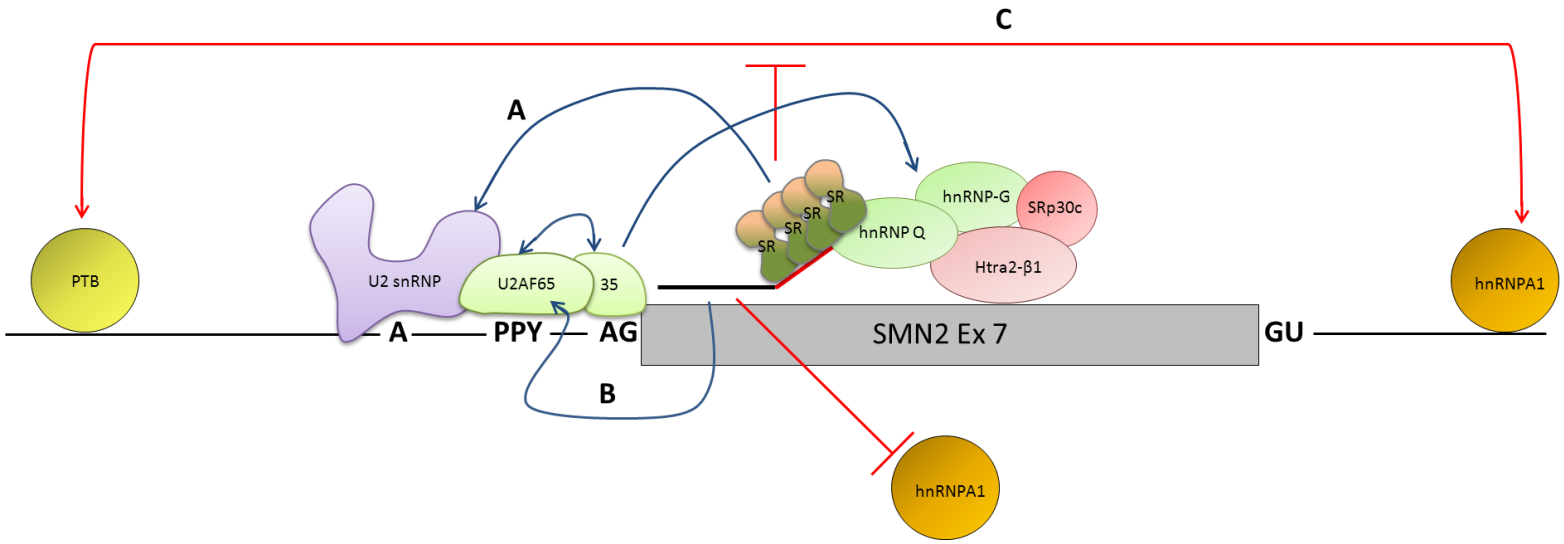

Figure 6.1. Diagram showing the action of the *SMN2* bifunctional oligonucleotide. (Oligonucleotide 1). **(A)** The tail of the oligonucleotide stimulates binding of U2 snRNP to the 3' splices site of intron 6. This is stimulated either through the direct action of SR proteins bound to the oligonucleotide tail or through the inhibition of a long range inhibitory interaction spanning the exon, by the tail binding bulky proteins and steric ally hindering this **(C).** The annealing domain of the oligonucleotide stimulates U2AF65 binding **(B)**, which in turn can stimulate U2AF35 binding and visa versa. Inhibition of the long range inhibitory interaction across the exon may also allow positive regulators of splicing to bind at the SE2 element within the exon. The binding of these factors may then stimulate further association of U2AF35 and 65 with the 3' splice site. U snRNPs and regulatory proteins are shown as colours circles. The RNA annealing region of the oligonucleotide is shown in black and the non-complementary tail region is shown in red. Interactions shown to stimulate splicing and splicesomal complex formation are shown by blue arrows and inhibitory interactions are shown by red arrows.

6.2. RON – A candidate for TOES? Identification of the Factors Limiting Splicing

6.2.1. *RON* Bifunctional Oligonucleotide Action and *RON*$^{1-692}$ Splicing Analysis

Oligonucleotide 8 has been seen to stimulate re-inclusion of *RON* exon 11 and reduce the expression of the RON Δ165 isoform *in vivo* (Ghigna et al., 2010). However, the present study has shown that oligonucleotide 8 does not display the same effect *in vitro.* Oligonucleotide 8 did not induce inclusion of *RON* exon 11 in a construct containing *RON* exons 10, 11 and 12 with intervening introns (*RFL*$^{1-692}$) (Figure 4.1.) or single intron *RON* constructs (Figure 4.3.). The oligonucleotide also did not enhance splicing of a *RON*/β-globin construct (R$^{298-484}$/βG$^{280-385}$) containing exon 11 (Figure 4.7.). Importantly, in the absence of oligonucleotide 8 the *RFL*$^{1-692}$ construct also did not splice to produce *RON* Δ165 mRNA, indicating that splicing of this region is intrinsically poor and that *in vitro* the system is fundamentally unable to splice (Figure 4.1. and Figure 4.2.). In addition, splicing of *RFL*$^{1-692}$ pre-mRNA to produce exon 11 skipped *RON* Δ165 mRNA was also not stimulated by a nuclear extract prepared from KATO III cells (Figure 4.4. A), that have been shown previously to express *RON* Δ165 (Ghigna et al., 2005).

Poor U2AF65 and U2 snRNP binding, either together or separately, have previously been shown to stimulate exon skipping in a number of genes including *SMN2* exon 7, *Fas* exon 6 and *RB1* exon 9 (Lim and Hertel, 2001; Frappaz et al., 2002; Martins de Araújo et al., 2009; Corrionero et al., 2011). As analysis of splicing signals in *RFL*$^{1-692}$ pre-mRNA identified that both introns 10 and 11 contain weak 3‘ splice site polypyrimidine tracts and branch-point sequences, binding of U2AF65 and U2 snRNP may also be limiting splicing of exon 11 here.

As increasing the concentration of U2AF65/35 has been shown to previously compensate for weak polypyrimidine tract sequences and so stimulate splicing (Pacheco et al., 2006), the effect of increased U2AF65/35 was tested on the splicing of this *RFL*$^{1\text{-}692}$ pre-mRNA. U2AF65/35 enrichment did not stimulate *RFL*$^{1\text{-}692}$ pre-mRNA splicing (Figure 4.4. B). Therefore either the polypyrimidine tract sequences may not limiting splicing, a repressive factor may be binding to this region (or another) and so inhibiting splicing, or the increase in U2AF65 concentration has no effect, as the polypyrimidine tract sequence is so weak.

Analysis of the splicing of *RON* constructs with increased intron length showed that the short length of *RFL*$^{1\text{-}692}$ introns 10 and 11 does not contribute to the inhibition of splicing (Figure 4.5.). The regions in *RFL*$^{1\text{-}692}$ pre-mRNA identified to be responsible for its splicing inhibition were restricted to *RON* Int10$^{254\text{-}297}$ and Int11$^{485\text{-}526}$ intronic regions (Figure 4.6.). *RON* exons were also not seen to contribute to splicing inhibition (Figure 4.6. C), which goes against the conclusion drawn by Lefave et al. (2011), who identified an ESS for hnRNP H in *RON* exon 11 that was seen to stimulate skipping of this exon (Lefave et al., 2011). However, it is still possible that hnRNP H does have a fundamental role in the induction of exon 11 skipping, but the precise mechanism through which this occurs was not shown by Lefave et al. (2011). In addition, the presence of hnRNP H binding sites (GGG) in the identified *RON* Int10$^{254\text{-}297}$ and Int11$^{485\text{-}526}$ intronic regions indicates that these sites may play a part in inhibition, through binding both at these sites and within the exon. This potential method of regulation by hnRNP H binding was not investigated in the current study.

Reduced U2 snRNP binding has been shown to stimulate skipping of both *SMN2* exon 7 (Martins de Araújo et al., 2009) and *Fas* exon 6 (Corrionero et al., 2011). Therefore, as the

branch-point falls within the inhibitory *RON* Int10$^{254-297}$ and Int11$^{485-526}$ intronic regions, the effect of mutation of these branch-point sequences to the consensus branch-point sequence was tested for its effect on splicing. Branch-point up-regulation did not significantly stimulate splicing when tested in both one and two intron RON constructs (Figure 4.9. B and C, Figure 4.11.), indicating once more that another factor must also be contributing to *RFL*$^{1-692}$ splicing inhibition. Splicing was stimulated by replacement of the branch-point and polypyrimidine tract with that of β-globin, in single intron RON constructs (Figure 4.8. D and E). However, by replacing this obviously weak area in *RON* with a strong sequence that supports splicing, other mechanisms of splicing regulation could be concealed here. In addition, the replacement of a weak splicing signal would, of course, stimulate splicing and may override an inhibitory mechanism. However, potentially the branch-point and polypyrimidine tract of RON could still be having a role in inhibition of *RFL*$^{1-692}$ splicing.

Subsequent analysis of the splicing of a series of single intron hybrid *RON*/β-globin constructs then identified a 32 nucleotide region at the 3' end of *RON* intron 10 and a 20 nucleotide region at the 3' end of *RON* intron 11 (R$^{264-297}$ and R$^{504-524}$ respectively) as the minimal *RON* sequence required to inhibit β-globin splicing (Figure 4.8. B and C, Figure 4.10.). This sequence does not contain the branch-point of intron 10, but divide that of intron 11, now confirming that the polypyrimidine tract is weak and inhibits splicing in both instances. As U2AF65 binding to polypyrimidine tracts is required for their recognition in splicing (Banerjee, 2003) and to underpin poor U2AF65 binding to *RON* Int10$^{254-297}$ and Int11$^{485-526}$ intronic regions as inhibitory, U2AF65 cross-linking was next investigated.

In order to study whether oligonucleotide 8 could enhance the splicing of a two intron *RON* transcript, the sequence of *RFL*$^{1\text{-}692}$ pre-mRNA was enhanced via mutation to stimulate splicing. To stimulate *RFL*$^{1\text{-}692}$ pre-mRNA to splice the branch-point mutation in *RON* intron 11 was required, either alone or together with the branch-point mutation in *RON* intron 10 (Figure 4.11. B and D). The replacement of intron 11 with the β-globin intron in *RFL*$^{1\text{-}692}$ pre-mRNA also stimulated *RON* Δ165 mRNA production only (Figure 4.11. E). The mutation of both *RFL*$^{1\text{-}692}$ intron 10 and 11 branch-point sequences to the consensus sequence in the same construct stimulated production of *RON* Δ165 mRNA and a low level of *RFL* mRNA (Figure 4.11. D). The branch-point mutation in *RON* intron 10 alone does generate a very low level of splicing dependent bands, but the resulting products cannot be clearly identified (Figure 4.11. B). From the results of Figure 4.11. B, C, D and E together with the findings from Figure 4.9. B and C, where both intron 10 and 11 branch-point mutations stimulated splicing of single intron RON constructs, it can be concluded that intron 10 is weaker than intron 11 and thus is fundamental to the inhibition of *RFL*$^{1\text{-}692}$ splicing.

Coupling the exon 11 5' splice site mutation together with the double branch-point mutations of intron 10 and 11, in *RFL*$^{1\text{-}692}$ pre-mRNA, had a negligible effect on the amount of *RFL*$^{1\text{-}692}$ and *RON* Δ165 mRNA produced. In addition, coupling of the intron 10 branch-point mutation with the 5' splice site mutation also did not stimulate splicing (Figure 4.11. C, D and G). Hence, the intron 11 5' splice site sequence is having no role in the splicing inhibition of *RFL*$^{1\text{-}692}$, indicating that enhancing exon definition of exon 11 does not stimulate splicing (Figure 4.11. D). As the results demonstrated here indicate that *RFL*$^{1\text{-}692}$ splicing initiates via intron definition (Sterner et al., 1996), it would have been interesting to see whether the 5'

splice site mutation enhances production of *RON* Δ165 mRNA when coupled with the intron 11 branch-point mutation.

The finding that *RON* intron 10 is a weaker intron than 11 signifies that there must be a difference between intron 10 and 11 causing this. Noticeably the efficiency of splicing *RFL*$^{1-692}$ pre-mRNA constructs with either intron 10 or 11 replaced by the β-globin intron was dramatically increased in comparison to the splicing efficiency of *RFL*$^{1-692}$ constructs with mutations (Table 4.2.). This highlighted that an additional factor must be inhibiting splicing in intron 10 in particular. A key difference between intron 10 and the β-globin intron is the 3' splice site sequence. The consensus 3' splice site sequence (C/T)AG/G (Zhang, 1998) is identical to that of β-globin, but not intron 10 whose 3' splice site sequence is CAG/T. Previously in a number of cases, it has been shown that mutations affecting the first 'G' of exon sequences stimulates exon skipping through reduced U2AF35 binding (Fu et al., 2011). Importantly, U2AF35 has been shown to be a key factor in the recognition of weak 3' splice sites and supports the binding of U2AF65 to poor polypyrimidine tracts (Guth et al., 2001; Pacheco et al., 2006). Hence, in the case of RON, poor U2AF35 binding to the 3' splice site of intron 10 could stimulate skipping of this exon through reduced binding of U2AF65 to its weak polypyrimidine tract. However, the binding of U2AF35 to *RFL*$^{1-692}$ pre-mRNA was not investigated in the current study.

In addition oligonucleotide 8 did not enhance the splicing of the two intron *RFL*$^{1-692}$ constructs that had been mutated and stimulated to splice (Figure 4.13.). However, it was not tested if these constructs could respond to SRSF1, that has been shown to stimulate skipping of exon 11 (Ghigna et al., 2005). Therefore even though constructs have been stimulated to

splice by mutation their splicing mechanism may not replicate that of wild-type *RFL*$^{1\text{-}692}$ pre-mRNA and hence they may not be a viable way to assess the effect of oligonucleotide 8 on the splicing of this region.

It is also important to remember that the RFL$^{1\text{-}692}$ region does splice *in vivo*, be it to a low level, and that exon 11 is only skipped in some instances. Therefore the splicing signals within this region must be functional, even if they are weak. In the light of this and the observed inability of *RFL*$^{1\text{-}692}$ to splice *in vitro*, it may be that an *in vitro* co-transcriptional splicing assay is more apt for the study the regulation of *RFL*$^{1\text{-}692}$ splicing and therefore the activity of oligonucleotide 8 *in vitro* (Yu et al., 2010). In addition, even though the use of *in vitro* assays to study splicing mechanisms allows for the development of clear and definitive answers, it would be interesting to investigate the splicing of a *RFL*$^{1\text{-}692}$ mini-gene construct *in vivo*. This may permit splicing of this region of *RON* in a way that cannot be achieved *in vitro*, thus allowing for investigation into the regulation of exon 11 splicing in a physiological setting.

6.2.2. Protein Binding to the *RON* Inhibitory Region

hnRNP H/F was seen to bind to the downstream half of both *RON* introns 10 and 11 (Figure 4.15., Figure 7.1.). The same pattern of cross-linking was seen with the 44 nucleotide downstream half of intron 10 (*RON*Int10$^{254\text{-}297}$) and the 32 nucleotide minimal inhibitory region (R$^{264\text{-}297}$) of this intron. The binding site for hnRNP H/F has been identified as T/G GGG (Chen et al., 1999; Caputi and Zahler, 2001). The binding of hnRNP H/F to the downstream half of *RON* introns 10 and 11 (*RON* Int10$^{254\text{-}297}$ and Int11$^{485\text{-}526}$) is supported by

the presence of consensus hnRNP H/F binding motifs 5' of these sequences. However, cross-linking of hnRNP H/F to the $R^{264-297}$ region of *RON* intron 10 is not as easily explained, as there are no T/G GGG motifs its sequence (Figure 4.16. A). The cross-link designated as hnRNP H/F is lost in cross-linking to the 20 nt *RON* intron 11 inhibitory region ($R^{504-524}$), which is as expected, as the hnRNP H/F binding site is not present in this sequence (Figure 4.16. A and B).

The activity of hnRNP H/F has been previously found to be dependent on the specific transcript to which it is associated. Its binding has been shown to induce both inclusion and skipping of exons, commonly through intronic and exonic binding respectively (Fogel and McNally, 2000; Mauger et al., 2008; Fisette et al., 2010; Lefave et al., 2011). The inhibitory effect of hnRNP H/F on *RON* exon 11 splicing may be accompanied by poor 3' splice site spliceosomal complex formation and therefore this could have overshadowed a mechanism of splicing inhibition involving hnRNP H/F. As previously stated, hnRNP H binding to the 5' end of *RON* exon 11 has been shown to induce skipping of this exon (Lefave et al., 2011), but the current study did not implicate *RON* exon 11 in the inhibition of this splicing event. It is possible however that hnRNP H/F bound within exon 11 and introns 10 and 11 could interact to inhibit splicing of exon 11, via the looping out of either the whole of exon 11 or its 3' or 5' splice site (Martinez-Contreras et al., 2006; Fisette et al., 2010). Alternatively, it is possible that hnRNP H/F could propagate along the RNA from its binding sites within the introns and inhibit recognition of splice sites this way (Okunola and Krainer, 2009).

In addition, G triplets (GGG) have been shown previously to stimulate splice site recognition. An intronic GGG sequence was shown to stimulate U1 snRNP binding to an

upstream 5' splice site (McCullough and Berget, 1997; Mccullough and Berget, 2000). The GGG triplet present in the inhibitory *RON* intronic region could actually be having a stimulatory effect on *RON* Δ165 production by promoting U1 snRNP binding to the 5' splice site of intron 10, and stimulating coupling between this site and the 3' splice site of intron 11. The coupling of these sites across exon 11 may be further stimulated by the identified poor polypyrimidine tract sequence of intron 10, this sequence would additionally prevent coupling of the intron 10 3' splice site with the stimulated 5' splice site of intron 10. This conclusion suggests that the downstream half of *RON* intron 10 contains the fundamental ability to enhance skipping of exon 11 to produce *RON* Δ165 mRNA through hnRNP H binding.

6.2.3. Revised *RON* Bifunctional Oligonucleotide Design

A combination of the conclusions drawn on the action of the *SMN2* bifunctional oligonucleotide and a greater understanding of the splicing mechanisms of $RON^{1\text{-}692}$ pre-mRNA has allowed a new bifunctional oligonucleotide to be designed to stimulate *RON* exon 11 splicing and combat production of RON Δ165 in target cancers.

As oligonucleotide 1 was shown to enhance the binding of U2 snRNP and U2AF65 to the 3' splice site of *SMN2* intron 6, its target location at the 5' end of *SMN2* exon 7 may be fundamental for its action. This conclusion is supported by the results of Owen et al. (2010), where it was found that re-design of this oligonucleotide to anneal at other sites on *SMN2* exon 7 did not enhance, but reduced the oligonucleotide's effect on *SMN2* exon 7 splicing (Owen et al., 2011). In addition, analysis of *RON* exon 11 splicing identified that its weakness are

conveniently located at the 3' end of both introns 10 and 11 (Figure 4.7.), the region to which U2 snRNP and U2AF65 bind during the early stages of splicing.

Oligonucleotide 8 was designed to be central within *RON* exon 11, in line with the previous belief that the *SMN2* bifunctional oligonucleotide mediated its effect on factors binding to the 5' splice site of intron 7 and needed to be an optimum distance from this to have this effect (Skordis et al., 2003; Owen et al., 2011). Oligonucleotide 8 was also 2'-*O*-Me modified oligonucleotide, a chemistry which has been shown in the current study and others to be less effective at inducing splicing than the 2'-*O*-MePs modification with an unmodified RNA tail (Figure 3.4.) (Owen et al., 2011).

If the *RON* oligonucleotide was re-designed to mimic oligonucleotide 1 in chemistry and also target location, it may have a more successful effect on *RON* exon 11 inclusion. Importantly, re-design of the *RON* oligonucleotide, to anneal at the 5' end of exon 11 (nucleotides 2-16), could enable the weakness in the 3' splice site of *RON* intron 10 to be solved via the recruitment of U2 snRNP by the oligonucleotide's tail sequence – which is identical to that of oligonucleotide 1.

6.3. IgM Oligonucleotides

The action of 2'-*O*-Me oligonucleotides (10-13) that were designed to re-directed the splicing of the membrane binding domain of IgM were tested *in vivo* in B-CLL cells. Firstly, the production of a DsRed-eGFP construct containing the IgM region of interest (Cμ4-M1) was synthesized. This vector could have provided a quick assay for the action of the oligonucleotides, through the visualization of a particular fluorescence with either splicing or polyadenylation. However, transfection of this construct into HeLa cells induced cell death and therefore it was concluded that the vector was toxic (Figure 5.2. and 5.3.).

The effect of oligonucleotides 10-13 (Figure 5.1. C) on Cμ4-M1 splicing/polyadenylation was tested directly in Mec-1 B-CLL cells and the desired effect was not seen in any case (Figure 5.5.–5.8.). An effect opposite to what was desired was seen in the case of oligonucleotide 12 (Figure 5.7.), as transfection of oligonucleotide 12 stimulated a decrease in the polyadenylated, but not the spliced isoform. In addition, often the level of error see overwhelmed any alterations in ratio and where the error was minimal the effect of the oligonucleotide was not significant enough to be pursued.

In order to design the most effective ASO to stimulate exon 7 inclusion in *SMN2* an antisense walk technique has been widely used (Hua et al., 2007, 2008; Singh et al., 2009, 2010). Targeting of a series of ASOs throughout exon 7 and surrounding intronic regions allowed for the most effective ASO target location to be easily identified. Such a walk would be the most effective way of developing oligonucleotides to inhibit splicing of the Cμ4-M1 junction.

6.4. Prospects for use of Oligonucleotides to Control Splicing for Therapy

Oligonucleotide delivery, non-specific binding and toxicity have the potential to limit the use of oligonucleotides as a therapeutic. Delivery of oligonucleotides is a complex matter as they often have a large molecular mass, a charge and are required to be stable in a cellular environment in-order to have their desired effect. As with any therapeutic treatment the toxicity of splice-switching oligonucleotides has to be assessed in detail. Currently oligonucleotides are beginning to make their way through clinical trials and hence toxicity is a hurdle that must be overcome in order for oligonucleotide therapy to make its way to the bedside (Webb et al., 2001; Hua et al., 2010).

The positional-dependence of the action of the *SMN2* bifunctional oligonucleotide and the inefficiency of the *RON* bifunctional oligonucleotide (Ghigna et al., 2010; Owen et al., 2011), indicate that bifunctional oligonucleotides may not always be successful in every context. In addition, the action of the tail and annealing region of the *SMN2* bifunctional oligonucleotide were shown here to be independent, with the tail recruiting U2 snRNP and the annealing region recruiting U2AF65. In the case of U2AF65 recruitment to the polypyrimidine tract of *SMN2* intron 6, the oligonucleotide is annealing over an hnRNP A1 binding site at the 5' end of *SMN2* exon 7 potentially preventing hnRNP A1 binding and therefore allowing for U2AF65 recruitment. If U2AF65 recruitment is dependent on the inhibition of hnRNP A1 binding and not another mechanism, enhanced U2AF65 recruitment to other substrates may not occur and the activity of the oligonucleotide may be diminished. This effect would be especially dramatic if there is no correlation between initial U2 snRNP and U2AF65 recruitment in the new substrate, as has been shown for *SMN2* exon 7 (Martins de Araújo et

al., 2009). Therefore, if an oligonucleotide that recruited U2 snRNP but not U2AF65 was applied to an exon skipping event, the effect seen may not be as significant as that seen with the *SMN2* bifunctional oligonucleotide as the effect of the tail and annealing region on splicing is cumulative. It could be possible to design an oligonucleotide to recruit U2AF65 directly via a tail containing the U2AF65 consensus binding sequence. This would enable U2 snRNP recruitment directly (Valcárcel et al., 1996). In addition, the oligonucleotide could be annealed across mutations shown to reduce U2AF65 binding that lead to exon skipping and disease development, such as that seen in the exon 9 skipping event in the *RM1* gene (Frappaz et al., 2002).

In the case of *SMN2*, exon 7 splicing stimulation through the inhibition of repressor protein binding with non-tailed ASOs was successful. However, this approach of stimulating exon inclusion by blocking protein binding may not be available in the case of every skipped exon. Therefore, if obvious weak splice signals, in particular those at the 3' splice site, result in exon skipping, the use of bifunctional oligonucleotides to stimulate binding of spliceosomal factors to these weak sites does appear to be a straight forward method of stimulating exon inclusion. It therefore seems feasible to pursue the development of bifunctional oligonucleotides to stimulate inclusion of skipped exons in other substrates, as these skipped exons may not be so obviously inhibited through repressor protein binding. U2 snRNP recruitment has also been linked with the length of downstream exons, with U2 snRNP binding being limited when downstream exons are short (Tardiff et al., 2006). Hence, enhanced recruitment of U2 snRNP via the bifunctional oligonucleotide could also simply be

used to increase the splicing efficiency of an exon that is not completely inhibited, but whose splicing is in efficient.

6.5. Final Summary: How the Mechanism leads to the Application

Bifunctional oligonucleotides have proven to be a highly successful way of enhancing exon 7 inclusion in *SMN2*. The results of this study have identified the mechanism of how this is achieved and have highlighted that this oligonucleotide can be adapted to potentially stimulate splicing of skipped exons in other substrates.

It was predicted initially that the *SMN2* bifunctional oligonucleotide enhanced U1 snRNP recruitment to the 5' splice site of *SMN2* intron 7 (Skordis et al., 2003; Owen et al., 2011), and therefore the distance between the oligonucleotide annealing site and the 5' splice site was fundamental for its action. On this basis, an oligonucleotide to stimulate *RON* exon 11 splicing was designed and tested, however this oligonucleotide proved to be less successful than the *SMN2* bifunctional oligonucleotide at stimulating exon inclusion. This study has shown that the *SMN2* bifunctional oligonucleotide stimulates *SMN2* intron 6 3' splice site recognition. Importantly, this indicates a downfall in the design of the *RON* bifunctional oligonucleotide which was designed to anneal relative to the 5' splice site of *RON* intron 11, as this was initially thought to be the target of oligonucleotide action. Therefore as the *RON* bifunctional oligonucleotide anneals centrally in exon 11 its effect on intron 10 3' splice site recognition would be relatively weaker than that seen with the *SMN2* bifunctional oligonucleotide, which anneals at positions +1 to +16 within its target exon. Targeting the *RON* bifunctional oligonucleotide to anneal close to the upstream 3' splice, as the *SMN2* bifunctional oligonucleotide is, would in theory enhance its exon inclusion effect. In addition, with the discovery that the 3' splice site of intron 10 was inhibitory for splicing of *RON* exon 11, enhancement of 3' splice site recognition that the bifunctional oligonucleotide provides could

work well to enhance exon 11 splicing. Due to these factors the *RON* bifunctional oligonucleotide was redesigned to anneal to the same relative position within *RON* exon 11 as the *SMN2* bifunctional oligonucleotide in *SMN2* exon 7 (Figure 6.2.).

The chemistry of the new *RON* bifunctional oligonucleotide was also altered to mirror that of the *SMN2* bifunctional oligonucleotide, as chemistry also was shown to have an effect on exon inclusion activity. The initial *RON* oligonucleotide was 2'*O*-Me, a chemistry that was shown in the current study to be less effective at stimulating splicing of exon 7 with the *SMN2* bifunctional oligonucleotide than the 2'*O* MePs modification. In addition, the most successful *SMN2* bifunctional oligonucleotide also contained an RNA tail, which was protected from degradation via a Ps cap. The presence of unmodified RNA as oppose to 2'*O*-Me in the tail may have an effect on the ability of proteins to bind and therefore stimulate splicing.

In conclusion, analysis of the mechanism through which the *SMN2* bifunctional oligonucleotide acts to stimulate exon inclusion, has allowed for the further development of a bifunctional oligonucleotide to reverse the *RON* Δ165 pro-metastatic splicing event.

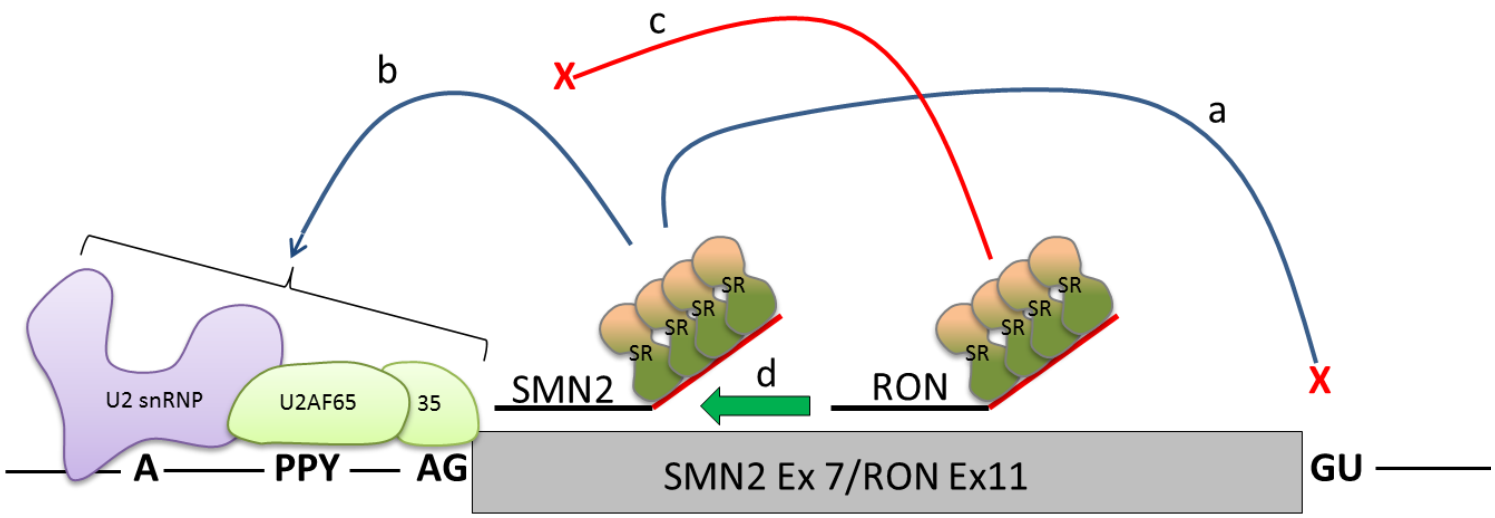

Figure 6.2. Diagram summarizing the mechanism of action of the *SMN2* bifunctional oligonucleotide, and the consequential re-design of the *RON* bifunctional oligonucleotide to stimulate *RON* exon 11 splicing and inhibit *RON* Δ165 expression. **a)** The *SMN2* bifunctional oligonucleotide does not stimulate recognition of the downstream 5' splice site. **b)** The *SMN2* bifunctional oligonucleotide stimulates 3' splice site recognition. **c)** The initial *RON* bifunctional oligonucleotide was designed to anneal relative to the downstream 5' splice site and so central to *RON* exon 11. However as the *SMN2* bifunctional oligonucleotide exerts its effect on the upstream 5' splice site, the *RON* oligonucleotide may be too far to have the same stimulatory effect. **d)** The *RON* bifunctional oligonucleotide was redesigned to anneal at the same relative position within *RON* exon 11 as the *SMN2* oligonucleotide in *SMN2* exon 7, therefore allowing it to have a stimulatory effect on 3' splice site recognition.

7. APPENDICES

7.1. Figures

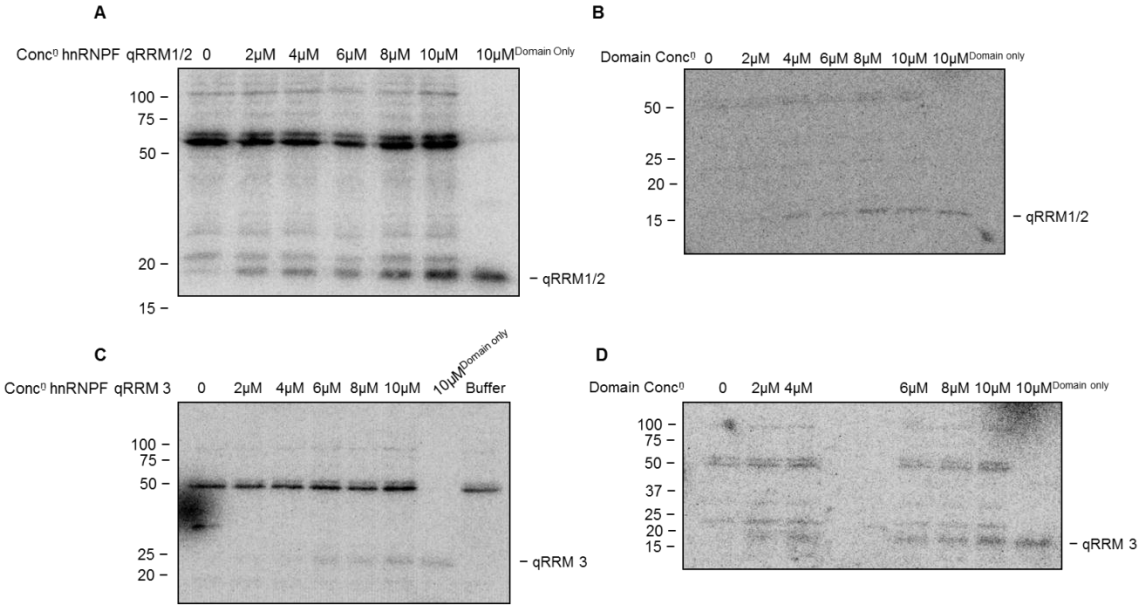

Figure 7.1. The qRRM domains 1/2 and 3 of hnRNP F bind to the downstream inhibitory regions of *RON* introns 10 ($R^{254\text{-}297}$) and 11 ($R^{485\text{-}526}$). Cross-linking was carried out as normal with splicing reactions supplemented with hnRNP F domains (gift from C Dominguez, (Dominguez and Allain, 2006)) at the shown concentrations. **(A)** $R^{254\text{-}297}$ with qRRM 1/2 **(B)** $R^{485\text{-}526}$ with qRRM 1/2 **(C)** $R^{254\text{-}297}$ with qRRM 3 **(D)** $R^{485\text{-}526}$ with qRRM 3.

7.2. Sequences

NB. Introns are underlined.

7.2.1. *RON* Sequence

```
  1  TGTGAGAGGCAGCTTCCAGAGCAGCAGCTGTGCCGCCTTCCTGAATATGTGGTCCGAGAC
 61  CCCCAGGGATGGGTGGCAGGGAATCTGAGTGCCCGAGGGGATGGAGCTGCTGGCTTTACA
121  CTGCCTGGCTTTCGCTTCCTACCCCCACCCCATCCACCCAGTGCCAACCTAGTTCCACTG
181  AAGCCTGAGGAGCATGCCATTAAGTTTGAGGTAAGTGTAAGGGATAGGGGCAGGGACAGT
241  TGGGGATCTGAAAGTAGGGGCCAGCCTACTGGCTGGTCCTCATGACCCTCTCTGCAGTAT
301  ATTGGGCTGGGCGCTGTGGCTGACTGTGTGGGTATCAACGTGACCGTGGGTGGTGAGAGC
361  TGCCAGCACGAGTTCCGGGGGGGACATGGTTGTCTGCCCCCTGCCCCCATCCCTGCAGCTT
421  GGCCAGGATGGTGCCCCATTGCAGGTAGGCAGCCCAGCTGGACCTCCCTGGGAAACACGG
481  GCAGAGGGCCTACAGGCTGGGCCTGAGTTGCCACCTGCCCCCAGGTCTGCGTAGATGGTG
541  AATGTCATATCCTGGGTAGAGTGGTGCGGCCAGGGCCAGATGGGGTCCCACAGAGCACGC
601  TCCTTGGTATCCTGCTGCCTTTGCTGCTGCTTGTGGCTGCACTGGCGACTGCACTGGTCT
661  TCAGCTACTGGTGGCGGAGGAAGCAGCTAG
```

7.2.2. β-globin Sequence

```
  1  GGGCTGCTGGTTGTCTACCCATGGACCCAGAGGTTCTTCGAGTCCTTTGGGGACCTGTCC

 61  TCTGCAAATGCTGTTATGAACAATCCTAAGGTGAAGGCTCATGGCAAGAAGGTGCTGGCT

121  GCCTTCAGTGAGGGTCTGAGTCACCTGGACAACCTCAAAGGCACCTTTGCTAAGCTGAGT

181  GAACTGCACTGTGACAAGCTGCACGTGGATCCTGAGAACTTCAGGGTGAGTTTGGGGACC

241  CTTGATTGTTCTTTCTTTTTCGCTATTGTAAAATTCATGTTATATGGTCGACTCTGCTAA

301  CCATGTTCATGCCTTCTTCTTTTTCCTACAGCTCCTGGGCAACGTGCTGGTTATTGTGCT

361  GTCTCATCATTTTGGCAGGTAAGTT
```

7.2.3. *SMN2* Sequence

The β-globin sequence is shown in italics.

```
   1  AGGGCTGCTGGTTGTCTACCCATGGACCCAGAGGTTCTTCGAGTCCTTTGGGGACCTGTC
  61  CTCTGCAAATGCTGTTATGAACAATCCTAAGGTGAAGGCTCATGGCAAGAAGGTGCTGGC
 121  TGCCTTCAGTGAGGGTCTGAGTCACCTGGACAACCTCAAAGGCACCTTTGCTAAGCTGAG
 181  TGAACTGCACTGTGACAAGCTGCACGTGGATCCTGAGAACTTCAGGGTGAGTTTGGGGAC
 241  CCTTGATTGTTCTTTCTTTTTCGCTATTGTAAAATTCATGTTATATGGTCGACAGACTAT
 301  CAACTTAATTTCTGATCATATTTTGTTGAATAAAATAAGTAAAATGTCTTGTGAAACAAA
 361  ATGCTTTTTAACATCCATATAAAGCTATCTATATATAGCTATCTATATCTATATAGCTAT
 421  TTTTTTTAACTTCCTTTATTTTCCTTACAGGGTTTTAGACAAAATCAAAAAGAAGGAAGG
 481  TGCTCACATTCCTTAAATCAGGAGTAAGTCTGCCAGCATTATGAAAGTGAATCTTACTTT
 541  TGTAAAACTTTATGGTTTGTGGAAAACAAATGTTTTTGAACATTTAAAAAGTTCAGATGT
 601  TAGAAAGTTGAAAGGTTAATGTAAAACAATCAATATTAAAGAATTTTGATGCCAAAACTA
 661  TTAGATAAAAGGTTAATCTACATCCCTACTAGAATTCTCATACTTAACTGGTTGGTTGTG
 721  TGGAAGAAACATACTTTCACAATAAAGAGCTTTAGGATATGATGCCATTTTATATCACGT
 781  CGACTCTGCTAACCATGTCATGCCTTCTTCTTTTTCCTACAGCTCCTGGGCAACCGTGCT
 841  GGGTATTGGGCTGGCTCAACAATTTTGGCAGGTAAGTT
```

8. BIBLIOGRAPHY

Abes, S., Turner, J.J., Ivanova, G.D., Owen, D., Williams, D., Arzumanov, A., Clair, P., Gait, M.J., Lebleu, B., 2007. Efficient splicing correction by PNA conjugation to an R6-Penetratin delivery peptide. Nucleic acids research 35, 4495-502.

Alfarano, A., Indraccolo, S., Circosta, P., Minuzzo, S., Vallario, A., Zamarchi, R., Fregonese, A., Calderazzo, F., Faldella, A., Aragno, M., Camaschella, A., Amadori, A., Caligaris-Cappio, F., 1999. An alternatively spliced form of CD79b gene may account for altered B-cell receptor expression in B-chronic lymphocytic leukemia. Blood 93, 2327-2335.

Alter, J., Lou, F., Rabinowitz, A., Yin, H., Rosenfeld, J., Wilton, S.D., Partridge, T. a, Lu, Q.L., 2006. Systemic delivery of morpholino oligonucleotide restores dystrophin expression bodywide and improves dystrophic pathology. Nature medicine 12, 175-7.

Andersson, R., Enroth, S., Rada-Iglesias, A., Wadelius, C., Komorowski, J., 2009. Nucleosomes are well positioned in exons and carry characteristic histone modifications. Genome research 19, 1732-41.

Andreassi, C., Angelozzi, C., Tiziano, F.D., Vitali, T., De Vincenzi, E., Boninsegna, A., Villanova, M., Bertini, E., Pini, A., Neri, G., Brahe, C., 2004. Phenylbutyrate increases SMN expression in vitro: relevance for treatment of spinal muscular atrophy. European journal of human genetics 12, 59-65.

BIBLIOGRAPHY

Ashiya, M., Grabowski, P.J., 1997. A neuron-specific splicing switch mediated by an array of pre-mRNA repressor sites: evidence of a regulatory role for the polypyrimidine tract binding protein and a brain-specific PTB counterpart. RNA (New York, N.Y.) 3, 996-1015.

Avila, A.M., Burnett, B.G., Taye, A.A., Gabanella, F., Knight, M.A., Hartenstein, P., Cizman, Z., Prospero, N.A.D., Pellizzoni, L., Fischbeck, K.H., Sumner, C.J., 2007. Trichostatin A increases SMN expression and survival in a mouse model of spinal muscular atrophy. J Clin Invest 117, 659-671.

Bakkour, N., Lin, Y.-L., Maire, S., Ayadi, L., Mahuteau-Betzer, F., Nguyen, C.H., Mettling, C., Portales, P., Grierson, D., Chabot, B., Jeanteur, P., Branlant, C., Corbeau, P., Tazi, J., 2007. Small-molecule inhibition of HIV pre-mRNA splicing as a novel antiretroviral therapy to overcome drug resistance. PLoS pathogens 3, 1530-9.

Banerjee, H., 2003. Sex lethal and U2 small nuclear ribonucleoprotein auxiliary factor (U2AF65) recognize polypyrimidine tracts using multiple modes of binding. RNA 9, 88-99.

Baughan, T., Shababi, M., Coady, T.H., Dickson, A.M., Tullis, G.E., Lorson, C.L., 2006. Stimulating full-length SMN2 expression by delivering bifunctional RNAs via a viral vector. Molecular therapy 14, 54-62.

BIBLIOGRAPHY

Baughan, T.D., Dickson, A., Osman, E.Y., Lorson, C.L., 2009. Delivery of bifunctional RNAs that target an intronic repressor and increase SMN levels in an animal model of spinal muscular atrophy. Human molecular genetics 18, 1600-11.

Bauman, J. a, Li, S.-D., Yang, A., Huang, L., Kole, R., 2010. Anti-tumor activity of splice-switching oligonucleotides. Nucleic acids research 38, 8348-56.

Behrens, S.E., Luhrmann, R., 1991. Immunoaffinity purification of a [U4/U6.U5] tri-snRNP from human cells. Genes & Development 5, 1439-1452.

Behzadnia, N., Golas, M.M., Hartmuth, K., Sander, B., Kastner, B., Deckert, J., Dube, P., Will, C.L., Urlaub, H., Stark, H., Lührmann, R., 2007. Composition and three-dimensional EM structure of double affinity-purified, human prespliceosomal A complexes. The EMBO journal 26, 1737-48.

Bellosillo, B., Villamor, N., Colomer, D., Pons, G., Gil, J., 1999. In Vitro Evaluation of Fludarabine in Combination With Cyclophosphamide and/or Mitoxantrone in B-Cell Chronic Lymphocytic Leukemia. Blood 2836-2843.

Benvenuti, S., Lazzari, L., Arnesano, A., Li Chiavi, G., Gentile, A., Comoglio, P.M., 2011. Ron kinase transphosphorylation sustains MET oncogene addiction. Cancer research 71, 1945-55.

Berget, S.M., 1995. Exon recognition in vertebrate splicing. J Biol Chem. 270, 2411-2414.

BIBLIOGRAPHY

Berglund, J. a, Abovich, N., Rosbash, M., 1998. A cooperative interaction between U2AF65 and mBBP/SF1 facilitates branchpoint region recognition. Genes & development 12, 858-67.

Bernal, A., 2001. Survival of leukemic B cells promoted by engagement of the antigen receptor. Blood 98, 3050-3057.

Bessonov, S., Anokhina, M., Krasauskas, A., Golas, M.M., Sander, B., Will, C.L., Urlaub, H., Stark, H., Lührmann, R., 2010. Characterization of purified human Bact spliceosomal complexes reveals compositional and morphological changes during spliceosome activation and first step catalysis. RNA (New York, N.Y.) 16, 2384-403.

Bessonov, S., Anokhina, M., Will, C.L., Urlaub, H., Lührmann, R., 2008. Isolation of an active step I spliceosome and composition of its RNP core. Nature 452, 846-50.

Bezerra, J., Laney, D., Friezner Degen, S., 1994. Increased expression of mRNA for hepatocyte growth factor-like protein during liver regeneration and inflammation. Biochemical and biophysical research communications 203, 666-673.

Black, D.L., 2003. Mechanisms of alternative pre-messenger RNA splicing. Annual review of biochemistry 72, 291-336.

Black, D.L., Chabot, B., Steitz, J. a, 1985. U2 as well as U1 small nuclear ribonucleoproteins are involved in premessenger RNA splicing. Cell 42, 737-50.

BIBLIOGRAPHY

Blankinship, M.J., Gregorevic, P., Chamberlain, J.S., 2006. Gene therapy strategies for Duchenne muscular dystrophy utilizing recombinant adeno-associated virus vectors. Molecular therapy : the journal of the American Society of Gene Therapy 13, 241-9.

Bogdahn, U., Hau, P., Stockhammer, G., Venkataramana, N.K., Mahapatra, a K., Suri, a, Balasubramaniam, a, Nair, S., Oliushine, V., Parfenov, V., Poverennova, I., Zaaroor, M., Jachimczak, P., Ludwig, S., Schmaus, S., Heinrichs, H., Schlingensiepen, K.-H., 2011. Targeted therapy for high-grade glioma with the TGF-β2 inhibitor trabedersen: results of a randomized and controlled phase IIb study. Neuro-oncology 13, 132-42.

Bonnal, S., Martínez, C., Förch, P., Bachi, A., Wilm, M., Valcárcel, J., 2008. RBM5/Luca-15/H37 regulates Fas alternative splice site pairing after exon definition. Molecular cell 32, 81-95.

Boutz, P.L., Stoilov, P., Li, Q., Lin, C.-H., Chawla, G., Ostrow, K., Shiue, L., Ares, M., Black, D.L., 2007. A post-transcriptional regulatory switch in polypyrimidine tract-binding proteins reprograms alternative splicing in developing neurons. Genes & development 21, 1636-52.

Brow, D. a, 2002. Allosteric cascade of spliceosome activation. Annual review of genetics 36, 333-60.

Buckanovich, R.J., Posner, J.B., Darnell, R.B., 1993. Nova, the paraneoplastic Ri antigen, is homologous to an RNA-binding protein and is specifically expressed in the developing motor system. Neuron 11, 657-72.

BIBLIOGRAPHY

Burghes, A.H.M., McGovern, V.L., 2010. Antisense oligonucleotides and spinal muscular atrophy: skipping along. Genes & development 24, 1574-9.

Burglen, L., Lefebvre, S., Clermont, O. et al, 1995. Structure and Organization of the Human Survival Motor. Genomics 482, 479-482.

Burnett, B.G., Muñoz, E., Tandon, A., Kwon, D.Y., Sumner, C.J., Fischbeck, K.H., 2009. Regulation of SMN protein stability. Molecular and cellular biology 29, 1107-15.

Bushby, K., Finkel, R., Birnkrant, D., Case, L., Clemens, P., Cripe, L., Kaul, A., Kinnett, K., McDonald, C., Pandya, S., Poysky, J., Shapiro, F., Tomezsko, J., Constantin, C., 2010. Diagnosis and management of Duchenne muscular dystrophy, part 1: diagnosis, and pharmacological and psychosocial management. Lancet neurology 9, 77-93.

Caceres, J.F., Krainer, a R., 1993. Functional analysis of pre-mRNA splicing factor SF2/ASF structural domains. The EMBO journal 12, 4715-26.

Calarco, J. a, Superina, S., O'Hanlon, D., Gabut, M., Raj, B., Pan, Q., Skalska, U., Clarke, L., Gelinas, D., van der Kooy, D., Zhen, M., Ciruna, B., Blencowe, B.J., 2009. Regulation of vertebrate nervous system alternative splicing and development by an SR-related protein. Cell 138, 898-910.

Caligaris-Cappio, F., Hamblin, T.J., 1999. B-cell chronic lymphocytic leukemia: a bird of a different feather. Journal of clinical oncology 17, 399-408.

BIBLIOGRAPHY

Camp, E.R., Liu, W., Fan, F., Yang, A., Somcio, R., Ellis, L.M., 2005. RON, a tyrosine kinase receptor involved in tumor progression and metastasis. Annals of surgical oncology 12, 273-81.

Caputi, M., Zahler, a M., 2001. Determination of the RNA binding specificity of the heterogeneous nuclear ribonucleoprotein (hnRNP) H/H'/F/2H9 family. The Journal of biological chemistry 276, 43850-9.

Carmel, I., 2004. Comparative analysis detects dependencies among the 5' splice-site positions. RNA 10, 828-840.

Carothers, A.M., Urlaub, G., Grunberger, D., Chasin, L.A., 1993. Splicing mutants and their second-site suppressors at the dihydrofolate reductase locus in Chinese hamster ovary cells. Molecular and cellular biology 13, 5085-98.

Carstens, R.P., Wagner, E.J., Mariano, A., 2000. An Intronic Splicing Silencer Causes Skipping of the IIIb Exon of Fibroblast Growth Factor Receptor 2 through Involvement of Polypyrimidine Tract Binding Protein. Mol Cell Biol 20, 7388-7400.

Cartegni, L., Chew, S.L., Krainer, A.R., 2002. Listening to silence and understanding nonsense: exonic mutations that affect splicing. Nature reviews. Genetics 3, 285-98.

Cartegni, L., Hastings, M.L., Calarco, J.A., de Stanchina, E., Krainer, A.R., 2006. Determinants of exon 7 splicing in the spinal muscular atrophy genes, SMN1 and SMN2. American journal of human genetics 78, 63-77.

BIBLIOGRAPHY

Cartegni, L., Krainer, A.R., 2002. Disruption of an SF2/ASF-dependent exonic splicing enhancer in SMN2 causes spinal muscular atrophy in the absence of SMN1. Nature genetics 30, 377-84.

Cartegni, L., Krainer, A.R., 2003. Correction of disease-associated exon skipping by synthetic exon-specific activators. Nature structural biology 10, 120-5.

Chandler, S.D., Mayeda, a, Yeakley, J.M., Krainer, a R., Fu, X.D., 1997. RNA splicing specificity determined by the coordinated action of RNA recognition motifs in SR proteins. Proceedings of the National Academy of Sciences of the United States of America 94, 3596-601.

Chen, C.D., Kobayashi, R., Helfman, D.M., 1999. Binding of hnRNP H to an exonic splicing silencer is involved in the regulation of alternative splicing of the rat β -tropomyosin gene. Genes & Development 13, 593-606.

Chen, H.-H., Chang, J.-G., Lu, R.-M., Peng, T.-Y., Tarn, W.-Y., 2008. The RNA binding protein hnRNP Q modulates the utilization of exon 7 in the survival motor neuron 2 (SMN2) gene. Molecular and cellular biology 28, 6929-38.

Chen, Q., Seol, D.W., Carr, B., Zarnegar, R., 1997. Co-expression and regulation of Met and Ron proto-oncogenes in human hepatocellular carcinoma tissues and cell lines. Hepatology 26, 59-66.

BIBLIOGRAPHY

Cheng, H.-L., Liu, H.-S., Lin, Y.-J., Chen, H.H.-W., Hsu, P.-Y., Chang, T.-Y., Ho, C.-L., Tzai, T.-S., Chow, N.-H., 2005. Co-expression of RON and MET is a prognostic indicator for patients with transitional-cell carcinoma of the bladder. British journal of cancer 92, 1906-14.

Cherny, D., Gooding, C., Eperon, G.E., Coelho, M.B., Bagshaw, C.R., Smith, C.W.J., Eperon, I.C., 2010. Stoichiometry of a regulatory splicing complex revealed by single-molecule analyses. The EMBO journal 29, 2161-72.

Cho, S., Hoang, A., Sinha, R., Zhong, X.-Y., Fu, X.-D., Krainer, A.R., Ghosh, G., 2011. Interaction between the RNA binding domains of Ser-Arg splicing factor 1 and U1-70K snRNP protein determines early spliceosome assembly. Proceedings of the National Academy of Sciences of the United States of America 108, 8233-8238.

Cho, S.-B., Park, Y.-L., Song, Y.-A., Kim, K.-Y., Lee, G.-H., Cho, D.-H., Myung, D.-S., Park, K.-J., Lee, W.-S., Chung, I.-J., Choi, S.-K., Kim, K.-K., Joo, Y.-E., 2011. Small interfering RNA-directed targeting of RON alters invasive and oncogenic phenotypes of human hepatocellular carcinoma cells. Oncology Reports 26, 1581-1586.

Chodavarapu, R.K., Feng, S., Bernatavichute, Y.V., Chen, P.-Y., Stroud, H., Yu, Y., Hetzel, J. a, Kuo, F., Kim, J., Cokus, S.J., Casero, D., Bernal, M., Huijser, P., Clark, A.T., Krämer, U., Merchant, S.S., Zhang, X., Jacobsen, S.E., Pellegrini, M., 2010. Relationship between nucleosome positioning and DNA methylation. Nature 466, 388-92.

BIBLIOGRAPHY

Chou, M.-yuan, Rooke, N., Turck, C.W., Black, D.L., 1999. hnRNP H Is a Component of a Splicing Enhancer Complex That Activates a c- src Alternative Exon in Neuronal Cells. Mol 19, 68-77.

Cirak, S., Arechavala-Gomeza, V., Guglieri, M., Feng, L., Torelli, S., Anthony, K., Abbs, S., Garralda, M.E., Bourke, J., Wells, D.J., Dickson, G., Wood, M.J., Wilton, S.D., Straub, V., Kole, R., Shrewsbury, S.B., Sewry, C., Morgan, J.E., Bushby, K., Muntoni, F., 2011. Exon skipping and dystrophin restoration in patients with Duchenne muscular dystrophy after systemic phosphorodiamidate morpholino oligomer treatment: an open-label, phase 2, dose-escalation study. Lancet 378, 595-605.

Clarke, L. a, Veiga, I., Isidro, G., Jordan, P., Ramos, J.S., Castedo, S., Boavida, M.G., 2000. Pathological exon skipping in an HNPCC proband with MLH1 splice acceptor site mutation. Genes, chromosomes & cancer 29, 367-70.

Cléry, A., Jayne, S., Benderska, N., Dominguez, C., Stamm, S., Allain, F.H.-T., 2011. Molecular basis of purine-rich RNA recognition by the human SR-like protein Tra2-β1. Nature structural & molecular biology 18, 443-50.

Cohen, J.B., Snow, J.E., Spencer, S.D., Levinson, a D., 1994. Suppression of mammalian 5' splice-site defects by U1 small nuclear RNAs from a distance. Proceedings of the National Academy of Sciences of the United States of America 91, 10470-4.

BIBLIOGRAPHY

Collesi, C., Santoro, M.M., Gaudino, G., Comoglio, P.M., 1996. A splicing variant of the RON transcript induces constitutive tyrosine kinase activity and an invasive phenotype. Molecular and cellular biology 16, 5518-26.

Conrotto, P., Corso, S., Gamberini, S., Comoglio, P.M., Giordano, S., 2004. Interplay between scatter factor receptors and B plexins controls invasive growth. Oncogene 23, 5131-7.

Cooper, T. a, Wan, L., Dreyfuss, G., 2009. RNA and disease. Cell 136, 777-93.

Corrionero, A., Raker, V.A., Izquierdo, J.M., 2011. Strict 3 ′ splice site sequence requirements for U2 snRNP recruitment after U2AF binding underlie a genetic defect leading to autoimmune disease. RNA 17, 401-411.

Cortes, J.J., Sontheimer, E.J., Seiwert, S.D., Steitz, J.A., 1993. the conserved loop of human U5 snRNA. The EMBO journal 12, 5181 -5189.

Crotti, L.B., Horowitz, D.S., 2009. Exon sequences at the splice junctions affect splicing fidelity and alternative splicing. Proceedings of the National Academy of Sciences of the United States of America 106, 18954-9.

Cusin, V., Clermont, O., Gerard, B., Elion, J., 2011. Prevalence of Specific Learning Disabilities Among Primary School Children in a South Indian City. Indian journal of pediatrics 2-5.

BIBLIOGRAPHY

Czeizel, A., Hamula, J., 1990. Werdnig-Hoffmann disease: myosin isoform expression not arrested at prenatal stage of development. Journal of the Neurological Sciences 95, 183-192.

Cáceres, J.F., Stamm, S., Helfman, D.M., Krainer, a R., 1994. Regulation of alternative splicing in vivo by overexpression of antagonistic splicing factors. Science (New York, N.Y.) 265, 1706-9.

Damle, R.N., 2002. B-cell chronic lymphocytic leukemia cells express a surface membrane phenotype of activated, antigen-experienced B lymphocytes. Blood 99, 4087-4093.

Das, R., Reed, R., 1999. Resolution of the mammalian E complex and the ATP-dependent spliceosomal complexes on native agarose mini-gels. RNA 5, 1504-1508.

Das, R., Zhou, Z., Reed, R., 2000. Functional Association of U2 snRNP with the ATP-Independent Spliceosomal Complex E. Molecular Cell 5, 779-787.

Dias, N., Stein, C.A., 2002. Antisense Oligonucleotides : Basic Concepts and Mechanisms. Molecular Cancer Therapeutics 1, 347-355.

Dickson, A., Osman, E., Lorson, C.L., 2008. A Negatively Acting Bifunctional RNA Increases Survival Motor Neuron Both In Vitro and In Vivo. Human Gene Therapy 19, 1307-1315.

BIBLIOGRAPHY

Doktor, T.K., Schroeder, L.D., Vested, A., Palmfeldt, J., Andersen, H.S., Gregersen, N., Andresen, B.S., 2011. SMN2 exon 7 splicing is inhibited by binding of hnRNP A1 to a common ESS motif that spans the 3' splice site. Human mutation 32, 220-30.

Dominguez, C., Allain, F.H.-T., 2006. NMR structure of the three quasi RNA recognition motifs (qRRMs) of human hnRNP F and interaction studies with Bcl-x G-tract RNA: a novel mode of RNA recognition. Nucleic acids research 34, 3634-45.

Dominski, Z., Kole, R., 1993. Restoration of correct splicing in thalassemic pre-mRNA by antisense oligonucleotides. PNAS 90, 8673-8677.

Dreyfuss, G., Kim, V.N., Kataoka, N., 2002. Messenger-RNA-binding proteins and the messages they carry. Nature reviews. Molecular cell biology 3, 195-205.

Du, H., Rosbash, M., 2002. The U1 snRNP protein U1C recognizes the 5' splice site in the absence of base pairing. Nature 419, 1-5.

Dubowitz, V., 1989. A colour atlas of muscle disorders in childhood. London: Wolfe Medical Publications Ltd ISBN 07234.

Dunckley, M.G., Manoharan, M., Villiet, P., Eperon, I.C., Dickson, G., 1998. Modification of splicing in the dystrophin gene in cultured Mdx muscle cells by antisense oligoribonucleotides. Human molecular genetics 7, 1083-90.

BIBLIOGRAPHY

Dönmez, G., Hartmuth, K., Kastner, B., Will, C.L., Lührmann, R., 2007. The 5' end of U2 snRNA is in close proximity to U1 and functional sites of the pre-mRNA in early spliceosomal complexes. Molecular cell 25, 399-411.

Eckerich, C., Schulte, A., Martens, T., Zapf, S., Westphal, M., Lamszus, K., 2009. RON receptor tyrosine kinase in human gliomas: expression, function, and identification of a novel soluble splice variant. Journal of neurochemistry 109, 969-80.

Egholm, M., Buchardt, O., Christensen, L., Behrens, C., Freier, S., Driver, D., Berg, R., Kim, S., Norden, B., Nielsen, P., 1993. PNA hybridizes to complementary oligonucleotides obeying the watson-crick hydrogen-bonding rules. Nature 365, 566-568.

Elsheikh, B., Prior, T., Zhang, X., Miller, R., Kolb, S.J., Moore, D., Bradley, W., Barohn, R., Bryan, W., Gelinas, D., Iannaccone, S., Leshner, R., Mendell, J.R., Mendoza, M., Russman, B., Smith, S., King, W., Kissel, J.T., 2009. An analysis of disease severity based on SMN2 copy number in adults with spinal muscular atrophy. Muscle & nerve 40, 652-6.

Emery, A., 1991. Population Frequencies of Inherited Neuromuscular Diseases a world survey. Neuromuscular Disorders 1, 19-29.

Eperon, I.C., Ireland, D.C., Smith, R.A., Mayeda, A., Krainer, A.R., 1993. Pathways for selection of 5' splice sites by U1 snRNPs and SF2/ASF. The EMBO journal 12, 3607-17.

BIBLIOGRAPHY

Eperon, I.C., Makarova, O.V., Mayeda, A., Munroe, S.H., Cáceres, J.F., Hayward, D.G., Krainer, A.R., 2000. Selection of alternative 5' splice sites: role of U1 snRNP and models for the antagonistic effects of SF2/ASF and hnRNP A1. Molecular and cellular biology 20, 8303-18.

Estibeiro, P., Godfray, J., 2001. Antisense as a neuroscience tool and therapeutic agent. Trends in neurosciences 24, S56–S62.

Fairbrother, W.G., Yeh, R.-F., Sharp, P. a, Burge, C.B., 2002. Predictive identification of exonic splicing enhancers in human genes. Science (New York, N.Y.) 297, 1007-13.

Fais, F., Ghiotto, F., Hashimoto, S., Sellars, B., Valetto, a, Allen, S.L., Schulman, P., Vinciguerra, V.P., Rai, K., Rassenti, L.Z., Kipps, T.J., Dighiero, G., Schroeder, H.W., Ferrarini, M., Chiorazzi, N., 1998. Chronic lymphocytic leukemia B cells express restricted sets of mutated and unmutated antigen receptors. The Journal of clinical investigation 102, 1515-25.

Faà, V., Incani, F., Meloni, A., Corda, D., Masala, M., Baffico, a M., Seia, M., Cao, A., Rosatelli, M.C., 2009. Characterization of a disease-associated mutation affecting a putative splicing regulatory element in intron 6b of the cystic fibrosis transmembrane conductance regulator (CFTR) gene. The Journal of biological chemistry 284, 30024-31.

Feldkötter, M., Schwarzer, V., Wirth, R., Wienker, T.F., Wirth, B., 2002. Quantitative analyses of SMN1 and SMN2 based on real-time lightCycler PCR: fast and highly

reliable carrier testing and prediction of severity of spinal muscular atrophy. American journal of human genetics 70, 358-68.

Fischer, U., Liu, Q., Dreyfuss, G., 1997. The SMN-SIP1 complex has an essential role in spliceosomal snRNP biogenesis. Cell 90, 1023-9.

Fisette, J.-F., Toutant, J., Dugré-Brisson, S., Desgroseillers, L., Chabot, B., 2010. hnRNP A1 and hnRNP H can collaborate to modulate 5' splice site selection. RNA 16, 228-38.

Fletcher, S., Honeyman, K., Fall, A.M., Harding, P.L., Johnsen, R.D., Steinhaus, J.P., Moulton, H.M., Iversen, P.L., Wilton, S.D., 2007. Morpholino oligomer-mediated exon skipping averts the onset of dystrophic pathology in the mdx mouse. Molecular therapy 15, 1587-92.

Fogel, B.L., McNally, M.T., 2000. A cellular protein, hnRNP H, binds to the negative regulator of splicing element from Rous sarcoma virus. The Journal of biological chemistry 275, 32371-8.

Follenzi, a, Bakovic, S., Gual, P., Stella, M.C., Longati, P., Comoglio, P.M., 2000. Cross-talk between the proto-oncogenes Met and Ron. Oncogene 19, 3041-9.

Foust, K.D., Wang, X., Mcgovern, V.L., Braun, L., Bevan, A.K., Haidet, A.M., Le, T.T., Morales, P.R., Rich, M.M., Burghes, A.H.M., Kaspar, B.K., 2010. Rescue of the spinal muscular atrophy phenotype in a mouse model by early postnatal delivery of SMN. Nature Biotechnology 28, 271-274.

BIBLIOGRAPHY

Fox-Walsh, K.L., Hertel, K.J., 2009. Splice-site pairing is an intrinsically high fidelity process. Proceedings of the National Academy of Sciences of the United States of America 106, 1766-71.

Fox-walsh, K.L., Dou, Y., Lam, B.J., Hung, S.-pin, Baldi, P.F., Hertel, K.J., 2005. The architecture of pre-mRNAs affects mechanisms of splice-site pairing. Proceedings of the National Academy of Sciences 2005, 16176-16181.

Frappaz, D., Dutrillaux, B., Chevillard, S., Malfoy, B., 2002. A T to C mutation in the polypyrimidine tract of the exon 9 splicing site of the RM1 gene responsible for low penetrance hereditary retinoblastoma. Journal of Medical Genetics 39, e21.

Fried, K., Emery, A., 1971. Spinal muscular atrophy type II. A separate genetic and clinical entity from type I (Werdnig-Hoffmann disease) and type 3 (Kugelberg-Welander disease). Clinical Genetics 2, 203-209.

Fu, X.D., 1993. Specific commitment of different pre-mRNA to splicing by single SR proteins. Nature 365, 82-85.

Fu, X.D., Mayeda, a, Maniatis, T., Krainer, a R., 1992. General splicing factors SF2 and SC35 have equivalent activities in vitro, and both affect alternative 5’ and 3' splice site selection. Proceedings of the National Academy of Sciences of the United States of America 89, 11224-8.

BIBLIOGRAPHY

Fu, Y., Masuda, A., Ito, M., Shinmi, J., Ohno, K., 2011. AG-dependent 3'-splice sites are predisposed to aberrant splicing due to a mutation at the first nucleotide of an exon. Nucleic acids research 39, 4396-404.

Gama-Carvalho, M., Krauss, R.D., Chiang, L., Valcárcel, J., Green, M.R., Carmo-Fonseca, M., 1997. Targeting of U2AF65 to sites of active splicing in the nucleus. J Cell Biol 137, 975-87.

Gaudino, G., Follenzi, a, Naldini, L., Collesi, C., Santoro, M., Gallo, K. a, Godowski, P.J., Comoglio, P.M., 1994. RON is a heterodimeric tyrosine kinase receptor activated by the HGF homologue MSP. The EMBO journal 13, 3524-32.

Gaur, R.K., Valcárcel, J., Green, M.R., 1995. Sequential recognition of the pre-mRNA branch point by U2AF65 and a novel spliceosome-associated 28-kDa protein. RNA 1, 407-17.

Geib, T., Hertel, K.J., 2009. Restoration of full-length SMN promoted by adenoviral vectors expressing RNA antisense oligonucleotides embedded in U7 snRNAs. PloS one 4, e8204.

Ghigna, C., Giordano, S., Shen, H., Benvenuto, F., Castiglioni, F., Comoglio, P.M., Green, M.R., Riva, S., Biamonti, G., 2005. Cell motility is controlled by SF2/ASF through alternative splicing of the Ron protooncogene. Molecular cell 20, 881-90.

Ghigna, C., Toledo, M.D., Bonomi, S., Valacca, C., Gallo, S., Apicella, M., Eperon, I., Tazi, J., Biamonti, G., Molecolare, G., Nazionale, C., Ii, M., Genetics, M., De, C.N., 2010. Pro-

metastatic splicing of Ron proto-oncogene mRNA can be reversed therapeutic potential of bifunctional oligonucleotides and indole derivatives. RNA Biology 7, 495-503.

Ghosh, G., Adams, J. a, 2011. Phosphorylation mechanism and structure of serine-arginine protein kinases. The FEBS journal 278, 587-97.

Goemans, N.M., Tulinius, M., Johanna T. van den Akker, B.E.B., Ekhart, P.F., Heuvelmans, N., Holling, T., Janson, A.A., Platenburg, G.J., Sipkens, J.A., Sitsen, J.M.A., Annemieke Aartsma-Rus, G.-J.B. van O., Buyse, G., Darin, N., Verschuuren, J.J., Campion, G.V., Kimpe, S.J. de, Deutekom, J.C. van, 2011. Systemic Administration of PRO051 in Duchenne's Muscular Dystrophy. N. Engl. J. Med 364, 1513-1522.

Goyenvalle, A., Babbs, A., Powell, D., Kole, R., Fletcher, S., Wilton, S.D., Davies, K.E., 2010. Prevention of dystrophic pathology in severely affected dystrophin/utrophin-deficient mice by morpholino-oligomer-mediated exon-skipping. Molecular therapy : the journal of the American Society of Gene Therapy 18, 198-205.

Goyenvalle, A., Vulin, A., Fougerousse, F., Leturcq, F., Kaplan, J.-C., Garcia, L., Danos, O., 2004. Rescue of dystrophic muscle through U7 snRNA-mediated exon skipping. Science (New York, N.Y.) 306, 1796-9.

Gozani, O., Potashkin, J., Reed, R., Gozani, O.R., 1998. A Potential Role for U2AF-SAP 155 Interactions in Recruiting U2 snRNP to the Branch Site. Molecular and cellular biology 18, 4752-4760.

BIBLIOGRAPHY

Grabowski, P.J., Nasim, F.U., Kuo, H.C., Burch, R., 1991. Combinatorial splicing of exon pairs by two-site binding of U1 small nuclear ribonucleoprotein particle. Molecular and cellular biology 11, 5919-28.

Graveley, B.R., Hertel, K.J., Maniatis, T., Graveley, B.R., Hertel, K.J., Maniatis, T.O.M., 2001. The role of U2AF35 and U2AF65 in enhancer-dependent splicing. RNA 7, 806-818.

Gregorevic, P., Allen, J.M., Minami, E., Blankinship, M.J., Haraguchi, M., Meuse, L., Finn, E., Adams, M.E., Froehner, S.C., Murry, C.E., Chamberlain, J.S., 2006. rAAV6-microdystrophin preserves muscle function and extends lifespan in severely dystrophic mice. Nature medicine 12, 787-9.

Griffey, R.H., Monia, B.P., Cummins, L.L., Freier, S., Greig, M.J., Guinosso, C.J., Lesnik, E., Manalili, S.M., Mohan, V., Owens, S., Ross, B.R., Sasmor, H., Wancewicz, E., Weiler, K., Wheeler, P.D., Cook, P.D., 1996. 2'-O-aminopropyl ribonucleotides: a zwitterionic modification that enhances the exonuclease resistance and biological activity of antisense oligonucleotides. Journal of medicinal chemistry 39, 5100-9.

Guo, X., Chen, Q.-R., Song, Y.K., Wei, J.S., Khan, J., 2011. Exon array analysis reveals neuroblastoma tumors have distinct alternative splicing patterns according to stage and MYCN amplification status. BMC medical genomics 4, 35.

Guth, S., Tange, T.O., Kellenberger, E., Thomas, O., 2001. Dual Function for U2AF 35 in AG-Dependent Pre-mRNA Splicing. Molecular and cellular biology 21, 7673-7681.

BIBLIOGRAPHY

Görnemann, J., Kotovic, K.M., Hujer, K., Neugebauer, K.M., 2005. Cotranscriptional Spliceosome Assembly Occurs in a Stepwise Fashion and Requires the Cap Binding Complex. Molecular Cell 19, 53-63.

Hall, S.L., Padgett, R. a, 1996. Requirement of U12 snRNA for in vivo splicing of a minor class of eukaryotic nuclear pre-mRNA introns. Science (New York, N.Y.) 271, 1716-8.

Han, S.P., Tang, Y.H., Smith, R., 2010. Functional diversity of the hnRNPs: past, present and perspectives. The Biochemical journal 430, 379-92.

Hartmuth, K., Urlaub, H., Vornlocher, H.-P., Will, C.L., Gentzel, M., Wilm, M., Lührmann, R., 2002. Protein composition of human prespliceosomes isolated by a tobramycin affinity-selection method. Proceedings of the National Academy of Sciences of the United States of America 99, 16719-24.

Hastings, M.L., Allemand, E., Duelli, D.M., Myers, M.P., Krainer, A.R., 2007. Control of pre-mRNA splicing by the general splicing factors PUF60 and U2AF(65). PloS one 2, e538.

Heinrichs, V., Bach, M., Winkelmann, G., Lührmann, R., 1990. U1-specific protein C needed for efficient complex formation of U1 snRNP with a 5' splice site. Science (New York, N.Y.) 247, 69-72.

Hermann, H., Fabrizio, P., Raker, V. a, Foulaki, K., Hornig, H., Brahms, H., Lührmann, R., 1995. snRNP Sm proteins share two evolutionarily conserved sequence motifs which are involved in Sm protein-protein interactions. The EMBO journal 14, 2076-88.

BIBLIOGRAPHY

Hicks, M.J., Mueller, W.F., Shepard, P.J., Hertel, K.J., 2010. Competing upstream 5' splice sites enhance the rate of proximal splicing. Molecular and cellular biology 30, 1878-86.

Hodges, C., Bintu, L., Lubkowska, L., Kashlev, M., Bustamante, C., 2009. Nucleosomal fluctuations govern the transcription dynamics of RNA polymerase II. Science (New York, N.Y.) 325, 626-8.

Hoffman, B.E., Grabowski, P.J., 1992. U1 snRNP targets an essential splicing factor, U2AF65, to the 3' splice site by a network of interactions spanning the exon. Genes & development 6, 2554-68.

Hoffman, E., Brown, R.J., Kunkel, L., 1987. Dystrophin: the protein product of the Duchenne muscular dystrophy locus. Cell 51, 919-928.

Hoffman, J., Hallam, S., Venne, V., Lyon, E., Ward, K., 1998. Implications of a novel cryptic splice site in the BRCA1 gene. American journal of medical genetics 80, 140-144.

Hoffmann, J., 1893. Uber chronische spinale Muskulatrophie in Kindesalter auf familiarer Basis. Dtsch Z Nervenheilkd 3, 427.

Hofmann, Y., Lorson, C.L., Stamm, S., Androphy, E.J., Wirth, B., 2000. Htra2-beta 1 stimulates an exonic splicing enhancer and can restore full-length SMN expression to survival motor neuron 2 (SMN2). Proceedings of the National Academy of Sciences of the United States of America 97, 9618-23.

BIBLIOGRAPHY

Hofmann, Y., Wirth, B., 2002. hnRNP-G promotes exon 7 inclusion of survival motor neuron (SMN) via direct interaction with Htra2-beta1. Human molecular genetics 11, 2037-49.

Holmila, R., Fouquet, C., Cadranel, J., Zalcman, G., Soussi, T., 2003. Splice mutations in the p53 gene: case report and review of the literature. Human mutation 21, 101-2.

House, A.E., Lynch, K.W., 2006. An exonic splicing silencer represses spliceosome assembly after ATP-dependent exon recognition. Nature structural & molecular biology 13, 937-44.

House, A.E., Lynch, K.W., 2008. Regulation of alternative splicing: more than just the ABCs. The Journal of biological chemistry 283, 1217-21.

Hsieh-li, H.M., Chang, J.-gowth, Jong, Y.-jyh, Wu, M.-hsiang, Wang, N.M., Tsai, C.H., Li, H., 2000. A mouse model for spinal muscular atrophy. Nature genetics 24, 66-70.

Hua, Y., Sahashi, K., Hung, G., Rigo, F., Passini, M. a, Bennett, C.F., Krainer, A.R., 2010. Antisense correction of SMN2 splicing in the CNS rescues necrosis in a type III SMA mouse model. Genes & development 24, 1634-1644.

Hua, Y., Vickers, T. a, Baker, B.F., Bennett, C.F., Krainer, A.R., 2007. Enhancement of SMN2 exon 7 inclusion by antisense oligonucleotides targeting the exon. PLoS biology 5, e73.

BIBLIOGRAPHY

Hua, Y., Vickers, T.A., Okunola, H.L., Bennett, C.F., Krainer, A.R., 2008. Antisense Masking of an hnRNP A1 / A2 Intronic Splicing Silencer Corrects SMN2 Splicing in Transgenic Mice. The American Journal of Human Genetics 834-848.

Huang, T., Vilardell, J., Query, C.C., 2002. Pre-spliceosome formation in S.pombe requires a stable complex of SF1-U2AF(59)-U2AF(23). The EMBO journal 21, 5516-26.

Hwang, D.Y., Cohen, J.B., 1996. U1 snRNA promotes the selection of nearby 5' splice sites by U6 snRNA in mammalian cells. Genes & Development 10, 338-350.

Ibrahim, E.C., Schaal, T.D., Hertel, K.J., Reed, R., Maniatis, T., 2005. Serine/arginine-rich protein-dependent suppression of exon skipping by exonic splicing enhancers. Proceedings of the National Academy of Sciences of the United States of America 102, 5002-7.

Indraccolo, S., Minuzzo, S., Zamarchi, R., Calderazzo, F., Piovan, E., Amadori, A., 2002. Alternatively spliced forms of Igα and Igβ prevent B cell receptor expression on the cell surface. European Journal of Immunology 32, 1530.

Ivanova, G.D., Arzumanov, A., Abes, R., Yin, H., Wood, M.J. a, Lebleu, B., Gait, M.J., 2008. Improved cell-penetrating peptide-PNA conjugates for splicing redirection in HeLa cells and exon skipping in mdx mouse muscle. Nucleic acids research 36, 6418-28.

BIBLIOGRAPHY

Izquierdo, J.M., Majós, N., Bonnal, S., Martínez, C., Castelo, R., Guigó, R., Bilbao, D., Valcárcel, J., 2005. Regulation of Fas alternative splicing by antagonistic effects of TIA-1 and PTB on exon definition. Molecular cell 19, 475-84.

Jensen, K.K., Orum, H., Nielsen, P.E., Nordén, B., 1997. Kinetics for hybridization of peptide nucleic acids (PNA) with DNA and RNA studied with the BIAcore technique. Biochemistry 36, 5072-7.

Jin, Y., Suzuki, H., Maegawa, S., Endo, H., Sugano, S., Hashimoto, K., Yasuda, K., Inoue, K., 2003. A vertebrate RNA-binding protein Fox-1 regulates tissue-specific splicing via the pentanucleotide GCAUG. The EMBO journal 22, 905-12.

Juliano, R., Bauman, J., Kang, H., Ming, X., 2009. Biological barriers to therapy with antisense and siRNA oligonucleotides. Molecular pharmaceutics 6, 686-95.

Jurica, M.S., Licklider, L.J., Gygi, S.R., Grigorieff, N., Moore, M.J., 2002. Purification and characterization of native spliceosomes suitable for three-dimensional structural analysis. RNA 8, 426-439.

Jurica, M.S., Moore, M.J., 2003. Pre-mRNA splicing: awash in a sea of proteins. Molecular cell 12, 5-14.

Kaida, D., Motoyoshi, H., Tashiro, E., Nojima, T., Hagiwara, M., Ishigami, K., Watanabe, H., Kitahara, T., Yoshida, T., Nakajima, H., Tani, T., Horinouchi, S., Yoshida, M., 2007.

Spliceostatin A targets SF3b and inhibits both splicing and nuclear retention of pre-mRNA. Nature chemical biology 3, 576-83.

Kan, J.L., Green, M.R., 1999. Pre-mRNA splicing of IgM exons M1 and M2 is directed by a juxtaposed splicing enhancer and inhibitor. Genes & development 13, 462-71.

Kandels-lewis, S., Seraphin, B., 1993. Role of U6 snRNA in 5' Splice Site Selection. Science 262, 2035-39.

Kanopka, A., Muhlemann, O., Akusjarvi, G., 1996. Inhibition by SR proteins of splicing of a regulated adenovirus pre-mRNA. Nature 535-538.

Karni, R., de Stanchina, E., Lowe, S.W., Sinha, R., Mu, D., Krainer, A.R., 2007. The gene encoding the splicing factor SF2/ASF is a proto-oncogene. Nature structural & molecular biology 14, 185-93.

Kashima, T., Manley, J.L., 2003. A negative element in SMN2 exon 7 inhibits splicing in spinal muscular atrophy. Nature genetics 34, 460-3.

Kashima, T., Rao, N., Manley, J.L., 2007. An intronic element contributes to splicing repression in spinal muscular atrophy. Proceedings of the National Academy of Sciences of the United States of America 104, 3426-31.

Kennedy, C.F., Krämer, A., Susan, M., Kra, A., 1998. A Role for SRp54 during Intron Bridging of Small Introns with Pyrimidine Tracts Upstream of the Branch Point. Molecular and cellular biology 18, 5425-5434.

BIBLIOGRAPHY

Kent, O. a, Reayi, A., Foong, L., Chilibeck, K.A., MacMillan, A.M., 2003. Structuring of the 3' splice site by U2AF65. The Journal of biological chemistry 278, 50572-7.

Kent, O.A., Ritchie, D.B., Macmillan, A.M., 2005. Characterization of a U2AF-Independent Commitment Complex (E') in the Mammalian Spliceosome Assembly Pathway. Molecular and cellular biology 25, 233-240.

Keriel, A., Mahuteau-Betzer, F., Jacquet, C., Plays, M., Grierson, D., Sitbon, M., Tazi, J., 2009. Protection against retrovirus pathogenesis by SR protein inhibitors. PloS one 4, e4533.

Kim, D.-W., Kim, J.-H., Park, M., Yeom, J.-H., Go, H., Kim, S., Han, M.S., Lee, K., Bae, J., 2011. Modulation of biological processes in the nucleus by delivery of DNA oligonucleotides conjugated with gold nanoparticles. Biomaterials 32, 2593-2604.

Kinali, M., Arechavala-Gomeza, V., Feng, L., Cirak, S., Hunt, D., Adkin, C., Guglieri, M., Ashton, E., Abbs, S., Nihoyannopoulos, P., Garralda, M.E., Rutherford, M., McCulley, C., Popplewell, L., Graham, I.R., Dickson, G., Wood, M.J. a, Wells, D.J., Wilton, S.D., Kole, R., Straub, V., Bushby, K., Sewry, C., Morgan, J.E., Muntoni, F., 2009. Local restoration of dystrophin expression with the morpholino oligomer AVI-4658 in Duchenne muscular dystrophy: a single-blind, placebo-controlled, dose-escalation, proof-of-concept study. Lancet neurology 8, 918-28.

BIBLIOGRAPHY

King, L.B., Norvell, A., Monroe, J.G., 1999. Antigen receptor-induced signal transduction imbalances associated with the negative selection of immature B cells. Journal of immunology 162, 2655-62.

Kitada, S., Andersen, J., Akar, S., Zapata, J.M., Takayama, S., Krajewski, S., Wang, H.G., Zhang, X., Bullrich, F., Croce, C.M., Rai, K., Hines, J., Reed, J.C., 1998. Expression of apoptosis-regulating proteins in chronic lymphocytic leukemia: correlations with In vitro and In vivo chemoresponses. Blood 91, 3379-89.

Koenig, M., Beggs, a H., Moyer, M., Scherpf, S., Heindrich, K., Bettecken, T., Meng, G., Müller, C.R., Lindlöf, M., Kaariainen, H., 1989. The molecular basis for Duchenne versus Becker muscular dystrophy: correlation of severity with type of deletion. American journal of human genetics 45, 498-506.

Kohtz, J., Jamison, S., Will, C., Zuo, P., Luhurmann, R., Garcia-Blanco, A., Manley, J., 1994. Protein-proetin interactions and 5'-splice site recognition in mammalian mRNA precurors. Nature 368, 119-124.

Kolasinska-Zwierz, P., Down, T., Latorre, I., Liu, T., Liu, X.S., Ahringer, J., 2009. Differential chromatin marking of introns and expressed exons by H3K36me3. Nature genetics 41, 376-81.

Konarska, M.M., Vilardell, J., Query, C.C., 2006. Repositioning of the reaction intermediate within the catalytic center of the spliceosome. Molecular cell 21, 543-53.

BIBLIOGRAPHY

Kornblihtt, A.R., de la Mata, M., Fededa, J.P., Munoz, M.J., Nogues, G., 2004. Multiple links between transcription and splicing. RNA 10, 1489-98.

Kotake, Y., Sagane, K., Owa, T., Mimori-Kiyosue, Y., Shimizu, H., Uesugi, M., Ishihama, Y., Iwata, M., Mizui, Y., 2007. Splicing factor SF3b as a target of the antitumor natural product pladienolide. Nature chemical biology 3, 570-5.

Kramer, A., Utans, U., 1991. Three protein factors (SF1, SF3 and U2AF) function in pre-splicing complex formation in addition to snRNPs. The EMBO journal 57, 2054-2058.

Kugelberg, E., Welander, L., 1956. Heredofamilial Juvenile muscular Atrophy Simulating muscular Dystrophy. Archives of neurology and psychiatry 75, 500-509.

Kumar, P., Wu, H., McBride, J.L., Jung, K.-E., Kim, M.H., Davidson, B.L., Lee, S.K., Shankar, P., Manjunath, N., 2007. Transvascular delivery of small interfering RNA to the central nervous system. Nature 448, 39-43.

Kuo, H.C., Nasim, F.H., Grsowski, P.J., 1991. Control of Alternative Splicing by the Differential Binding of U1 Small Nuclear Ribonucleoprotein Particle. Science 251, 1045-1050.

Kurahashi, H., Takami, K., Oue, T., 1995. Biallelic Inactivation of the APC Gene in Hepatoblastoma. Cancer 55, 5007-5011.

BIBLIOGRAPHY

Kurihara, N., Iwama, a, Tatsumi, J., Ikeda, K., Suda, T., 1996. Macrophage-stimulating protein activates STK receptor tyrosine kinase on osteoclasts and facilitates bone resorption by osteoclast-like cells. Blood 87, 3704-10.

Lacadie, S.A., Rosbash, M., Street, S., 2005. Dynamics and the Role of U1 snRNA : 5' ss Base Pairing in Yeast. Yeast 19, 65-75.

Lallena, M.J., Chalmers, K.J., Llamazares, S., Lamond, A.I., Valcárcel, J., 2002. Splicing regulation at the second catalytic step by Sex-lethal involves 3' splice site recognition by SPF45. Cell 109, 285-96.

Langer, W., Sohler, F., Leder, G., Beckmann, G., Seidel, H., Gröne, J., Hummel, M., Sommer, A., 2010. Exon array analysis using re-defined probe sets results in reliable identification of alternatively spliced genes in non-small cell lung cancer. BMC genomics 11, 676.

Le, T.T., Pham, L.T., Butchbach, M.E.R., Zhang, H.L., Monani, U.R., Coovert, D.D., Gavrilina, T.O., Xing, L., Bassell, G.J., Burghes, A.H.M., 2005. SMNDelta7, the major product of the centromeric survival motor neuron (SMN2) gene, extends survival in mice with spinal muscular atrophy and associates with full-length SMN. Human molecular genetics 14, 845-57.

Lefave, C.V., Squatrito, M., Vorlova, S., Rocco, G.L., Brennan, C.W., Holland, E.C., Pan, Y.-X., Cartegni, L., 2011. Splicing factor hnRNPH drives an oncogenic splicing switch in gliomas. The EMBO journal 30, 4084-4097.

BIBLIOGRAPHY

Lefebvre, S., Bürglen, L., Reboullet, S., Clermont, O., Burlet, P., Viollet, L., Benichou, B., Cruaud, C., Millasseau, P., Zeviani, M., 1995. Identification and characterization of a spinal muscular atrophy-determining gene. Cell 80, 155-65.

Leonis, M. a, Toney-Earley, K., Degen, S.J.F., Waltz, S.E., 2002. Deletion of the Ron receptor tyrosine kinase domain in mice provides protection from endotoxin-induced acute liver failure. Hepatology 36, 1053-60.

Lesser, C.F., Guthrie, C., 1993. Mutations in U6 snRNA that alter splice site specificity: implications for the active site. Science (New York, N.Y.) 262, 1982-8.

Li, Y., Blencowe, B.J., 1999. Distinct factor requirements for exonic splicing enhancer function and binding of U2AF to the polypyrimidine tract. Journal of Biological Chemistry 274, 35074-35079.

Lim, S.R., Hertel, K.J., 2001. Modulation of survival motor neuron pre-mRNA splicing by inhibition of alternative 3' splice site pairing. The Journal of biological chemistry 276, 45476-83.

Lim, S.R., Hertel, K.J., 2004. Commitment to splice site pairing coincides with A complex formation. Molecular cell 15, 477-83.

Lin, C.H., Patton, J.G., 1995. Regulation of alternative 3' splice site selection by constitutive splicing factors. RNA 1, 234-45.

BIBLIOGRAPHY

Liu, L., Siegmund, A., Xi, N., Kaplan-Lefko, P., Rex, K., Chen, A., Lin, J., Moriguchi, J., Berry, L., Huang, L., Teffera, Y., Yang, Y., Zhang, Y., Bellon, S.F., Lee, M., Shimanovich, R., Bak, A., Dominguez, C., Norman, M.H., Harmange, J.-C., Dussault, I., Kim, T.-S., 2008. Discovery of a potent, selective, and orally bioavailable c-Met inhibitor: 1-(2-hydroxy-2-methylpropyl)-N-(5-(7-methoxyquinolin-4-yloxy)pyridin-2-yl)-5-methyl-3-oxo-2-phenyl-2,3-dihydro-1H-pyrazole-4-carboxamide (AMG 458). Journal of medicinal chemistry 51, 3688-91.

Liu, Q., Fischer, U., Wang, F., Dreyfuss, G., 1997. The spinal muscular atrophy disease gene product, SMN, and its associated protein SIP1 are in a complex with spliceosomal snRNP proteins. Cell 90, 1013-21.

Liu, Z., Luyten, I., Bottomley, M.J., Messias, a C., Houngninou-Molango, S., Sprangers, R., Zanier, K., Krämer, a, Sattler, M., 2001. Structural basis for recognition of the intron branch site RNA by splicing factor 1. Science (New York, N.Y.) 294, 1098-102.

Lorson, C.L., Androphy, E.J., 2000. An exonic enhancer is required for inclusion of an essential exon in the SMA-determining gene SMN. Human molecular genetics 9, 259-65.

Lorson, C.L., Hahnen, E., Androphy, E.J., Wirth, B., 1999. A single nucleotide in the SMN gene regulates splicing and is responsible for spinal muscular atrophy. Proceedings of the National Academy of Sciences of the United States of America 96, 6307-11.

BIBLIOGRAPHY

Lu, Q.L., Mann, C.J., Lou, F., Bou-Gharios, G., Morris, G.E., Xue, S.-an, Fletcher, S., Partridge, T. a, Wilton, S.D., 2003. Functional amounts of dystrophin produced by skipping the mutated exon in the mdx dystrophic mouse. Nature medicine 9, 1009-14.

Lu, Q.L., Rabinowitz, A., Chen, Y.C., Yokota, T., Yin, H., Alter, J., Jadoon, A., Bou-Gharios, G., Partridge, T., 2005. Systemic delivery of antisense oligoribonucleotide restores dystrophin expression in body-wide skeletal muscles. Proceedings of the National Academy of Sciences of the United States of America 102, 198-203.

Lu, Y., Yao, H.-P., Wang, M.-H., 2007. Multiple variants of the RON receptor tyrosine kinase: biochemical properties, tumorigenic activities, and potential drug targets. Cancer letters 257, 157-64.

López-Bigas, N., Audit, B., Ouzounis, C., Parra, G., Guigó, R., 2005. Are splicing mutations the most frequent cause of hereditary disease? FEBS letters 579, 1900-3.

Lømo, J., Smeland, E.B., Krajewski, S., Lymphocytes, B.B., Lã, J., Smeland, B., Reed, J.C., Blomhoff, H.K., 1996. Expression of the Bcl-2 Homologue Mcl-1 Correlates with Survival of Peripheral Blood B Lymphocytes Expression of the Bcl-2 Homologue Md-i Correlates with Survival of Peripheral. Cancer Research 56, 40-43.

Ma, Q.I., Zhang, K.U.N., Yao, H.-ping, Zhou, Y.-qing, Padhye, S., Wang, M.-hai, 2010. Inhibition of MSP-RON signaling pathway in cancer cells by a novel soluble form of RON comprising the entire sema sequence. International journal of oncology 36, 1551-1561.

BIBLIOGRAPHY

Mackereth, C.D., Madl, T., Bonnal, S., Simon, B., Zanier, K., Gasch, A., Rybin, V., Valcárcel, J., Sattler, M., 2011. Multi-domain conformational selection underlies pre-mRNA splicing regulation by U2AF. Nature 2-7.

Madocsai, C., Lim, S.R., Geib, T., Lam, B.J., Hertel, K.J., 2005. Correction of SMN2 Pre-mRNA splicing by antisense U7 small nuclear RNAs. Molecular therapy 12, 1013-22.

Maggiora, P., 2003. The RON and MET oncogenes are co-expressed in human ovarian carcinomas and cooperate in activating invasiveness. Experimental Cell Research 288, 382-389.

Makeyev, E.V., Zhang, J., Carrasco, M. a, Maniatis, T., 2007. The MicroRNA miR-124 promotes neuronal differentiation by triggering brain-specific alternative pre-mRNA splicing. Molecular cell 27, 435-48.

Manoharan, M., 1999. 2′-Carbohydrate modifications in antisense oligonucleotide therapy: importance of conformation, configuration and conjugation. Biochimica et Biophysica Acta (BBA) - Gene Structure and Expression 1489, 117-130.

Markovtsov, V., Nikolic, J.M., Goldman, J. a, Turck, C.W., Chou, M.Y., Black, D.L., 2000. Cooperative assembly of an hnRNP complex induced by a tissue-specific homolog of polypyrimidine tract binding protein. Molecular and cellular biology 20, 7463-79.

Marquis, J., Meyer, K., Angehrn, L., Kämpfer, S.S., Rothen-Rutishauser, B., Schümperli, D., 2007. Spinal muscular atrophy: SMN2 pre-mRNA splicing corrected by a U7 snRNA derivative carrying a splicing enhancer sequence. Molecular therapy 15, 1479-86.

Marshall, N.B., Oda, S.K., London, C. a, Moulton, H.M., Iversen, P.L., Kerkvliet, N.I., Mourich, D.V., 2007. Arginine-rich cell-penetrating peptides facilitate delivery of antisense oligomers into murine leukocytes and alter pre-mRNA splicing. Journal of immunological methods 325, 114-26.

Martinez-Contreras, R., Fisette, J.-F., Nasim, F.-ul H., Madden, R., Cordeau, M., Chabot, B., 2006. Intronic binding sites for hnRNP A/B and hnRNP F/H proteins stimulate pre-mRNA splicing. PLoS biology 4, e21.

Martins de Araújo, M., Bonnal, S., Hastings, M.L., Krainer, A.R., Valcárcel, J., 2009. Differential 3' splice site recognition of SMN1 and SMN2 transcripts by U2AF and U2 snRNP. RNA 15, 515-23.

Mattis, V.B., Fosso, M.Y., Chang, C.-W., Lorson, C.L., 2009. Subcutaneous administration of TC007 reduces disease severity in an animal model of SMA. BMC neuroscience 10, 142.

Matzke, A., Herrlich, P., Ponta, H., Orian-Rousseau, V., 2005. A five-amino-acid peptide blocks Met- and Ron-dependent cell migration. Cancer research 65, 6105-10.

BIBLIOGRAPHY

Mauger, D.M., Lin, C., Garcia-Blanco, M. a, 2008. hnRNP H and hnRNP F complex with Fox2 to silence fibroblast growth factor receptor 2 exon IIIc. Molecular and cellular biology 28, 5403-19.

Mayeda, a, Krainer, A.R., 1992. Regulation of alternative pre-mRNA splicing by hnRNP A1 and splicing factor SF2. Cell 68, 365-75.

Mayeda, a, Ohshima, Y., 1988. Short donor site sequences inserted within the intron of beta-globin pre-mRNA serve for splicing in vitro. Molecular and cellular biology 8, 4484-91.

Mayeda, a, Screaton, G.R., Chandler, S.D., Fu, X.D., Krainer, a R., 1999. Substrate specificities of SR proteins in constitutive splicing are determined by their RNA recognition motifs and composite pre-mRNA exonic elements. Molecular and cellular biology 19, 1853-63.

Mayes, a E., Verdone, L., Legrain, P., Beggs, J.D., 1999. Characterization of Sm-like proteins in yeast and their association with U6 snRNA. The EMBO journal 18, 4321-31.

McCullough, A., Berget, S.M., 1997. G triplets located throughout a class of small vertebrate introns enforce intron borders and regulate splice site selection. Molecular and cellular biology 17, 4562-4571.

McNally, E.M., 2007. New approaches in the therapy of cardiomyopathy in muscular dystrophy. Annual review of medicine 58, 75-88.

BIBLIOGRAPHY

Mccullough, A.J., Berget, S.M., 2000. An Intronic Splicing Enhancer Binds U1 snRNPs To Enhance Splicing and Select 5 ′ Splice Sites. Mol Cell Biol 20, 9225-9235.

Meister, G., Bühler, D., Pillai, R., Lottspeich, F., Fischer, U., 2001. A multiprotein complex mediates the ATP-dependent assembly of spliceosomal U snRNPs. Nature cell biology 3, 945-9.

Melki, J., Lefebvre, S., Burglen, L., Burlet, P., Clermont, O., Millasseau, P., Reboullet, S., Bénichou, B., Zeviani, M., Le Paslier, D., 1994. De novo and inherited deletions of the 5q13 region in spinal muscular atrophies. Science (New York, N.Y.) 264, 1474-7.

Mera, a, Suga, M., Ando, M., Suda, T., Yamaguchi, N., 1999. Induction of cell shape changes through activation of the interleukin-3 common beta chain receptor by the RON receptor-type tyrosine kinase. The Journal of biological chemistry 274, 15766-74.

Meyer, K., Marquis, J., Trüb, J., Nlend Nlend, R., Verp, S., Ruepp, M.-D., Imboden, H., Barde, I., Trono, D., Schümperli, D., 2009. Rescue of a severe mouse model for spinal muscular atrophy by U7 snRNA-mediated splicing modulation. Human molecular genetics 18, 546-55.

Misquitta-Ali, C.M., Cheng, E., O'Hanlon, D., Liu, N., McGlade, C.J., Tsao, M.S., Blencowe, B.J., 2011. Global profiling and molecular characterization of alternative splicing events misregulated in lung cancer. Molecular and cellular biology 31, 138-50.

Miyajima, H., Miyaso, H., Okumura, M., Kurisu, J., Imaizumi, K., 2002. Identification of a cis-acting element for the regulation of SMN exon 7 splicing. The Journal of biological chemistry 277, 23271-7.

Miyaso, H., Okumura, M., Kondo, S., Higashide, S., Miyajima, H., Imaizumi, K., 2003. An intronic splicing enhancer element in survival motor neuron (SMN) pre-mRNA. The Journal of biological chemistry 278, 15825-31.

Moulton, H.M., Moulton, J.D., 2010. Morpholinos and their peptide conjugates: therapeutic promise and challenge for Duchenne muscular dystrophy. Biochimica et biophysica acta 1798, 2296-303.

Munsat, T., Davies, K., 1992. Metting Report: International SMA Consortium Meeting. Neuromuscular Disorders 2, 423-428.

Murray, H.L., Jarrell, K. a, 1999. Flipping the switch to an active spliceosome. Cell 96, 599-602.

Nahkuri, S., Taft, R.J., Mattick, J.S., 2009. Nucleosomes are preferentially positioned at exons in somatic and sperm cells. Cell cycle 8, 3420-4.

Nakamura, A., Takeda, S., 2009. Exon-skipping therapy for Duchenne muscular dystrophy. Neuropathology 29, 494-501.

Nasim, F.-ul H., Hutchison, S., Cordeau, M., 2002. High-affinity hnRNP A1 binding sites and duplex-forming inverted repeats have similar effects on 5 ’ splice site selection in

support of a common looping out and repression mechanism . High-affinity hnRNP A1 binding sites and duplex-forming inverted repea. RNA 8, 1078-1089.

Nelson, K.K., Green, M.R., 1988. Splice site selection and ribonucleoprotein complex assembly during in vitro pre-mRNA splicing. Genes & Development 2, 319-329.

Neri, M., Torelli, S., Brown, S., Ugo, I., Sabatelli, P., Merlini, L., Spitali, P., Rimessi, P., Gualandi, F., Sewry, C., Ferlini, A., Muntoni, F., 2007. Dystrophin levels as low as 30% are sufficient to avoid muscular dystrophy in the human. Neuromuscular disorders : NMD 17, 913-8.

Newman, a J., Norman, C., 1992. U5 snRNA interacts with exon sequences at 5' and 3' splice sites. Cell 68, 743-54.

Newman, a, Norman, C., 1991. Mutations in yeast U5 snRNA alter the specificity of 5' splice-site cleavage. Cell 65, 115-23.

Newman, A.J., 1997. The role of U5 snRNP in pre-mRNA splicing. The EMBO journal 16, 5797-5800.

Ney, P.A., Andrea, A.D.D., Dc, W., 2011. Friend erythroleukemia revisited. Blood 96, 3675-3680.

Nicole, S., Diaz, C.C., Frugier, T., Melki, J., 2002. Spinal muscular atrophy: recent advances and future prospects. Muscle & nerve 26, 4-13.

BIBLIOGRAPHY

Nizzardo, M., Nardini, M., Ronchi, D., Salani, S., Donadoni, C., Fortunato, F., Colciago, G., Falcone, M., Simone, C., Riboldi, G., Govoni, A., Bresolin, N., Comi, G.P., Corti, S., 2011. Beta-lactam antibiotic offers neuroprotection in a spinal muscular atrophy model by multiple mechanisms. Experimental neurology 229, 214-25.

Okunola, H.L., Krainer, A.R., 2009. Cooperative-binding and splicing-repressive properties of hnRNP A1. Molecular and cellular biology 29, 5620-31.

Owen, N., Zhou, H., Malygin, A. a, Sangha, J., Smith, L.D., Muntoni, F., Eperon, I.C., 2011. Design principles for bifunctional targeted oligonucleotide enhancers of splicing. Nucleic acids research 39, 7194-7208.

O'Mullane, L., Eperon, I.C., 1998. The pre-mRNA 5' cap determines whether U6 small nuclear RNA succeeds U1 small nuclear ribonucleoprotein particle at 5' splice sites. Molecular and cellular biology 18, 7510-20.

O'Toole, J.M., Rabenau, K.E., Burns, K., Lu, D., Mangalampalli, V., Balderes, P., Covino, N., Bassi, R., Prewett, M., Gottfredsen, K.J., Thobe, M.N., Cheng, Y., Li, Y., Hicklin, D.J., Zhu, Z., Waltz, S.E., Hayman, M.J., Ludwig, D.L., Pereira, D.S., 2006. Therapeutic implications of a human neutralizing antibody to the macrophage-stimulating protein receptor tyrosine kinase (RON), a c-MET family member. Cancer research 66, 9162-70.

Pacheco, T.R., Coelho, M.B., Desterro, J.M.P., Carmo-fonseca, M., 2006. In Vivo Requirement of the Small Subunit of U2AF for Recognition of a Weak 3' Splice Site. Molecular and cellular biology 26, 8183-8190.

Padhye, S.S., Guin, S., Yao, H.-P., Zhou, Y.-Q., Zhang, R., Wang, M.-H., 2011. Sustained Expression of the RON Receptor Tyrosine Kinase by Pancreatic Cancer Stem Cells as a Potential Targeting Moiety for Antibody-Directed Chemotherapeutics. Molecular pharmaceutics.

Pan, Q., Shai, O., Lee, L.J., Frey, B.J., Blencowe, B.J., 2008. Deep surveying of alternative splicing complexity in the human transcriptome by high-throughput sequencing. Nature genetics 40, 1413-5.

Park, J.S., Park, J.H., Khoi, P.N., Joo, Y.E., Jung, Y.D., 2011. MSP-induced RON activation upregulates uPAR expression and cell invasiveness via MAPK, AP-1 and NF-κB signals in gastric cancer cells. Carcinogenesis 32, 175-81.

Park, J.S.U.N., Park, J.I.H.Y.E., Lee, S., Joo, Y.E.U.N., Jung, Y.D.O., 2010. Small interfering RNA targeting of Recepteur d'Origine Nantais induces apoptosis via modulation of nuclear factor- κ B and Bcl-2 family in gastric cancer cells. Oncology Reports 24, 709-714.

Passini, M., Bu, J., Richards, A., Kinnecom, C., 2011. Antisense oligonucleotides delivered to the mouse CNS ameliorate symptoms of severe spinal musclar atrophy. Science Translational Medicine 3, 72ra18.

Passini, M.A., Bu, J., Roskelley, E.M., Richards, A.M., Sardi, S.P., Riordan, C.R.O., Klinger, K.W., Shihabuddin, L.S., Cheng, S.H., 2010. CNS-targeted gene therapy improves survival and motor function in a mouse model of spinal muscular atrophy 120.

Peace, B.E., Hill, K.J., Degen, S.J.., Waltz, S.E., 2003. Cross-talk between the receptor tyrosine kinases Ron and epidermal growth factor receptor. Experimental Cell Research 289, 317-325.

Pearn, J., 1973. The gene frequency of acute Werdnig-Hoffmann disease (SMA type 1). A total population survey in North-East England. Journal of medical genetics 10, 260-5.

Pearn, J., 1978. Incidence, prevalence, and frequency studies of chronic childhood spinal muscular atrophy. Journal of medical Genetics 15, 409-413.

Pedrotti, S., Bielli, P., Paronetto, M.P., Ciccosanti, F., Fimia, G.M., Stamm, S., Manley, J.L., Sette, C., 2010. The splicing regulator Sam68 binds to a novel exonic splicing silencer and functions in SMN2 alternative splicing in spinal muscular atrophy. The EMBO journal 29, 1235-47.

Pellizzoni, L., Baccon, J., Rappsilber, J., Mann, M., Dreyfuss, G., 2002. Purification of native survival of motor neurons complexes and identification of Gemin6 as a novel component. The Journal of biological chemistry 277, 7540-5.

Petersen, M., Nielsen, C.B., Nielsen, K.E., Jensen, G. a, Bondensgaard, K., Singh, S.K., Rajwanshi, V.K., Koshkin, a a, Dahl, B.M., Wengel, J., Jacobsen, J.P., 2000. The conformations of locked nucleic acids (LNA). Journal of molecular recognition 13, 44-53.

BIBLIOGRAPHY

Peterson, M.L., 2007. of Membrane and Secreted Immunoglobulin During B Cell Development. Immunologic Research 37, 33-46.

Peterson, M.L., Bryman, M.B., Peiter, M., Cowan, C., 1994. Exon size affects competition between splicing and cleavage-polyadenylation in the immunoglobulin u gene. Molecular and cellular biology 14, 77-86.

Peterson, M.L., Gimmi, E.R., Perry, R.P., 1991. The developmentally regulated shift from membrane to secreted mu mRNA production is accompanied by an increase in cleavage-polyadenylation efficiency but no measurable change in splicing efficiency. Molecular and cellular biology 11, 2324-7.

Peterson, M.L., Perry, R.P., 1989. The regulated production of um and us mRNA is dependent on the relative efficiencies of us poly(A) site usage and the cu4-to-M1 splice. Molecular and cellular biology 9, 726-38.

Petlickovski, A., Laurenti, L., Li, X., Marietti, S., Chiusolo, P., Sica, S., Leone, G., Efremov, D.G., 2005. Sustained signaling through the B-cell receptor induces Mcl-1 and promotes survival of chronic lymphocytic leukemia B cells. Blood 105, 4820-7.

Pollex, R.L., Hegele, R. a, 2004. Hutchinson-Gilford progeria syndrome. Clinical genetics 66, 375-81.

Polydorides, a D., Okano, H.J., Yang, Y.Y., Stefani, G., Darnell, R.B., 2000. A brain-enriched polypyrimidine tract-binding protein antagonizes the ability of Nova to regulate neuron-

specific alternative splicing. Proceedings of the National Academy of Sciences of the United States of America 97, 6350-5.

Pomeranz Krummel, D. a, Oubridge, C., Leung, A.K.W., Li, J., Nagai, K., 2009. Crystal structure of human spliceosomal U1 snRNP at 5.5 A resolution. Nature 458, 475-80.

Prior, T.W., Krainer, A.R., Hua, Y., Swoboda, K.J., Snyder, P.C., Bridgeman, S.J., Burghes, A.H.M., Kissel, J.T., 2009. A positive modifier of spinal muscular atrophy in the SMN2 gene. American journal of human genetics 85, 408-13.

Query, C.C., Moore, M.J., Sharp, P. a, 1994. Branch nucleophile selection in pre-mRNA splicing: evidence for the bulged duplex model. Genes & Development 8, 587-597.

Raeppel, S., Gaudette, F., Mannion, M., Claridge, S., Saavedra, O., Isakovic, L., Déziel, R., Beaulieu, N., Beaulieu, C., Dupont, I., Nguyen, H., Wang, J., Macleod, a R., Maroun, C., Besterman, J.M., Vaisburg, A., 2010. Identification of a novel series of potent RON receptor tyrosine kinase inhibitors. Bioorganic & medicinal chemistry letters 20, 2745-9.

Raker, V. a, Plessel, G., Lührmann, R., 1996. The snRNP core assembly pathway: identification of stable core protein heteromeric complexes and an snRNP subcore particle in vitro. The EMBO journal 15, 2256-69.

Rampino, T., Gregorini, M., Soccio, G., Maggio, M., Rosso, R., Malvezzi, P., Collesi, C., Dal Canton, A., 2003. The Ron proto-oncogene product is a phenotypic marker of renal oncocytoma. The American journal of surgical pathology 27, 779-85.

BIBLIOGRAPHY

Reed, R., 1989. The organization of 3' splice-site sequences in mammalian introns. Genes & Development 3, 2113-2123.

Reed, R., 2003. Coupling transcription, splicing and mRNA export. Current Opinion in Cell Biology 15, 326-331.

Reed, R., Maniatis, T., 1986. A role for exon sequencing and splice site proximity in splice site selection. Cell 46, 681-690.

Reth, M., 1992. Antigen receptors on B lymphocytes. Annual review of immunology 10, 97-121.

Richard, J.P., Melikov, K., Vives, E., Ramos, C., Verbeure, B., Gait, M.J., Chernomordik, L.V., Lebleu, B., 2003. Cell-penetrating peptides. A re-evaluation of the mechanism of cellular uptake. The Journal of biological chemistry 278, 585-90.

Rigo, F., Martinson, H.G., 2009. Polyadenylation releases mRNA from RNA polymerase II in a process that is licensed by splicing. RNA 15, 823-36.

Rimessi, P., Sabatelli, P., Fabris, M., Braghetta, P., Bassi, E., Spitali, P., Vattemi, G., Tomelleri, G., Mari, L., Perrone, D., Medici, A., Neri, M., Bovolenta, M., Martoni, E., Maraldi, N.M., Gualandi, F., Merlini, L., Ballestri, M., Tondelli, L., Sparnacci, K., Bonaldo, P., Caputo, A., Laus, M., Ferlini, A., 2009. Cationic PMMA nanoparticles bind and deliver antisense oligoribonucleotides allowing restoration of dystrophin expression in the mdx mouse. Molecular therapy 17, 820-7.

Robberson, B.L., Cote, G.J., Berget, S.M., 1990. Exon definition may facilitate splice site selection in RNAs with multiple exons. Molecular and cellular biology 10, 84-94.

Roberts, D.F., Chavez, J., Court, S.D., 1970. The genetic component in child mortality. Archives of disease in childhood 45, 33-8.

Roca, X., Krainer, A.R., 2009. Recognition of atypical 5' splice sites by shifted base-pairing to U1 snRNA. Nature structural & molecular biology 16, 176-82.

Roca, X., Olson, A.J., Rao, A.R., Enerly, E., Kristensen, V.N., Børresen-Dale, A.-L., Andresen, B.S., Krainer, A.R., Sachidanandam, R., 2008. Features of 5'-splice-site efficiency derived from disease-causing mutations and comparative genomics. Genome research 18, 77-87.

Romano, M., Marcucci, R., Baralle, F.E., 2001. Splicing of constitutive upstream introns is essential for the recognition of intra-exonic suboptimal splice sites in the thrombopoietin gene. Nucleic acids research 29, 886-94.

Romfo, C.M., Maroney, P.A., Wu, S., 2001. 3' splice site recognition in nematode trans - splicing involves enhancer-dependent recruitment of U2 snRNP. RNA 7, 785-792.

Ruskin, B., Zamore, P.D., Green, M.R., 1988. A factor, U2AF, is required for U2 snRNP binding and splicing complex assembly. Cell 52, 207-19.

Sander, B., Golas, M.M., Makarov, E.M., Brahms, H., Kastner, B., Lührmann, R., Stark, H., 2006. Organization of core spliceosomal components U5 snRNA loop I and U4/U6 Di-

snRNP within U4/U6.U5 Tri-snRNP as revealed by electron cryomicroscopy. Molecular cell 24, 267-78.

Sanford, J.R., Coutinho, P., Hackett, J. a, Wang, X., Ranahan, W., Caceres, J.F., 2008. Identification of nuclear and cytoplasmic mRNA targets for the shuttling protein SF2/ASF. PloS one 3, e3369.

Scaffidi, P., Misteli, T., 2005. Reversal of the cellular phenotype in the premature aging disease Hutchinson-Gilford progeria syndrome. Nature medicine 11, 440-5.

Scholl, R., Meyer, K., Schümperli, D., 2007. Position and functional importance of the branch site preceding SMN exon 7. RNA Biology 4, 34-37.

Schrank, B., Götz, R., Gunnersen, J.M., Ure, J.M., Toyka, K.V., Smith, a G., Sendtner, M., 1997. Inactivation of the survival motor neuron gene, a candidate gene for human spinal muscular atrophy, leads to massive cell death in early mouse embryos. Proceedings of the National Academy of Sciences of the United States of America 94, 9920-5.

Schroeder, G.M., An, Y., Cai, Z.-wei, Chen, X.-tao, Clark, C., Cornelius, L.A.M., Dai, J., Gullo-brown, J., Gupta, A., Henley, B., Hunt, J.T., Jeyaseelan, R., Kamath, A., Kim, K., Lippy, J., Lombardo, L.J., Manne, V., Oppenheimer, S., Sack, J.S., Schmidt, R.J., Shen, G., Stefanski, K., Tokarski, J.S., Trainor, G.L., Wautlet, B.S., Wei, D., Williams, D.K., Zhang, Y., Zhang, Y., Fargnoli, J., Borzilleri, R.M., 2009. Discovery of N-(4-(2-Amino-3-chloropyridin-4-yloxy)-3-fluorophenyl)-4-ethoxy-1-(4-fluorophenyl)-2-oxo-1,2-

dihydropyridine-3-carboxamide (BMS-777607), a Selective and Orally Efficacious Inhibitor of the Met Kinase Superfamily. Journal of medicinal chemistry 52, 1251-1254.

Schwartz, S., Meshorer, E., Ast, G., 2009. Chromatin organization marks exon-intron structure. Nature structural & molecular biology 16, 990-5.

Selenko, P., Gregorovic, G., Sprangers, R., Stier, G., Rhani, Z., Krämer, A., Sattler, M., 2003. Structural basis for the molecular recognition between human splicing factors U2AF65 and SF1/mBBP. Molecular cell 11, 965-76.

Selvakumar, M., Helfman, D.M., 1999. Exonic splicing enhancers contribute to the use of both 3’ and 5' splice site usage of rat beta-tropomyosin pre-mRNA. RNA 5, 378-94.

Shapiro, I.M., Cheng, A.W., Flytzanis, N.C., Balsamo, M., Condeelis, J.S., Oktay, M.H., Burge, C.B., Gertler, F.B., 2011. An EMT-Driven Alternative Splicing Program Occurs in Human Breast Cancer and Modulates Cellular Phenotype. PLoS genetics 7, e1002218.

Sharma, S., Falick, A.M., Black, D.L., 2005. Polypyrimidine tract binding protein blocks the 5’ splice site-dependent assembly of U2AF and the prespliceosomal E complex. Molecular cell 19, 485-96.

Sharma, S., Kohlstaedt, L. a, Damianov, A., Rio, D.C., Black, D.L., 2008. Polypyrimidine tract binding protein controls the transition from exon definition to an intron defined spliceosome. Nature structural & molecular biology 15, 183-91.

BIBLIOGRAPHY

Sharma, S., Maris, C., Allain, F.H.-T., Black, D.L., 2011. U1 snRNA Directly Interacts with Polypyrimidine Tract-Binding Protein during Splicing Repression. Molecular cell 41, 579-88.

Shaw, S.D., Chakrabarti, S., Ghosh, G., Krainer, A.R., 2007. Deletion of the N-terminus of SF2/ASF permits RS-domain-independent pre-mRNA splicing. PloS one 2, e854.

Shen, H., Green, M.R., 2004. A pathway of sequential arginine-serine-rich domain-splicing signal interactions during mammalian spliceosome assembly. Molecular cell 16, 363-373.

Shen, H., Green, M.R., 2006. RS domains contact splicing signals and promote splicing by a common mechanism in yeast through humans. Genes & development 20, 1755-65.

Shen, H., Green, M.R., 2007. RS domain-splicing signal interactions in splicing of U12-type and U2-type introns. Nature structural & molecular biology 14, 597-603.

Shen, H., Kan, J.L., Green, M.R., 2004. Arginine-serine-rich domains bound at splicing enhancers contact the branchpoint to promote prespliceosome assembly. Molecular cell 13, 367-376.

Shen, H., Kan, J.L.C., Ghigna, C., Biamonti, G., Green, M.R., 2004. A single polypyrimidine tract binding protein (PTB) binding site mediates splicing inhibition at mouse IgM exons M1 and M2. RNA 10, 787-794.

BIBLIOGRAPHY

Sheth, N., Roca, X., Hastings, M.L., Roeder, T., Krainer, A.R., Sachidanandam, R., 2006. Comprehensive splice-site analysis using comparative genomics. Nucleic acids research 34, 3955-67.

Shieh, J.-J., Liu, K.-T., Huang, S.-W., Chen, Y.-J., Hsieh, T.-Y., 2009. Modification of alternative splicing of Mcl-1 pre-mRNA using antisense morpholino oligonucleotides induces apoptosis in basal cell carcinoma cells. The Journal of investigative dermatology 129, 2497-506.

Shin, C., Manley, J.L., 2004. Cell signalling and the control of pre-mRNA splicing. Nature reviews. Molecular cell biology 5, 727-38.

Sierakowska, H., Sambade, M.J., Agrawal, S., Kole, R., 1996. Repair of thalassemic human beta-globin mRNA in mammalian cells by antisense oligonucleotides. Proceedings of the National Academy of Sciences of the United States of America 93, 12840-4.

Singh, N.K., Singh, N.N., Androphy, E.J., Singh, R.N., 2006. Splicing of a Critical Exon of Human Survival Motor Neuron Is Regulated by a Unique Silencer Element Located in the Last Intron. Molecular and cellular biology 26, 1333-1346.

Singh, N.N., Androphy, E.J., Singh, R.N., 2004a. In vivo selection reveals combinatorial controls that define a critical exon in the spinal muscular atrophy genes. RNA 10, 1291-305.

BIBLIOGRAPHY

Singh, N.N., Androphy, E.J., Singh, R.N., 2004b. An extended inhibitory context causes skipping of exon 7 of SMN2 in spinal muscular atrophy. Biochemical and biophysical research communications 315, 381-8.

Singh, N.N., Hollinger, K., Bhattacharya, D., Singh, R.N., 2010. An antisense microwalk reveals critical role of an intronic position linked to a unique long-distance interaction in pre-mRNA splicing. RNA (New York, N.Y.) 16, 1167-81.

Singh, N.N., Seo, J., Ottesen, E.W., Shishimorova, M., Bhattacharya, D., Singh, R.N., 2011. TIA1 prevents skipping of a critical exon associated with spinal muscular atrophy. Molecular and cellular biology 31, 935-54.

Singh, N.N., Shishimorova, M., Cao, L.C., Gangwani, L., Singh, R.N., 2009. A short antisense oligonucleotide masking a unique intronic motif prevents skipping of a critical exon in spinal muscular atrophy. RNA biology 6, 341-50.

Singh, N.N., Singh, R.N., Androphy, E.J., 2007. Modulating role of RNA structure in alternative splicing of a critical exon in the spinal muscular atrophy genes. Nucleic acids research 35, 371-89.

Singh, R., Valcárcel, J., Green, M.R., 1995. Distinct binding specificities and functions of higher eukaryotic polypyrimidine tract-binding proteins. Science (New York, N.Y.) 268, 1173-6.

BIBLIOGRAPHY

Singh, S.K., Nielsen, P., Koshkin, A., Wengel, J., 1998. LNA (locked nucleic acids): synthesis and high-affinity nucleic acid recognition nucleic acids. Chemical communications 4, 455-456.

Sinha, R., Allemand, E., Zhang, Z., Karni, R., Myers, M.P., Krainer, A.R., 2010. Arginine methylation controls the subcellular localization and functions of the oncoprotein splicing factor SF2/ASF. Molecular and cellular biology 30, 2762-74.

Skordis, L. a, Dunckley, M.G., Yue, B., Eperon, I.C., Muntoni, F., 2003. Bifunctional antisense oligonucleotides provide a trans-acting splicing enhancer that stimulates SMN2 gene expression in patient fibroblasts. Proceedings of the National Academy of Sciences of the United States of America 100, 4114-4119.

Smith, C.W., Valcárcel, J., 2000. Alternative pre-mRNA splicing: the logic of combinatorial control. Trends in biochemical sciences 25, 381-8.

Smith, D.J., Query, C.C., Konarska, M.M., 2008. '"Nought May Endure but Mutability "': Spliceosome Dynamics and the Regulation of Splicing. Molecular Cell 30, 657-666.

Sontheimer, E.J., Steitzt, J.A., 1993. The U5 AND U6 small nuclear RNAs as Active Site Components of the Spliceosome. Science 262, 1989-96.

Spies, N., Nielsen, C.B., Padgett, R. a, Burge, C.B., 2009. Biased chromatin signatures around polyadenylation sites and exons. Molecular cell 36, 245-54.

BIBLIOGRAPHY

Staknis, D., Reed, R., 1994a. SR proteins promote the first specific recognition of Pre-mRNA and are present together with the U1 small nuclear ribonucleoprotein particle in a general splicing enhancer complex. Molecular and cellular biology 14, 7670-82.

Staknis, D., Reed, R., 1994b. Direct Interactions between Pre-mRNA and Six U2 Small Nuclear Ribonucleoproteins during Spliceosome Assembly. Molecular and cellular biology 14, 2994-3005.

Staley, J.P., Guthrie, C., 1998. Mechanical devices of the spliceosome: motors, clocks, springs, and things. Cell 92, 315-26.

Stamm, S., Zhang, M.Q., Marr, T.G., Helfman, D.M., 1994. A sequence compilation and comparison of exons that are alternatively spliced in neurons. Nucleic acids research 22, 1515-26.

Sterner, D. a, Carlo, T., Berget, S.M., 1996. Architectural limits on split genes. Proceedings of the National Academy of Sciences of the United States of America 93, 15081-5.

Sun, S., Zhang, Z., Fregoso, O., Krainer, a. R., 2012. Mechanisms of activation and repression by the alternative splicing factors RBFOX1/2. RNA 18, 274-83.

Sun, S., Zhang, Z., Sinha, R., Karni, R., Krainer, A.R., 2010. SF2/ASF autoregulation involves multiple layers of post-transcriptional and translational control. Nature structural & molecular biology 17, 306-12.

Tacke, R., Chen, Y., Manley, J.L., 1997. Sequence-specific RNA binding by an SR protein requires RS domain phosphorylation: creation of an SRp40-specific splicing enhancer. Proceedings of the National Academy of Sciences of the United States of America 94, 1148-53.

Takagaki, Y., Manley, J.L., 1998. Levels of polyadenylation factor CstF-64 control IgM heavy chain mRNA accumulation and other events associated with B cell differentiation. Molecular cell 2, 761-71.

Takagaki, Y., Seipelt, R.L., Peterson, M.L., Manley, J.L., 1996. The polyadenylation factor CstF-64 regulates alternative processing of IgM heavy chain pre-mRNA during B cell differentiation. Cell 87, 941-52.

Talerico, M., Berget, S.M., 1990. Effect of 5' splice site mutations on splicing of the preceding intron. Molecular and cellular biology 10, 6299-6305.

Tanackovic, G., Kra, A., 2005. Human splicing factor SF3a ,sbut not SF1 , is essential for pre-mRNA splicing in vivo. Molecular Biology of the Cell 16, 1366 -1377.

Tanackovic, G., Ransijn, A., Thibault, P., Abou Elela, S., Klinck, R., Berson, E.L., Chabot, B., Rivolta, C., 2011. PRPF mutations are associated with generalized defects in spliceosome formation and pre-mRNA splicing in patients with retinitis pigmentosa. Human molecular genetics 20, 2116-30.

BIBLIOGRAPHY

Tanko, Q., Franklin, B., Lynch, H., Knezetic, J., 2002. A hMLH1 genomic mutation and associated novel mRNA defects in a hereditary non-polyposis colorectal cancer family. Mutation research 503, 37-42.

Tardiff, D.F., Lacadie, S.A., Rosbash, M., 2006. A Genome-Wide Analysis Indicates that Yeast Pre-mRNA Splicing Is Predominantly Posttranscriptional. Molecular Cell 24, 917-929.

Taylor, J.K., Zhang, Q.Q., Wyatt, J.R., Dean, N.M., 1999. Induction of endogenous Bcl-xS through the control of Bcl-x pre-mRNA splicing by antisense oligonucleotides. Nature biotechnology 17, 1097-100.

Taylor, M.D., Gokgoz, N., Andrulis, I.L., Mainprize, T.G., Drake, J.M., Rutka, J.T., 2000. Familial posterior fossa brain tumors of infancy secondary to germline mutation of the hSNF5 gene. American journal of human genetics 66, 1403-6.

Tennyson, C.., Kalmut, H.., Worton, R.G., 1995. The human dystrophin gene requires 16 hours to be transcribed and is cotranscriptionally spliced. Nature genetics 9, 184-190.

Teplova, M., Wallace, S.T., Tereshko, V., Minasov, G., Symons, a M., Cook, P.D., Manoharan, M., Egli, M., 1999. Structural origins of the exonuclease resistance of a zwitterionic RNA. Proceedings of the National Academy of Sciences of the United States of America 96, 14240-5.

BIBLIOGRAPHY

Thiery, J.P., Sleeman, J.P., 2006. Complex networks orchestrate epithelial-mesenchymal transitions. Nature reviews. Molecular cell biology 7, 131-42.

Thobe, M.N., Gurusamy, D., Pathrose, P., Waltz, S.E., 2010. The Ron receptor tyrosine kinase positively regulates angiogenic chemokine production in prostate cancer cells. Oncogene 29, 214-26.

Thomas, R.M., Toney, K., Fenoglio-Preiser, C., Revelo-Penafiel, M.P., Hingorani, S.R., Tuveson, D. a, Waltz, S.E., Lowy, A.M., 2007. The RON receptor tyrosine kinase mediates oncogenic phenotypes in pancreatic cancer cells and is increasingly expressed during pancreatic cancer progression. Cancer research 67, 6075-82.

Tian, M., Maniatis, T., 1994. A splicing enhancer exhibits both constitutive and regulated activities. Genes & Development 8, 1703-1712.

Tilgner, H., Nikolaou, C., Althammer, S., Sammeth, M., Beato, M., Valcárcel, J., Guigó, R., 2009. Nucleosome positioning as a determinant of exon recognition. Nature structural & molecular biology 16, 996-1001.

Tollervey, J.R., Wang, Z., Hortobagyi, T., Witten, J.T., Zarnack, K., Kayikci, M., Clark, T. a., Schweitzer, a. C., Rot, G., Curk, T., Zupan, B., Rogelj, B., Shaw, C.E., Ule, J., 2011. Analysis of alternative splicing associated with aging and neurodegeneration in the human brain. Genome Research 1572-1582.

Townsend, D., Yasuda, S., Li, S., Chamberlain, J.S., Metzger, J.M., 2008. Emergent dilated cardiomyopathy caused by targeted repair of dystrophic skeletal muscle. Molecular therapy : the journal of the American Society of Gene Therapy 16, 832-5.

Trabulo, S., Resina, S., Simões, S., Lebleu, B., Pedroso de Lima, M.C., 2010. A non-covalent strategy combining cationic lipids and CPPs to enhance the delivery of splice correcting oligonucleotides. Journal of controlled release 145, 149-58.

Trusolino, L., Comoglio, P.M., 2002. Scatter-factor and semaphorin receptors: cell signalling for invasive growth. Nature reviews. Cancer 2, 289-300.

Tsukahara, T., Casciato, C., Helfman, D.M., 1994. Alternative splicing of beta-tropomyosin pre-mRNA: multiple cis-elements can contribute to the use of the 5'- and 3'-splice sites of the nonmuscle/smooth muscle exon 6. Nucleic acids research 22, 2318-25.

Ule, J., Stefani, G., Mele, A., Ruggiu, M., Wang, X., Taneri, B., Gaasterland, T., Blencowe, B.J., Darnell, R.B., 2006. An RNA map predicting Nova-dependent splicing regulation. Nature 444, 580-6.

Underwood, J.G., Boutz, P.L., Dougherty, J.D., Stoilov, P., Black, D.L., 2005. Homologues of the Caenorhabditis elegans Fox-1 Protein Are Neuronal Splicing Regulators in Mammals. Molecular and cellular biology 25, 10005-10016.

Valacca, C., Bonomi, S., Buratti, E., Pedrotti, S., Baralle, F.E., Sette, C., Ghigna, C., Biamonti, G., 2010. Sam68 regulates EMT through alternative splicing-activated

nonsense-mediated mRNA decay of the SF2/ASF proto-oncogene. The Journal of cell biology 191, 87-99.

Valcárcel, J., Gaur, R.K., Singh, R., Green, M.R., 1996. Interaction of U2AF65 RS region with pre-mRNA branch point and promotion of base pairing with U2 snRNA [corrected]. Science (New York, N.Y.) 273, 1706-9.

Venables, J.P., Klinck, R., Koh, C., Gervais-Bird, J., Bramard, A., Inkel, L., Durand, M., Couture, S., Froehlich, U., Lapointe, E., Lucier, J.-F., Thibault, P., Rancourt, C., Tremblay, K., Prinos, P., Chabot, B., Elela, S.A., 2009. Cancer-associated regulation of alternative splicing. Nature structural & molecular biology 16, 670-6.

Venkatesh, S., Wower, J., Byrne, M.E., 2009. Nucleic acid therapeutic carriers with on-demand triggered release. Bioconjugate chemistry 20, 1773-82.

Vezain, M., Saugier-Veber, P., Goina, E., Touraine, R., Manel, V., Toutain, A., Fehrenbach, S., Frébourg, T., Pagani, F., Tosi, M., Martins, A., 2010. A rare SMN2 variant in a previously unrecognized composite splicing regulatory element induces exon 7 inclusion and reduces the clinical severity of spinal muscular atrophy. Human mutation 31, E1110-25.

Villemaire, J., Dion, I., Elela, S.A., Chabot, B., 2003. Reprogramming alternative pre-messenger RNA splicing through the use of protein-binding antisense oligonucleotides. The Journal of biological chemistry 278, 50031-9.

Vinogradov, S.V., Batrakova, E.V., Kabanov, A.V., 2004. Nanogels for oligonucleotide delivery to the brain. Bioconjugate chemistry 15, 50-60.

Wagh, P.K., Gray, J.K., Zinser, G.M., Vasiliauskas, J., James, L., Monga, S.P., Waltz, S.E., 2011. β-Catenin is required for Ron receptor-induced mammary tumorigenesis. Oncogene 30, 3694-704.

Wagner, E.J., Garcia-Blanco, M.A., 2001. Polypyrimidine Tract Binding Protein Antagonizes Exon Definition. Molecular and cellular biology 21, 3281-3288.

Wahl, M.C., Will, C.L., Lührmann, R., 2009. The spliceosome: design principles of a dynamic RNP machine. Cell 136, 701-18.

Waltz, S.E., Eaton, L., Hess, K.A., Peace, B.E., Ihlendorf, J.R., Wang, M.-hai, Kaestner, K.H., Degen, S.J.F., 2001. Ron-mediated cytoplasmic signaling is dispensable for viability but is required to limit inflammatory responses. Journal of clinical investigation 108, 567-576.

Waltz, S.E., Toms, C.L., McDowell, S. a, Clay, L. a, Muraoka, R.S., Air, E.L., Sun, W.Y., Thomas, M.B., Degen, S.J., 1998. Characterization of the mouse Ron/Stk receptor tyrosine kinase gene. Oncogene 16, 27-42.

Wang, E.T., Sandberg, R., Luo, S., Khrebtukova, I., Zhang, L., Mayr, C., Kingsmore, S.F., Schroth, G.P., Burge, C.B., 2008. Alternative isoform regulation in human tissue transcriptomes. Nature 456, 470-6.

Wang, J., Steinbacher, S., Augustin, M., Schreiner, P., Epstein, D., Mulvihill, M.J., Crew, A.P., 2010. The crystal structure of a constitutively active mutant RON kinase suggests an intramolecular autophosphorylation hypothesis. Biochemistry 49, 7972-4.

Wang, J., Xiao, S.-H., Manley, J.L., 1998. Genetic analysis of the SR protein ASF/SF2: interchangeability of RS domains and negative control of splicing. Genes & Development 12, 2222-2233.

Wang, M.-H., Lao, W.-F., Wang, D., Luo, Y.L., Yao, H.-P., 2007. Blocking tumorigenic activities of colorectal cancer cells by a splicing RON receptor variant defective in the tyrosine kinase domain. Cancer biology & therapy 6, 1121-9.

Wang, M.-H., Wang, D., Chen, Y.-Q., 2003. Oncogenic and invasive potentials of human macrophage-stimulating protein receptor, the RON receptor tyrosine kinase. Carcinogenesis 24, 1291-300.

Wang, M.H., Cox, G.W., Yoshimura, T., Sheffler, L. a, Skeel, a, Leonard, E.J., 1994. Macrophage-stimulating protein inhibits induction of nitric oxide production by endotoxin- or cytokine-stimulated mouse macrophages. The Journal of biological chemistry 269, 14027-31.

Wang, M.H., Dlugosz, a a, Sun, Y., Suda, T., Skeel, a, Leonard, E.J., 1996. Macrophage-stimulating protein induces proliferation and migration of murine keratinocytes. Experimental cell research 226, 39-46.

Wang, M.H., Iwama, a, Skeel, a, Suda, T., Leonard, E.J., 1995. The murine stk gene product, a transmembrane protein tyrosine kinase, is a receptor for macrophage-stimulating protein. Proceedings of the National Academy of Sciences of the United States of America 92, 3933-7.

Wang, Y., Wang, J., Gao, L., Stamm, S., Andreadis, A., 2011. An SRp75/hnRNPG complex interacting with hnRNPE2 regulates the 5' splice site of tau exon 10, whose misregulation causes frontotemporal dementia. Gene 485, 130-8.

Wang, Z., Burge, C.B., 2008. Splicing regulation: from a parts list of regulatory elements to an integrated splicing code. RNA 14, 802-13.

Wang, Z., Xiao, X., Van Nostrand, E., Burge, C.B., 2006. General and specific functions of exonic splicing silencers in splicing control. Molecular cell 23, 61-70.

Warzecha, C.C., Sato, T.K., Nabet, B., Hogenesch, J.B., Carstens, R.P., 2009. ESRP1 and ESPR2 Are Epithelial Cell-Type-Specific Regultors of FGFR2 Splicing. Molecular Cell 33, 591-601.

Webb, M.S., Tortora, N., Cremese, M., Kozlowska, H., Blaquiere, M., Devine, D.V., Kornbrust, D.J., Al, W.E.T., 2001. Toxicity and Toxicokinetics of a Phosphorothioate Oligonucleotide Against the c-myc Oncogene in Cynomolgus Monkeys. Blood 163, 155-163.

Werdnig, G., 1894. Die fruhinfantile progressive spinale Amyotrophie. Arch Psychiatr Nervenkr 26, 706-44.

Wijnhoven, B.P., Dinjens, W.N., Pignatelli, M., 2000. E-cadherin-catenin cell-cell adhesion complex and human cancer. The British journal of surgery 87, 992-1005.

Will, C.L., Lührmann, R., 2001. Spliceosomal UsnRNP biogenesis, structure and function. Current opinion in cell biology 13, 290-301.

Williams, J.H., Schray, R.C., Patterson, C.A., Ayitey, S.O., Tallent, M.K., Lutz, G.J., 2009. Oligonucleotide-mediated survival of motor neuron protein expression in CNS improves phenotype in a mouse model of spinal muscular atrophy. The Journal of neuroscience : the official journal of the Society for Neuroscience 29, 7633-8.

Wilton, S.D., Lloyd, F., Carville, K., Fletcher, S., Honeyman, K., Agrawal, S., Kole, R., 1999. Specific removal of the nonsense mutation from the mdx dystrophin mRNA using antisense oligonucleotides. Neuromuscular disorders : NMD 9, 330-8.

Wirth, B., Brichta, L., Hahnen, E., 2006. Spinal muscular atrophy: from gene to therapy. Seminars in pediatric neurology 13, 121-31.

Wu, B., Moulton, H.M., Iversen, P.L., Jiang, J., Li, J., Li, J., Spurney, C.F., Sali, A., Guerron, A.D., Nagaraju, K., Doran, T., Lu, P., Xiao, X., Lu, Q.L., 2008. Effective rescue of dystrophin improves cardiac function in dystrophin-deficient mice by a modified

morpholino oligomer. Proceedings of the National Academy of Sciences of the United States of America 105, 14814-9.

Wu, J.Y., Maniatis, T., 1993. Specific interactions between proteins implicated in splice site selection and regulated alternative splicing. Cell 75, 1061-70.

Wu, R.P., Youngblood, D.S., Hassinger, J.N., Lovejoy, C.E., Nelson, M.H., Iversen, P.L., Moulton, H.M., 2007. Cell-penetrating peptides as transporters for morpholino oligomers: effects of amino acid composition on intracellular delivery and cytotoxicity. Nucleic acids research 35, 5182-91.

Wu, S., Romfo, C.M., Nilsen, T.W., Green, M.R., 1999. Functional recognition of the 3' splice site AG by the splicing factor U2AF35. Nature 402, 832-5.

Wyatt, J.R., Sontheimer, E.J., Steitz, J. a, 1992. Site-specific cross-linking of mammalian U5 snRNP to the 5' splice site before the first step of pre-mRNA splicing. Genes & Development 6, 2542-2553.

Xie, J., Black, D.L., 2001. A CaMK IV responsive RNA element mediates depolarization-induced alternative splicing of ion channels. Nature 410, 936-9.

Xu, Q., Lee, C., 2003. Discovery of novel splice forms and functional analysis of cancer-specific alternative splicing in human expressed sequences. Nucleic Acids Research 31, 5635-5643.

BIBLIOGRAPHY

Yang, X., Koh, C.G., Liu, S., Pan, X., Santhanam, R., Yu, B., Peng, Y., Pang, J., Golan, S., Talmon, Y., Jin, Y., Muthusamy, N., Byrd, J.C., Chan, K.K., Lee, L.J., Marcucci, G., Lee, R.J., 2008. Transferrin Receptor-Targeted Lipid Nanoparticles for Delivery of an Antisense Oligodeoxyribonucleotide against Bcl-2. Molecular Pharmaceutics 6, 221-230.

Yao, H.-P., Zhou, Y.-Q., Ma, Q., Guin, S., Padhye, S.S., Zhang, R.-W., Wang, M.-H., 2011. The monoclonal antibody Zt/f2 targeting RON receptor tyrosine kinase as potential therapeutics against tumor growth-mediated by colon cancer cells. Molecular cancer 10, 82.

Yeung, E.W., Whitehead, N.P., Suchyna, T.M., Gottlieb, P. a, Sachs, F., Allen, D.G., 2005. Effects of stretch-activated channel blockers on [Ca2+]i and muscle damage in the mdx mouse. The Journal of physiology 562, 367-80.

Yin, H., Moulton, H.M., Betts, C., Seow, Y., Boutilier, J., Iverson, P.L., Wood, M.J. a, 2009. A fusion peptide directs enhanced systemic dystrophin exon skipping and functional restoration in dystrophin-deficient mdx mice. Human molecular genetics 18, 4405-14.

Yin, H., Moulton, H.M., Seow, Y., Boyd, C., Boutilier, J., Iverson, P., Wood, M.J.A., 2008. Cell-penetrating peptide-conjugated antisense oligonucleotides restore systemic muscle and cardiac dystrophin expression and function. Human molecular genetics 17, 3909-3918.

Yokota, T., Lu, Q.-L., Partridge, T., Kobayashi, M., Nakamura, A., Takeda, S., Hoffman, E., 2009. Efficacy of systemic morpholino exon-skipping in Duchenne dystrophy dogs. Annals of neurology 65, 667-76.

Yoshida, K., Sanada, M., Shiraishi, Y., Nowak, D., Nagata, Y., Yamamoto, R., Sato, Y., Sato-Otsubo, A., Kon, A., Nagasaki, M., Chalkidis, G., Suzuki, Y., Shiosaka, M., Kawahata, R., Yamaguchi, T., Otsu, M., Obara, N., Sakata-Yanagimoto, M., Ishiyama, K., Mori, H., Nolte, F., Hofmann, W.-K., Miyawaki, S., Sugano, S., Haferlach, C., Koeffler, H.P., Shih, L.-Y., Haferlach, T., Chiba, S., Nakauchi, H., Miyano, S., Ogawa, S., 2011. Frequent pathway mutations of splicing machinery in myelodysplasia. Nature 478, 64-69.

Young, P.J., DiDonato, C.J., Hu, D., Kothary, R., Androphy, E.J., Lorson, C.L., 2002. SRp30c-dependent stimulation of survival motor neuron (SMN) exon 7 inclusion is facilitated by a direct interaction with hTra2 beta 1. Human molecular genetics 11, 577-87.

Yu, Y., Das, R., Folco, E.G., Reed, R., 2010. A model in vitro system for co-transcriptional splicing. Nucleic acids research 38, 7570-7578.

Yu, Y., Maroney, P. a, Denker, J. a, Zhang, X.H.-F., Dybkov, O., Lührmann, R., Jankowsky, E., Chasin, L. a, Nilsen, T.W., 2008. Dynamic regulation of alternative splicing by silencers that modulate 5' splice site competition. Cell 135, 1224-36.

Yuan, N., Wang, C.H., Trela, A., Albanese, C.T., 2007. Laparoscopic Nissen fundoplication during gastrostomy tube placement and noninvasive ventilation may improve survival in type I and severe type II spinal muscular atrophy. Journal of child neurology 22, 727-31.

Zahler, a M., Neugebauer, K.M., Lane, W.S., Roth, M.B., 1993. Distinct functions of SR proteins in alternative pre-mRNA splicing. Science (New York, N.Y.) 260, 219-22.

Zamore, P.D., Green, M.R., 1989. Identification, purification, and biochemical characterization of U2 small nuclear ribonucleoprotein auxiliary factor. Proceedings of the National Academy of Sciences 86, 9243-9247.

Zamore, P.D., Patton, J.., Green, G.., 1992. Cloning and domain structure of the mammalian splicing factor U2AF. Nature 355, 609-614.

Zhang, M.Q., 1998. Statistical features of human exons and their flanking regions. Human molecular genetics 7, 919-32.

Zhang, R., So, B.R., Li, P., Yong, J., Glisovic, T., Wan, L., Dreyfuss, G., 2011. Structure of a Key Intermediate of the SMN Complex Reveals Gemin2's Crucial Function in snRNP Assembly. Cell 146, 384-95.

Zhang, X.H.F., Chasin, L.A., 2004. Computational definition of sequence motifs governing constitutive exon splicing. Genes & development 18, 1241-50.

Zhang, Y., Kaplan-Lefko, P.J., Rex, K., Yang, Y., Moriguchi, J., Osgood, T., Mattson, B., Coxon, A., Reese, M., Kim, T.-S., Lin, J., Chen, A., Burgess, T.L., Dussault, I., 2008.

Identification of a novel recepteur d'origine nantais/c-met small-molecule kinase inhibitor with antitumor activity in vivo. Cancer research 68, 6680-7.

Zhang, Z., Kelemen, O., van Santen, M. a, Yelton, S.M., Wendlandt, A.E., Sviripa, V.M., Bollen, M., Beullens, M., Urlaub, H., Lührmann, R., Watt, D.S., Stamm, S., 2011. Synthesis and characterization of pseudocantharidins, novel phosphatase modulators that promote the inclusion of exon 7 into the survival of motoneuron (SMN) pre-mRNA. The Journal of biological chemistry 286, 10126-36.

Zhang, Z., Lotti, F., Dittmar, K., Younis, I., Wan, L., Kasim, M., Dreyfuss, G., 2008. SMN deficiency causes tissue-specific perturbations in the repertoire of snRNAs and widespread defects in splicing. Cell 133, 585-600.

Zhou, D., Pan, G., Zheng, C., Zheng, J., Yian, L., Teng, X., 2008. Expression of the RON receptor tyrosine kinase and its association with gastric carcinoma versus normal gastric tissues. BMC cancer 8, 353.

Zhou, Y.-Q., He, C., Chen, Y.-Q., Wang, D., Wang, M.-H., 2003. Altered expression of the RON receptor tyrosine kinase in primary human colorectal adenocarcinomas: generation of different splicing RON variants and their oncogenic potential. Oncogene 22, 186-97.

Zhou, Z., Licklider, L.J., Gygi, S.P., Reed, R., 2002. Comprehensive proteomic analysis of the human spliceosome. Nature 419, 182-5.

Zhu, J., Mayeda, A., Krainer, A.R., Brook, S., York, N., 2001. Exon Identity Established through Differential Antagonism between Exonic Splicing Silencer-Bound hnRNP A1 and Enhancer-Bound SR Proteins. Cell 8, 1351-1361.

Zhuang, Y. a, Goldstein, a M., Weiner, a M., 1989. UACUAAC is the preferred branch site for mammalian mRNA splicing. Proceedings of the National Academy of Sciences of the United States of America 86, 2752-6.

Zuo, P., Maniatis, T., 1996. The splicing factor U2AF35 mediates critical protein-protein interactions in constitutive and enhancer-dependent splicing. Genes & Development 10, 1356-1368.

Zuo, P., Manley, J.L., 1993. Functional domains of the human splicing factor ASF/SF2. The EMBO journal 12, 4727-37.

Zuo, P., Manley, J.L., 1994. The human splicing factor ASF/SF2 can specifically recognize pre-mRNA 5' splice sites. Proceedings of the National Academy of Sciences 91, 3363-7.

Zupo, S., Massara, R., Dono, M., Rossi, E., Malavasi, F., Cosulich, M.E., Ferrarini, M., 2000. Apoptosis or plasma cell differentiation of CD38-positive B-chronic lymphocytic leukemia cells induced by cross-linking of surface IgM or IgD. Blood 95, 1199-1206.